Delineating debris-flow hazards on alluvial fans in the Coromandel and Kaimai regions, New Zealand, using GIS

A thesis submitted in partial fulfilment of the requirements for the degree of

Master of Science in Environmental Science

at the

University of Canterbury

Andrew J. Welsh

University of Canterbury

2007

Abstract

Debris-flows pose serious hazards to communities in mountainous regions of the world and are often responsible for loss of life and damages to infrastructure. Characterised by high flow velocity, large impact forces and long runout, debris-flows have potential discharges several times greater than clear water flood discharges and possess much greater erosive and destructive potential. In combination with poor temporal predictability, they present a significant hazard to settlements, transport routes and other infrastructure located at the drainage points (fan-heads).of watersheds. Thus, it is important that areas vulnerable to debris-flows are identified in order to aid decisions on appropriate land-uses for alluvial fans.

This research has developed and tested a new GIS-based procedure for identifying areas prone to debris-flow hazards in the Coromandel/Kaimai region, North Island, New Zealand. The procedure was developed using ESRI Arc View software, utilising the NZ 25 x 25 m DEM as the primary input. When run, it enabled watersheds and their associated morphometric parameters to be derived for selected streams in the study area. Two specific parameters, Melton ratio (R) and watershed length were then correlated against field evidence for debris-flows, debris-floods and fluvial processes at stream watershed locations in the study area. Overall, strong relationships were observed to exist between the evidence observed for these phenomena and the parameters, thus confirming the utility of the GIS procedure for the preliminary identification of hydrogeomorphic hazards such as debris-flow in the Coromandel/Kaimai region study area.

In consideration of the results, the procedure could prove a useful tool for regional councils and CDEM groups in regional debris-flow hazard assessment for the identification of existing developments at risk of debris-flow disaster. Furthermore, the procedure could be used to provide justification for subsequent, more intensive local investigations to fully quantify the risk to people and property at stream fan and watershed locations in such areas.

Table of Contents

Abstract……...i
Table of contents……....ii
List of figures…….....v
List of tables……...x
Acknowledgements.....xi

Chapter One 1
Introduction.....1
1.1 Background 1
1.2 Research Rationale.....4
1.3 Aims and Objectives 7
1.4 Thesis structure 9

Chapter Two.....11
Definitions and distinctions between processes.....11
2.1 Introduction.....11
2.2 Approaches to distinguishing and defining processes 11
2.3 Terminology of processes 20
2.4 Case studies.....32
2.5 Summary 39

Chapter Three.....41
Past research into the recognition of debris-flow hazard.....41
3.1 Introduction.....41
3.2 Debris-flow hazard recognition overview 42
3.3 Spatial recognition of debris-flows using fan-basin morphometry.....48

Chapter Four 56
Study area and methodology 56
4.1 Introduction 56
4.2 Study area 56
4.3 Research methodology – GIS methods 64
4.4 Research methodology – Field reconnaissance approach 83
4.5 Research methodology – Air photograph approach 90
4.6 Statistical processing and analysis methodology 91

Chapter Five 93
GIS and Field investigation results 93
5.1 Introduction 93
5.2 Melton ratio (*R*) and watershed length values derived for stream watershed locations in the study area 93
5.3 Criteria observed at stream locations in the study area 97
and watershed length 104
5.4 Relationships between Melton ratio (R) and watershed length, and observed evidence for hydrogeomorphic processes in the study area 107
5.5 Melton ratio (R) and watershed length values derived for other stream watershed locations outside the study area 115

Chapter Six 120
Discussion 120
6.1 Introduction 120
6.2 The use of Melton ratio (*R*) for the identification of areas prone to debris-flow, debris-flood and fluvial-flood hazards in the study area 121
6.3 The use of watershed length for the identification of areas prone to debris-flow, debris-flood and fluvial-flood hazards 128
6.4 Results derived for stream watersheds outside the study area 130
6.5 Combinations of *R* and watershed length for the identification of debris-flow hazards in the study area 132

6.6 Implied debris-flow hazard at stream locations in the Coromandel/Kaimai region 134
6.7 Limitations of the research 138

Chapter Seven 143
Summary and Conclusions 143
7.1 Introduction 143
7.2 Restatement of thesis aims and objectives 143
7.3 Summary of the main findings 144
7.4 Conclusions 148
7.5 Suggestions for future research 148
References: 150
Appendices 170

List of Figures

Figure 1.1: The devastating amount of sediment and debris transported to fans as a result of major debris-flows in the state of Vargas, Venezuela 1999……2

Figure 1.2: Graphical representation of the differences between the vector and raster data models used to represent real world phenomena in a GIS ……..4

Figure 1.3: Bouldery debris-flow deposits at Matata, 2006……..7

Figure 2.1: Pierson and Costa's (1987) rheological classification of water-sediment mixtures……..14

Figure 2.2: Lorenzini and Mazza's (2004) proposed sediment-water mixture classification based on the graph proposed by Pierson and Costa (1987)…….16

Figure 2.3: Diagram showing the characteristics of a debris-flow surge ……22

Figure 2.4: Approximate ranges in limiting thresholds for experimental (a & b) and natural hyperconcentrated flows (c, d & e) in comparison to Beverage and Culbertson's (1964) proposed limits……...25

Figure 2.5: Hyperconcentrated flow observed at Matata, North Island, New Zealand, following the debris-flow event of June 2005 ……..26

Figure 2.6: Location of Venezuela, South America, and areas worst affected in the state of Vargas during the 1999 storm event …….32

Figure 2.7: Devastation in the settlement of Los Corales, Vargas, due to occurrence of numerous debris-flows and debris-floods in the 1999 storm ……33

Figure 2.8: Rainfall measurements at Maiquetia Weather Station during the month of December 1999. ……33

Figure 2.9: Giant boulders up to 6m in size and large amounts of tree debris brought down from the slopes of Avila Mountain during the 1999 debris-flow event in Venezuela, South America……...35

Figure 2.10: Locations of Te Aroha and Matata, North Island, New Zealand…….36

Figure 2.11: Devastation and destruction as a result of debris-flows in the small town of Te Aroha 1985 ……..38

Figure 2.12: Giant boulder transported downstream in the Matata debris-flows of June 2005 ……..38

Figure 3.1: Debris-flow channel observed in the Canadian Rockies, showing levee deposits and pronounced super-elevation of the flow in the two bends, as marked by the lines ……...45

Figure 3.2: Conceptual sketch showing the difference between supply-unlimited and supply-limited basins with regard to debris-flow initiation …….……47

Figure 3.3: Plot of Melton's Ratio and Fan Gradient, showing thresholds used to distinguish debris-flow from fluvially dominated fans (and hence their contributing basins) in the Southern Alps of the South Island New Zealand ……53

Figure 4.1: Location of the Coromandel/Kaimai region study area ……57

Figure 4.2: Geological map of the Coromandel/Kaimai region ……..59

Figure 4.3: Annual precipitation, wind speed and wind direction for the Coromandel/Kaimai region ……...62

Figure 4.4: Process followed to extract the DEM of the study area and derive the drainage network (Part 1 of the 'Watershed model'; constructed using the Spatial Analyst Model Builder)……...66

Figure 4.5: Process followed to derive watersheds and their associated morphometric parameters for the study area (Part 2 of the 'Watershed model'; constructed using the Spatial Analyst Model Builder)……67

Figure 4.6: Coding for the 8 possible flow directions out of each cell and example flow direction raster output, created using the spatial analyst 'flow direction' tool ……69

Figure 4.7: Zones of high flow accumulation, displayed on top of the region's topography as represented by the hillshade DEM output……..71

Figure 4.8: Profile view of a sink in the data before and after running the Fill tool…...72

Figure 4.9: Example slope output raster derived using the Slope tool (displayed on hillshade DEM background; DEM Location: Matata, New Zealand)……...73

Figure 4.10: NZTM wrap aerial photograph showing a digitized house location within the desired 100 m ground distance buffer (4 cells = Distance A) of the active stream channel……...75

Figure 4.11: Pour points placed in stream channels adjacent to relevant house locations……77

Figure 4.12: Example of Watershed DEM output and associated pour point, displayed on the hillshade DEM background…….79

Figure 4.13: Example of the Euclidean distance output (displayed on the hillshade DEM background) showing concentric distance rings radiating outward from the pour point origin. ……81

Figure 4.14: DEM of the Coromandel Range region showing the location of specific stream sites surveyed in the field investigation ……88

Figure 4.15: DEM of the Kaimai Range region showing the location of specific stream sites surveyed in the field investigation ……89

Figure 5.1: Scatterplot of Melton ratio (*R*) and watershed lengths for all stream watersheds in the study area. ……94

Figure 5.2: The geographic distribution of stream watersheds in the study area according to categories of *R* and watershed length…….96

Figure 5.3: Percentage of debris-flow criteria observed at stream watershed locations in the study area…….98

Figure 5.4: Enormous boulders up to 6 m in size (note cap for scale) were observed in the stream channel and on the fan at Lipsy Stream……98

Figure 5.5: An example of one of the many 'debris dams' observed in the channel at Lipsy Stream……..99

Figure 5.6: Poorly sorted, matrix supported and gravely topped lobes observed in the stream channel at Waitoitoi Stream……...99

Figure 5.7: Percentage of debris-flood criteria observed at stream watershed locations in the study area……...100

Figure 5.8: Boulder-topped, lobed deposits observed beyond the stream channel on the fan at Wahine Stream……...101

Figure 5.9: Tree trunks and branches and loose mixtures of woody debris, gravel and sand observed at Gordon Stream…….101

Figure 5.10: Percentage of fluvial criteria observed at stream watersheds locations in the study area…….102

Figure 5.11: The large width to depth ratio and the presence of bars, sheets and splays in the stream channel observed at Te Puru Stream……..103

Figure 5.12: Clast supported deposits observed in a stream cut at Stanley Stream……103

Figure 5.13: Evidence observed for all processes (debris-flows, debris-floods and fluvial processes) at stream watershed locations exhibiting *R* values <0.30 and lengths >2.7 km (category A)…….104

Figure 5.14: Evidence observed for all processes at stream locations in categories C and D……...…105

Figure 5.15: Evidence observed for all processes at stream locations in category F…..106

Figure 5.16: Relationship between observed evidence for debris-flows (DF) and Melton ratio (*R*) for stream watershed locations in the study area……...108

Figure 5.17: Relationship between observed evidence for debris-floods (DFld) and Melton's *R* for stream watershed locations in the study area……..108

Figure 5.18: Relationship between the amounts of criteria observed for fluvial processes (Flu) and Melton's *R* for stream watershed locations in the study area……...109

Figure 5.19: Evidence observed for debris-flows (DF) at stream locations in the study area in terms of categories of Melton's *R*……110

Figure 5.20: Evidence observed for debris-floods (DFld) at stream locations in the study area in terms of categories of Melton's *R*……111

Figure 5.21: Evidence observed for fluvial processes (Flu) at stream locations in the study area in terms of categories of Melton's *R*……..111

.

Figure 5.22: Relationship between observed evidence for debris-flows (DF) and watershed length for stream locations in the study area……..112

Figure 5.23: Relationship between observed evidence for debris-floods (DFld) and watershed length for stream locations in the study area……..113

Figure 5.24: Relationship between observed evidence for fluvial processes (Flu) and watershed length for stream locations in the study area……..113

Figure 5.25: Evidence observed for debris-flows (DF) at stream locations in the study area in terms of categories of watershed length (WSL)……..114

Figure 5.26: Evidence observed for debris-floods (DFld) at stream locations in the study area in terms of categories of watershed length (WSL)……...115

Figure 5.27: Evidence observed for fluvial processes (Flu) at stream locations in the study area in terms of categories of watershed length (WSL)…….116

Figure 5.28: South Island locations and allocated Melton ratio (*R*)/watershed length (WL) categories for stream watersheds outside the study area known to have produced debris-flows……..117

Figure 5.29: North Island locations and allocated Melton ratio (*R*)/watershed length (WL) categories for stream watersheds outside the study area known to have produced debris-flows……..118

Figure 5.30: Scatterplot of Melton ratio (*R*) and watershed lengths for stream watersheds outside the study area known to have experienced debris-flows. ……...119

Figure 6.1: Correlation trends between observed evidence for debris-flows, debris-floods and fluvial processes at drainage points of watersheds in the study area and Melton's *R* of the contributing watershed. …….122

Figure 6.2: Melton ratios (*R*) of debris-flow-prone watersheds in the study area……..125

Figure 6.3: Melton ratios (*R*) of fluvially-prone watersheds in the study area ……..125

Figure 6.4: Correlation trends between observed evidence for processes at stream locations in the study area and Melton's R of contributing watersheds. ……126

Figure 6.5: Correlation trends between evidence for debris-flow and fluvial processes and watershed length for stream watershed locations in the study area. ……129

Figure 6.6: Scatterplot showing debris-flow hazard levels assigned for/to each categorical combination of *R* and watershed length (A-F). ……133

Figure 6.7: Stream watersheds in the Coromandel region exhibiting moderate, moderate-high and high debris-flow hazard. ……..135

Figure 6.8: Stream watersheds in the Kaimai region exhibiting moderate, moderate-high and high debris-flow hazard levels. ……136

List of tables

Table 2.1: Classification of flow-type landslides (Hungr et al. 2001)……..18

Table 4.1: Category combinations of Melton ratio (*R*) and Watershed Length (WL)…..83

Table 4.2: Values of *R* and watershed length for stream watershed locations in the study area…….85

Table 4.3: Example calculation of criteria observed in the field……..91

Table 4.4: Stream watershed locations outside the study area……..92

Table 5.1: Frequency of stream watersheds within categorical combinations of *R* and watershed length……....94

Table 5.2: Melton ratio (*R*) and watershed lengths (WSL) derived for 'other' stream locations outside the study area ……..116

Table 6.1: Comparison between mean *R* and standard deviation ranges of *R* for debris-flow and fluvially-prone watersheds ……...124

Table 6.2: Comparison of ranges in watershed lengths (km) identified for specific hydrogeomorphic processes by Wilford et al. (2004) and the present study. …….130

Table 6.3: Frequency of stream watersheds within categories of *R*/WL and associated debris-flow hazard ……...134

Table 6.4: Names for stream watersheds in the study area, their respective R/WL categories and associated debris-flow hazard levels ……...137

Acknowledgements

I would like to say a big thank you to my two supervisors, Associate Professor Tim Davies and Dr. Tom Cochrane. Your ongoing help, guidance, encouragement and insightful comments were invaluable and it has been a real privilege working with you both. Also, thank you to Dr. Clive Sabel for help during the early stages of the thesis.

Thank you to Dr. Mauri McSaveney for helping with initial field reconnaissance during April 2006. To John Thyne, Graham Furniss and Paul Bealing, thank you for providing expert assistance with the development of the GIS procedure. A massive thank you must go to Tim Applehans for providing invaluable assistance and advice on anything and everything to do with the writing of this thesis.

To Adam Munro and Bevan Jenkins at Environment Waikato, thank you for providing maps, NZTM aerial photographs and GIS data. Thank you to EQC for providing funding for the project. To Pat Roberts, cheers for all your help with the ordering of air photographs and financial issues.

Thank you to all my fellow friends at uni, in particular Rei, Nita, Paul, Einor, Justin, Kim, Wybren, Sam, Tristan, Lis and Simon A, for all your encouragement and support during this ordeal! Special thanks to Alex Fletcher and James Veale for providing me with a place to stay during my field excursions, and to all my other friends outside uni, notably Pete Irvine, Shawn Baty, Kate Ryder, Marissa Blackley, Tapper, Goodie, Jony Pow, Matty J, Matt A, Hamish Lough, Catherine Tisch and Carly and Shona Sluys for providing outstanding support over the course of this research.

Most importantly, a huge thank you must go to my parents David and Frances and my brothers Simon and Lachie for providing endless love and support during my studies at university – I couldn't have done it without you.

Chapter One

Introduction

1.1 Background

In the last two decades of the twentieth century, over 30 000 people lost their lives to geohazards such as earthquakes, volcanoes, mass-movements such as debris-avalanches and debris-flows, and flash floods (Smith, 2001). Couple this with the billions of dollars worth of property damages and it is apparent that more emphasis needs to be placed on the evaluation and mitigation of such hazards.

One of the most destructive of all geohazards is the debris-flow (Takahashi, 1991). Debris-flows can loosely be described as sediment gravity flows, comprising a viscous mix of water, soil, boulders and organic material, capable of reaching speeds of up to 10 meters/sec in mountainous terrain (Stiny, 1910; Sharpe, 1938; Hutchinson, 1969; Varnes, 1978; Jakob and Hungr, 2005). They are amongst the most energetic of geomorphic processes and play a significant role in the denudation of mountainous terrain (Lorenzini and Mazza, 2004; Rowbotham et al, 2005).

In combination with normal fluvial processes, debris-flows are a prominent mechanism by which fans are constructed at the mouths of small tributary basins in steep terrain (de Scally and Owens, 2004). When human activity encroaches on such regions, debris-flows transform from being just a natural process of erosion and sediment transport, to become also a natural hazard posing significant danger to settlements, transport routes and other infrastructure located on depositional fans (Figure 1.1) (Jakob and Hungr, 2005; Davies, 1997; Whitehouse and McSaveney, 1992).

In recent times, a combination of urban sprawl and an ever-increasing desire of individuals to reside in secluded locations with a view have lead to a greater number of people living in debris-flow prone areas (Staley et al., 2006). This has exacerbated the

debris-flow hazard in these areas, leading to more instances in which the unexpected occurrence of debris flow has lead to loss of life. A good example of this is seen in Japan, where in the twenty years between 1967 and 1987, 1257 fatalities out of a total 4598 caused by natural disasters were attributed to debris-flows (Takahashi, 1991).

Figure 1.1: Debris-flows can present a significant hazard to people and property residing on the depositional fans of steep drainage basins. This photograph shows the devastating amount of sediment and debris transported to fans as a result of major debris-flows in the state of Vargas, Venezuela 1999 (Wieczorek et al., 2001).

In order to avoid the lethal consequences associated with the occurrence of debris-flow, governments and research institutions worldwide have invested much time and resources into assessing the hazard and portraying its spatial distribution (Guzzetti et al., 1999). This is well observed in Chile, Italy, Japan and Taiwan where frequent debris-flow activity has prompted a good deal of research into the evaluation and mitigation of the hazard (e.g. Aleotti and Chowdhury, 1999; Pasuto and Soldati, 2004; Takahashi, 1991; Lin et al., 2002).

In general, assessment of debris-flow hazards has included the use of two distinct approaches:

1. those at regional scale, in which Geographic Information Systems (GIS) have been used predominantly in combination with statistical analysis, simple dynamic approaches and interpretation of aerial photographs or satellite imagery to predict 'where' the phenomena occur in a particular region; and
2. those at local scale, in which numerical models and comprehensive fieldwork have been used to undertake detailed investigation of individual events and susceptible slopes (Hurlimann et al., 2006; Guzzetti, 1999).

Geographic Information Systems (GIS) provide an invaluable tool in the assessment and evaluation of hazards such as debris-flow. A GIS can be defined as a system of computer hardware, software, and procedures designed to support the capture, management, manipulation, analysis, modelling and display of spatial data for solving complex planning and management problems (Demers, 2002). Two distinct data models are utilized in a GIS to represent real world phenomena: that of the vector data model and the raster data model (Figure 1.2). The vector data model represents space as a series of discrete entities, defined as either points, lines or polygons, that are geographically referenced by Cartesian co-ordinates (rectilinear two-dimensional or three-dimensional co-ordinates) (Burrough and McDonnell, 1998). The raster data model, on the other hand, represents space as a regular grid (or matrix) of cells, in which each cell is given a specific value corresponding to some particular characteristic of that location (e.g. in the case of a land surface, a value of 1 maybe ascribed to all cells covered by barren land, 2 to that covered by a water body, 3 to vegetation and so on) (ESRI, 2006; Burrough and McDonnell, 1998). Examples of raster-based datasets include that of satellite imagery and digital elevation models (DEM), whilst vector-based datasets include that of coverages (georelational data models that store vector data containing spatial and attribute data for geographic features) and triangular irregular networks (vector equivalent of the raster DEM in which triangulation of a set of points are used to represent surface morphology) (Burrough and McDonnell, 1998; ESRI, 2006).

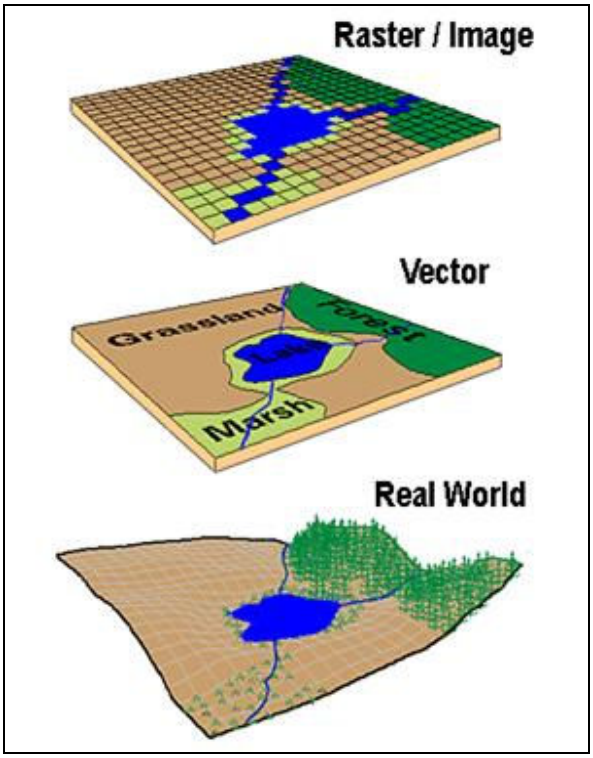

Figure 1.2: Graphical representation of the differences between the vector and raster data models used to represent real world phenomena in a GIS (Inovative GIS Solutions, 2007).

GIS technologies allow efficient analysis of large complex datasets that may contain numerous categorical and continuous variables with varying degrees of spatial resolution (Wohl and Oguchi, 2004). The statistical evaluation of correlations among variables, the continual updating of records as new information becomes available and the development and calibration of predictive models is also greatly facilitated through the use of GIS, thus underlining its value in the evaluation of debris-flow and related natural hazards (Burrough and McDonnell, 1998; Walsh et al., 1998; Wohl and Oguchi, 2004).

1.2 Research Rationale

Characterised by high flow velocity, large impact forces and long runout, debris-flows have potential discharges several times greater than clear water flood discharges from the same catchment and possess much greater erosive and destructive potential (Jakob and Hungr, 2005; De Scally and Owens, 2004; Davies, 1997; Morgan et al, 1992). In

addition, debris-flows are effectively unmanageable by fan or catchment modification (Davies, 1997). Thus, it is important that areas vulnerable to debris-flows are identified in order to aid decisions on appropriate land-uses for alluvial fans (Wilford et al., 2004).

Despite this, there is as yet little appreciation of the threat posed by such phenomena (Jakob and Hungr, 2005.) This is especially true in New Zealand, where the infrequent nature of such events has led to a tendency to neglect debris-flows as a hazard (McSaveney and Davies, 2005). This is exemplified by the fact that recent rapid development in New Zealand has led to increasing use of alluvial/stream fans for residential structures with little regard for debris-flow hazard.

There remains some uncertainty as to definitions and distinctions between debris-flow and related stream-flow water floods (Lorenzini and Mazza, 2004; Jakob and Hungr, 2005). Between-country differences in terminology and the many limitations associated with modeling such complex flows have led to some confusion amongst experts as to the distinction of concentrated sediment-water mixtures. This has significant implications for the hazard management of such phenomena as debris-flows and stream-flow water floods present very different hazards (Wilford et al., 2004; McSaveney et al., 2005) (discussed in Chapter 2).

Conventional clear water floods, debris flows and associated debris-laden water-floods (debris-floods) have proven a very dangerous and destructive force in the north-east of the North Island, New Zealand, particularly in the Coromandel/Kaimai region. For example, the Thames area over its 138 year history has been repeatedly flooded by debris-laden waters originating in the steep drainage catchments of the Coromandel Range (McSaveney and Beetham, 2006). In addition, several streams are considered to have produced major debris-flows prior to settlement in the region, the deposits of which underlie significant parts of the Thames residential area (McSaveney and Beetham, 2006).

In Te Aroha, 1985 and more recently in Matata, 2005, debris-flows have caused considerable damage to property and infrastructure as well as loss of life in the case of the former. In both localities, the debris flow hazard was not widely recognised prior to the event (Montz, 1993; McSaveney et al., 2005). In the 1985 Te Aroha event, intense precipitation in the vicinity of Te Aroha triggered debris flows which caused 3 deaths and caused several million dollars in damages to property and infrastructure (Montz, 1993). The town of Matata suffered a similar fate in June 2005, when intense rainstorms in the catchments behind the coastal township produced major debris flows (Figure 1.3). Although there were no casualties in this event, the debris flows, in conjunction with landslips and severe flooding, destroyed 27 homes, damaged 87 properties and closed the main highway and railway routes for 12 and 20 days respectively (McSaveney et al., 2005) (for further description of these events, see Chapter 2, sections 2.4.2 and 2.4.3). Such events clearly illustrate the destructive capability of debris flow hazards and emphasize the need to reliably assess risk to life and property from such events and establish the acceptability of existing or proposed land uses (Morgan et al., 1992).

A number of previous studies have used basin morphometric variables to differentiate debris-flow and non-debris-flow-prone stream fans (Jackson et al., 1987; Kostaschuck et al., 1986; de Scally et al, 2001; de Scally and Owens, 2004; Wilford et al., 2004; Rowbotham et al., 2005). Many of these studies have found significant differences between the morphometric characteristics of basins that predominantly produce fans formed by debris-flows and those which produce fans largely formed by fluvial processes. In particular, a handful of morphometric variables including basin area (Kostaschuck et al., 1986; de Scally and Owens, 2004), Melton Ratio (an index of basin ruggedness that normalizes basin relief by area; Melton, 1965) (Jackson et al., 1987; de Scally and Owens, 2004; Wilford et al., 2004) and watershed length (distance from fan apex to most distant point on watershed boundary) (Wilford et al., 2004) have been identified as reliable for identifying and differentiating debris-flow and non-debris-flow basins and their respective fans (further discussed in Chapter 3, section 3.3) . There is hence, scope to test the ability of these variables to predict fans subject to debris-flows in areas such as the Coromandel/Kaimai region where flash-flood events are frequent.

Figure 1.3: Bouldery debris-flow deposits still remained on the roadside in April 2006, following the devastating debris-flow event which destroyed many houses in Matata, June 2005.

1.3 Aims and Objectives

The primary objective of the research is to develop and test a new procedure for identifying debris-flow hazard-prone areas in the Coromandel/Kaimai region study area that can potentially be applied to any region of New Zealand. The procedure will be developed around/according to/using/in relation to the following hypothesis:

"That debris-flow, debris-flood and flood hazards can be related to specific catchment/watershed parameters and these parameters used to indicate hazard levels at the drainage points of watersheds in the Coromandel/Kaimai study area"

In order to test the hypothesis and hence validate the utility of the GIS procedure, the primary aims of the research will be to:

1. Generate useful definitions and distinctions between debris-flows, debris-floods and conventional floods as these phenomena present vastly different hazards

2. Identify suitable morphometric parameters to be derived using the procedure to be developed

3. Develop a simple, automated GIS-based procedure to drive watersheds and their morphometric parameters for selected stream locations in the study area

4. Validate and apply the procedure by:

   (a) Examining selected stream locations for geomorphic evidence indicative of debris-flow, debris-flood and flood processes

   (b) Correlating the field evidence observed at selected stream locations for each hazard with the GIS-derived morphometric measures to enumerate relations between these variables

   (c) Using the GIS procedure to derive watershed morphometric measures for streams in other areas of New Zealand known to have produced debris-flows and compare these values to those derived for the Coromandel/Kaimai region study area.

5. Imply debris-flow hazard levels at specific stream locations in the study area and produce indicative debris-flow hazard map(s) for the Coromandel/Kaimai region.

1.4 Thesis structure

This thesis is comprised of five main sections, excluding introductory and concluding chapters. Chapter 2 provides an overview of the terminology for debris-flow and associated stream-flow phenomena in order to provide useful definitions and distinctions between processes. In addition, three case studies are reviewed which clearly demonstrate the destructive potential of debris-flows and their significance in terms of hazard.

Chapter 3 sets the context for the present research, through review of past research into the recognition of debris-flows. Spatial and temporal techniques for debris-flow hazard recognition are assessed before a review of works which have used fan-basin morphometry to delineate basins subject to debris-flows and related hydro-geomorphic hazards is provided. To conclude, fan and/or basin morphometric parameters identified by previous studies to be most useful for distinguishing basin by dominant fan-formative process, are identified and discussed.

Chapter 4 introduces the Coromandel/Kaimai region study area and methodological procedure used in the research. A brief description of the location, geology, regional structure, vegetation, climate and land-use of the study area is provided. This is followed by a description of the research methodology, including an outline of the GIS procedure used to derive watersheds and their morphometric characteristics (e.g. Melton ratio and watershed length) for selected stream locations in the study area. The final section provides a description of the field investigation and statistical methods utilized to test the utility of the GIS procedure.

Chapter 5 presents the results obtained through the GIS procedure and field investigation. Trends in the values of Melton ratio (R) and watershed length (derived using the GIS procedure) for stream locations in the study area are described. This is followed by an account of the evidence observed for debris-flow, debris-flood and flood processes at selected stream locations in the study area. Relationships between the two datasets are then investigated. Finally, a description of the trends in the values of R and watershed

length for stream watershed locations outside the study area known to have experienced debris-flows is presented.

Chapter 6 provides an interpretation and discussion of the key results with respect to the literature and in order to evaluate the hypothesis for the research. Implications for debris-flow hazard in the study area are then discussed utilising results outlined in sections 5.2 and 5.3. Finally, a critical appraisal of the methods used in this research is provided. To conclude, Chapter 7 summarises and concludes the main findings of this research and suggests a direction for future research into the recognition debris-flow hazards.

Chapter Two

Definitions and distinctions between processes

2.1 Introduction

The objectives of this chapter are to overview the terminology of debris-flow and associated stream-flow phenomena in order to provide useful definitions and distinctions between processes. In addition, three case studies will be reviewed which clearly demonstrate the destructive potential of debris-flows and their significance in terms of hazard.

2.2 Approaches to distinguishing and defining processes

2.2.1 Early definitions and distinctions

First attempts at describing and classifying mass wasting phenomena were mainly concentrated on landslides (Lorenzini and Mazza, 2004). Of these attempts, Stiny (1910) was one of the first to devote an entire monologue to a specific type of landslide, describing debris-flow. In his book 'Die Muren', Stiny (1910) noted debris flow to initiate as a flood in a mountain torrent and change into a viscous mass of water, soil, gravel and organics as the sediment concentration in flow increased (Jakob and Hungr, 2005).

Soon after, Sharpe (1938) in the USA devised a classification based on two main parameters, relative velocity and sediment concentration. The classification was utilized to make the important distinction between debris-avalanche and debris-flow. The former was defined as a rapid flow of saturated, unsorted debris in a steep channel and the latter as a rapid shallow landslide from a steep slope resembling that of a snow avalanche in morphology (Jakob and Hungr, 2005, Lorenzini and Mazza, 2004).

Following Sharpe (1938), Varnes (1954, 1978), in works carried out for the US Transportation Research Board proposed a similar classification based on two main

characteristics: the type of material and the type of movement involved. This enabled identification and distinction between block stream, debris avalanche, debris-flow/mud-flow, earth-flow, solifluction and creep phenomena (Lorenzini and Mazza, 2004). The classification later became a reference point for the terminology of these processes and thus became fairly well-established in North American usage (Jakob and Hungr, 2005). In addition to Stiny (1910), Sharpe (1938) and Varnes (1954, 1978), Hutchinson (1968) in England, also recognized debris-flow and later divided it into channelised and hill-slope varieties (Hutchinson, 1988), corresponding respectively to the debris-flow and debris-avalanche of Varnes (1954).

2.2.2 Recent approaches and quantitative means of distinction

The earlier classification systems for water-sediment mixtures, as briefly described above, were mainly based on criteria obtained from direct observations and/or morphological analysis of deposits. More recent classifications have attempted to systemize established terminology by introducing quantitative criteria concerned with the flow mechanics and constituents of water-sediment flows (Lorenzini and Mazza, 2004). Furthermore, many of the recent attempts to succinctly classify debris-flow and related water-sediment mixtures have focused on the predominant mechanism by which transport of sediment is accomplished in these phenomena.

In the approach taken by Takahashi (1981), mass wasting is defined as “the fall, slide or flow of a conglomerate or dispersed mixture of sediment in which gravity moves all the particles and the interstitial fluid, so that the relative velocity between the solid and liquid phases in the main direction of motion merely plays a minor role, whereas in a fluid flow, the forces of lift and resistance caused by relative velocity are essential for the transport of each single particle” (Lorenzini and Mazza, 2004, p19). In this approach processes are distinguished on the basis of the mechanism that supports the clasts, the properties of the interstitial liquid, velocity and distance reached. Utilizing this criterion Takahashi (1981) distinguishes four specific phenomena: falls (single particles move separately with relatively small internal deformation), sturzstroms (rapid moving rock-fall avalanches or

rock-flow rubble streams (Rogers and Beckmann, 2003), pyroclastic flows (rapid and explosive volcanogenic events in which suspension is linked to expansion of gas within the flow) and debris-flows (grains are dispersed in water-clay interstitial fluid). The last three of these phenomena constitute continuous processes that require a certain force for grain suspension and thus can be collectively termed as gravitational sediment flows (Lorenzini and Mazza, 2004).

Further attempts to classify sediment-water mixtures were carried out by O'Brien and Julien (1985) and involved classifying phenomena according to the properties controlled by sediment concentrations. More specifically, this involved classifying the characteristic stresses predominant in the flow responsible for the transport of the sediment component and affected by the volumetric concentration of the sediment: yield stress, viscous stress, turbulent stress in the fluid and the dispersive stress caused by inertial impact of the coarser sediments (Lorenzini and Mazza, 2004). The classification is based on laboratory experimental results on debris samples from Colorado and yields three distinctive categories of water-sediment phenomena which lie between conventional stream flooding on one hand and landslides on the other: that of mud-floods, mud-flows and debris-flows (Lorenzini and Mazza, 2004).

Perhaps one of the more recognized classifications for sediment-water mixtures however, is that proposed by Pierson and Costa (1987) in which the various types of flow are classified using a bi-dimensional graph (Figure 2.1) that considers mean flow velocity and volumetric sediment concentration. Processes are classified according to their rheological properties (i.e. stream capacity to suspend clasts) and estimated flow velocity, characteristics that can be determined by deposit analysis (Lorenzini and Mazza, 2004).

In Figure 1, vertical divisions A, B and C are dependant on grain size and concentration and denote the approximate thresholds at which one flow type will change to another, whilst the horizontal velocity limits are identified by the stress mechanism that acts between the particles during the flow. Reading from left to right, limit A represents the development of yield stress in the flow, limit B the beginning of fluidification and limit C

the stoppage of fluidification. If the mixture is composed of a high proportion of fine and/or cohesive materials it may be necessary to shift the vertical divisions which separate the various rheological behaviors to the left, and similarly to the right for coarser, less cohesive and well sorted materials (Lorenzini and Mazza, 2004).

Lorenzini and Mazza (2004) note two main flow categories to be recognized when using this classification, those of apparently fluid mixtures and plastic-fluid mixtures, separated by vertical rheological division B on the graph. Apparently-fluid mixtures include both stream-flows, in which there is little interaction between particles, and the flow maintains the characteristics of a Newtonian fluid (i.e. deforms under any applied shear stress, has no measurable yield strength); and hyperconcentrated stream flows, in which the mixture attains measurable static yield strength as a result of particle interactions to exhibit non-Newtonian flow behavior and exceed vertical limit A (Pierson and Costa, 1987; Pierson, 2005).

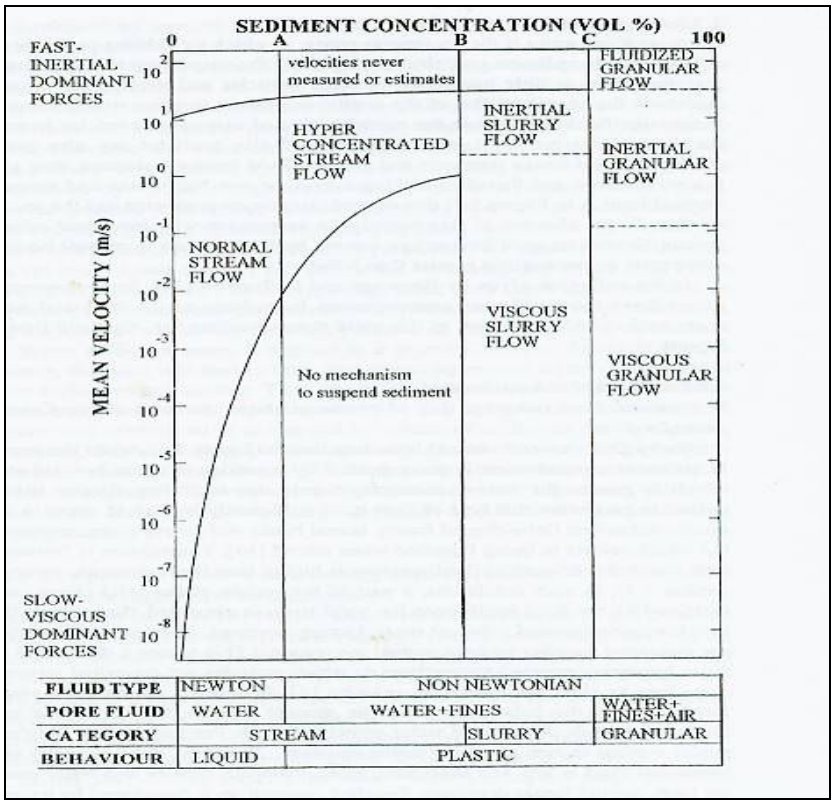

Figure 2.1: Pierson and Costa's (1987) rheological classification of water-sediment mixtures (Lorenzini and Mazza, 2004).

Plastic-fluid mixtures on the other hand, include slurry flows and granular flows. Slurry-flows are water-saturated mixtures that have sufficiently high internal friction to show plastic behavior (e.g. lobe-shaped fronts, lateral-banks and coarse-grained suspension), as part of the weight of the solid phase can be sustained by the fluid itself due to the interstitial fluid pressure being higher than the hydrostatic value. In granular flows however, the interstitial fluid pressure is no longer greater than the hydrostatic pressure and, as granule concentration by volume is very high, the entire weight of the granular mass is sustained by contacts or collisions, with vertical limit C exceeded on the graph (Lorenzini and Mazza, 2004; Pierson and Costa, 1987; Pierson, 2005).

According to Lorenzini and Mazza (2004), Pierson and Costa's (1987) classification attempts to categorize sediment-water mixtures according to rheological behavior alone (i.e. the forces which dominate each process, such as inertial, viscosity and friction, and the presence or absence of yield stress), have enabled a convenient grouping of the relevant terminology. Accordingly, Lorenzini and Mazza, (2004) utilize Pierson and Costa's (1987) graph to specifically categorize the terminology (Figure 2.2), noting viscous and inertial slurry-flows to include the wide phenomenological range of mudflows and debris-flows respectively, and granular flows to include sturzstroms, debris avalanches, earth-flows and creep. Lorenzini and Mazza, (2004) thus note the classification to constitute a reference point in this field, as it proposes a univocal classification of water-sediment mixtures, helping to overcome some of the confusion that has increased as studies have proliferated.

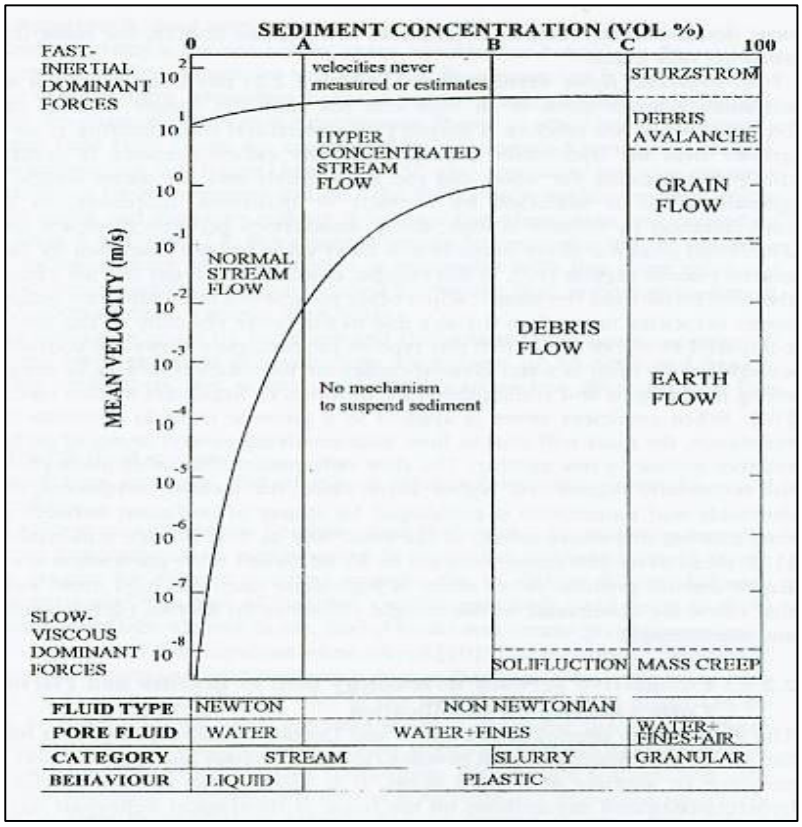

Figure 2.2: Lorenzini and Mazza's (2004) proposed sediment-water mixture classification based on the graph proposed by Pierson and Costa (1987).

2.2.3 Debris-flow and flow-like landslide terminology confusion

Despite the definitive works of authors such as Stiny (1910), Sharpe (1938), Varnes (1978), Pierson and Costa (1987), some confusion still remains as to the terminology of sediment-water mixtures. In particular, debris-flow terminology has been the subject of considerable uncertainty in the past, with a variety of names used to describe the phenomena. For instance, a number of other authors (e.g. Bull, 1964; Broscoe and Thompson, 1969) have preferred the term mud-flow to that of debris-flow. The term mudflow however, has also been used by Skempton and Hutchinson (1969) to describe slow moving clayey earth flows with no coarse material present. This usage thus created confusion as to the terminology of both processes (Lorenzini and Mazza, (2004) and consequently has since been abandoned (Hungr, 2005).

'Debris-torrent' is another term that has been used to describe the debris-flow process (Hungr, 2005). 'Debris-torrent' was first coined by Swanston (1974) to describe organic-rich landslides in the forested steep lands of western North America and is still in use in western USA and Canada, although, according to Slaymaker (1988) its use is declining as the term is considered by many to be linguistically questionable (Jakob and Hungr, 2005).

In order to reconcile the confused state of terminology for debris-flows, Cruden and Varnes (1996) proposed to restrict the term debris-flow to its literal meaning (i.e. phase of a landslide characterized by flowage of coarse debris). This proposal is questioned by Hungr (2005), who note that, under this usage, many landslide types (e.g. rock avalanches, dry granular flow) could exhibit a phase termed debris-flow. Hungr (2005) instead suggests preserving the term debris-flow as an established key word representing the entire phenomenon, including an initial slide, flow in a steep channel, and deposition on a debris fan. The revised classification system of Varnes (1978) proposed by Cruden and Varnes (1996) is also criticized by Hungr et al. (2001) who describe the two types of material distinguished in the scheme (debris and earth) as being rather arbitrary in definition. Hungr et al. (2001) consequently propose to replace these terms with new ones derived from geomorphology, and use the newly defined material components to devise formal definitions for several types of flow-like landslide (Table 2.1). Hungr (2005) notes that, as these new definitions do not stray far from North American and British terminology, they should prove useful in terms of research and practical application, because they provide some clarity as to the terminology of debris-flow and related flow-like landslides, something that has been lacking at times in the past.

Table 2.1: Classification of flow-type landslides (Hungr et al., 2001)

Material	Water content[1]	Special condition	Velocity	Name
Silt, sand, gravel, and debris (talus)	Dry, moist, or saturated	No excess pore-pressure Limited volume	Various	*Non-liquefied sand (silt, gravel, debris) flow*
Silt, sand, debris, and weak rock[2]	Saturated at rupture surface	Liquefiable material[3] Constant water content	Extremely rapid	*Sand (silt, debris, rock) flow slide*
Sensitive clay	At or above liquid limit	Liquefaction *in situ*[3] Constant water content[4]	Extremely rapid	*Clay flow slide*
Peat	Saturated	Excess pore-pressure	Slow to very rapid	*Peat flow*
Clay or earth	Near plastic limit	Slow movements Plug flow (sliding)	Less than rapid	*Earth flow*
Debris	Saturated	Established channel[5] Increased water content[4]	Extremely rapid	*Debris flow*
Mud	At or above liquid limit	Fine-grained debris flow	Greater than, very rapid	*Mud flow*
Debris	Free water present	Flood[6]	Extremely rapid	*Debris flood*
Debris	Partly or fully saturated	No established channel[5] Relatively shallow, steep source	Extremely rapid	*Debris avalanche*
Fragmented rock	Various, mainly dry	Intact rock at source Large volume[7]	Extremely rapid	*Rock avalanche*

[1] Water content of material in the vicinity of the rupture surface at the time of failure.
[2] Highly porous, weak rock (examples: weak chalk, weathered tuff, pumice).
[3] The presence of full or partial *in situ* liquefaction of the source material of the flow slide may be observed or implied.
[4] Relative to *in situ* source material.
[5] Presence or absence of a defined channel over a large part of the path, and an established deposition landform (fan). *Debris flow* is a recurrent phenomenon within its path, while *debris avalanche* is not.
[6] Peak discharge of the same order as that of a major flood or an accidental flood. Significant tractive forces of free flowing water. Presence of floating debris.
[7] Volume greater than 10,000 m^3 approximately. Mass flow, contrasting with fragmental rock fall.

2.2.4 Deficiencies in the rheological approach to defining debris-flows

Much of the confusion regarding debris-flow terminology is linked to shortcomings in the characterization of the material that composes such flows and hence the flow behavior itself (Lorenzini and Mazza, (2004). Lorenzini and Mazza, (2004) note that a suitable constitutive law, (equation describing the relationship between shear stress and strain in a moving fluid) must be defined before any forecasts can be made on a specific flow field. Summarizing this relationship however, is an extremely complex matter when applied in the context of debris-flows as such phenomena have a wide variety of constituents and are Non-Newtonian in nature.

Lorenzini and Mazza (2004) note two ways in which the subject can be handled:
(A) Considering the entire mass (fluid and solid) as a single material with particular properties, or
(B) Considering the coarser material and the water (sometimes together with the fine fraction) separately.
Utilizing these approaches, a number of rheological models have been proposed (e.g. Bingham's plastic model, Herschel-Bulkley's viscoplastic model) yet there still remains a lack of consensus as to which constitutive equation best approximates the behavior of debris-flow (Lorenzini and Mazza (2004). Furthermore, variation in the characteristics of the same phenomena in different geographical areas has lead to the development of studies on the topic in specific directions. Studies in Japan, for example, often use the dilatant model to describe events characterized by a greater quantity of coarser material, whilst those in China predominantly employ the visco-plastic model to describe events dominated by large quantities of the fine fraction (Lorenzini and Mazza, 2004).

Difficulty also exists in relation to the experimental testing of debris-flow samples. One such problem is caused by the fact debris-flows often have high coarse material contents for which bulky and expensive lab equipment is required. In addition, this coarse content can have a significant influence on the flow behavior, thus alternative attempts to test debris-flow samples using the fine fraction alone are likely to prove insufficient (Lorenzini and Mazza, 2004).

2.3 Terminology of processes

Having considered some of the main approaches to classifying sediment water mixtures in section 2.1, it is now appropriate to take a closer look at the terminology of specific stream flow processes with an aim to further clarify their definitive characteristics.

2.3.1 Debris-flow and Mudflows

Debris-flows and Mud-flows are complex, highly concentrated gravitational flows of sediment and water. In particular, debris-flows are characterized by sediment concentrations often in excess of 60 % by volume (80 % by weight) (Pierson and Costa, 1987; Wan and Wang, 1994). According to Hungr (2005, p14) debris-flow is defined as 'a very rapid to extremely rapid flow of saturated non-plastic debris in a steep channel'. Such flows are considered to carry more than 50 % particles larger than sand size (Varnes, 1978) with the sediment component playing an integral role in the mechanics and behavior of the flow (Coussot and Piau, 1994; Coussot, 1995; Iverson, 1997; Pierson, 2005).

Similarly, mudflow is defined by Hungr (2005) as 'a very rapid flow of saturated plastic debris in a steep channel, involving significantly greater water content relative to the source material'. According to Pierson (2005), mudflows are effectively the fine-grained equivalent of debris-flow. They are chiefly composed of silt, some clay and fine sand and flow behavior is largely determined by a combination concentration-dependant and shear-rate-dependant, electrochemical and frictional interactions between particles (Coussot and Piau, 1994; Hungr et al., 2001; Pierson, 2005). Accordingly, some authors (Pierson, 2005) refer to debris-flow and mud-flow as pseudo-one-phase phenomena, as the solid and fluid components do not appear to remain separate or clearly distinct from each other in the flow.

The flow mechanics of debris-flow involve complex combinations of physical particle interactions between clasts (friction and momentum transfer between coarse particles) and between the clasts and the fluid (Pierson, 2005; Iverson, 2005). This causes the flow to exhibit non-Newtonian, plastic-fluid characteristics characterized by the development

of lobe-shaped fronts and lateral banks (Pierson and Costa, 1987; Lorenzini and Mazza, 2004). Additionally, as the concentration of sediment in the flow increases, so does yield stress, which, in combination with buoyancy provided by the fluid and grain to grain frictional contact, enables the flow to transport large amounts of coarse sediment (gravel and larger) in full dynamic suspension (Coussot and Piau, 1994; Wan and Wang, 1994; Pierson, 2005). As a consequence, huge boulders (up to 4 meters diameter in some cases) can be carried in the flow at high velocity, presenting a serious hazard to people and their property in debris-flow prone areas (Davies, 1997; Whitehouse and McSaveney, 1992).

The strong interaction between the water and sediment in debris-flows ensures the fast-moving sediment carries the water along with it, much faster than in a conventional stream-flow water flood (McSaveney et al., 2005). Moreover, for the same amount of rain, a debris-flow has much higher discharge, moves faster and contains more large rocks and debris. Peak discharge in debris-flow can be as much as 40 - 50 times that of a conventional flood due to erosion and incorporation of sediment from the streams bed and banks as the flow surges down the channel (McSaveney et al., 2005, Wilford et al., 2004). In addition, debris-flows commonly move as distinct surges, in which an event may consist of one to many tens of surges. These surges are characterized by ‘boulder fronts’ (Figure 2.3) comprising considerable sized clasts and large debris (trees) that can reach heights of more than 2 meters above the channel floor (McSaveney et al., 2005). A finer, liquefied mass of debris makes up the main body of the surge and a dilute, turbulent flow of sediment-charged water comprises the tail.

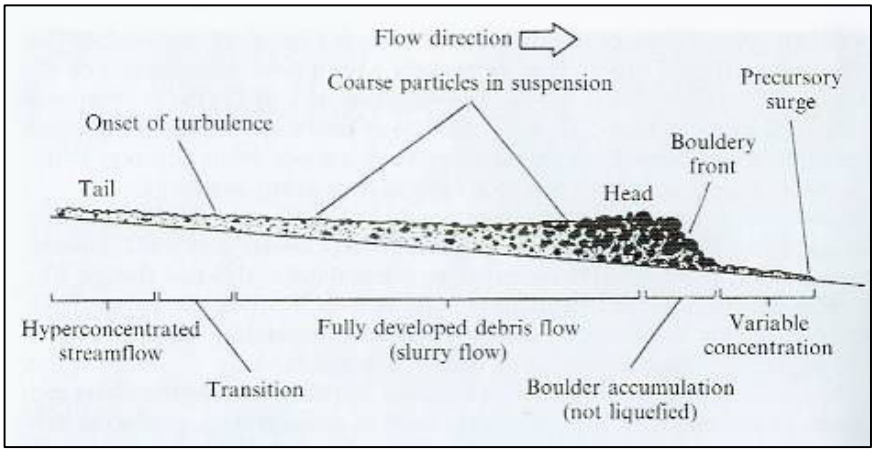

Figure 2.3: Diagram showing the characteristics of a debris-flow surge (Hungr, 2005)

Debris-flows are generally restricted to small steep streams where channel gradients are sufficient to maintain motion and an abundant supply of sediment is available for transport. Debris-flows often initiate as a slope failure in the headwall of a stream channel, following high rainfall and/or earthquake events (Hungr, 2005). The breach of a landslide dam, or in some instances, spontaneous initiation in the steep bed of the channel as the channel becomes unstable during extreme discharge, are two further ways in which debris-flow can ensue. In the case of slope failure, the gradient of the affected slope generally ranges between 20 and 45° where sufficient potential energy exists to start failure of granular soil and where soil cover is thick and continuous enough to be vulnerable to sliding (Hungr, 2005).

Deposition of debris-flow usually occurs on an established ‘debris-flow fan’, following slope reduction and loss of confinement (Hungr, 2005; Ikeya, 1981). Debris-flow fans characteristically have marginal levees or terminal lobes (Wilford et al., 2004) and are thus steeper and ‘more hummocky’ in morphology than normal stream flow fans (Davies, T.R. pers.comm, 21/02/2007). Deposits usually exhibit a wide range of grain sizes, from small amounts of fines (clay, silt) to large boulders, mixed with varying amounts of debris (tree logs). Moreover, due to dense grain packing, debris-flows cannot selectively deposit transported solid particles by size when the flow slows or stops, resulting in

massive (non-stratified) and poorly sorted sediment textures (Pierson, 2005). In addition, deposits are often matrix supported, with the long-axis of clasts (A-axis) frequently either oriented parallel to the direction of flow or randomly oriented and angular to sub-angular in geometry (Coe et al., 2003; De Scally and Owens, 2001; Wilford et al., 2004). Deposits can also sometimes show reverse grading, although grading can range from absent to normal (Wilford et al., 2004). Despite their characteristic signatures, debris-flow fans are often heavily reworked by subsequent water flow (Hungr, 2005). Consequently, only limited evidence of their passage often remains, providing substantial challenges for those wishing to identify such areas for hazard mitigation purposes (Davies, 1997).

Debris-flows present a significant hazard to settlements, transport routes and other infrastructure located on fans (Jakob and Hungr, 2005; Davies, 1997; Whitehouse and McSaveney, 1992). During acceleration, debris-flows can be extremely erosive and generate impact forces comparable to rock and snow avalanches (Watanabe and Ikeya, 1981). The viscous nature of the flow and its ability to transport large boulders and debris in suspension contribute to the destructive potential of such phenomena. Thus, debris-flows are capable of destroying houses, roads and bridges, sweeping away trees and motor vehicles and inflicting loss of life. Large areas can also be inundated by as much as several hundred cubic meters of mud, rock and other debris, blocking roads and damming streams. Massive deposition of material at the debris-flow-fan head can also cause the direction of flow on the fan to be quite unpredictable, resulting in the diversion of successive pulses by the deposits of earlier pulses and possibly culminating in the overwhelming of conventional flood protection measures (Wilson and Wieczorek, 1995; McSaveney et al., 2005). By comparison, mud-flows are less hazardous than debris-flow in that their fine-grained nature means they carry less of the large boulders responsible for impact damage in debris-flows. It is thus important that distinction be made between the two in hazard evaluation studies to ensure correct mitigation measures are implemented where necessary.

2.3.2 Hyperconcentrated floods

In steep granular stream channels, most practitioners and researchers recognize a continuum between stream-flow water floods and debris-flow, as normal bedload transport processes such as rolling and saltation are replaced by massive bed instability with increasing slope angle (Hungr, 2005). Beverage and Culbertson (1964) coined the term hyperconcentrated flood to describe flows intermediate between these two end members, using the term to distinguish these sediment-rich flows from normal stream-flow because of their tendency to clog irrigation channels and aggrade natural stream beds (McSaveney et al., 2005; Hungr, 2005; Pierson, 2005).

Beverage and Culbertson (1964) defined hyperconcentrated flood to have suspended sediment concentrations of at least 20% by volume (40% by weight) and not more than 60% by volume (80 by weight). This approach to defining hyperconcentrated flood is criticized by Pierson (2005) who notes that the range in limiting thresholds for experimental and natural hyperconcentrated flows involving mostly fine sediments (Figure 2.4) can be entirely below both the upper and lower limits proposed by Beverage and & Culbertson (1964). Pierson (2005) thus argues that suspended sediment concentration should not be used alone to define sediment water mixtures, as grain size distribution and grain density to also play extremely important roles in determining the properties of sediment water suspensions.

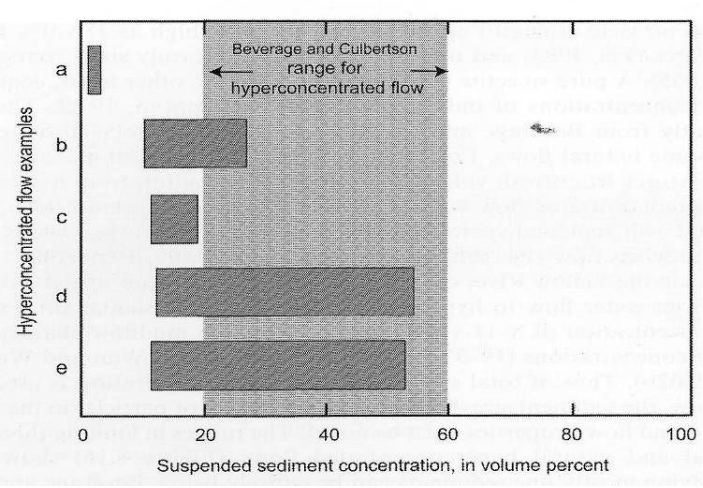

Figure 2.4: Approximate ranges in limiting thresholds for experimental (a & b) and natural hyperconcentrated flows (c, d & e) in comparison to Beverage and Culbertson's (1964) proposed limits (see Pierson, 2005 for further explanation).

According to Pierson (2005, p193) hyperconcentrated flood is defined as 'a two-phase flow of water and sediment, intermediate in concentration between conventional stream flow and debris-flow/mudflow and in which viscosity, turbulence and collision-maintained suspension of fines in water (the carrier fluid) enables the intermittent, dynamic suspension of large quantities of coarser sediment' (i.e. sand, gravel). Pierson (2005) notes hyperconcentrated flow to be distinctive in terms of processes acting to transport the sediment. In this regard, the mixture develops the ability to carry large amounts of sand and some gravel in prolonged suspension due to increased viscosity, grain collisions, buoyancy and turbulence, associated with increasing fines concentrations. Additionally, as the flow velocity decreases, the coarse suspended load settles out of suspension and is selectively deposited according to grain size; this contrasts that of debris-flow in which selective settling is hindered by dense grain packing and all particles settle at the same rate (Pierson, 2005).

Laboratory and field evidence indicate that a minimum volumetric concentration of 3-10% fines must be achieved before the mixture can suspend coarse particles. This sudden change from a Newtonian to a Non-Newtonian fluid is utilized by a number of authors to

identify the transition from stream flow to hyperconcentrated flow (Qian et al., 1981; Pierson and Costa, 1987; Rickenmann, 1991; Xu, 2002b, 2003). The upper threshold of hyperconcentrated flow (i.e. transformation to debris-flow/mudflow) can also be defined in terms of yield strength, notably the point at which buoyancy, in conjunction with mixture dynamics or yield strength, is sufficient to suspend gravel-size particles, whether or not the flow is moving (Pierson and Costa, 1987).

In addition to rheological criteria, Pierson (2005) notes that suspended sand concentration can be used to identify the lower boundary for hyperconcentrated flow. Hyperconcentrated flows are characterized by the transport of large amounts of sand with concentrations often exceeding that of the fines concentration. Thus, the point at which the proportion of sand in suspension abruptly increases relative to the suspended fines can be used to define the lower boundary of hyperconcentrated flow.

Figure 2.5: Hyperconcentrated flow observed at Matata, North Island, New Zealand, following the debris-flow event of June 2005 (McSaveney et al., 2005)

Hyperconcentrated flows (Figure 2.5) commonly occur in semi-arid to arid regions characterized by ample supplies of easily erodible, relatively fine-grained sediment (Pierson, 2005). This is well observed in the Loess Plateau of central China, where the sub-humid to semi-arid climate, in combination with steep terrain underlain by an abundant supply of erodible silts and fine sands, has lead to a particularly high incidence

of hyperconcentrated flows (Cheng et al., 1999; Xu, 1999). In addition, hyperconcentrated flows frequently occur in volcanic landscapes recently impacted by explosive eruptions, commonly acting as the main mechanism for sediment transport in Lahars (volcanic debris-flows and/or hyperconcentrated flows). In both landscapes, such flows can readily occur at high and low discharges, often initiating after water floods acquire added suspended sediment through erosion and entrainment or when debris-flows lose coarse sediment through dilution (Pierson, 2005).

A variety of depositional features can be attributed to hyperconcentrated flows. Where flow velocities significantly decrease and/or the flow halts, deposition usually occurs by suspension fallout (where grains settle out of suspension) forming normally graded relatively massive and well sorted deposits that seldom exhibit stratification (Pierson, 2005). Deposition also occurs by traction carpet accretion (grains deposited as sheets or layers accreted from the base of the flow) when flow velocities and bed shear stresses are high. In this instance, deposits are often typified by pronounced horizontal stratification but without high-angle cross-bedding, the coarse bedload enveloped by finer accretionary strata or left stranded on surfaces of berms or terraces (Pierson, 2005). In addition to these deposits, massive moderately compacted and very poorly sorted diamicts of sand and gravel are sometimes observed in channels following the passage of hyperconcentrated flow, possibly representing a submerged debris-flow phase that flows beneath more dilute surface flow (Cronin et al., 2000; Pierson, 2005). Hyperconcentrated flow deposits are also distinctive in that they are relatively similar over hundreds of meters along a channel, in contrast to normal water flood deposits where abrupt changes in mean grain-size and stratification are frequently observed over short distances (Cronin et al., 2000).

In comparison to debris-flow, hyperconcentrated flows are generally less hazardous to riverside communities. Flow velocities are usually lower, and they seldom carry the large boulders that are responsible for impact damage in debris-flows (Pierson, 2005). They are however, considered more dangerous than conventional water floods of similar magnitude as they possess much greater potential for doing geomorphic work (Pierson,

2005). Hyperconcentrated flows can be extremely erosive in steep terrain, possessing the ability to rapidly incise their channels by up to tens of meters (probably, like debris-flows, by nick-point recession; Davies et al., 1992). Such erosion can cause significant damage to bridges, roads and other infrastructure in the vicinity of affected channels (Pierson, 2005; Rodolfo et al., 1996).

In addition to their powerful erosive capabilities, hyperconcentrated flows can also be dangerous in terms of their depositional characteristics. Where river beds widen or channel gradients decrease, rapid deposition and river bed aggradation can cause incremental filling of channels and channel shifting, reduction in flood conveyance capacity, and burial of low lying areas and structures in sediment (Rodolfo, 1996; Scott et al., 1996). A prime example of such aggradation was well observed in the rivers draining Mt Pinatubo (Philippines) following the 1991 eruption of the volcano, where close to 25m of channel aggradation as a result of numerous lahars (some debris-flows but mostly hyperconcentrated flows) lead to the widespread burial of housing, roads and farms and the displacement of thousands of families in the months and years following the event (Major et al., 1996; Scott et al., 1996; Rodolfo et al., 1996).

2.3.3 Debris-flood and Mud-floods

The terms debris-flood and mud-flood are used in the literature to describe extreme magnitude sediment-rich flood events in which prodigious quantities of sediment and debris are transported downstream in steep catchments (Pierson, 2005). Bates and Jackson (1987) describe debris flood in a general sense as a flood intermediate between that of a turbid mountain stream and a true mudflow. A more concise description of debris-flood however, is proposed by Hungr (2005, pg.15) who defines the phenomenon as ‘a very rapid surging flow of water, heavily charged with debris in a steep channel’. Mud-flood is regarded as the approximately synonymous term to this, the distinction between the two phenomena based on the predominant grainsize of the transported sediment, mud-floods being characterized by the finer fraction and debris floods by coarser material (Gagoshidze, 1969; Commission On Methodologies For Predicting Mud-

flow Areas, 1982; Lorenzini and Mazza, 2004; Pierson, 2005). Such events are believed to have peak discharges 2 – 3 times that of normal floods and have sediment concentrations between 20 - 47% by volume (Wilford et al., 2004; GNS, 2005). In consideration of the definitions above, floods that could qualify as debris-flood or mud-floods might include landslide-dam or thunderstorm-generated flash floods in steep narrow canyons. The 1996 Barranco de Aras flood in Spain (Alcoverro et al., 1999; Batalla et al., 1999) and the 1982 Lawn lake dam-failure flood in Colorado (Jarrett and Costa, 1986) are two published examples of such events (Pierson, 2005). Debris-floods can also ensue when debris-flows enter large, wide channels at flood stage. Upon entering such large volumes of water, debris-flows will often lose their viscous properties and deposit or disintegrate to form a debris-flood downstream (Benda, 1985; Lorenzini and Mazza, 2004).

Scoot and Gravlee (1968) also note that debris-floods or mud-floods can in some cases achieve debris-flow characteristics towards the front of the flood wave or may include a submerged debris-flow phase along the channel bed. In contrast, Aulitzky (1980) notes debris-flood to presumably maintain the characteristics of a Newtonian fluid and to not exhibit surging or pulsating behavior. This point is backed up by Pierson (2005) who argues debris-floods to be primarily normal water-floods or hyperconcentrated floods that are able to move large quantities of coarse sediment because of high discharges and/or steep channel slopes. In this instance, Pierson (2005) refers to works by Mizuyama (1981) and Komar (1988) which reveal that dramatic increases in coarse sediment transport can be expected in normal floods where high velocities are maintained and abundant coarse sediment is available. Pierson (2005) thus argues that with the exception of minor debris-flow phases, there is as yet neither data nor compelling arguments to suggest that (1) basic bedload transport mechanics are not sufficient to account for the large scale bedload movement in debris-floods/mud-floods, or that (2) debris-floods/mud-floods should be classified as a separate process.

Debris-flood and mud-flood deposits include bars, fans, sheets and splays, and significant amounts of sediment are often deposited beyond the channel on the fan. Poorly stratified,

loose mixtures of coarse gravel and sand are typical of such deposits, the coarser fraction of the deposits (cobbles and boulders) exhibiting weak imbrication and an openwork texture throughout. Furthermore, clast orientations can often be mixed, the long axis (A-axis) of large cobble to boulder clasts perpendicular to flow and pebbles and small cobbles parallel to flow (Wilford et al., 2004).

Debris-floods and mud-floods are far less hazardous than debris-flows. Debris-flows can have peak discharges up to 20 times greater than debris-floods and carry much larger boulders in greater quantities (Wilford et al., 2004). Debris-floods in comparison are characterized by relatively low flow depths, limiting their destructive potential. Despite this, the phenomena are still more than capable of inflicting major damage to housing and infrastructure through the inundation of houses with mud and silt and through impact damage from floating debris (large trees) (Hungr, 2005).They thus, in addition to debris-flows and hyperconcentrated floods, pose a significant hazard to people and property in the vicinity of affected stream courses and should be duly considered in hazard studies.

2.3.4 Stream-flow water floods

Conventional water floods are normally characterized by the transport of much more water than sediment, with the fine fraction carried in suspension and the coarser sediment dragged along the channel floor as bedload (Pierson, 2005; McSaveney et al., 2005). Concentrations of suspended sediment are generally less than 4% by volume (vol %) or 10% by weight (wt %), the entrained sediment grains having little meaningful interaction with each other and therefore little effect on the behavior of the flow (Pierson, 2005; Waananen et al., 1970). According to Pierson (2005) sufficiently low suspended sediment concentrations ensure the flow behaves as a Newtonian fluid with any particles larger than sand in grainsize principally transported as bedload. In addition, the vertical concentration profile in the flow is predominantly non-uniform and the sand concentration is generally less than the fines concentration. In large water floods in steep channels however, some sand or even fine gravel can be forced into intermittent

suspension as a consequence of strong turbulence and high bed shear stress associated with steep water surface slopes and valley constrictions (Pierson, 2005; Komar, 1988).

Conventional stream-flow water flood deposits are similar to debris-floods in that they include bars, fans, sheets and splays. Sediment concentrations in water floods however, are much less (less than 20 % by volume), meaning the channel can usually contain the sediment load, resulting in few deposits beyond the channel on the fan. Furthermore, deposits are typically well sorted, clasts are well imbricated and the A-axis of clasts is predominantly oriented perpendicular to flow (Wilford et al., 2004; Boggs, 1995).Water flood deposits can also exhibit layering and pronounced stratification in which a host of sedimentary features (e.g.. cross-bedding, flame structures) can be found; in stark contrast to debris-flows for example, which are characterized by massive, matrix-supported, chaotic mixtures of poorly sorted sediment and debris (Boggs, 1995; Wilford et al, 2004; Lorezini and Mazza, 2004).

In terms of hazard, clear water floods are much less destructive than debris-flows, hyperconcentrated flows and debris-floods. As they are typified by much lower sediment-concentrations, they lack the ability to transport the large boulders responsible for impact damage in debris-flows, and are much less erosive than hyperconcentrated flows (Hungr, 2005). Large debris in the form of tree branches can however, be carried by such flows at high peak discharges, which, in combination with inundation can present a significant hazard to people and their property.

2.4 Case studies

Some of the world's most devastating landslide disasters, in terms of fatalities and economic loss, have been attributed to debris-flows (Jakob and Hungr, 2005). Described below are three events which clearly illustrate the destructive capability of debris-flows and thus the hazard such phenomena pose to people and their property.

2.4.1 World event: Debris-flows in Venezuela 1999

One of the most spectacular debris-flow events in recent Latin American history occurred in December 1999 on the north central Venezuelan coast of South America (Figure 2.6). High intensity rainfall induced numerous debris-flows in 24 streams across a 50 km coastal strip in the northern state of Vargas, Venezuela, resulting in the devastation and destruction of many coastal settlements (Figure 2.7) and the loss of thousands of lives (Wieczorek et al, 2001; Garcia-Martinez and Lopez, 2005).

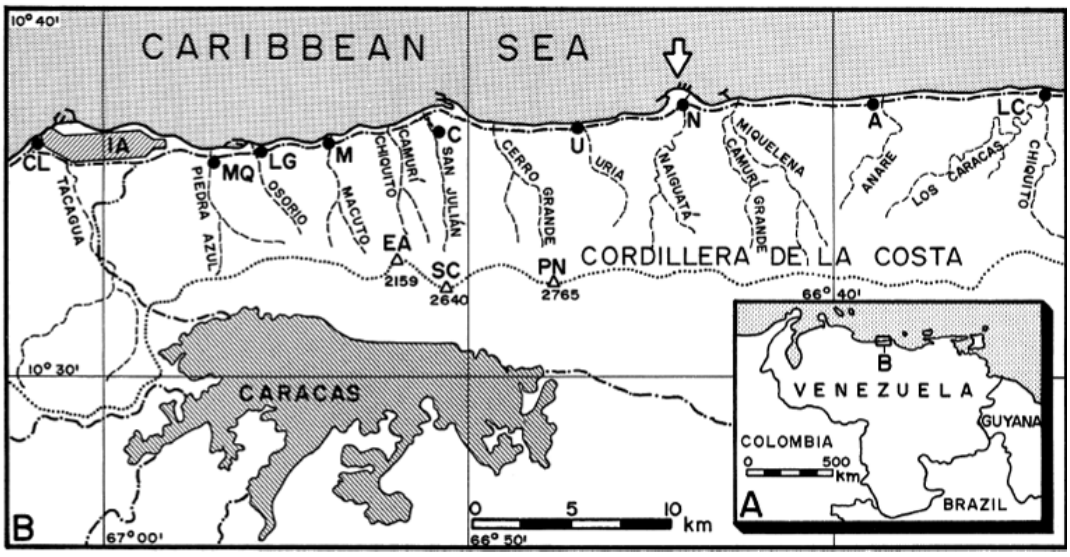

Figure 2.6: Location of Venezuela, South America, and areas worst affected in the state of Vargas during the 1999 storm event (Wieczorek et al., 2001)

Figure 2.7: Devastation in the settlement of Los Corales, Vargas, due to occurrence of numerous debris-flows and debris-floods in the 1999 storm (Wieczorek et al., 2001).

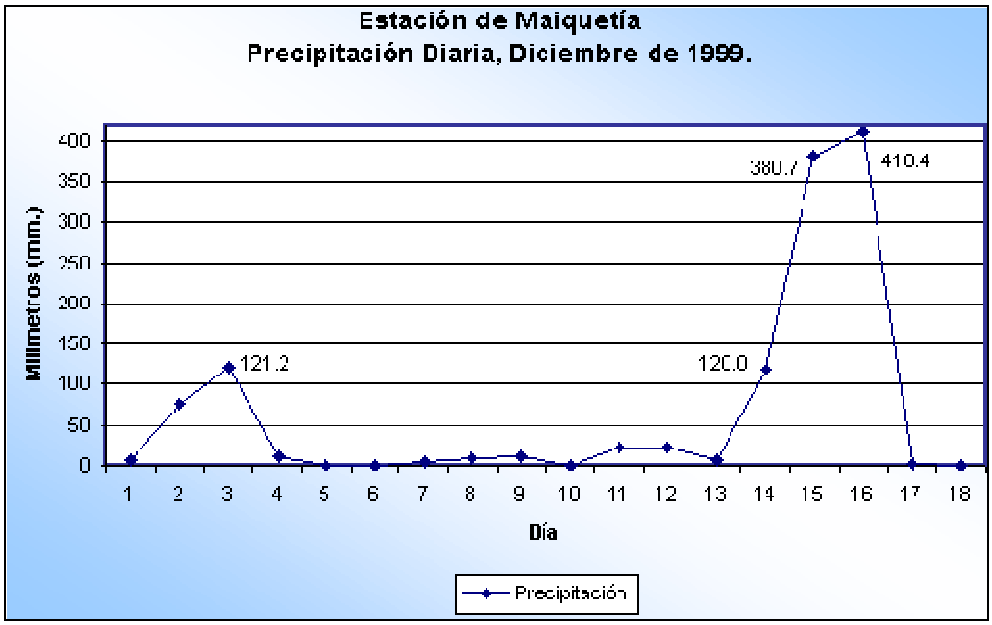

Figure 2.8: Rainfall measurements at Maiquetia Weather Station during the month of December 1999. (Y-axis show measurement in mm; X-axis shows day of the month) (Wieczorek et al., 2001)

Much of the devastation and destruction occurred on December 14 – 16th as a result of an intense rainstorm developed through the interaction of a cold front with moist southwesterly flow from the Pacific Ocean toward the Caribbean Sea (Wieczorek et al., 2001). Rainfall measurements (Figure 2.8) at Maiquetia weather station (43 m above sea level) revealed a colossal 911 mm of precipitation in 72 hours, and 72 mm in one hour during the storm, well above the annual mean of 523 mm (Garcia-Martinez and Lopez, 2005).

As well as the extreme amounts of precipitation during the storm of December 14-16, persistent rain of low intensity from December 1-13 also played a major role in the event. Measurements at Maiquetia revealed precipitation of 293 mm during December 1-13, more than half the annual average (Garcia-Martinez and Lopez, 2005). This persistent rainfall saturated the underlying metamorphic and sedimentary rocks in the steep catchments of Avila Mountain, substantially reducing the stability of slopes in the region. These slopes subsequently failed catastrophically during the storm to form debris-flows and debris-floods of giant proportions.

The debris-flows and debris-floods transported huge amounts of mud, rock and debris downstream from the steep slopes of Avila Mountain National Park, carrying boulders in excess of 6 m in size and debris in the form of tree trunks, some exceeding over 30 m in length (Figure 2.9). The debris-flows and debris-floods proceeded to wreck total destruction in the settlements located on the alluvial fans of the streams, destroying buildings, roads and bridges and severely disrupting electricity, water and sewerage systems. In total an estimated 23 000 houses were destroyed with a further 65 000 severely damaged (Garcia-Martinez and Lopez, 2005). Economic losses totaled nearly $US 2 billion and over 15 000 people were killed. In addition, over 20 million cubic meters of sediment and debris was estimated to have been deposited on the alluvial fans along 50 km of the coastal strip from La Guaira to Naiguita. This material modified the coastline to create new lands with aerial extents estimated at 150 ha, totaling some of the largest volumes of deposited material on record for rainfall-induced debris-flows (Wieczorek et al., 2001; Garcia-Martinez and Lopez, 2005).

Figure 2.9: Giant boulders up to 6m in size and large amounts of tree debris brought down from the slopes of Avila Mountain during the 1999 storm (Garcia-Martinez and Lopez, 2005).

2.4.2 New Zealand events – Te Aroha 1985

One of the better known debris-flow events to take place in New Zealand occurred on February 17, 1985 in the small township of Te Aroha (Figure 2.10). Following a long, hot and dry summer, the town of Te Aroha, situated on a shingle fan between Mt Te Aroha (937 m), the highest point on the Kaimai Range, and the low lying flood-prone Waihau River, experienced damaging debris-flows which cascaded through the town, destroying housing and infrastructure and causing loss of life (Jones, 1985; Hutchins, 2006).

A major storm involving a period of extremely heavy rainfall in the ranges above Te Aroha during the morning of February 17, 1985, is thought to have been the main cause of the disaster. In addition, steady precipitation 24 hours beforehand is also thought to have facilitated proceedings, seeping through the dry, cracked surface soil on the steep slopes of Mt Te Aroha, saturating the ground at depth and lubricating planes of weakness (Jones, 1985; Hutchins, 2006).

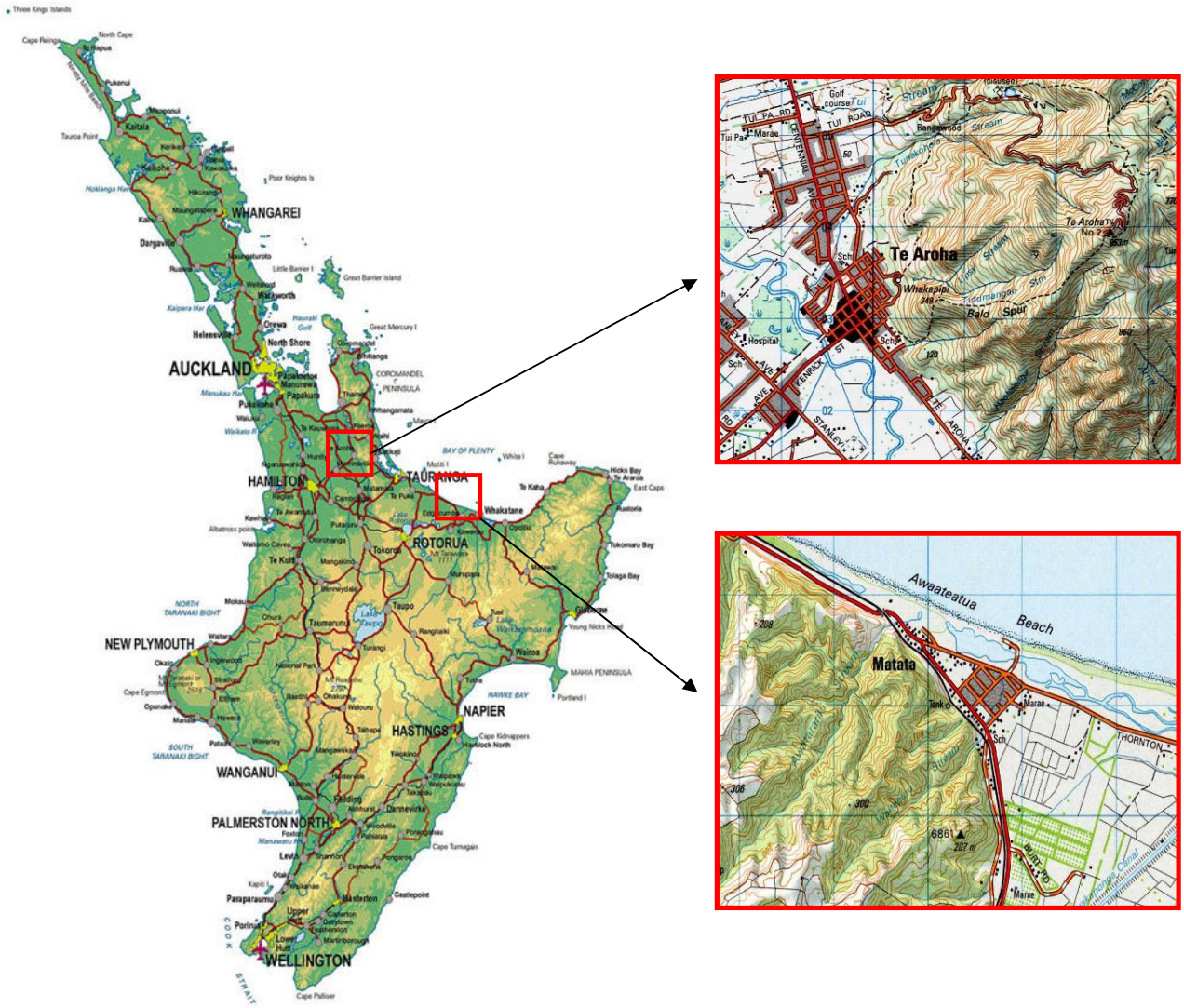

Figure 2.10: Locations of Te Aroha (top insert) and Matata (lower insert), North Island, New Zealand

The storm ensued when a cold front embedded in a trough unexpectedly deepened into a depression while passing over the region in the early hours of February 17. Warnings were unable to be provided as the Auckland Weather Service had closed down for the

weekend (Jones et al., 1985). As the cold front passed over Mt Te Aroha, orographic rainfall intensified and thunderstorms developed. Over 600 mm of precipitation fell between 6 pm February 16 and 6 am February 17, causing substantial slope failure in the already saturated soils of steep catchments above Te Aroha. Strong winds accompanied the rain, facilitating the uprooting of unstable trees on the slopes. These slope failures then liquefied into debris-flows upon entering Tutumangao stream and proceeded to surge downstream as chaotic mixtures of mud, rock and tree debris into the township below (Jones et al., 1985).

Houses in the path of the debris-flows were either completely destroyed or suffered extensive impact damage from the boulders and large tree debris in the flow (Figure 2.11) (Jones, 1985; Hutchins, 2006; Piako Post, 1985). Three people were killed and a fourth left critically injured when a house was swept off its foundation and subsequently demolished by the flows. Flows and torrents of water smashed through the rears of many buildings, damaging more than 20 businesses and piling motor vehicles on top of each other along the main street (Piako Post, 1985; Hutchins, 2006; Jones et al., 1985). In addition, the torrents of mud, rock and debris broke sewerage lines, inundated residences with considerable amounts of debris-laden water and damaged the town's water supply reservoir, cutting off water supplies for 12 days (Jones, 1985).

Figure 2.11: Devastation and destruction as a result of debris-flows in the small town of Te Aroha1985 (www.teara.govt.nz, 2000)

Figure 2.12: Giant boulder transported downstream in the Matata debris-flows of June 2005 (McSaveney et al., 2005)

2.4.3 New Zealand events – Matata 2005

Another debris-flow event of note occurred recently on 18 May, 2005, in the coastal settlement of Matata, North Island, New Zealand (Figure 2.10). As in the Te Aroha and Venezuela events described previously, the debris-flows of Matata were largely induced by substantial rainfall in the catchments above the township (McSaveney et al., 2005).

Following a day of moderately heavy rain (153 mm in 17.75 hours at Awakaponga) on 18 May, 2005, a band of intense rain (130 mm in 1.75 hours) passed over the catchments behind Matata, triggering widespread slope failures and inducing flooding and debris-flow activity in the many streams draining the catchments (McSaveney et al., 2005). These flows carried boulders up to 7 m in length (Figure 2.12) and large amounts of tree debris downstream into parts of Matata, destroying 27 homes and causing substantial damage to 87 properties. In addition, the railway and State Highway 2 incurred extensive damage leading to closure for more than 20 days and 12 days respectively. Despite the destruction, there were no serious injuries or fatalities in the event, an extremely fortuitous outcome considering the damage incurred (McSaveney et al., 2005).

2.5 Summary

Despite the definitive works of early practitioners and researchers such as Stiny (1910) and Varnes (1958) with regard to the classification and terminology of debris-flow and related processes, there still remains some uncertainty as to definitions and distinctions between phenomena. Between-country differences in terminology and the many limitations associated with modeling such complex flows have facilitated confusion amongst experts as to the distinction of concentrated sediment-water mixtures. This has significant implications for the hazard management of such phenomena as debris-flows and stream-flow water floods present very different hazards.

Debris-flow can best be defined as a rapid, highly concentrated, homogenous flow of saturated non-plastic debris and sediment in a steep channel, possessing the ability to transport huge boulders in permanent suspension due to physical interactions between

clasts and clasts and the fluid during flow. The term Mud-flow is roughly synonymous with this and is usually used to describe debris-flows of fine-grained nature. Stream-flow water floods in contrast, are characterized by substantially more water than sediment in the mixture, resulting in the sediment having no real influence on the flow behavior and hence exhibiting Newtonian fluid characteristics.

Hyperconcentrated flow is a distinct flow process, fine-grained in nature in which viscous and yield strength maintained suspension of fines in water (the carrier fluid) enables the intermittent suspension of large quantities of coarser sediment (sand and some gravel). The term debris-flood is used to describe extreme magnitude sediment-rich flood events in which prodigious quantities of sediment and debris are transported downstream in steep catchments and in which the flow maintains the characteristics of a Newtonian fluid. Mud-flood is the synonymous term to this, describing floods dominated by the finer (clays, silts) fraction. Debris-floods and mud-floods are thus argued to be analogous with normal stream-flow water floods at high discharge.

Due to their ability to transport large boulders and debris in suspension, debris-flows possess substantially greater destructive potential than hyperconcentrated flows, debris-floods and stream-flow water floods. In the Venezuela (section 2.4.1), Te Aroha (section 2.4.2) and Matata (section 2.4.3) events, this destructive potential is clearly demonstrated (i.e. In the Venezuela event, over 15 000 lives were lost and over $US 2 billion in damages was incurred). In light of such disaster, it can be argued that more emphasis needs to be placed on the assessment of such hazards in terms of risk to life and property in order to establish the acceptability of existing or proposed land uses.

Chapter Three

Past research into the recognition of debris-flow hazard

3.1 Introduction

Hazard recognition is a key element of debris-flow hazard assessment. It provides the essential basis for subsequent, more localized studies in an area of interest and facilitates the development of appropriate hazard management and mitigation strategies through the provision of vital information on the estimated whereabouts, magnitude and timing of probable future events (Wilford et al., 2004; Jakob, 2005).

Recognition of past debris-flows has proven a stern challenge for scientific experts and practitioners alike, due to the complex nature of the phenomena and the great variety of conditions and/or factors that can influence their occurrence. Climatic extremes, underlying geology, seismic events, antecedent soil moisture conditions, the presence or absence of vegetation and anthropogenic activities such as logging are just some of the factors that affect the spatial and temporal distribution of debris-flow phenomena and the nature of their deposits (Wieczorek et al., 2000; Lorente et al., 2002). Consequently, a variety of methods have been utilized to evaluate debris-flow hazard, varying substantially between countries, between regions and between practitioners (Jakob, 2005).

This chapter initially provides a broad overview of past research into the recognition of debris-flow hazard in order to provide a context for the research carried out in this thesis, before focusing more specifically on the use of fan-basin morphometry for the spatial recognition debris-flow and associated hydro-geomorphic hazards - the broad approach taken for this research. Accordingly, the chapter begins with a review of spatial and temporal approaches to debris-flow hazard recognition. This is followed by review of works which have used fan-basin morphometry to delineate basins subject to debris-flows and related hydro-geomorphic hazards. To conclude, fan and/or basin morphometric

parameters identified by previous studies to be most useful for distinguishing basin by dominant fan-formative process, are identified and discussed, in order to facilitate meeting the aims and objectives of this research (see section 1.3, Chapter 1).

3.2 Debris-flow hazard recognition overview

In order to gain an appreciation of the way in which past research into the recognition of debris-flow phenomena has been carried out and to further give context to this research, it is useful to look at the variety of approaches that have been utilized to quantify the spatial and temporal occurrence of debris-flow.

3.2.1 Spatial recognition of debris-flow hazard

The spatial identification of debris-flow hazard provides the essential basis for subsequent temporal recognition of such phenomena. Hence, the spatial recognition of debris-flow hazards can be argued to be the most important step in any debris-flow hazard analysis, for it is only when debris-flow occurrence has been determined in space, that the timing and magnitude of individual events can be accurately quantified and appropriate site-specific mitigation measures and related management decisions proposed (Jakob, 2005).

Previous studies have primarily employed geomorphic field investigation (e.g. Glade, 2005, Sterling and Slaymaker, 2006), remote sensing (RS) (e.g. Volker, 2006; Bisson et al., 2005), geographic information system (GIS) (Lin et al., 2002) and quantitative techniques (de Scally and Owens, 2004; Wilford et al., 2004) to identify the spatial distribution of debris-flow hazards. Geomorphic and aerial photograph investigation has long since been a fundamental element in any debris-flow hazard assessment, particularly in regions where supplementary data in the form of historical, botanical, geological and/or climatic records have been readily available (Wohl and Oguchi, 2004; Jakob, 2005). In many areas however (e.g. in sparsely populated regions), such records rarely exist in complete form (Ni et al., 2006). In such cases, relying only on geomorphic field

investigations can prove time consuming and costly, as a greater area must often be surveyed (i.e. due to lack of knowledge on spatial extent) to ensure the hazard is assessed in adequate detail (Ni et al., 2006).

Accordingly, recent research has focused on the use of other techniques such as GIS, RS and quantitative analyses, usually in combination with geomorphic field and aerial photograph investigations, to promote a more efficient and cost-effective assessment of the hazard. Notable examples of such work employing GIS and RS technologies include that by Lin et al. (2002), in which GIS techniques are used to identify and rank factors believed to be critical to the occurrence of debris-flows in the Chen-Yu-Lan River, Taiwan; Bisson et al. (2005), who use a combination of GIS and RS to evaluate the potential of wild-fire-affected areas as a source for debris-flows in Sicily, southern Italy; and Volker et al. (2006) who utilize a 1m high-resolution digital elevation model (DEM), derived from airborne laser swath mapping (ALSM) to identify morphometric parameters that can possibly be used to classify alluvial fans according to their formative processes (i.e. debris-flow, fluvial flow) in the Death Valley, Basin and Range Province, California.

In addition to GIS and RS technologies, a number of studies have used quantitative methodologies to identify areas susceptible to debris-flows (e.g. Jackson et al., 1987; Kostaschuck et al. 1986; de Scally et al. 2001; de Scally and Owens, 2004; Wilford et al., 2004; Rowbotham et al., 2005). Such studies have predominantly focused on the identification and application of fan and/or basin-specific morphological parameters to classify fans and/or their contributing basins according to dominant fan-formative, sediment-transport processes (e.g. debris-flow, debris-flood, and flood). In works by de Scally et al. (2001) and de Scally and Owens (2004) for example, morphometric variables associated with fan and/or basins (e.g. fan and/or basin gradient, relief, area) in the Cascade Mountains of British Columbia and the Southern Alps of New Zealand are examined by various statistical methods (e.g. discriminant analysis, Pearson product-moment correlation) to identify those variables that can be used to classify fans/basins according to process and hence ultimately identify those subject to debris-flows. More recent works by Wilford et al. (2004) and Rowbotham et al. (2005) carry out similar

research utilizing GIS technology applied to DEM's to identify the morphometric characteristics associated with basins and examine them in relation to specific basin types (i.e. fluvial, debris-flow dominated). The present thesis uses a similar GIS-based approach to identify possible debris-flow prone areas in the Coromandel and Kaimai regions of New Zealand; accordingly, research utilizing morphological parameters for debris-flow recognition is discussed in greater detail in section 3.3.

3.2.2 Temporal recognition of debris-flow

Following the spatial recognition of debris-flow hazard, more localized investigation can be carried out to identify the temporal nature of past events and formulate estimates for the probability (likelihood and frequency of debris-flow occurrence in the future) and magnitude (scale of an event in terms of volume, peak discharge characteristics of flows) of future occurrence (Jakob, 2005).

Studies have utilized geomorphic field investigation and aerial photograph/remote sensing techniques (often in combination) to examine the characteristics of debris-flow deposits (Jakob and Podor, 1995; Bovis and Jakob, 1999; Jakob et al., 2005). Field investigation has generally involved dating and measurement of existing deposits and the contributing channel to allow age determination and estimate the volume and peak discharge of the flow, respectively. Dating of debris-flow deposits has included the use of either relative methods such as lichenometry, soil development and weathering rinds on surface boulders (Birkeland, 1999; Decaule and Saemundson, 2003), in which the relative age of debris-flow deposits are compared (e.g. deposit A is older than deposit B) or absolute methods such as radiocarbon dating and dendrochronology (Jakob et al., 2005; Bovis and Jakob, 1999), whereby a fixed date or age range is attributed to the deposit(s) (Jakob, 2005).

Measurement of existing deposits and the channel have typically involved inspection of super-elevation in channel bends (Figure 3.1), as evidenced by mud lines or trim lines (lines of vegetation damage) on the channel banks, along with general observations on

the dimensions of depositional lobes and related subsurface stratigraphy (e.g. using trenches, boreholes) (Jakob et al., 2005; Jakob, 2005). In addition to detailed field investigation, aerial photograph and remote sensed imagery have also proven useful for the estimation of debris-flow volumes (Jakob and Podor, 1995) and dating of deposits (e.g. through repeat photography (Griffiith et al., 1996)).

Figure 3.1: Debris-flow channel observed in the Canadian Rockies, showing levee deposits and pronounced super-elevation of the flow in the two bends, as marked by the lines (Hungr, 2005).

A number of studies have also employed the use of empirical methods to predict the volume and travel distance of debris-flows, including that by Benda (1985) and Benda and Cundy (1990), who use channel slope and tributary junction angle; Cannon (1993) who use regression analysis incorporating the transverse radius of channel curvature and slope angle for volume prediction; and Fannin and Wise (2001) who use material entrainment, slope angle and reach length to predict volume changes along debris-flow paths (Jakob et al., 2005). These studies are criticized by Jakob et al. (2005) who note that channel recharge rates, as a function of sediment supply conditions in the basin, should also be considered in order to accurately predict the volume of future debris-flow events. In this instance, Jakob et al. (2005) note that the contributing channel is often

scoured clear of debris and sediment by the passage of a debris-flow, so that any subsequent occurrence will largely be dependent on the time required for the channel to recharge with sufficient sediment and debris to permit debris-flow development. In addition, supplies of sediment available for transport are considered to vary considerably both in space and time between basins, rendering some basins capable of producing damaging debris-flows more often than others (Jakob, 2005).

In this context, Jakob et al. (2005) propose to differentiate basins according to their sediment supply characteristics, classifying them as either transport-limited (supply-unlimited), in which channels cut into readily mobilizable glacial, colluvial or volcanic materials provide an almost continual supply of sediment to the channel, hence acting to ensure fast rates of channel recharge following an event; or weathering-limited (supply-limited), in which channels are cut into more competent bedrock, resulting in a more limited supply of sediment to the channel and consequently slower rates of channel recharge (Bovis and Jakob, 1999; Jakob, 2005). Accordingly, debris-flows tend to be more frequent in transport-limited basins than in weathering-limited basins (Figure 3.2). Jakob et al. (2005) thus conclude that channel recharge rates (and associated basin sediment supply conditions) should be considered in studies aiming to predict the temporal nature of debris-flows because neglect of such rates may lead to underestimation of debris-flow volumes and miscalculation of probability, frequency and magnitude estimates, particularly in basins with rare debris-flow occurrence.

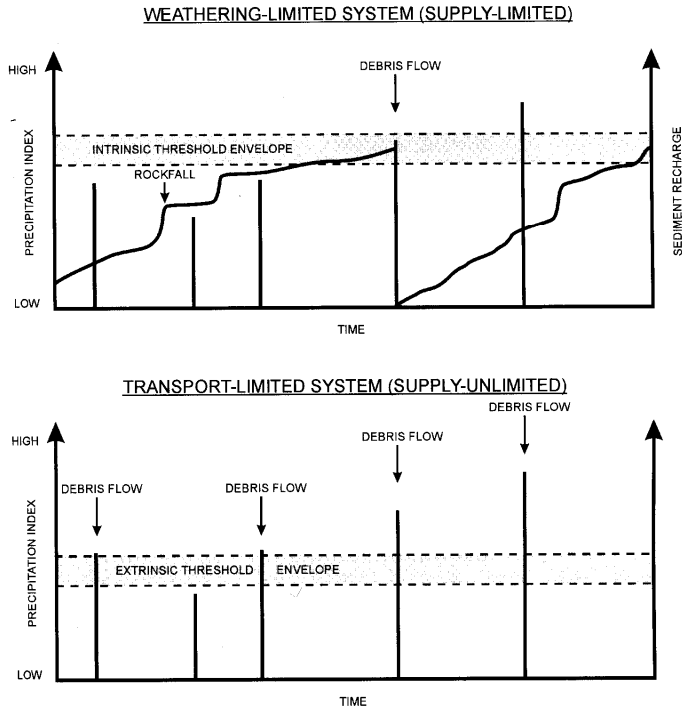

Figure 3.2: Conceptual sketch showing the difference between supply-unlimited and supply-limited basins with regard to debris-flow initiation (Hungr, 2005).

Many studies have also investigated the influence of climatic factors on the frequency of debris-flow occurrence. Such studies have predominantly utilized numerical models based on records and observations of past debris-flow-initiating storms in order to determine rainfall thresholds and/or critical soil moisture conditions above which debris-flow occurrence is probable (Wieczorek and Glade, 2005). Examples of such studies include that by Cannon and Ellen (1985) who derive thresholds for the San Francisco Bay region based on rainfall records and debris-flow observations from previous storm events; Wilson and Wieczorek (1995) who use a simple numerical model based on the physical analogy of a leaky barrel to derive a rainfall/debris-flow threshold for the La Honda area, central Santa Cruz Mountains, California; and Wieczorek et al. (2000) who use GIS technology to define a minimum threshold necessary to trigger debris-flows in granitic rocks of Madison County, Virginia. The present review now refocuses attention back on

to the use of morphometric parameters and GIS technology for the spatial recognition of debris-flows, as this is the broad approach employed for this research.

3.3 Spatial recognition of debris-flows using fan-basin morphometry

Most studies utilizing fan-basin morphometry for the spatial recognition of debris-flows have been carried out post-1980. Prior to this time, studies largely focused on examining broader fan-basin relationships (i.e. relationships between size of alluvial fans and their contributing basins) to understand the mechanisms of fan construction (e.g. Bull, 1964; Hooke, 1968), as opposed to attempting explicit differentiation between debris-flow and non-debris-flow-prone basins (de Scally et al., 2001). Notable examples of earlier works in which fan-basin morphometry has been employed to classify basin by dominant fan-forming process, hence ultimately enabling identification of basins susceptible to debris-flows, include those by Desloges and Gardner (1984), Kostaschuck et al. (1986) and Jackson et al. (1987). In the earlier study by Deslodges and Gardner (1984), explicit differentiation between debris-flow, snow avalanche and conventional water-flood dominated basins in the Front Ranges of the Canadian Rockies, Canada, was achieved through the use of field survey techniques, aerial photograph analysis and measurements of basin and fan morphometry from topographic maps. Subsequent works by Kostaschuck et al. (1986) and Jackson et al. (1987) utilized similar techniques to classify basins according to dominant fan-forming process in the Canadian Rockies, but also employed quantitative statistical methods to test for significant differences between morphometric variables characteristic of specific basins, and to determine which of these variables could be used to differentiate basin by dominant fan-forming process.

Following the application of field and aerial photograph techniques, in conjunction with basin and fan morphometric measurements from topographic maps to classify basins by dominant debris-flow or fluvial process, Kostaschuck et al. (1986) used statistical methods to enumerate relations between the morphometric variables alluvial fan area, fan slope, basin area and ruggedness (after Melton, 1965, see below) to examine form and process relations in the two types of basin. A clear relationship was confirmed: the small,

less rugged basins were found to produce small, steep fans dominated by debris-flows, and the large, less rugged basins produced large, gently sloping fans dominated by fluvial processes.

Works by Jackson et al. (1987) on basins in British Columbia, more specifically used statistical methods to determine those variables most useful for distinguishing basins by process. Through such research, the Melton Ratio (an index of basin ruggedness that normalizes basin relief by area (Melton, 1965), Equation 1) and fan gradient were found to be the most useful parameters for distinguishing basins by process, values for each of the parameters being found to be clearly distinct between debris-flow and fluvial-dominated basins.

Equation 1: ***Melton ratio (R)*** = $H_b A_b^{-0.5} = H_b / \sqrt{A_b}$

H_b denotes basin relief (difference between maximum and minimum elevations in the basin) and A_b the total area of the basin

Similar quantitative analyses were carried out by de Scally et al. (2001) to differentiate between snow avalanche, debris-flow and fluvial basins in south-western British Columbia. In contrast to Jackson et al. (1987), Melton's *R* was not found to be particularly useful for differentiating basins by process, with lower threshold values of *R* for debris-flow basins significantly overlapping with that of upper threshold values of *R* for fluvial basins. Significant overlap was also observed in the critical threshold values of the other variables examined (e.g. basin area, fan gradient, basin elevation), complicating the differentiation of individual debris-flow and fluvial fans and their basins in the study area. The differentiation of debris-flow, snow avalanche and mixed debris-flow-snow avalanche basins and fans was more successful however, with two other variables, channel gradient and bottom elevation, found to be most effective for distinction of basins and fans subject to these processes.

De Scally and Owens (2004) used statistical techniques to distinguish debris-flow from fluvial dominated fans and hence their contributing basins in the Southern Alps of the

South Island, New Zealand. Through statistical analysis, 3 variables, (basin area, fan gradient and Melton's *R*) were all identified as useful variables for distinguishing basins by process in this region.

Studies by Wilford et al. (2004) and Rowbotham et al. (2005) have employed GIS (Geographic Information System) technology in combination with statistical methods to delineate and differentiate between debris-flow and non-debris-flow prone basins in the mountains of British Columbia. Wilford et al. (2004), like the previously mentioned studies, also initially used field survey techniques to classify basins by their sediment deposit signatures present on the fan. The morphometric characteristics associated with each type of basin were then derived from a digital elevation model (DEM) of the study area (as opposed to acquisition by field survey techniques and/or topographic measurements from topographic maps) and statistical analysis carried out to test the use of these morphometric variables for differentiating basin according to dominant fan-forming process; in this study as either debris-flow, debris-flood or conventional fluvial-flow. Overall, Melton's *R* and watershed length were determined to be the best variables for distinguishing between debris-flow, debris-flood and flood-prone basins.

Rowbotham et al. (2005) also used a DEM to derive morphometric parameters associated with basins in the Cascade Mountains of southwestern British Columbia; however alternative parameters were derived to those conventionally employed in previous studies, namely the first and second derivatives of elevation: slope gradient, slope aspect, profile curvature and mean curvature. The basins in the study area had already previously been classified by de Scally et al. (2001) as either snow avalanche, debris-flow or fluvial-flow-dominated, thus the main aim of this research was to test the use of the purely DEM-derived variables mentioned above, for distinction of debris-flow from non-debris-flow-dominated basins. Following statistical analysis within the GIS, the standard deviations of slope gradient and slope aspect were identified as the strongest predictors of the variables tested. In addition, Melton's *R* and basin area parameters (included in the database for comparative purposes) were also identified as useful, although weaker than the two strongest DEM-derived morphometric variables.

3.3.1 Morphometric criteria found to be most useful for distinction of basin by process

From section 3.3 (above), the morphometric variables basin area, fan gradient and Melton Ratio (*R*) have been found to offer the greatest potential for distinguishing basins according to dominant fan-forming process. Basin area has proven a useful variable for prediction of debris-flow-prone basins in a number of studies, with debris-flow basins generally found to be smaller in size than those dominated by fluvial activity (Van Dine, 1985; Kostaschuck, 1986; Jackson et al., 1987; de Scally and Owens, 2004; Wilford et al., 2004). Upper threshold values of basin area for debris-flow dominated basins have, however, been found to vary considerably between regions. For example, basin area values for debris-flow dominated basins in the Canadian Cordillera have been found to have an upper threshold of about 10 km^2, in contrast to the 4-5 km^2 upper threshold identified in the Southern Alps of New Zealand by de Scally and Owens (2004). Consequently, no universal upper threshold has as yet been determined to allow identification of debris-flow basins in different geographic regions, casting some doubt as to the overall usefulness of this variable on its own for the recognition of fans and basins susceptible to debris-flows.

Correlations have been recognized between fan gradient and dominant fan-formative process, with fans formed by debris-flows generally found to exhibit steeper gradients than those predominantly formed by fluvial processes (Deslodges and Gardner, 1984; Kostaschuck et al., 1986; Jackson et al., 1987; de Scally et al., 2001; de Scally and Owens, 2004). Gradients of fans predominantly formed by debris-flow processes have however, been found to vary significantly between regions. For example, minimum threshold values for fan gradient of around 4° were found by Jackson et al. (1987) in the Canadian Rockies, in contrast to thresholds of 7-8° identified by de Scally and Owens (2004) in the Southern Alps of New Zealand. This variation is mainly related to the lithological characteristics of the contributing basin and the fan itself. Volcanic debris-flows (lahars) may form fans with slopes as low as 1-2°, while debris-flow fans formed in granitic terrain may show average fan gradients several degrees higher than the 4° quoted for the Canadian Rockies (Hungr, 2005; Lorenzini and Mazza, 2004). There is thus doubt

as to whether regional fan gradient thresholds can be readily transferred to other regions to facilitate the preliminary identification of basins and fans prone to debris-flows (Hungr, 2005; de Scally et al., 2001).

In addition, fan gradients can be significantly affected by anthropogenic modification (Bovis and Jakob, 1999; Jakob, 2005). For example, alteration of the fan surface through general building residence (i.e. land smoothed or cleared to enable housing construction or garden cultivation) or commercial activities such as timber logging or mining (common in the Coromandel/Kaimai region – see Chapter 4, section 4.2.6) can cause the fan to lose its morphology. Consequently, fans subject to infrequent debris-flows and those predominantly formed by fluvial processes may exhibit similar fan gradients, thus compromising the potential usefulness of this variable for unambiguous identification of debris-flow-prone fans (Bovis and Jakob, 1999; Jakob, 2005).

The Melton Ratio (R) has proved useful in a number of studies for the preliminary identification of basins and fans prone to debris-flows (de Scally and Owens, 2004; Jackson et al., 1987; Wilford et al., 2004). de Scally et al. (2004) note that this index of basin ruggedness may potentially be useful because the lower threshold of R theoretically reflects the minimum gradient necessary for maintaining debris-flow motion when other factors, such as moisture and clay content of sediment, are optimal (Van Dine, 1985; de Scally and Owens, 2001).

A handful of studies have identified thresholds of R which have enabled differentiation of fluvially-dominated basins from those dominated by debris-flows. Jackson et al. (1987) for example, identified a threshold of 0.30 as useful for distinguishing between the two types of basin; basins prone to flooding identified as having ratios <0.30 and those prone to debris-flows >0.30. Wilford et al. (2004) also identified flood-prone watersheds to have ratios <0.30, however incorporated debris-flood into their workings so that the threshold of 0.30 was used to differentiate flood-prone basins from those susceptible to debris-floods, as opposed to debris-flows. Instead, a threshold value of 0.60 was established for debris-flow prone basins, with those prone to debris-floods determined to

have ratios between 0.30 and 0.60. de Scally and Owens (2004) also identified a higher threshold of *R* (0.75) which was used to separate debris-flow prone basins from fluvially-dominated basins, although in this case, and like Jackson et al. (1987), debris-floods were not incorporated in the schema, thus the upper threshold for fluvial basins may possibly exhibit a significantly lower value of *R* than that quoted.

In addition to the use of Melton's *R* for distinction of basin by process, other variables, when used in combination with *R*, have proved useful for the distinction of debris-flow, debris-flood and fluvial basins. Fan gradient, for example, when combined with Melton's *R* (Figure 3.3), has proven useful for distinguishing debris-flow and fluvial basins (de Scally and Owens, 2004; Jackson et al.; 1987) (although, as previously mentioned, this method may be limited in areas subject to anthropogenic modification). Additionally, watershed length combined with *R*, as demonstrated by Wilford et al. (2004) has been found to enable distinction of debris-flow from debris-flood and flood-prone basins.

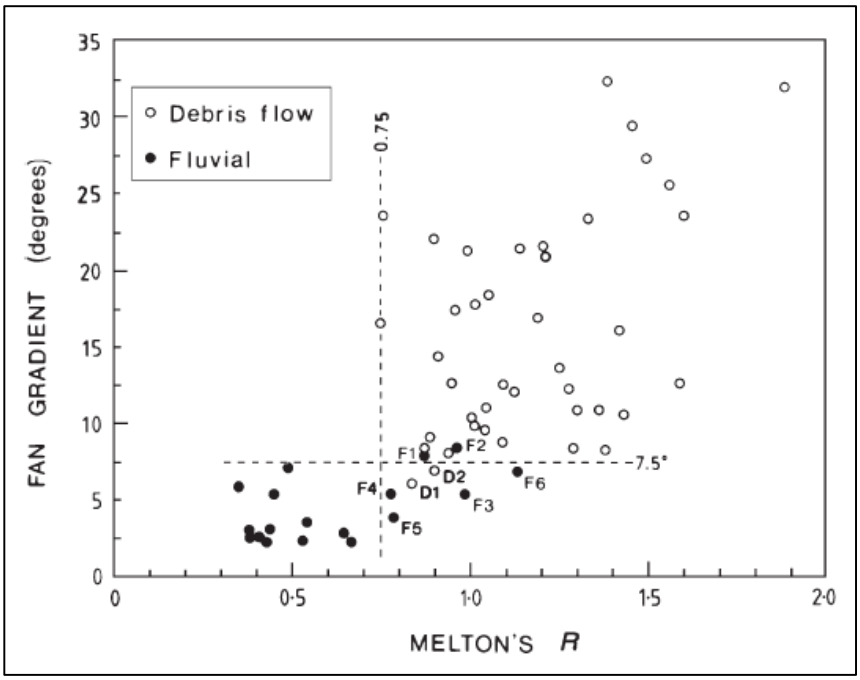

Figure 3.3: Plot of Melton's Ratio and Fan Gradient, showing thresholds used to distinguish debris-flow from fluvially dominated fans (and hence their contributing basins) in the Southern Alps of the South Island New Zealand (De Scally and Owens, 2004).

The use of Melton's *R* (and morphometric criteria in general) to identify fans and basins subject to debris-flow and related hydrogeomophic hazards can, however, be somewhat invalidated in regions which have experienced glaciation (Jackson et al., 1987). Basins may take on 'stepped' profile morphology as a result of glacial erosion (e.g. Rocky Mountain Main Ranges; Jackson et al., 1987), these low gradient steps acting to trap debris, hindering the ability of debris-flows to reach the fan. The debris-flow deposits may then be reworked and transported to the fan as fluvial sediments. Consequently, basins in such regions may exhibit Melton ratios greater than a definitive threshold (e.g. such as the 0.30 lower threshold defined for debris-flows by Jackson et al. (1987)), but may not be capable of producing debris-flows that reach the fan (de Scally and Owens, 2004; de Scally et al., 2001; Jackson et al., 1987). Despite this, Jackson et al. (1987) stipulate that, in unglacierized regions where such topographic constraints are less prevalent, the use of *R* and other relevant morphometric variables should have wide applicability for the primary discrimination of fans and basins with a debris-flow hazard. The Coromandel/Kaimai study area for the present research is such an unglacierized region, having not experienced glaciation in its short history (Newnhall, 1999), thus the use of morphometric approach to delineate debris-flow hazards on fans and basins in this region should be valid.

Overall, the Melton ratio (*R*) has shown to be one of the more robust morphometric variables used to classify basin by process, with a number of studies identifying similar critical threshold values of *R* for hydrogeomorphic phenomena in different regions (e.g. Jackson et al., 1987; Bovis and Jakob, 1999; de Scally and Owens, 2004; Wilford et al., 2004). Furthermore, when used in combination with watershed length, as demonstrated in the model devised by Wilford et al. (2004), the Melton ratio was found to be particularly useful for the discrimination of debris-flow, debris-flood and fluvial watersheds; the model correctly identifying 92 % of the debris-flow watersheds, 88 % of the flood watersheds and 82 % of the debris-flood watersheds, previously classified in the field according to stream fan sediment deposit signatures in the west central British Columbia study area for the research. In consideration of the above, the combination of Melton ratio and watershed length, based on the model proposed by Wilford et al. (2004), are deemed

to offer the greatest potential for the discrimination of basins and fans with a debris-flow hazard. Accordingly, the ability of these variables to predict and discriminate debris-flow prone basins in the Coromandel/Kaimai study area is tested as part of the research for this thesis.

Chapter Four

Study area and methodology

4.1 Introduction

This chapter provides an overview of the study area and methodological approach used in this research. The chapter begins with a brief description of the location, geology, regional structure, vegetation, climate and land-use of the Coromandel/Kaimai study area. This is followed by a description of the research methodology, including an outline of the GIS procedure used to derive watersheds and their morphometric characteristics (e.g. Melton ratio and watershed length) for selected stream locations in the study area. The final section provides a description of the field investigation and subsequent statistical analysis methods used to test the ability of the GIS-derived morphometric parameter's (Melton ratio and watershed length) to identify stream basins/watersheds and fans with a potential debris-flow hazard in the Coromandel/Kaimai region.

4.2 Study area

4.2.1 Location

The Coromandel and Kaimai ranges are located in the north east of the North Island, New Zealand between latitudes 175°21'E and 175°56'E, and longitudes 36°29'S and 37°55'S (Figure 4.1). The ranges trend NNW – SSE and extend approximately 163 km from Cape Colville in the north to Te Poi in the south, covering a total area close to 6500 km^2. Bounded on the western margin by the steep-faced eroded-back scarp of the Hauraki Fault, the ranges are typically rugged and well dissected, with ridge altitudes generally averaging between 400 and 600 m, and reaching a maximum of 952 m at Mt Te Aroha (Kaimai Range) (Christie et al., 2001). Accordingly, streams and rivers in the region are predominantly short and steep with the coastline typified by short beaches and bays separated by rocky cliffs. In addition, exposed areas are generally characterized by sandy beaches (particularly on the east coast) whilst mangroves and mudflats are common in more sheltered terrain (Christie et al., 2001).

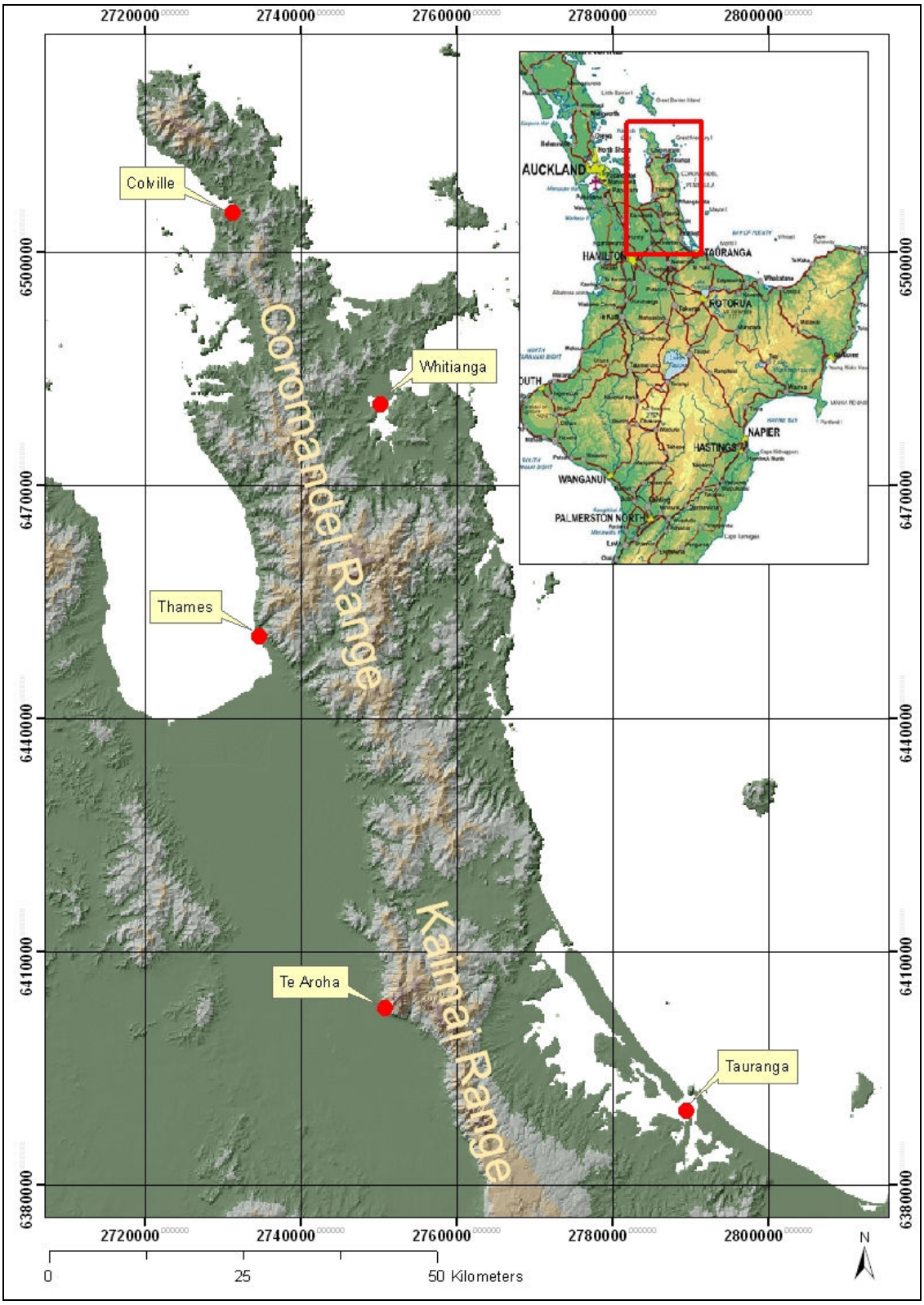

Figure 4.1: Location of the Coromandel/Kaimai region study area

4.2.2 Geology

The oldest rocks in the Coromandel region are late Jurassic basement greywacke and argillites of the Manaia Hill Group (Figure 4.2) (Christie et al., 2001). These rocks are unconformably overlain by much younger marine sediments (conglomerates, sandstones, siltstones, limestones and thin coal seams) of the Torehina formation (Te Kuiti Group) and Colville Formation (Waitemata Group), deposited during the Oligocene and early Miocene epochs respectively (Skinner, 1976). Both the late Jurassic greywacke and Cenezoic marine sediments have very limited exposure in the region, outcropping only in the north of the Coromandel Peninsula (Christie et al., 2001).

The most commonly exposed rocks in the Coromandel region comprise late Cenozoic, calc-alkaline to alkaline sub-aerial volcanics (Skinner, 1986; Christie et al., 2001; Thornton, 2000). Volcanic eruptions first broke out about 20 million years ago near the northern tip of the Coromandel Peninsula, and gradually spread southward over the course of the next 18 million years to form a chain of volcanoes, the remnants of which now comprise the 'backbone' of the Coromandel and Kaimai ranges (Homer and Moore, 1992). Andesites and dacites of the Coromandel Group (further sub-divided into three groups representing different phases of intermediate volcanism, that of the Kuaotunu Subgroup (early to mid Miocene in age), Waiwawa Subgroup (mid to late Miocene) and Omahine Subgroup (late Miocene to Pliocene) after Skinner, 1986)) make up about 70 % of the volcanics by area, while rhyolites of the Whitianga and Whakamarama Groups comprise close to 30%, and basalts of the Kerikeri Volcanic Group <0.1%. Most of the Coromandel Group andesites have been extensively altered by hydrothermal (most commonly propylitic and argillic activity (Christie et al., 2001; Thornton, 2000). The Coromandel Group also includes a large (15 km^2) quartz diorite to granodiorite pluton (Paritu plutonics, Miocene to Pliocene age (Skinner, 1976)) located at the northern end of the Coromandel peninsula, which intrudes the Manaia Hill Group basement greywackes and earliest Coromandel Group andesites; and subvolcanic dikes, stocks and plugs of andesitic and dacitic porphyry that intrude the basement and volcanic rocks of northern and central Coromandel (Christie et al, 2001).

In the eastern central and southern parts of the Coromandel/Kaimai region, rhyolitic rocks of the Whitianga Group (subdivided into Late Miocene to Pliocene flow and dome-forming rhyolites of the Minden Rhyolite Subgroup, rhyolitic pyroclastic rocks and sediments of the Coroglen Subgroup and Pliocene to early Pleistocene ignimbrites of the Ohinemuri Subgroup) are well exposed, with several calderas and volcano-tectonic depressions recognized (Skinner, 1995; Christie et al., 2001). In contrast, the Miocene to Pliocene basalts of the Kerikeri Volcanic Group are rare in the region, exposures largely restricted to the base and eastern end of the Kuaotuna Peninsula, and south-east of Whitianaga on the inner margins of the Kapowai Caldera (Adams et al., 1994; Christie et al., 2001). In addition to the abundant rhyolites and rare basalts, tephras of late Quaternary age erupted from the Central Volcanic Zone and Mayor Island blanket the east and south of the Coromandel region by up to 2 m (Hogg and McCraw, 1983).

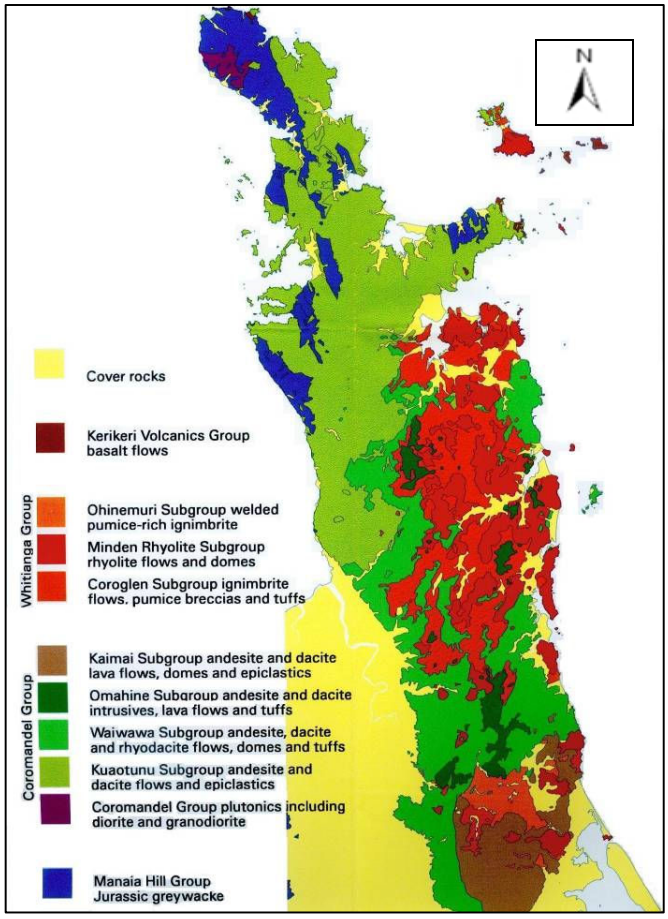

Figure 4.2: Geological map of the Coromandel/Kaimai region (Christie et al., 2001).

4.2.3 Regional structure

A well developed NNW and NNE to ENE fault block pattern is evident in the Coromandel/Kaimai region (Christie et al., 2001). This is considered to have formed initially as a result of extensive folding and faulting of the Manaia Hill Group greywacke basement during the early Cretaceous period, before rejuvenation and subsequent imposition on the overlying Tertiary volcanic rocks during the late Cenozoic (Skinner, 1986). Accordingly, several major structural corridors, indicated by aeromagnetic anomalies such as that observed in Coromandel-Waikawau Bay (Appendix 1) (Christie et al., 2001), major fault zones such as the Tapu-Whitianga Fault Zone (Appendix 2) (see Skinner, 1986) and the alignment of some epithermal veins (e.g. the Karangahake-Jubilee-Maoriland-Golden Cross-Wharekirauponga vein trend (Appendix 3); Irvine and Smith, 1990) cross the peninsula. The eastern side of the Coromandel region is characterized by a number of rhyolite and ignimbrite-filled volcano-tectonic depressions, whilst the west margin of the Coromandel peninsula is bounded by the asymmetric Hauraki Rift or Graben (Skinner, 1995; Christie et al., 2001). The graben has a downthrow of 1 to 3 km (the main displacement of which is believed to have initiated in the early Quaternary) and is estimated to contain over 700 m of unconsolidated Quaternary sediments that overlie 2 to 3 km of Pliocene and older sedimentary and volcanic rocks (Hochstein and Nixon, 1979).

4.2.4 Vegetation

The Coromandel and Kaimai regions are characterized by a diverse range of flora, from low-lying grassland and mixed indigenous scrub to towering indigenous Kauri trees and exotic forest (Newsome, 1987). In the Kaimai Range, summit-warm temperate forest such as Tawa (*Beilschmiedia tawa*), Tawari (*Ixerba brexiodes*), Silver (*Nothofagus menziesii*) and Red Beech (*Nothofagus fusca*) dominate on upper slopes and crests between 600 and 900 m altitude. Some of the other more prevalent canopy species in this region include Quintinia (Quintinia autifolia), Toro (*Myrsine_salincina*), Kamahi (*Weinmannia racemosa*), Kaikawaka (*Libocedrus bidwillii*) and Pink Pine (Halocarpus biformis) (Wardle, 1991; Newsome, 1987). In broken forested terrain where die-back and forest collapse is evident, trees have been replaced by the occupation of shrubby

communities dominated by Raurekau (*Coprosma grandilfolia*), Quintinia (*Q. autifolia*), Lowland Pepperwood (*Pseudowintera axillaris*) and Pigeonwood (*Hedycarya arborea*), in addition to swards of Bush-rice grass (*Microlaena avenacia*), Holy grass (*Hierochloe redolens*) and *Uncinia distans* (Wardle, 1991). Species such as Manuka (*Leptosprmum scoparium*) and Tamingi (*Epacris pauciflora*) are also common where the canopy is lower and more open.

Further north in the Kauaeranga Valley, vegetation is predominantly comprised of lowland-podocarp broadleaved forest, with mixed indigenous and sub-alpine scrub on the river flats and widely scattered Kauri (*Agathis australis*) on the ridges (Byrami et al., 2002; Newsome, 1987). Tawa (*Beilschmiedia tawa*), Kamahi (*Weinmannia racemosa*), Hinau (*Elaeocarpus dentatus*) and Hall's Totara (*Podocarpus hallii*) are prominent constituents of the lowland-podocarp broadleaved forest, whilst the mixed indigenous and sub-alpine scrubland communities comprise Five-finger (*Pseudopanax aboreus*) Manuka (*Leptosprmum scoparium*) and Tamingi (*Epacris pauciflora*) that are indicative of recent (i.e. <100 yr) disturbance (Byrami et al., 2002). Such disturbance is attributed to early European logging operations undertaken in the late 19th and early 20th centuries in which large areas of the Coromandel region were extensively logged for Kauri (Byrami et al., 2002; Tourism Coromandel, 2007).

4.2.5 Climate

Weather patterns in the Coromandel and Kaimai regions (and New Zealand in general) are largely influenced by the easterly movement of frontal systems, associated with prevailing westerly and southwesterly winds from the Tasman Sea. Weather in the summer months is generally dominated by the southeasterly movement of anticyclones from the north Tasman Sea, whilst in the winter, weather patterns are largely influenced by the northeasterly movement of troughs from the south (Environment Waikato, 2007; Jane and Green, 1984; Maunder, 1970). Rainfall is generally received from a westerly quarter (Jane and Green, 1984). Annual precipitation (Figure 4.3) often exceeds 3000 mm in the Coromandel range, with rainfalls in excess of 4500 mm p.a. not uncommon, whilst in the Kaimai Range, rainfalls generally amount to between 1500 and 2500 mm per

annum (Jane and Green, 1984; Environment Waikato, 2007). Extreme annual rainfalls in the Coromandel/Kaimai region are often attributed to the incidence two major storm patterns. Summer tropical cyclones, which originate to the north of New Zealand and sweep southwards along the east coast of the North Island before veering eastward out through East Cape, bringing intense rainstorms to the ranges. Winter storm fronts associated with the southeasterly movement of low pressure troughs that characteristically sweep northeastwards through the central North Island before veering at Mt Ruapehu towards east cape, bringing heavy rainfall and occasionally snow to the ranges (Jane and Green, 1984; Burrows and Greenland, 1979). Mean annual temperatures for the region generally vary between 12 to 14°C, ranging between 5 and 15°C in the winter months and 15 and 25°C during summer (NIWA Science, 2007; Hauraki District Council, 2007). The region receives between 1800 and 2000 hours of sunshine per annum (NIWA Science, 2007).

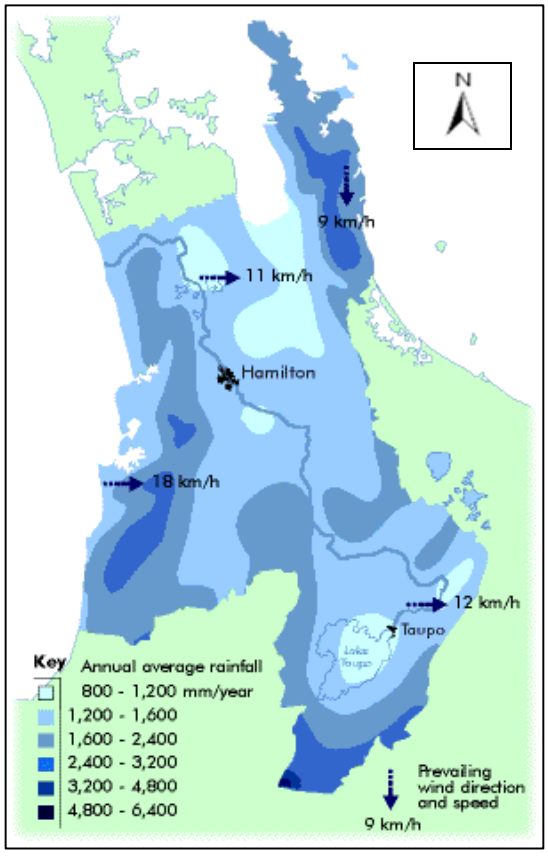

Figure 4.3: Annual precipitation, wind speed and wind direction for the Coromandel/Kaimai region (Environment Waikato, 2007).

4.2.6 Land-use and population

A large part of the land in the Coromandel/Kaimai region is administered by the Department of Conservation (DoC), and is zoned with levels of environmental protection ranging up to full reserve status (geological reserves, ecological areas and forest sanctuaries) (Christie et al., 2001). In addition, much of this land is only accessible on foot (particularly on the Coromandel Peninsula) meaning many of the major population centers are concentrated in coastal areas of the peninsula. Main population centers include Thames (population 6500), Paeroa (3700), Te Aroha (3700), Waihi (3700), Whitianga (2500) and Whangamata (2500), with tourism, horticulture, farming, fishing, forestry and mining being the main commercial activities in the region. There is high recreational use in coastal areas of the peninsula; the overall close proximity to Hamilton, Auckland and Rotorua, in addition to many attractive beaches, makes the Coromandel/Kaimai region a popular holiday and tourist destination (Christie et al., 2001).

The Coromandel region is also particularly well-known for its mineral resources, being recognized as one of the most mineral-rich regions in New Zealand (Christie et al., 2001; Thornton, 2000). It includes most of the Hauraki Goldfield and comprises a large number of epithermal gold-silver- lead-zinc-copper deposits, a few epithermal pyrite and mercury deposits, and several occurrences of porphyry copper style mineralization, all related to late Cenezoic volcanism (Thornton, 2000; Christie et al., 2001). Gold and silver continue to be mined from the Martha Hill open pit mine at Waihi, while rock aggregate (predominantly andesite), sand and limestone (extracted for local use as road aggregate and agricultural lime) are currently mined from numerous other localities in the region (Thornton, 2000; Christie et al., 2001).

4.3 Research methodology – GIS methods

The ESRI software package Arc GIS Arc View, versions 9.1 and 9.2, comprised the geographic information system (GIS) utilized for this research. This program is extremely useful for identifying and analyzing the hydrologic characteristics of a region as it contains a particular set of features (the hydrology toolset) specifically designed to facilitate the creation, manipulation and analysis of such information.

Tools (Arc GIS geoprocessing commands) within the 'spatial analyst' toolset in Arc Toolbox (user interface used for accessing, organizing, and managing geoprocessing tools, models, and scripts; ESRI, 2006) were primarily utilized to investigate the hydrologic characteristics of the Coromandel/Kaimai study area. These tools were linked within the 'Spatial Analyst Model Builder' (interface used to build and edit geoprocessing models in ArcGIS; ESRI, 2006) to construct a systematic flow diagram or model enabling the delineation of watersheds in the study area and extraction of morphometric parameters associated with them. Input data was entered as a list into each tool to enable model iteration and hence processing of large amounts of data in an automated and simultaneous fashion.

The formulated model (referred to herein as the 'Watershed model') was divided into two parts: part 1 (Figure 4.4) used to extract a study area subset from an existing digital elevation model (DEM) of New Zealand, and to delineate a drainage network for the study region; and part 2 (Figure 4.5), used to delineate watersheds in the study area and extract the morphometric parameters associated with them. Once devised and run to produce outputs, the extracted morphometric parameters were exported into a Microsoft Excel spreadsheet where Melton Ratios and watershed lengths for each of the watersheds were calculated and prepared for subsequent analysis.

4.3.1 Input datasets

An existing digital elevation model (DEM) of the North Island, New Zealand, NZTM wrap aerial photographs and NZ 1:50 000 topographic map sheets were used as main inputs for the model.

4.3.1.1 NZ DEM

The NZ DEM, sourced from the University of Canterbury Geography Department (UCGD) data holdings inventory, was used to facilitate the creation of a DEM for the study area. The NZ DEM was initially formulated by Landcare Research in 1999 using Land Information New Zealand (LINZ) 1:50 000 photogrammetrically-derived topographic data sources, before acquisition by the UCGD in 2000. The DEM has a cell size of 25 x 25 m with 90% of the vertical data accurate to within 10 m of their true elevation (Landcare Research, 2000).

4.3.1.2 Aerial photographs

The NZTM wrap aerial photographs (taken in 2000) were utilized in the model to facilitate the identification and analysis of watersheds within the study area. They were acquired from Environment Waikato (EW) and have a spatial resolution of 1 m.

4.3.1.3 Map sheets

The NZ 1:50 000 topographic map sheets were sourced from the UCGD data holdings inventory and used in conjunction with the NZTM wrap aerial photographs in the model, to facilitate the identification and analysis of watersheds within the study area. They were originally derived using Land Information New Zealand (LINZ) 1:50 000 photogrammetrically-derived topographic data sources and purchased from Terralink NZ by the UCGD in late 2000.

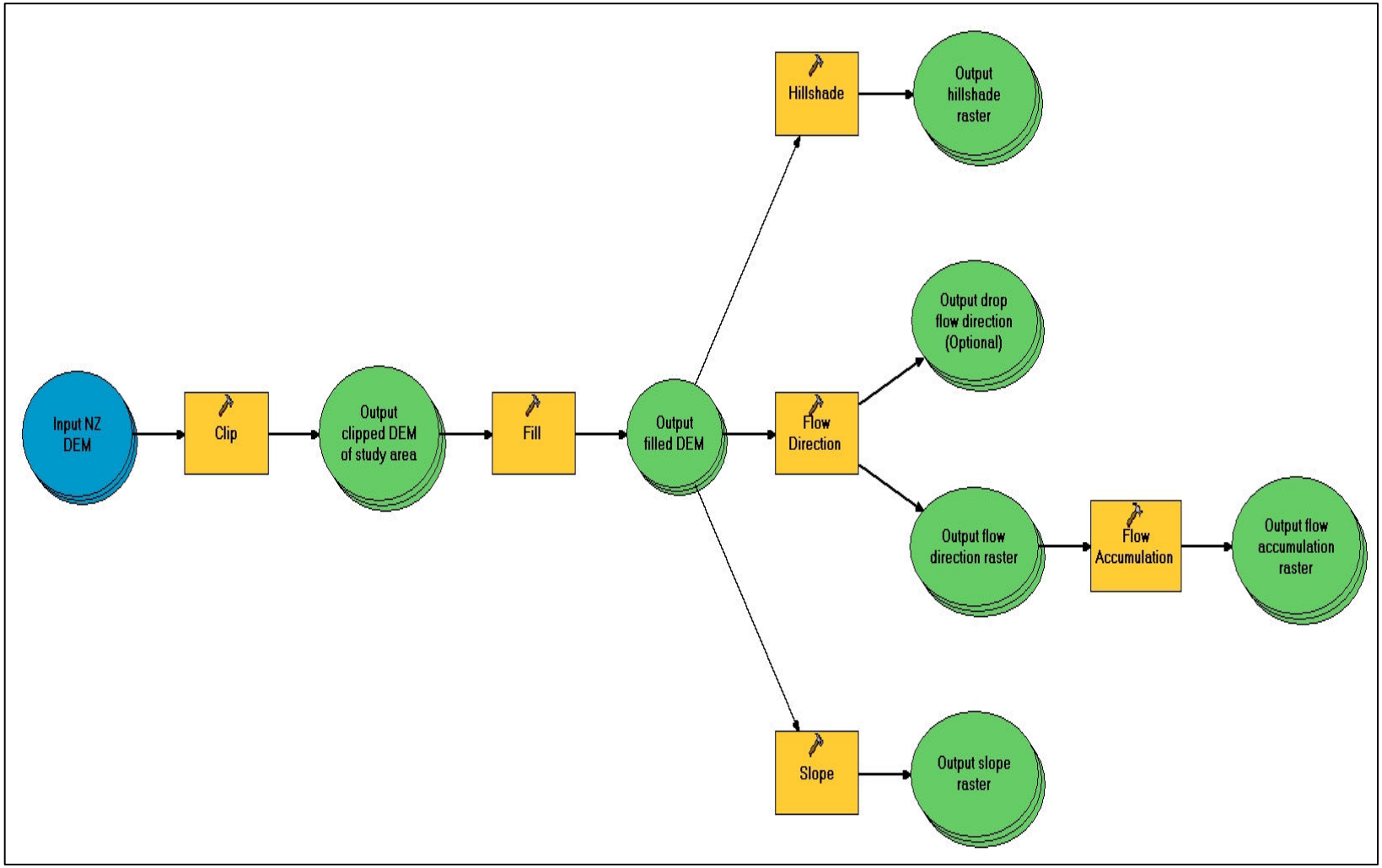

Figure 4.4: Process followed to extract the DEM of the study area and derive the drainage network (Part 1 of the 'Watershed model'; constructed using the Spatial Analyst Model Builder).

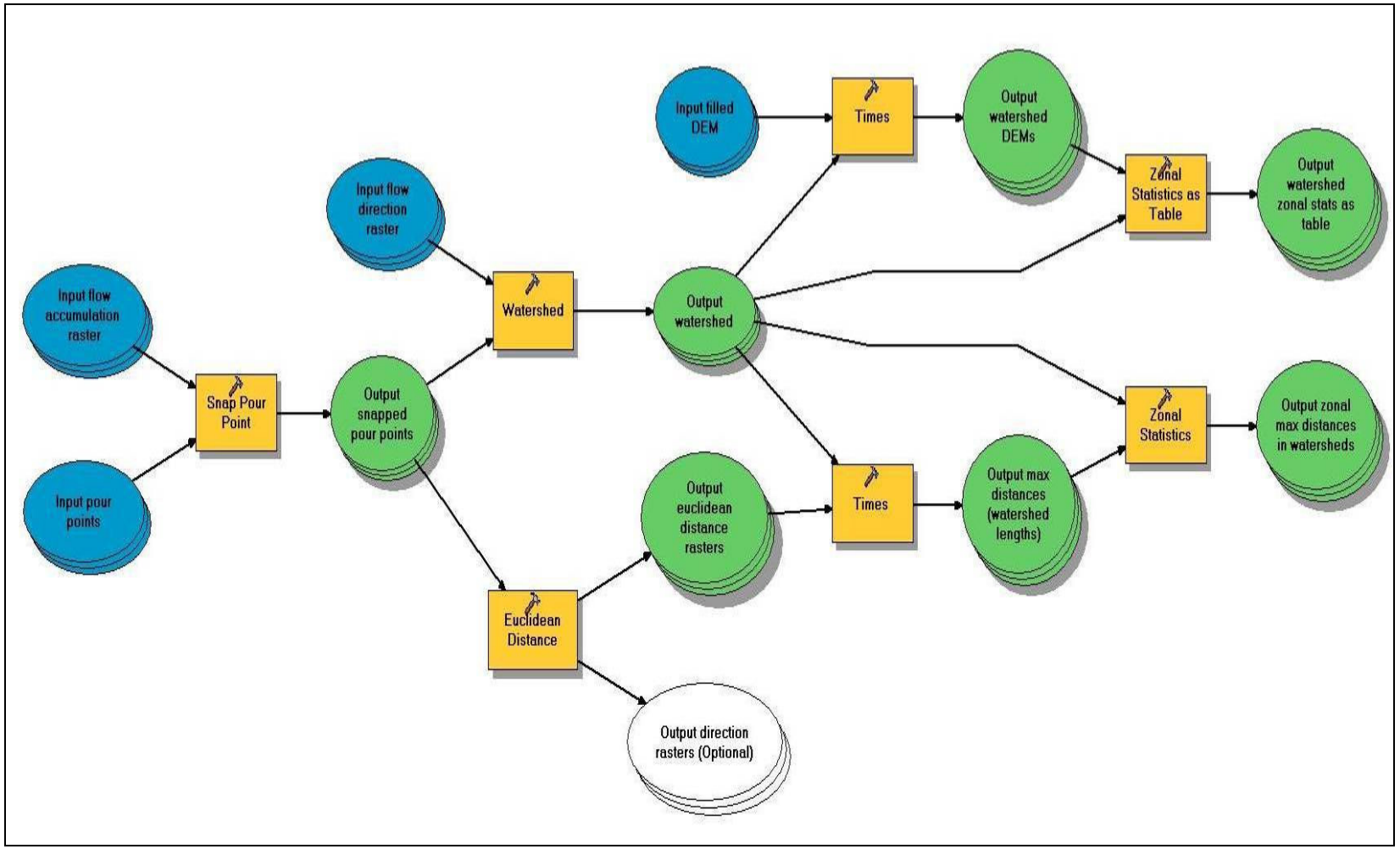

Figure 4.5: Process followed to derive watersheds and their associated morphometric parameters for the study area (Part 2 of the ' Watershed model'; constructed using the Spatial Analyst Model Builder)

4.3.2 Watershed Model: Part 1 – Extraction of the study area DEM and delineation of the drainage network

NB: The reader is referred to figures 4.4 and 4.5 to follow all processes in part 1 and 2 of the watershed model, unless otherwise stated.

4.3.2.1 Extraction of study area DEM

The first step in the GIS procedure involved the extraction of a study area-defined subset from the larger North Island DEM in order to facilitate study area-specific processing. This was carried out using the 'Clip' tool from the data management toolset within Arc toolbox. The x and y co-ordinate spatial extent of the study area was specified within the Clip tool's dialogue box as the subset to be extracted/clipped from the North Island DEM. The clip tool process was then run within spatial analyst model builder to produce a specific DEM of the Coromandel/Kaimai region study area (output clipped DEM).

4.3.2.2 Delineation of drainage network

The next step in the GIS procedure involved delineating the drainage network for the study area. To accomplish this, the flow directions of each cell in the newly derived study area DEM (i.e. directions in which water would theoretically flow out of each cell under the influence of gravity) had to be determined. Prior to carrying out this process, however, the DEM had to first be corrected for possible errors in the data. In order to understand how such errors affect the construction of a drainage network and the way in which they are manifested in the data, it is first necessary to describe the process by which flow direction and flow accumulations for cells in the DEM are determined so as to provide a conceptual basis for the reader.

Flow direction

Flow directions for each of the cells in the DEM were determined utilizing the spatial analyst 'Flow Direction' tool. Each cell was assigned a flow direction corresponding to one of the eight adjacent cells into which flow could travel (Figure 4.6), which is determined by the direction of steepest descent from each cell. The resulting raster

output (flow direction) was then used to facilitate determination of high flow accumulation zones in the study area DEM.

NB: In addition to flow direction, an optional output raster (the 'drop raster') was also created showing the ratio of the maximum change in elevation from each cell along the direction of flow to the path length between centers of cells (expressed in percentages), however this output was not used as input to any other processes in the model.

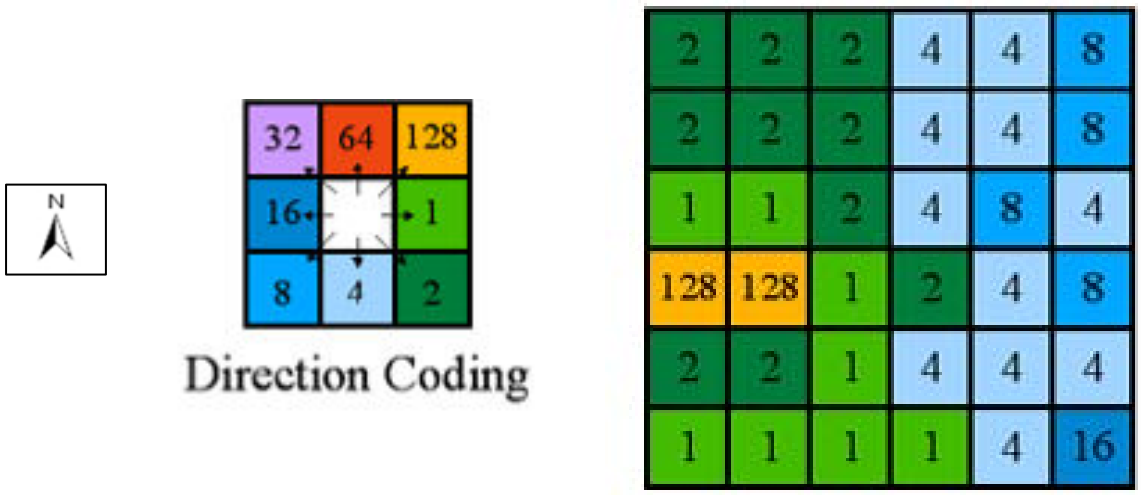

Figure 4.6: Coding for the 8 possible flow directions out of each cell and example flow direction raster output, created using the spatial analyst 'flow direction' tool (ESRI, 2006)

Flow accumulation

Zones of flow accumulation in the study area were delineated using the 'flow accumulation' tool from within the spatial analyst hydrology toolset. Using the previously created flow direction raster as input, this tool created a raster output of accumulated flow to each cell, by determining the cumulative number of all upslope cells flowing into each down slope cell (Figure 4.7). Cells in the output (flow accumulation) with high flow accumulation were interpreted as areas of concentrated flow and used to identify stream channels, and hence the drainage network for the study area.

Correction of DEM for errors in the data

Prior to carrying out the processes described above to define the drainage network for the study area, the input DEM was examined and corrected for possible errors in the data, so as to ensure the accuracy of subsequently derived outputs. In general, DEM's often inherit errors during generation, due to sampling effects and rounding of elevations to integer numbers. These errors in the data are generally termed 'sinks' and can best be defined as individual cells or sets of spatially connected cells whose flow direction cannot be assigned one of eight valid values in a flow direction raster, either because all neighboring cells are higher (have higher values) than the processing cell (Figure 4.8) or because the cells flow into each other, creating a two-cell loop. As a result, sinks can act as areas of internal drainage in the dataset (i.e. cells may flow in but will not flow out). Sinks thus must be corrected for in the input dataset to ensure a derived drainage network is continuous and to guarantee the accuracy of all subsequently derived outputs. This of course is based on the assumption that sinks are indeed errors or artifacts in the data and not actual features in the landscape (i.e. according to Goodchild and Mark (1987) sinks are generally rare in natural landscapes and largely restricted to glacial or karst terrain; two characteristics which are not typical of the Coromandel/Kaimai region study area).

Correction of the DEM was carried out using of the 'Fill' tool from the hydrology toolset. Using this tool, all sinks in the study area DEM were identified and filled (e.g. DEM values were altered to ensure continuous flow routing throughout the DEM) to produce a new depressionless DEM output (filled DEM). This output was then used as input to the flow direction tool process (to facilitate delineation of the drainage network, as described in sections 4.3.2.1.1 and 4.3.2.1.2) and to the slope and hillshade tool processes (described below) to create raster outputs of slope angle and hillshade effect, respectively.

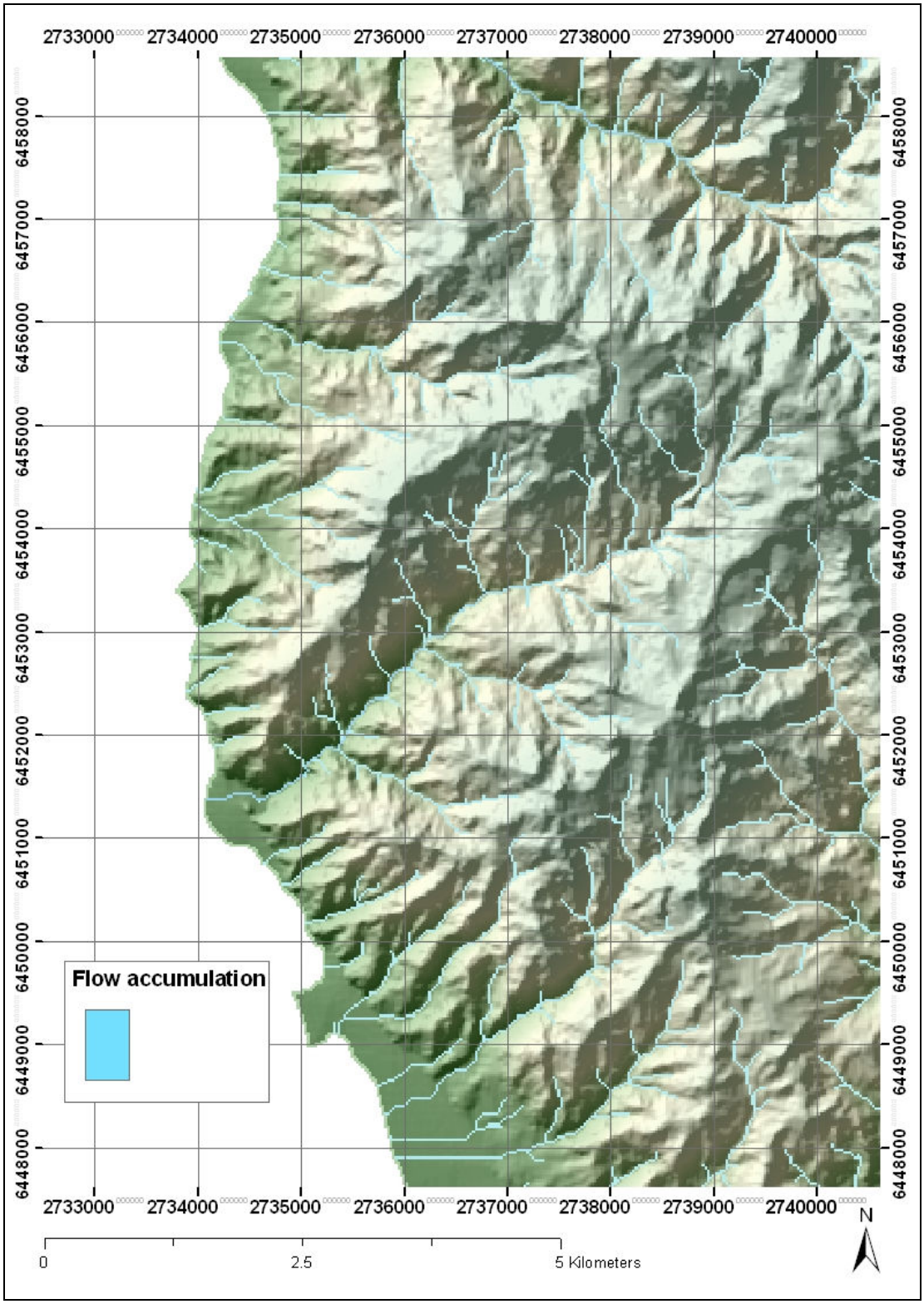

Figure 4.7: Zones of high flow accumulation, displayed on top of the region's topography as represented by the hillshade DEM output.

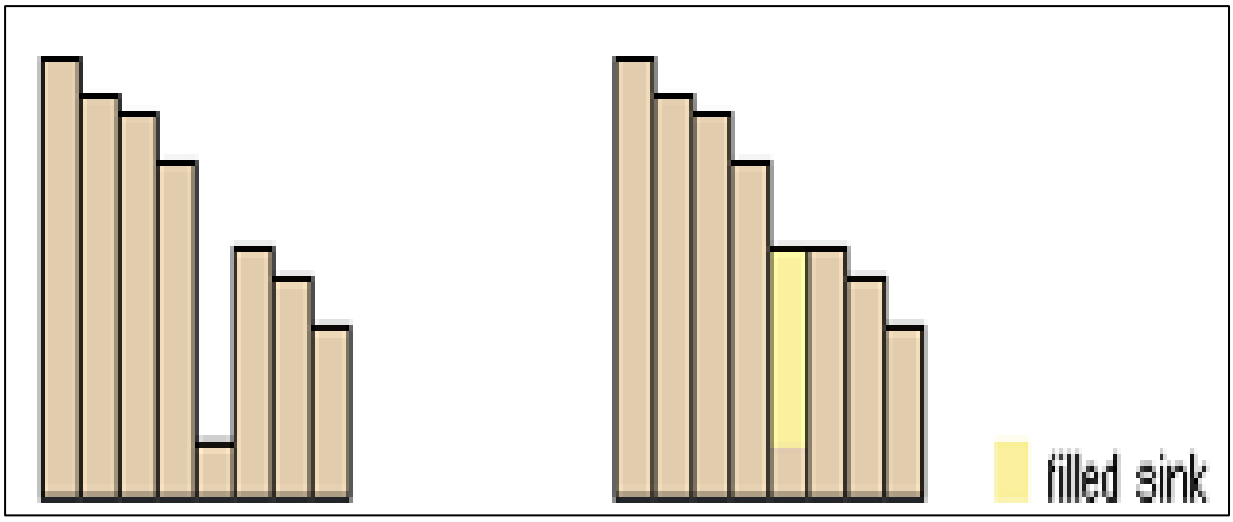

Figure 4.8: Profile view of a sink in the data before and after running the Fill tool

4.3.2.3 Formulation of slope and hillshade rasters

Slope and hillshade rasters were formulated to facilitate spatial analysis of the derived drainage network and enable the identification of watershed outlet (pour) points (described in section 4.3.3.1). The slope output raster (Figure 4.9) was derived using the 'Slope' tool from the spatial analyst-surface toolbox. This tool determined slope (expressed in degrees) for each cell in the output raster by calculating the maximum change in elevation over the distance between that cell and its eight neighbours.

The hillshade raster output (Figure 4.7) was created using the 'Hillshade' tool within the spatial analyst-surface toolbox. Each cell was assessed in terms of the position of a specified hypothetical light source and assigned a corresponding illumination value. The direction of the light source was specified at 315° and the altitude angle of the light source above the horizon was set to 45° to produce a shaded relief raster of the study area. When viewed in conjunction with subsequently derived outputs (i.e. as an underlying base layer to other derived outputs) the hillshade DEM greatly enhanced visualization and overall graphical display.

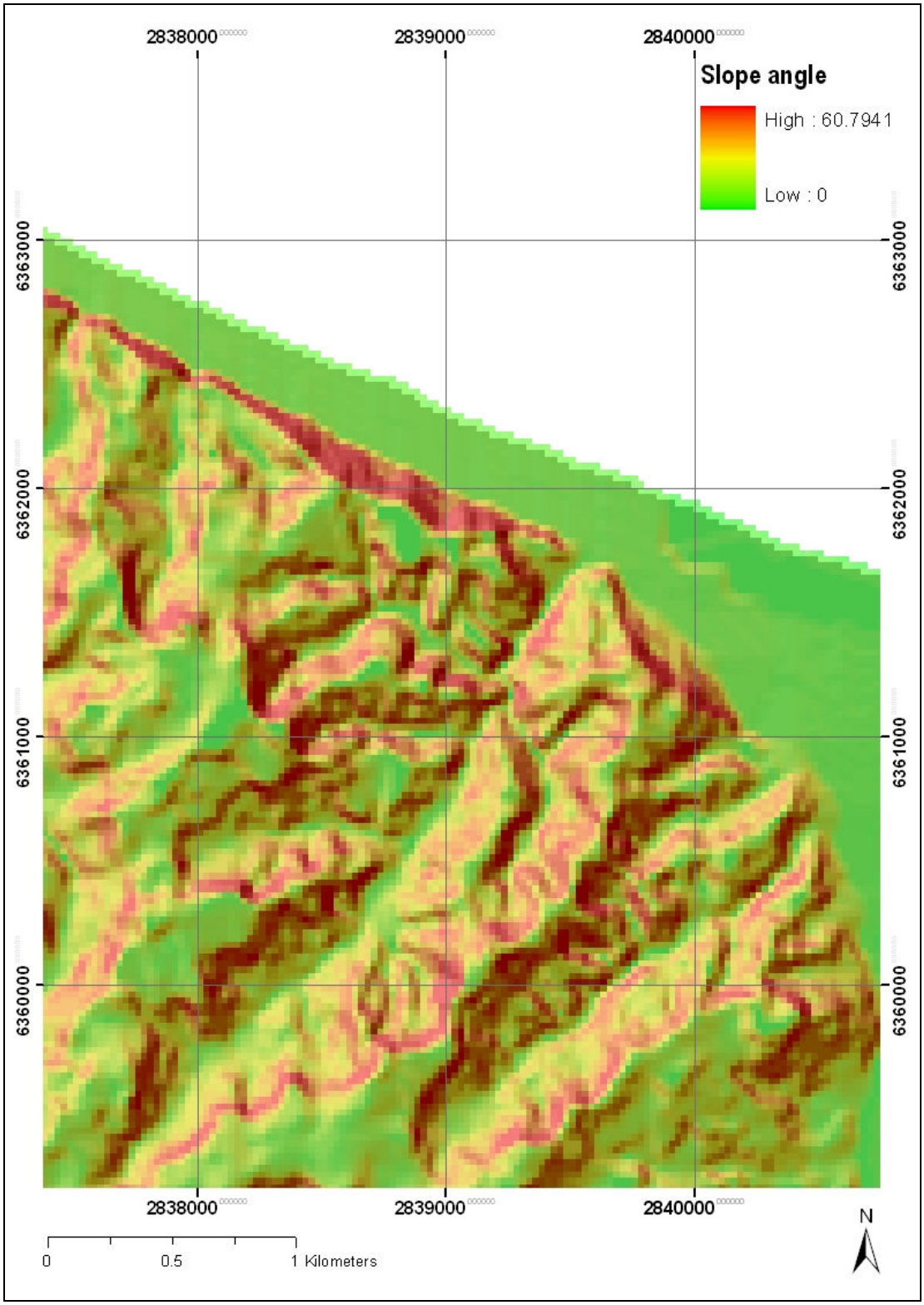

Figure 4.9: Example slope output raster derived using the Slope tool (displayed on hillshade DEM background; DEM Location: Matata, New Zealand).

4.3.3 Watershed Model: Part 2 – Delineation of watersheds and extraction of morphometric parameters

Following delineation of the drainage network, a second part to the watershed model (Figure 4.5) was constructed to derive watersheds for selected stream watershed locations in the study area, and to extract morphometric parameters associated with them. Prior to running this part of the model, new vector-based input datasets (pour point data – locations to which watersheds drain) had to first be created to identify suitable stream locations for which to generate watersheds.

4.3.3.1 Identification of suitable stream fans for watershed generation

Stream fans deemed as suitable for watershed generation included those interpreted to have a possible debris-flow hazard. Two simple criteria were used to identify such stream fans on this basis, these being that of:

(a) The presence of steep slopes adjacent to the stream channel in the upstream area draining to the fan, and
(b) The presence of housing on the stream fan in close proximity to the active stream channel

For criterion (a) steep slopes were defined as slopes >20° in angle. At least one third (visually estimated onscreen) of the upstream drainage network draining to the fan had to have steep slopes adjacent to some part of the stream channel. According to Hungr (2005) slopes between 20 and 45° are necessary to promote the initiation of debris-flows (i.e. by slope failure) and to maintain their momentum down-channel to reach the stream fan (see chapter 2, section 2.3.1 for further information).

For criterion (b) housing included all building types (e.g. large buildings, family homes, hay sheds) acting as residence for human beings (i.e. in which humans work or live). Housing on the stream fan was defined to be within close proximity to the active stream channel if within a 100 m radius (i.e. 4 cells; each cell 25 x 25 m) of that channel (estimated visually onscreen). The radius of 100 m was an arbitrarily defined distance considered adequate by the author, based on the assumption that debris-flows are generally limited in their spatial extent and that housing closest to the

stream channel is likely to be at greatest risk of damage in the event of a debris-flow or flows.

Steep slopes adjacent to the channel in the upstream area draining to the fan and housing on the stream fan in close proximity to the active stream channel were identified through examination of NZTM wrap aerial photography and 1:50 000 topographic map sheets for the study area, in conjunction with the flow accumulation (showing drainage network), slope and hillshade rasters derived in part 1 of the watershed model (all layers viewed simultaneously in the main Arc Map spatial analysis window). Upon visual identification, each house was then digitized (Figure 4.10) onscreen (the process of creating new digital data from existing digital sources by computer-based spatial query) to create a new vector-based layer, signposting the spatial location of suitably identified stream fans.

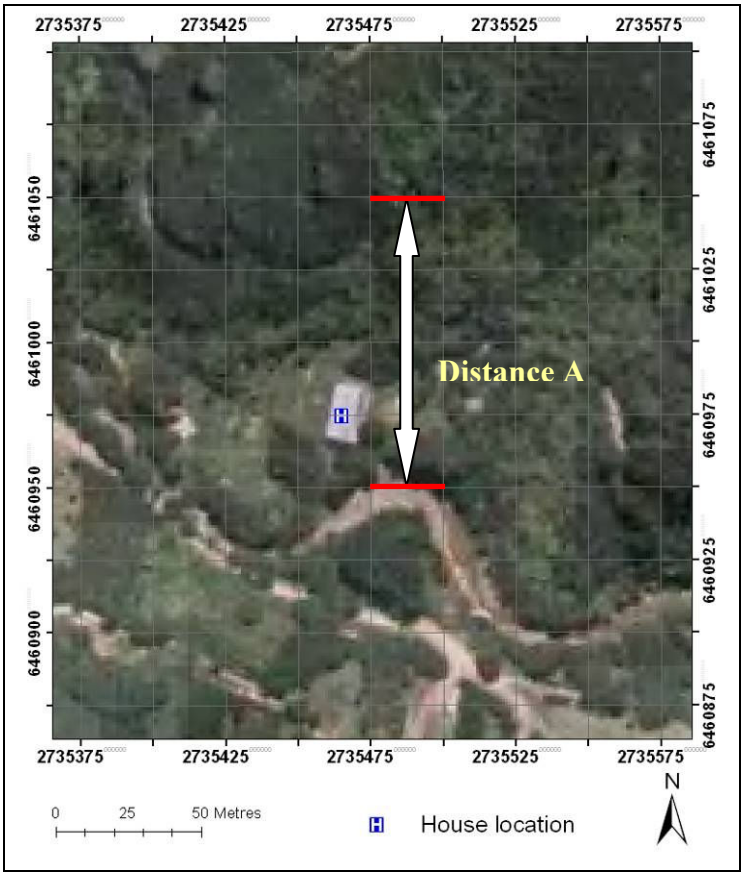

Figure 4.10: NZTM wrap aerial photograph showing a digitized house location within the desired 100 m ground distance buffer (4 cells = Distance A) of the active stream channel.

Digitizing of the housing layer

To craft the housing layer, an empty shapefile (file used to store point, line, polyline or polygon vector features) was initially created within Arc Catalog to hold subsequent data to be created. Utilizing the spatial analyst 'editor' feature within Arc Map, and the NZTM aerial photographs, topographic map sheets, flow accumulation and slope rasters as base maps, points were plotted on top of the identified houses and polylines linked to form vector polygons encompassing major built up areas (e.g. towns such as Thames). Not all houses were digitized into the layer. Instead, only the closest houses to the fan apex and drainage source were digitized, as these were considered to have the greatest debris-flow hazard. This data was then saved in the newly created shapefile to create the housing layer.

Pour points and watershed generation

A watershed is defined as the total upstream area contributing flow of water and related substances to a given hydrologic point (generally termed a 'pour point') in a landscape (ESRI, 2006). In Arc GIS, to identify the contributing watershed for a particular location, a specific pour point must first be defined for that locality. Accordingly, for the present research, pour points had to be defined for the active streams on stream fans considered to have a possible debris-flow hazard (in accordance with the criteria described in section 4.3.3.1) in order to delineate their relevant watersheds.

Identification and digitizing of pour points

Individual pour points were identified and digitized in the active stream channel for each stream fan. Before digitizing the points, empty shapefiles for each location were created (as with the housing layer) in Arc Catalog to hold each vector data point to be digitized. Spatial analyst 'Editor' was then used to facilitate onscreen digitization of the pour points (plotted as vector points), using the NZTM aerial photographs, topographic map sheets, flow accumulation and slope rasters as base maps.

The housing layer was used as an objective guide for the placement of pour points in the active stream channel on the stream fans. In this regard, pour points were placed in the stream channel (defined by the flow accumulation raster output) adjacent to

those houses (Figure 4.11) in the housing layer closest to the fan apex and/or drainage source upstream. To ensure the accurate placement of each pour point in the relevant stream channel, the display was magnified to local cell level (i.e. each individual cell made visible) using the conventional zoom function, and the pour point placed in the relevant cell corresponding to high flow accumulation. The existence of small, steep tributaries feeding the main channel and in close proximity to the stream fan were also digitized with pour points, these placed at the junction with the main channel. This was done to ensure those tributaries to the main channel with perhaps a higher potential for producing debris-flows to reach the fan were adequately represented in terms of the Melton ratio (*R*) derived for the watershed. Data were then saved for each shapefile, to produce individual point datasets for each stream fan location. In all, 302 different stream locations within the study area and an additional 18 outside the study area were digitized with pour points for which to derive watersheds.

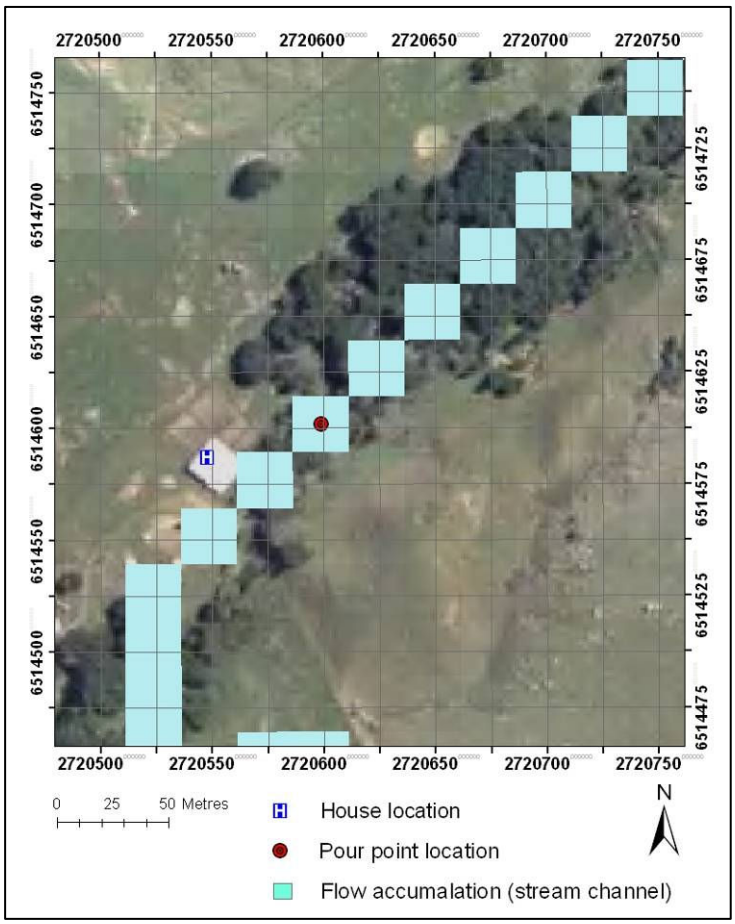

Figure 4.11: Pour points were placed in stream channels adjacent to relevant house locations.

4.3.3.2 Snapping of pour points to cells of highest flow accumulation

The next step in the GIS procedure involved utilizing the 'Snap Pour' tool from the spatial analyst hydrology toolset to assure the accurate location of pour points in cells of high accumulated flow (i.e. the relevant stream channel); the correct location of these points is critical for the accurate subsequent delineation of the desired watersheds. In the previous step (section 4.3.3.1), the accurate placement of pour points was, to an extent, dependent on the resolution of the display at the time (i.e. to ensure the correct cell was selected, each cell had to be visible onscreen; at lesser display resolution, accurate pour point placement could not be assured as individual cells were comparatively much less visible). The snap pour tool provided a means by which to rectify any inaccuracies associated with the initial placement of pour points, since the tool is designed to identify and snap a specific pour point to the cell of highest flow accumulation within a specified distance from that particular pour point. Accordingly, the pour point data and flow accumulation raster were used as the input data to the tool and a snap distance of 25 m (size of one cell in the display) specified; this distance was considered appropriate, as initial placement of the pour points was deemed to be accurate to individual cell level. The tool was then run to create an accurate raster representation of each pour point dataset, and this raster output used as input to the subsequent 'Watershed' (described below) and 'Euclidean Distance' (described in section 4.3.3.5) tool processes in the model.

4.3.3 3 Creation of watersheds

Initial watershed raster

Watersheds were derived for each pour point using the 'Watershed' tool from within the spatial analyst hydrology toolbox. The newly created pour point rasters (snapped pour points) and the flow direction raster comprised the input data for the tool. Each watershed for each stream was then calculated as the total number of upstream cells draining to the specific pour point defined for that location. Each cell identified as watershed was assigned a value of 1 and all other cells classified as 'no data' to produce a single class raster output displaying the spatial extent of the derived watershed for each pour-point defined stream location. These outputs were then used to create digital elevation models of each stream watershed.

Creation of watershed DEM's

DEM's for each watershed were created using the times tool from within the spatial analyst math toolbox. Using the initial watershed rasters and the 'filled' DEM of the study area as inputs, this tool simply multiplied the values of the two rasters (i.e. each watershed multiplied by the filled DEM) on a cell by cell basis to produce specific DEM's for each watershed; these containing the relevant topographic information from which to derive morphometric parameters for each stream watershed.

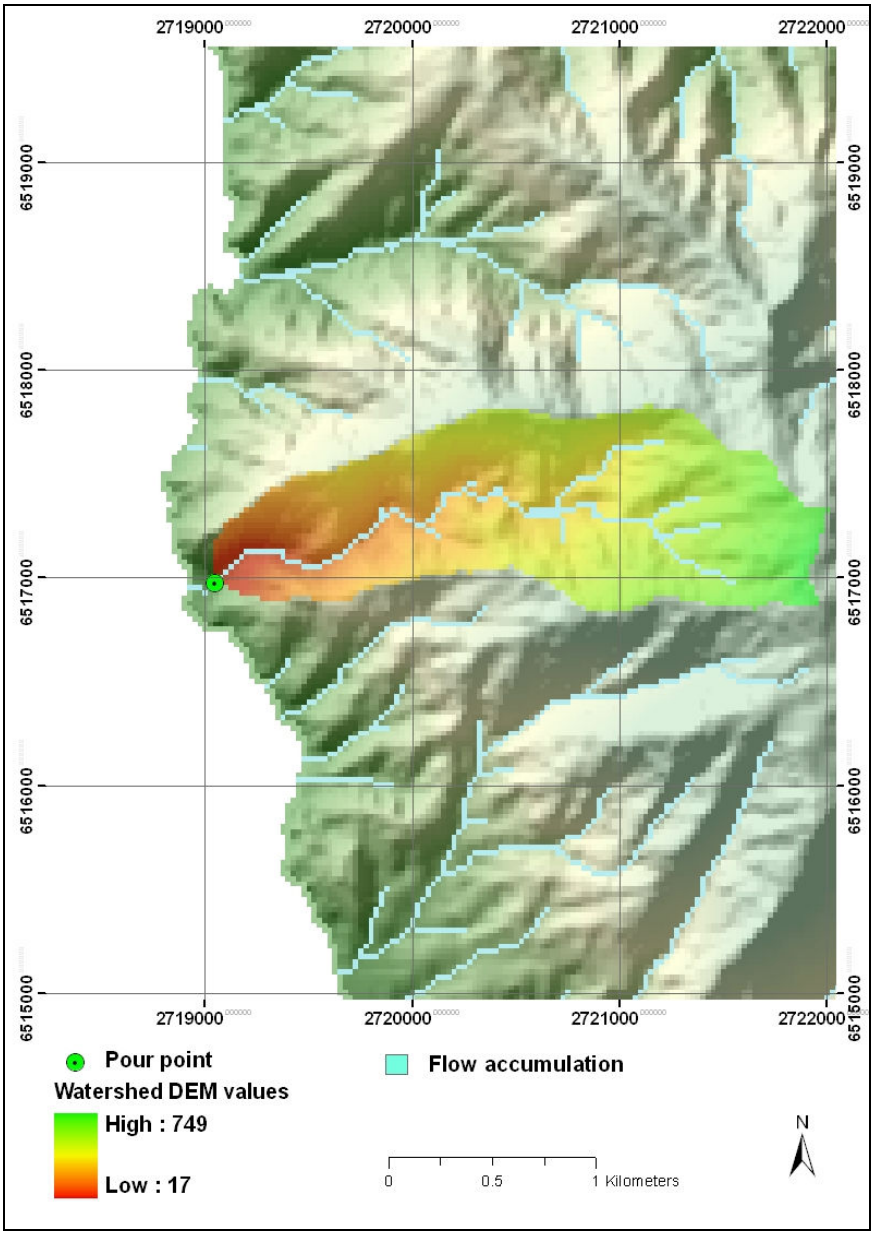

Figure 4.12: Example of Watershed DEM output and associated pour point, displayed on the hillshade DEM background.

4.3.3.4 Extraction of watershed morphometric parameters

Morphometric parameters associated with each stream watershed were extracted from the watershed DEM outputs utilizing the 'Zonal Statistics as Table' tool from within the spatial analyst zonal toolset. In order to run the tool, the zones from which statistics were to be derived had to first be specified; these relevant zones were defined by the initial watershed outputs. When run, this tool summarized the elevation statistics (extracted from the watershed DEM) for each watershed (the zone of interest) and reported the results as a table. Accordingly, this process derived all morphometric statistics associated with each stream watershed, with the exception of watershed length. Additional steps were required to derive length, as described below.

4.3.3.5 Creation of distance rasters to identify watershed lengths

Three main tools were utilized to facilitate the identification and extraction of watershed length parameters associated with each individual watershed, these being the 'Euclidean Distance' tool from the spatial analyst distance toolbox , the 'Times' tool from the spatial analyst math toolbox, and the 'Zonal Statistics' tool from the spatial analyst zonal toolbox.

The first step in the process involved utilizing the Euclidean Distance tool to identify the explicit radial distance outward from each pour point. An output raster was produced (Figure 4.13) displaying distances as concentric rings radiating outward from the point of origin (the pour point). These outputs were then multiplied by the initial watershed rasters using the Times tool, to produce a distance raster of each watershed (i.e. a distance raster showing distances outward from the pour point defined within the zone of the watershed for that point).

Finally, the Zonal Statistics tool was used to identify the cell (or cells) with the highest value in each distance raster (i.e. cell furtherest from the pour point), this corresponding to the maximum distance from the pour point in that particular watershed and hence defining the desired watershed length value. Accordingly, distance raster outputs were used as inputs to the tool and zonal maximum specified as the statistic to be calculated. This produced a raster output in which all cells were

coded as the maximum distance value identified for that specific watershed-defined zone

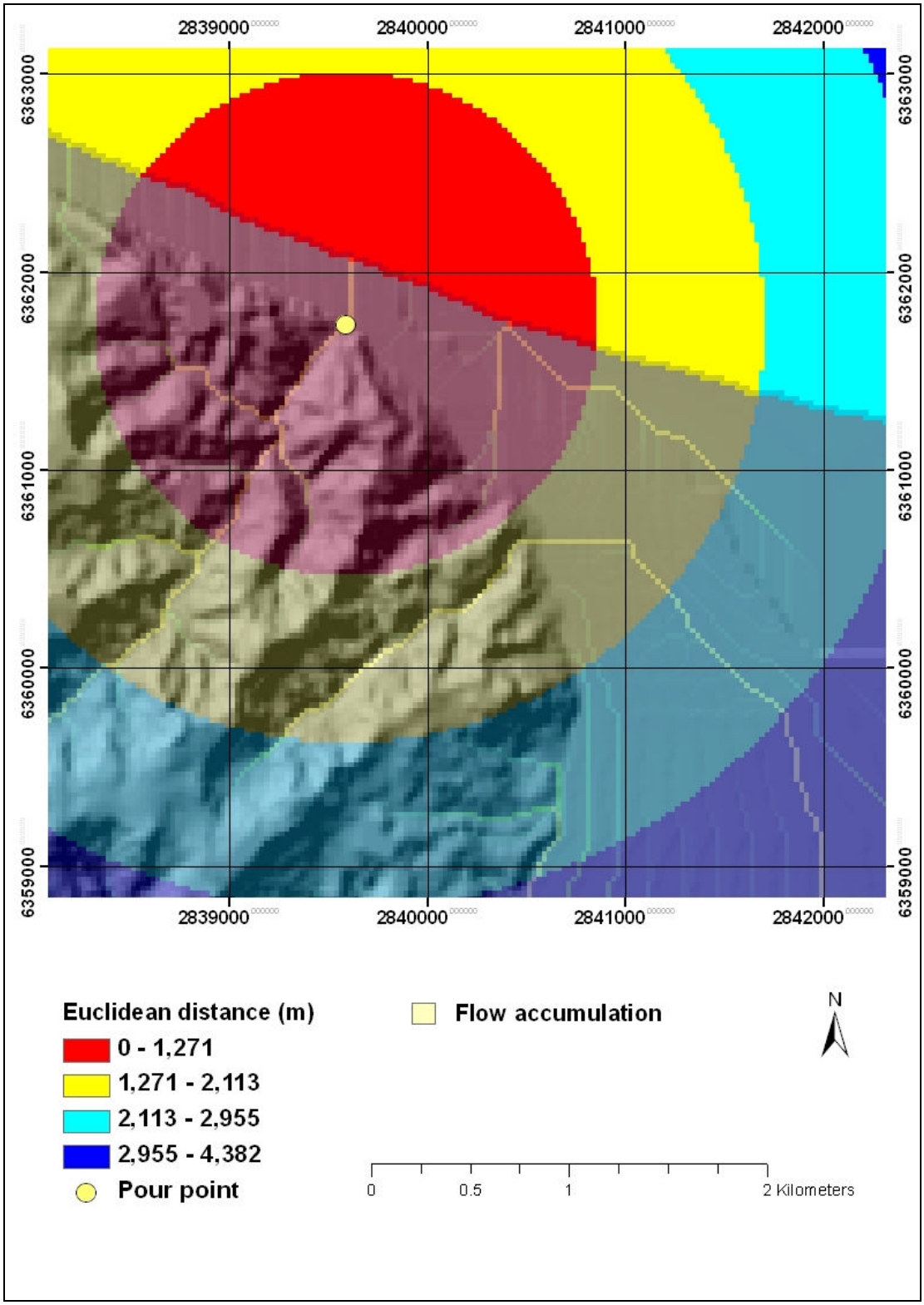

Figure 4.13: Example of the Euclidean distance output (displayed on the hillshade DEM background) showing concentric distance rings radiating outward from the pour point origin.

4.3.3.6 Export of watershed morphometric parameters into Microsoft Excel

Following extraction of morphometric statistics for each watershed, all relevant data were manually exported to dbf (database) files. These files were then opened in Microsoft Excel and copied to a common spreadsheet holding all the morphometric statistics for each stream watershed. All statistics were then converted into metric units to facilitate analysis.

4.3.3.7 Calculation of Melton's Ratio and identification of hazard thresholds

Melton ratio calculation

Melton ratio's *(R)* were calculated within excel according to the formula:

$(R) = H_b / \sqrt{A_b}$

where H_b is basin relief and A_b basin area, after Melton (1965)(see Chapter 3, section 3.3). Cells were accordingly formatted according the relevant equation to calculate values for each stream watershed derived for study area.

Hazard thresholds for Melton Ratio and Watershed length parameters

Melton ratio (*R)* values for each stream watershed were allocated into three categories, corresponding to the hazard thresholds for debris-flow, debris-flood and fluvial phenomena, defined by Wilford et al. (2004) and Jackson et al. (1987) (see Chapter 3, section 3.3.1). These categories are described below:

- *R* <0.30 - Identified by Jackson et al. (1987) and Wilford et al. (2004) as threshold below which conventional fluvial processes are generally the dominant fan-forming processes in a watershed

- *R* 0.30 – 0.60 - Identified by Wilford et al. (2004) as the threshold range for watersheds prone to debris-floods

- *R* >0.60 - Identified by Wilford et al. (2004) as the threshold above which watersheds are prone to debris-flows

In addition, threshold classes were also defined for values of watershed length (WL) (based on the model proposed by Wilford et al. (2004), these classes determined as:

- WL <2.7 km – Debris-flows are a prominent fan-forming process in the watershed
- WL >2.7 km – Conventional fluvial processes and/or debris-floods are the dominant fan-forming process in the watershed

This gave rise to 6 different categorical combinations (labeled A to F) of $\underline{R}$ and WL, as shown in Table 4.1 below:

Table 4.1: Category combinations of Melton ratio (*R*) and Watershed Length (WL)

Category	Combination
A	*R* <0.30; length >2.7 km
B	*R* <0.30; length <2.7 km
C	*R* 0.30 – 0.60; length >2.7 km
D	*R* 0.30 – 0.60; length <2.7 km
E	*R* >0.60; length >2.7 km
F	*R* >0.60; length <2.7km

4.4 Research methodology – Field reconnaissance approach

The main aim of the field investigation for this research was to test whether values of Melton's ratio (*R*) and watershed length for watersheds in the study area, could be used to give a preliminary indication of debris-flow hazard at their corresponding drainage points (fan). In order to do this, suitable sites were first selected according to values of *R* and watershed length obtained for each stream watershed through the GIS procedure. Geomorphic criteria corresponding to debris-flow, debris-flood and flood hazards were then formulated to aid identification of deposits in the field. This was followed by field excursion to each selected site to obtain the relevant data to test the hypothesis.

4.4.1 Site selection

Eighteen sites were selected for field investigation, 9 in each of the Coromandel and Kaimai regions to ensure a representative spread over the study area. These sites were selected according to combinations of the threshold categories defined for Melton's *R* and watershed length identified in section 4.3.3.7.; categories are described below:

Of the 9 locations selected for each region:

- 3 streams were selected exhibiting *R* <0.30 and watershed length >2.7 km (category A, Table 4.1);
- 3 with *R* 0.30 – 0.60 and watershed lengths >2.7 km and/or <2.7 km (categories C, D); and
- 3 with *R* >0.60 and watershed length <2.7 km (category F)

No category B streams were selected because they were assumed to show similar deposits to that found in category A (i.e. fluvial watersheds in the literature are observed to have R <0.30; Jackson et al., 1987; Wilford et al, 2004). Category A is identified in the literature to define the optimal range for watersheds prone to fluvial processes (fluvial processes dominant in watersheds with R<0.30 and WL <2.7 km; Wilford et al. (2004). Hence better evidence is likely to be observed at streams in this category than for category B. No category E streams were selected as only 3 watersheds in the study area plot in this category.

Values of *R* and watershed length (WL) for selected locations are shown in Table 4.2. The general geographical locations of the stream sites investigated are shown in Figures 4.14 and 4.15 and specific site and pour point locations in Appendix 4.

Table 4.2: Values of *R* and watershed length for stream watershed locations in the study area

Stream location & *R*/WL category	**Melton ratio (*R*)**	Watershed length (km)
(A) R <0.30; WL >2.7 km		
Waiwhango stream	0.15	4.31
Te Puru stream	0.14	6.49
Taruru stream	0.17	6.52
Waitoki stream	0.20	4.07
Putangi stream	0.19	4.05
Matutu stream	0.30	3.35
(C) & (F) *R* 0.30-0.60; WL >2.7 km & <2.7 km		
Otohi stream	0.35	3.31
Otuturu stream	0.39	1.98
Waiotahi stream	0.46	1.98
Wahine stream (2)	0.47	3.41
Gordon stream	0.41	4.14
Stanley stream	0.38	4.40
(F) *R* >0.60; WL <2.7 km		
Waitoitoi stream	0.68	2.66
Whakanekeneke stream (2)	0.71	1.65
Karaka stream (3)	0.61	1.16
Lipsy stream	0.76	2.21
Moonlight stream	0.95	1.89
Gordon Rd.: Unnamed stream	1.51	1.47

(*n*) Indicates watershed derived for an unnamed tributary draining into the main stream

4.4.2 Formulation of criteria to identify evidence for hydrogeomorphic hazards

Sedimentological and morphological geomorphic criteria corresponding to typical field evidence indicative of debris-flow, debris-flood and fluvial–flood phenomena were formulated through review of literature. The specific criteria utilized to identify evidence for debris-flow, debris-flood and fluvial processes in the field are briefly described below:

Debris-flow criteria:

- Narrow channel, small width to depth ratio
- Semi-circular to U-shaped channel
- Sinuous terraces formed by flow margins

- Channel scoured to bedrock
- Lobate areas of even age vegetation younger than the surrounding growth
- Old bark scars high on trunks and branches of trees
- Presence of scattered large, woody debris
- Coarse deposits beyond the channel on the fan
- Depositional lobes several meters high in the channel and on the fan surface
- Levees of coarse angular material aligned along the stream on upper fan
- Boulders rolled against trees on the channel banks or lodged high above stream channel
- Isolated boulders in the channel and on the fan surface with diameters >1m
- Massive boulders perched on top of finer deposits
- Deposits are massive, stratification absent, with no imbrication,
- Poorly-sorted and matrix supported deposits
- Angular to subangular clasts
- A-axis of clasts oriented parallel to flow or randomly oriented

Debris-flood criteria:

- Channel exhibits medium to large width to depth ratio
- Bars sheets, fans and splays notable at local scale in the channel
- Bouldery deposits beyond the channel on the fan
- Presence of large, woody debris in the channel and/or on the fan
- Moderate to poor sorting of deposits
- Clast-supported deposits
- Deposits have mixed clast orientation: A-axis of large boulders perpendicular to flow, pebbles and small cobbles parallel to flow direction
- Deposits exhibit weak imbrication and collapse packing in coarser sediment fraction
- Poorly stratified deposits, comprised of loose mixtures of coarse gravel and sand
- Clasts more rounded to sub-angular

Fluvial criteria:

- Meandering or braided channel morphology
- Large width to depth ratio
- Moderate to well-sorted deposits
- Deposits are clast supported
- Well imbricated deposits
- Presence of sedimentary features (e.g. cross-bedding, flame structures)
- Presence of stratification and layering
- Clasts more sub-rounded/rounded
- A-axis of larger clasts perpendicular to flow
- Rare deposits beyond the channel on the fan
- Bars sheets, fans and splays notable at local scale in the channel

4.4.3 Field reconnaissance

4.4.3.1 April-May 2006 reconnaissance

Initial field reconnaissance of the study area was undertaken between April 26 and May 1 2006, to familiarize with the study area and the evidence indicative of hydro-geomorphic processes. Reconnaissance was carried out with the help of Associate Professor Tim Davies (thesis supervisor) of the University of Canterbury, and Dr. Mauri McSaveney of GNS Science, New Zealand.

Localities that had previously experienced the occurrence of debris-flow hazard were visited and briefly explored. These included Te Aroha, a location that experienced devastating debris-flows in February 1985 (described in Chapter 2, section 2.4.2), Thames, an area which has experienced numerous flooding events (EW, 2007), and Matata, the location of a debris-flow event in June 2005 (described in Chapter 2, section 2.4.3).

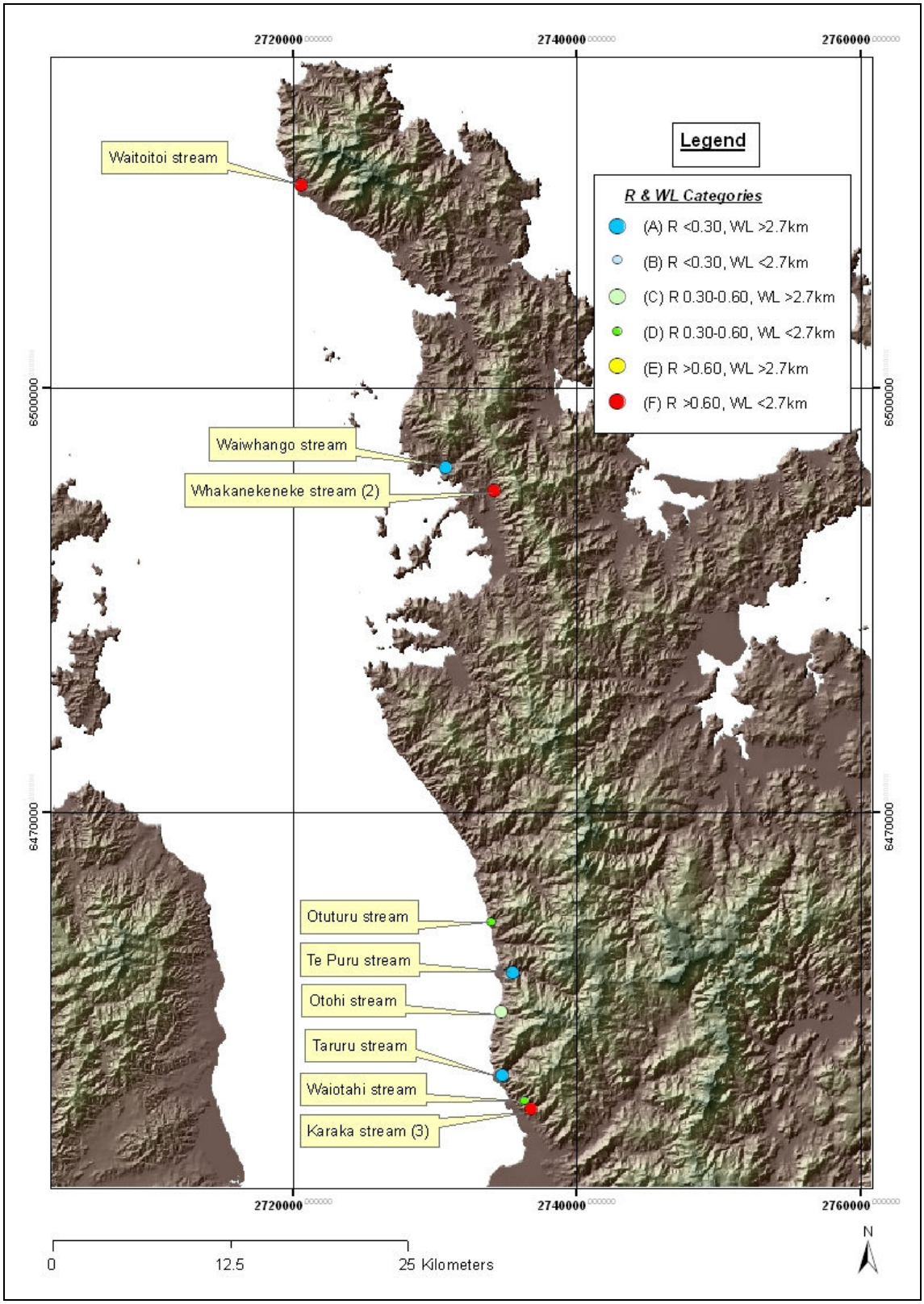

Figure 4.14: DEM of the Coromandel Range region showing the location of specific stream sites surveyed in the field investigation

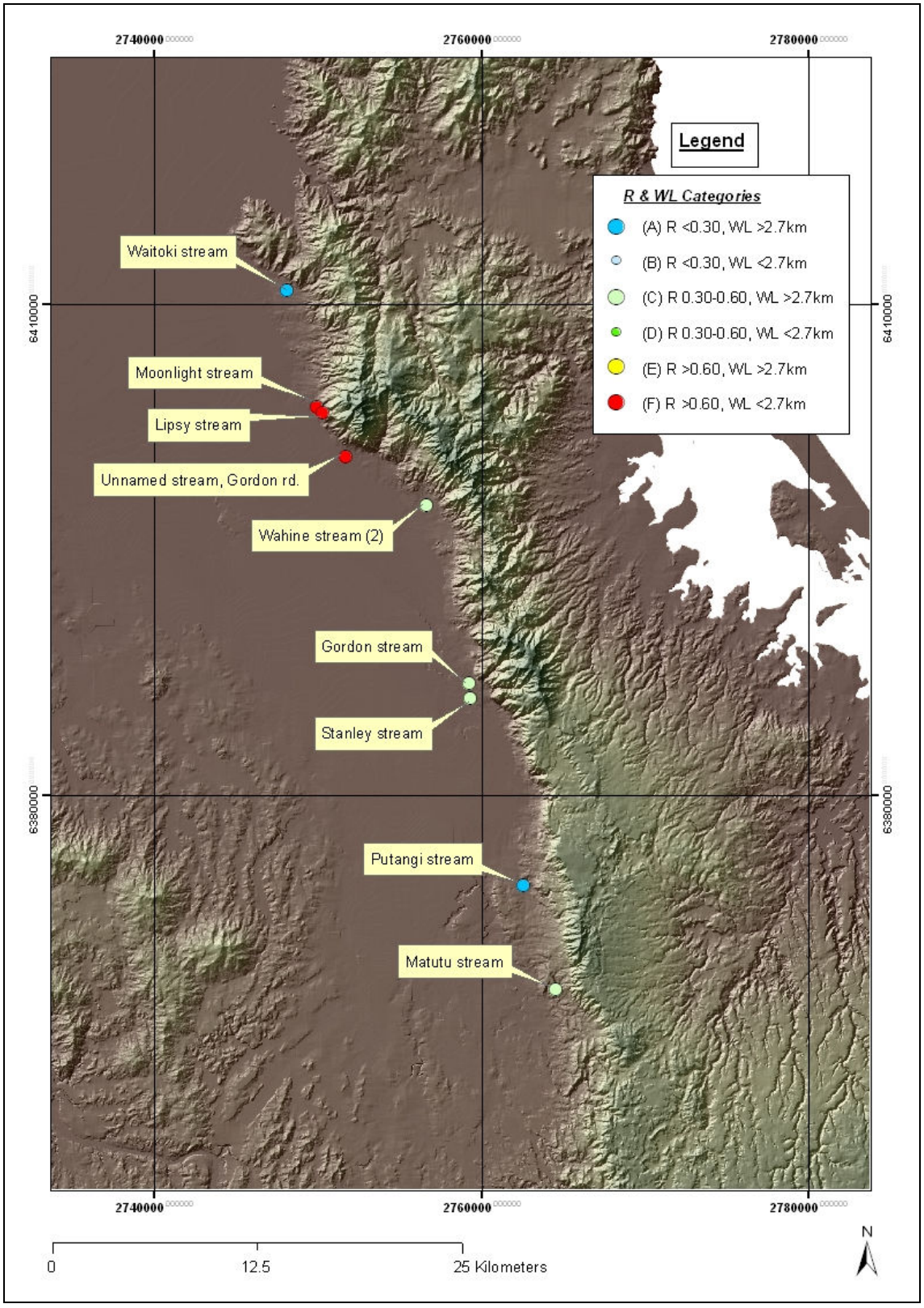

Figure 4.15: DEM of the Kaimai Range region showing the location of specific stream sites surveyed in the field investigation

4.4.3.2 December 2006 and January 2007 field survey

Field investigation of selected sites was carried out for the Coromandel region between December 11 – 20 2006, and for the Kaimai region, from January 13 – 24 2007. Prior to field excursion, letters were sent out to land owners to request permission for access to the relevant locations. Sites were visited by car and the channel and fan surveyed on foot. The stream channel and fan were investigated for 200 – 500 m up-stream and down-stream of the GIS-defined pour point location for that stream location. The presence or absence of the specific criteria corresponding to geomorphic surface and subsurface evidence (in river cut exposures) for debris-flow, debris-flood and fluvial processes were then recorded and photographs taken for each location, along with additional information on overall watershed morphological appearance, lithologies, and in cases, qualitative information from residents on the stream history.

4.5 Research methodology – Air photograph approach

To complement the field investigation methodology, stereo-pair aerial photographs of the study region were acquired from New Zealand Aerial Mapping Ltd. (NZAM). True colour hard copy images taken in 2002 and of scale 1:40 000 were initially obtained to facilitate broad inspection of the study area and individual watersheds identified in the GIS procedure. Once obtained however, it was found that the resolution of the photographs was insufficient to allow comprehensive scrutiny of the study region and individual sites. Consequently, additional 1:10 000 true colour hard copy stereo-pairs (2002) were acquired. Due to the expense of these photographs, only one stereo-pair was initially ordered to clarify whether acquisition of these photographs would be cost-effective. It was concluded that such photographs offered little in terms of use for the identification of watersheds with morphometric characteristics indicating an ability to generate debris-flow hazards, because a large proportion of relevant channels and fans were obscured by vegetation and/or modified by anthropogenic activity. Accordingly, no further use was made of aerial photographs.

4.6 Statistical processing and analysis methodology

4.6.1 Field data analysis and statistical processing methods

Following collection of the data in the field, data were entered into a Microsoft Excel spread-sheet for manipulation and analysis. Specifically, geomorphic evidence for debris-flows, debris-floods and fluvial-flood hazards was organized according to their respective criteria, and percentages of observed criteria calculated for each according to the following formula:

Observed % = Number of observed criteria / Total number of criteria

Where certain criteria were unable to be observed in the field (i.e. due to steep terrain, dense vegetation) N/A was recorded for that particular criterion and this element not included in the calculation, as shown, for example, in Table 4.3.

Table 4.3: Example calculation of criteria observed in the field

Debris-flow criteria	**Stream X**	**Stream Y**
Angular-subangular clasts	Y	N
Poorly-sorted and matrix supported deposits	Y	Y
Semi-circular to U-shaped channel	Y	N/A
Total no. observed criteria	**3/3**	**1/2**
Total observed %	**100**	**50**

Information on observed % of criteria for each hazard at each stream location was then exported into Statistica (version 7.0) and compared against the Melton ratio (*R*) and watershed length values defined for each stream watershed to quantify relationships between variables. This data was displayed graphically to aid interpretation of relationships using scatter-plots and box and whisker plots. Linear regression analysis was performed on the data to clarify the strength of relations between Melton's *R* and observed criteria % for locations in the entire region. To account for the small sample sizes examined, it was chosen to set α at 0.01 to test for significance (Hair et al, 2006).

In addition to the data derived for stream locations in the study area, the GIS 'Watershed model' was also run to produce watershed data for a number of other areas in New Zealand, known to have experienced debris-flows in the past. This data was derived to facilitate useful comparison between regions. Sixteen of the watersheds are located in the vicinity of the Southern Alps of the South Island, New Zealand (Figure 5.27, Chapter 5). These areas are characterized by metamorphic lithologies and widespread glacial and colluvial sediments, in contrast to the predominant volcanic geology of the Coromandel/ Kaimai region (de Scally and Owens, 2004; Christie et al. (2001); Skinner, 1986). The locations of each of these stream watersheds are detailed in Table 4.4. Notable locations to have experienced destructive debris-flows include Awatawarariki and Waitepuru streams, Matata in 2005 (see Chapter 2, section 2.4.3) and the Kowhai River, South Canterbury, in 1975 (Kimbu, 1991). Most occurrences at the other locations are not well documented, or are the subject of confidential client reports (Davies, T.R, pers.comm, 25/06/07). Debris-flow deposits are well observed at streams in Turiwhati and at Carew Creek, Lake Brunner, while Pipson Creek, Stony Creek, Boyle River, Yellow and Bullock Creeks have all been reported as active in recent times (i.e. 1990's – present) (Davies, T.R, pers.comm, 25/06/07).

Table 4.4: Stream watershed locations outside the study area

Name	Location	NZMG Easting	NZMG Northing
Bullock Creek	Mt Thomas, Canterbury	2461090	5781830
Havelock Creek	Karangarua	2257200	5736450
Stoney Creek	Tatare	2284260	5755780
Yellow Creek	Fox Glacier	2271520	5742110
Bullock Creek	Fox Glacier	2263040	5740440
Pipson Creek	Makarora	2209900	5657470
Waterfall Creek	Lake Hawea	2206760	5640820
Candy's Creek	Otira	2392320	5813020
Halpin Creek	Arthurs Pass	2393880	5802560
Greyneys Creek	Arthurs Pass	2394700	5800890
Unnamed Creek I	Boyle River	2460260	5856810
Unnamed Creek II	Boyle River	2462780	5854680
Carew Creek	Lake Brunner	2378720	5839170
Turiwate Creek	Turiwhate	2369000	5828530
Grahams Creek	Turiwhate	2370600	5828130
Unnamed Creek	Turiwhate	2368140	5829100
Kowhai River	Peel Forest, South Canterbury	2368000	5699220
Awatarariki Strm	Matata	2839520	6361710
Waitepuru Strm	Matata	2840440	6360630

Chapter Five

GIS and Field investigation results

5.1 Introduction

Chapter five presents the results obtained through the GIS procedure and field investigation. The chapter begins with a description of the trends in the values of Melton ratio (*R*) and watershed length derived for stream locations in the study area. This is followed by an account of the evidence observed for debris-flow, debris-flood and flood processes at selected stream locations in the study area. Relationships between the two datasets are then investigated. Finally, a description of the trends in the values of *R* and watershed length for stream watershed locations outside the study area known to have experienced debris-flows is presented. No attempt will be made in this chapter to interpret the results. Instead, a full discussion and interpretation of all results in the context of the thesis aims and objectives will be provided in Chapter 6.

5.2 Melton ratio (*R*) and watershed length values derived for stream watershed locations in the study area

Values of Melton ratio (*R*) and watershed length were calculated for 302 stream watersheds in the study area. A plot of *R* against watershed length for all stream watershed locations is illustrated in Figure 5.1. An exponential-like relationship is apparent between the variables, with those watersheds exhibiting low *R* values (<0.20) tending to have longer watershed lengths (>5 km), and vice-versa. In terms of variance, watersheds in the study area generally exhibit lengths between 1 and 7 km with only a small number exceeding lengths of 10 km. The majority of *R* values are distributed between 0.10 and 0.45 with only one watershed exhibiting a ruggedness value greater than 1.0 (1.51).

Figure 5.1 is divided into 6 different categorical combinations/quadrants of *R* and watershed length (A-F), based on the model proposed by Wilford et al. (2004) (see chapter 3). Table 5.1 shows the frequency distribution of values in each of these categories for watersheds in the study area The largest proportion of watersheds

(39%) fall into category A (watersheds with low ruggedness values (R <0.30) and longer watershed lengths (>2.7 km)). Only 10 % of the watersheds exhibit R values greater than 0.60, with the majority (60 %) having R values less than 0.30.

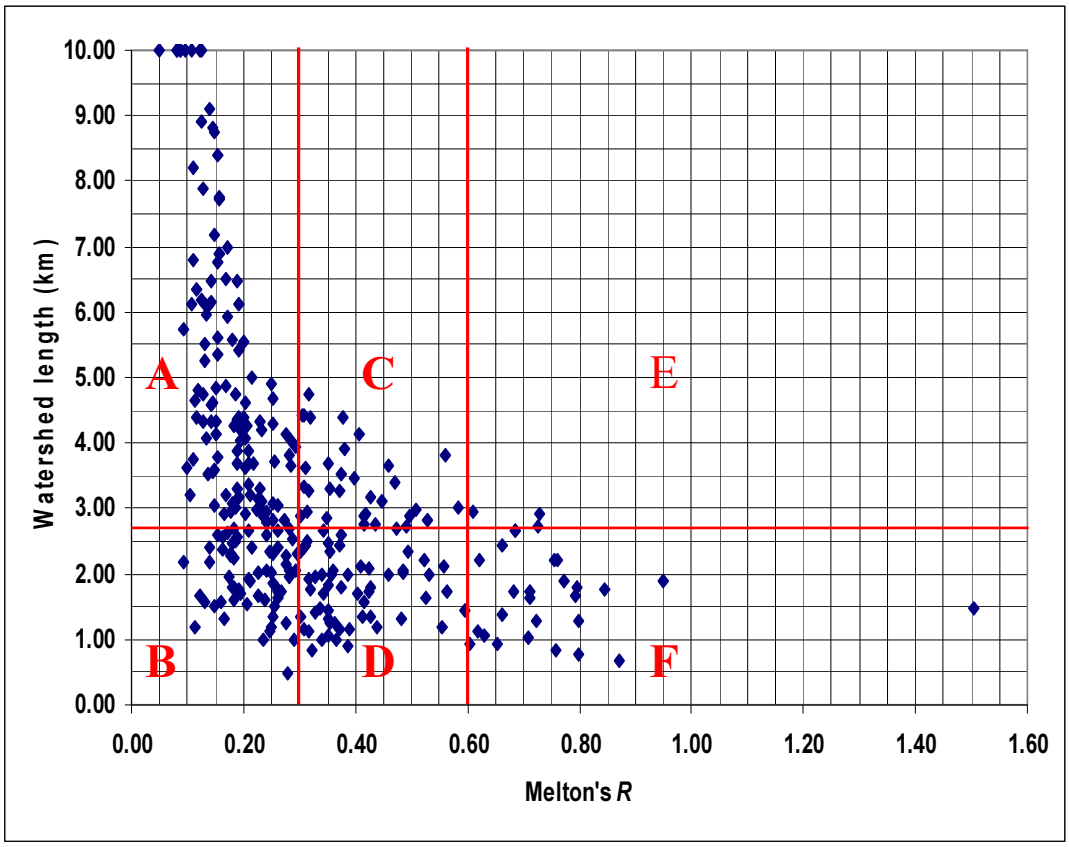

Figure 5.1: Scatterplot of Melton ratio (R) and watershed lengths for all stream watersheds in the study area. Quadrants A – F represent categorical combinations of R and watershed length based on the model proposed by Wilford et al. (2004).

Table 5.1: Frequency of stream watersheds within categorical combinations of R and watershed length

Melton's (R) and Watershed length (WL) categories	Frequency (no.)	Frequency (%)
(A) R <0.30 and WL >2.7 km	117	39
(B) R <0.30 and WL <2.7 km	64	21
(C) R 0.30 – 0.60 and WL >2.7 km	33	11
(D) R 0.30 – 0.60 and WL <2.7 km	58	19
(E) R >0.60 and WL >2.7 km	3	1
(F) R >0.60 and WL <2.7 km	27	9
Total:	302	100

Figure 5.2 illustrates the geographic distribution of watersheds in the study area according to the categories of *R* and watershed length shown in Table 5.1 and Figure 5.1. Watersheds in category A are well distributed across the study area, while those in category B are most common in the eastern (near Kuaotunu) and northern regions (in the vicinity of Coromandel Township and Colville) of the Coromandel peninsula. Category C watersheds are more restricted in their extent, being largely confined to the south of the Kaimai range between Te Aroha and adjacent to Wardville on the range front. Those in category D are particularly common on the western range front of the Coromandel and Kaimai ranges, the highest concentration of these watersheds located on the west coast of the Coromandel Peninsula between Thames and Kereta. Watersheds in categories E and F are comparatively rare in the study area and restricted to the western range front. All three watersheds in category E are located between Te Aroha and Wardville. The highest concentrations of Category F watersheds are located in the vicinity of Te Aroha and at the southern extent of the Kaimai range (adjacent to Matata). In addition, two smaller clusters exist in the vicinity of Thames and in the far north of the Coromandel Peninsula (just south of Port Jackson).

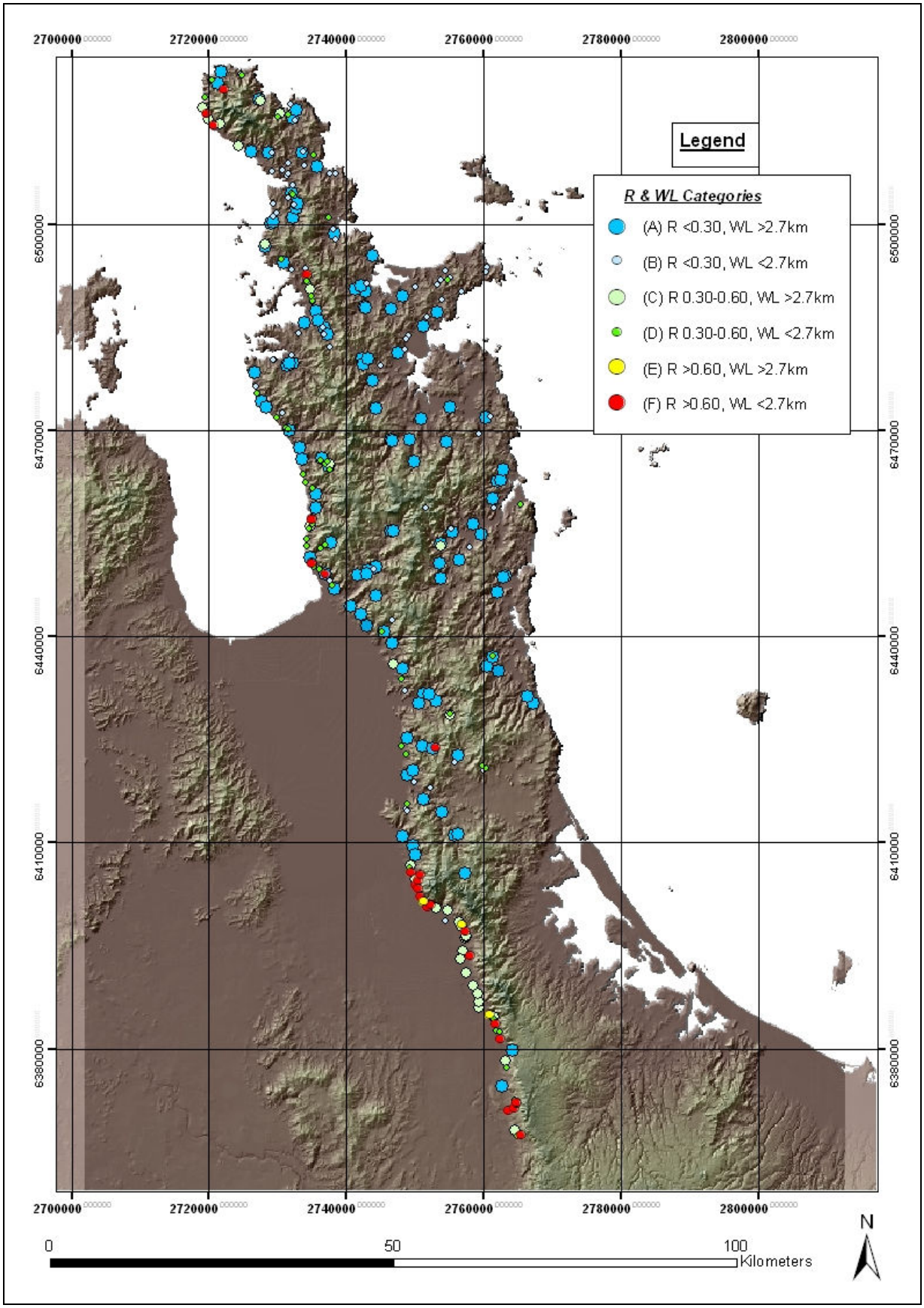

Figure 5.2: The geographic distribution of stream watersheds in the study area according to categories of *R* and watershed length.

5.3 Criteria observed at stream locations in the study area

As mentioned in Chapter 4, section 4.4.1, 18 stream watershed locations within the study area were selected for field investigation. This involved survey of the active stream channel and fan for geomorphologic and sedimentological evidence indicative of debris-flow, debris-flood and flood processes. A summary of the evidence found at each stream location is presented below.

5.3.1 Debris-flow evidence

Figure 5.3 shows the amount of criteria observed for debris-flows at stream watershed locations in the study area. Highest amounts of debris-flow criteria were observed at stream locations in the vicinity of Te Aroha in the Kaimai Range. Lispy Stream (94 % criteria observed) exhibited the highest amount of evidence for debris-flows, with huge isolated boulders up to 6 m in size (Figure 5.4) in the stream channel and on the fan, and 'debris-dams' comprised of crushed gravel, sizable boulders and tree trunks within the channel (Figure 5.5) observed at this location. Unnamed Stream on Gordon Rd. (87 %) and Moonlight Stream (76 %) also showed high amounts of evidence including scattered woody debris and abundant, large (2-4 m), sub-angular to angular boulders rolled against trees on the fan. Further north, good evidence for debris-flow depositional lobes was observed at Waitoitoi Stream (76 %) (Figure 5.6), while Karaka Stream (71 %) exhibited the characteristic semi-u-shaped channel scoured to bedrock that is often associated with channels prone to debris-flows (McSaveney and Betham, 2006). Other streams to also show good evidence for debris-flows included Whakanekeneke Stream (64 %), Otuturu Stream (59 %) and Wahine Stream (59 %).

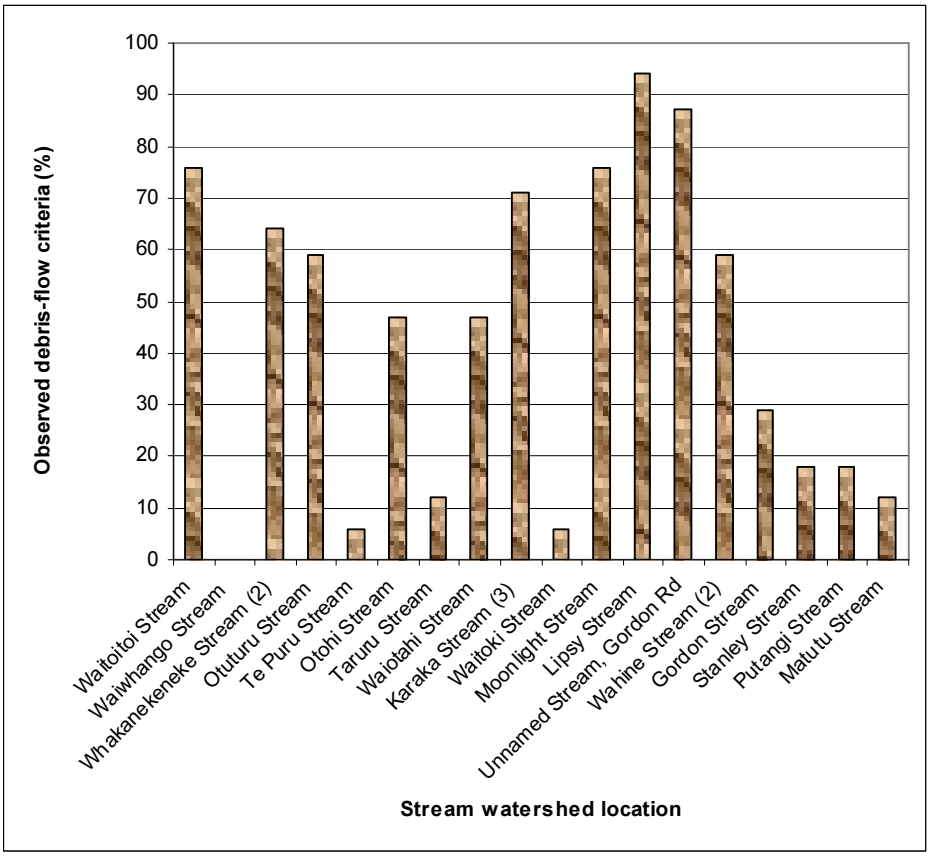

Figure 5.3: Percentage of debris-flow criteria observed at stream watershed locations in the study area.

Figure 5.4: Enormous boulders up to 6 m in size (note cap for scale) were observed in the stream channel and on the fan at Lipsy Stream.

Figure 5.5: An example of one of the many 'debris dams' observed in the channel at Lipsy Stream.

Figure 5.6: Poorly sorted, matrix supported and gravely topped lobes were observed at a number of locations in the stream channel at Waitoitoi Stream.

5.3.2 Debris-flood evidence

The amount of criteria observed for debris-floods at stream locations in the study area is shown in Figure 5.7. Wahine, Gordon and Stanley Streams were found to exhibit the highest amounts of evidence (80 %) for debris-floods. At Wahine Stream, cobble-boulder-topped, lobed deposits and large (1-2 m), sub-angular boulders were observed on the fan surface adjacent to the active channel (Figure 5.8). Loose mixtures of tree trunks/branches, boulders and gravel were noted in the stream channel at Gordon Stream (Figure 5.9), whilst clast-supported, weakly imbricated alluvium layers were identified in stream cuts at Stanley Stream. Significant evidence was also observed at Otohi Stream (78 %) where woody debris, large sub-rounded to sub-angular boulders (0.5 -1 m) and poorly stratified, loose mixtures of woody debris, gravel and sand were evident at a number of locations in the stream channel.

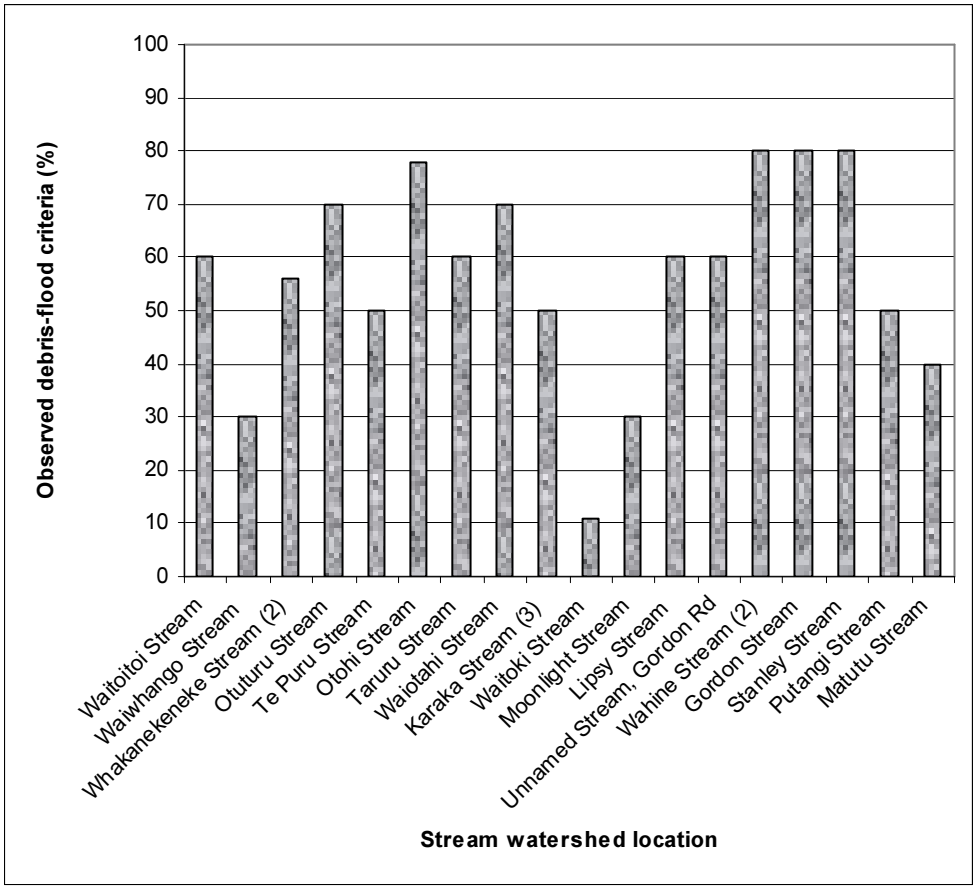

Figure 5.7: Percentage of debris-flood criteria observed at stream watershed locations in the study area.

Figure 5.8: Boulder-topped, lobed deposits observed beyond the stream channel on the fan at Wahine Stream.

Figure 5.9: Tree trunks and branches and loose mixtures of woody debris, gravel and sand were observed on numerous bends in the stream channel at Gordon Stream.

5.3.3 Fluvial evidence

Figure 5.10 shows the amount of fluvial criteria observed at stream watershed locations in the study area. Best evidence for fluvial processes was observed at Te Puru (82 %), Waiwhango (78 %) and Taruru (73 %) streams in the Coromandel Peninsula. At Te Puru and Taruru streams, prevalent fluvial features included the large width to depth ratio of the stream channels, the presence of point bars and the dominant orientation of cobble stones and boulders (A-axis) perpendicular to the flow direction (Figure 5.11). Further south in the Kaimai Range, clast supported stream cut deposits were observed at Stanley Stream (73 %) (Figure 5.12), while at Waitoki (71 %), Putangi (67 %) and Matutu (64 %) streams, a meandering morphology typical of shallow gradient, low energy, fluvially dominated streams was evident.

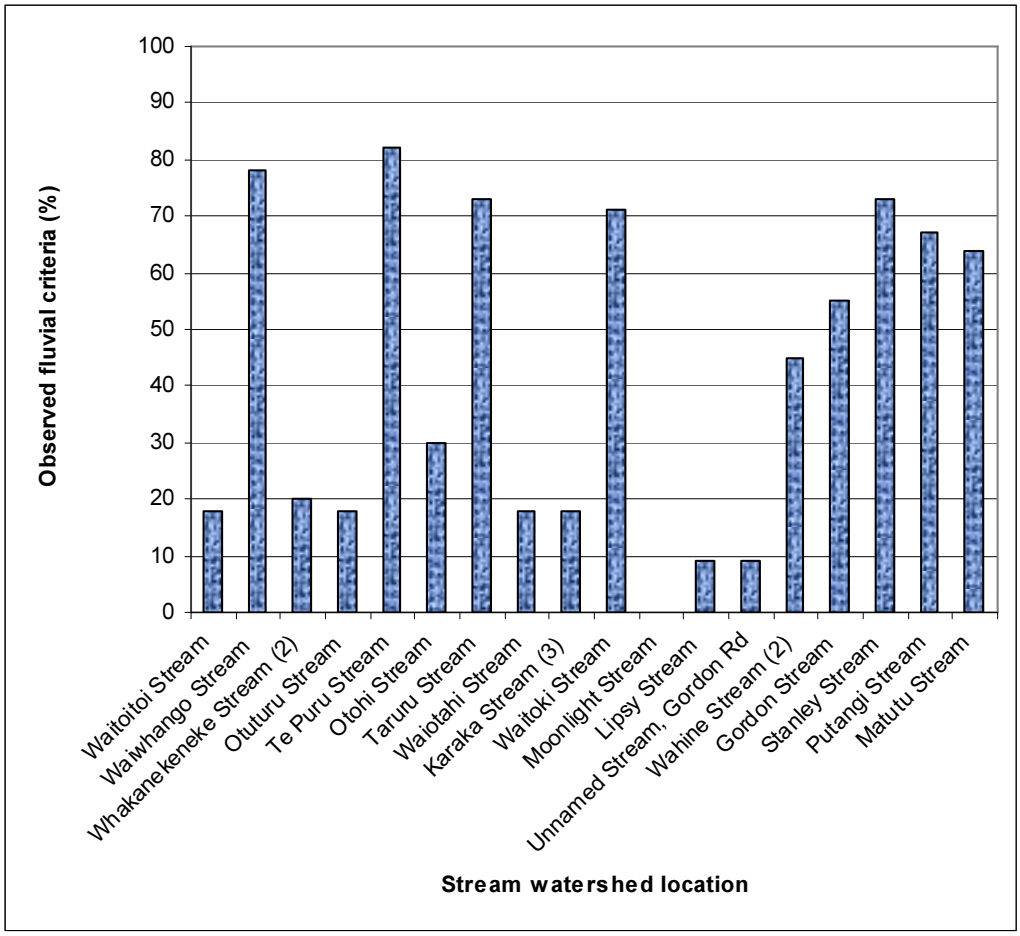

Figure 5.10: Percentage of fluvial criteria observed at stream watersheds locations in the study area.

Figure 5.11: The large width to depth ratio and the presence of bars, sheets and splays in the stream channel were some of the prominent fluvial features observed at Te Puru Stream.

Figure 5.12: Clast supported deposits observed in a stream cut at Stanley Stream

5.3.4 Evidence observed at stream locations in terms of categories of Melton's R and watershed length

5.3.4.1 Category A (R <0.30, WL >2.7 km)

Figure 5.13 shows the amount of evidence observed for debris-flow, debris-flood and fluvial processes at stream locations in category A. All streams exhibited high amounts of evidence for fluvial processes and conversely very low evidence (<18 % criteria observed) for debris-flows. In addition, at Taruru and Putangi streams, high amounts of evidence were observed for both fluvial processes and debris-floods.

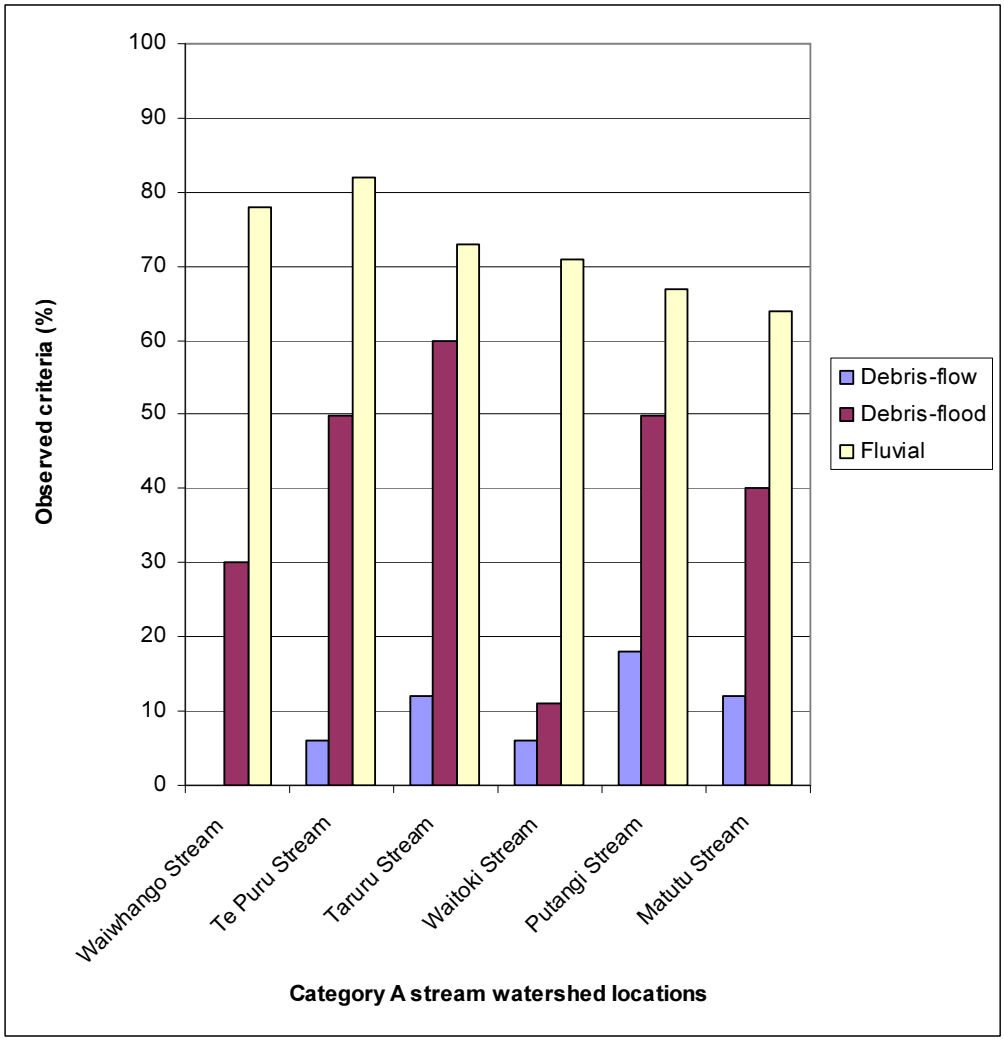

Figure 5.13: Evidence observed for all processes (debris-flows, debris-floods and fluvial processes) at stream watershed locations exhibiting *R* values <0.30 and lengths >2.7 km (category A).

5.3.4.2 Categories C and D (R 0.30 – 0.60, WL >2.7 km and <2.7 km)

The amount of evidence observed for debris-flows, debris-floods and fluvial processes at stream locations in categories C and D is shown in Figure 5.14. A high amount of evidence for debris-floods (>70 %) was observed at all stream locations in these categories. Good evidence (45 – 60 %) was also observed for debris-flows at a number of locations. Furthermore, at Otuturu stream high evidence was observed for both debris-floods and debris-flows, whilst at Stanley stream high evidence was observed for debris-floods and fluvial processes.

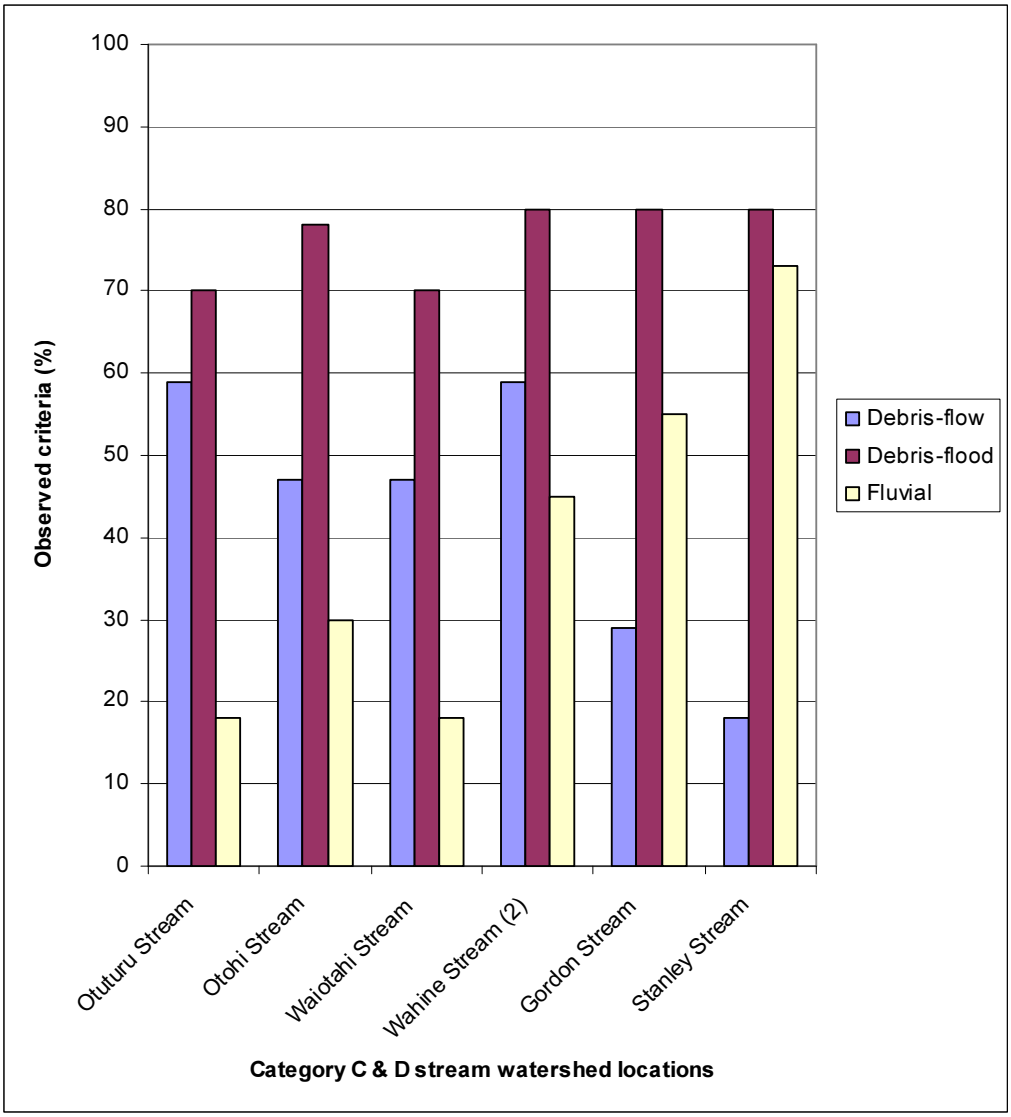

Figure 5.14: Evidence observed for all processes at stream locations in categories C and D.

5.3.4.3 Category F (R >0.60, WL <2.7 km)

Figure 5.15 shows the amount of criteria observed for all processes at stream watershed locations in category F. All streams in this category showed high evidence for debris-flows (5 out 6 locations >70 % criteria observed), with good evidence also observed for debris-floods (5 of 6 locations > 50% criteria observed). Conversely, very little evidence (<20 % observed) was identified for fluvial processes. Two streams in this category (Waitoitoi and Whakanekeneke (2) streams) exhibited high evidence for both debris-flows and debris-floods.

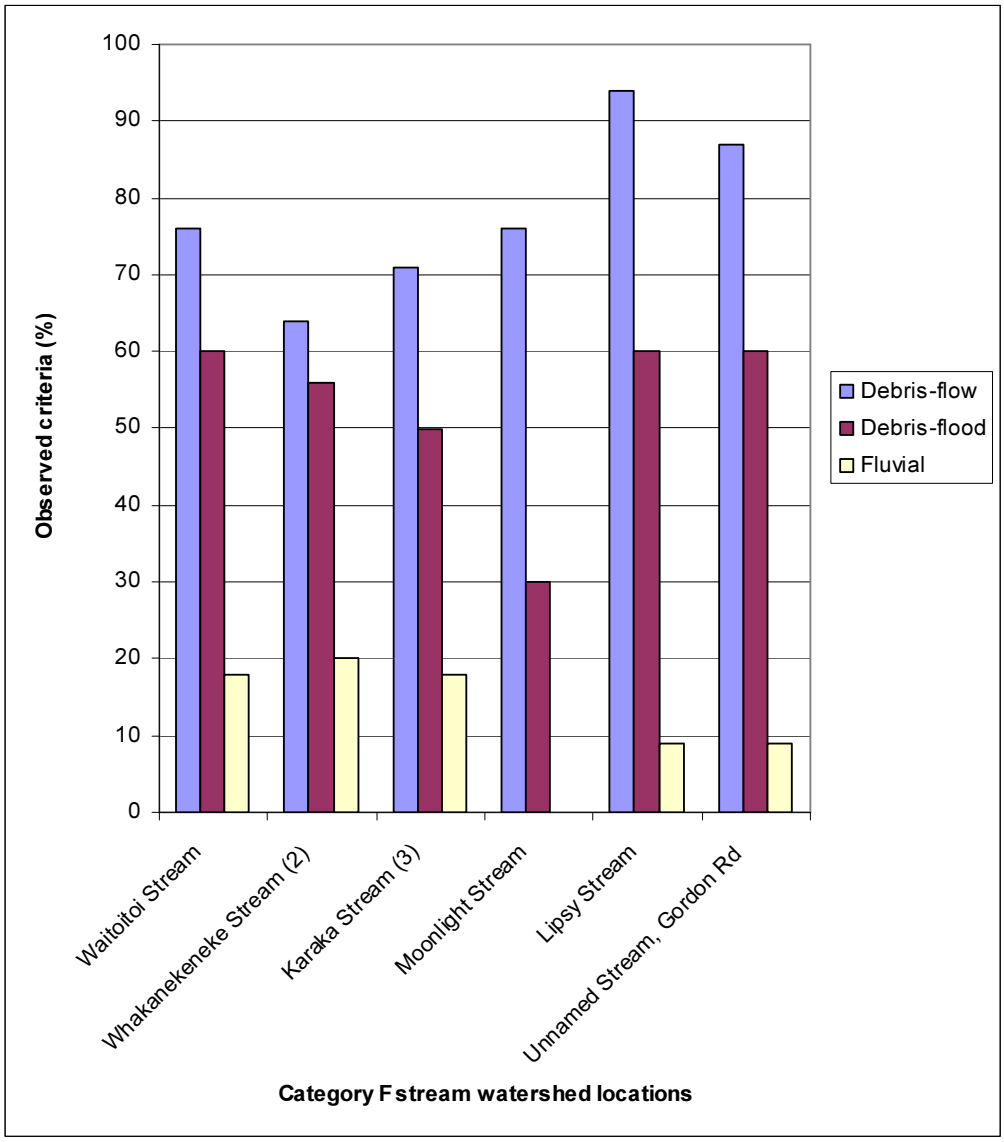

Figure 5.15: Evidence observed for all processes at stream locations in category F.

5.4 Relationships between Melton ratio (R) and watershed length, and observed evidence for hydrogeomorphic processes in the study area

Pearson product moment correlations (linear regressions) were calculated to ascertain relationships between observed evidence for debris-flows, debris-floods and fluvial processes, and individual morphometric parameters Melton's *R* and watershed length. In each regression, a co-efficient of determination (r^2; a value representing the proportion of common variation in the two variables: i.e. the strength or magnitude of the relationship), correlation co-efficient (r; value representing the linear relationship between two variables) and p-value (indicating statistical significance of a relationship; e.g. in this study $p < 0.01$ is considered statistically significant) were derived to evaluate the correlation between the variables (Statistica, 2005). Box-plots were also formulated to analyse relationships between observed evidence and specific categories of *R* and watershed length (see Chapter 4, section 4.3.3.7). For the analyses, one stream location ('Unnamed stream' on Gordon rd) was omitted as it was considered to be an outlier in the data ($R = 1.51$ – only stream location to have an *R* value greater than 1.0).

5.4.1 Melton ratio (R) vs observed evidence

5.4.1.1 R vs. debris-flow evidence

Figure 5.16 illustrates the relationship between Melton ratio (*R*) and observed evidence for debris-flows at stream watershed locations in the study area. A very strong, positive correlation exists between the variables with r^2 (0.81) and r (0.90) exhibiting values very close to 1 (perfect linear relationship). Furthermore; as the derived p-value is <0.01, the correlation is considered statistically significant.

5.4.1.2 R vs. debris-flood evidence

The relationship between *R* and evidence observed for debris-floods (Figure 5.17) is significantly different to that seen above for debris-flows. The correlation is not linear with values of r^2 and r being very close to 0 (0.01 and 0.09 respectively). A subtle pattern is evident in the data however, with the highest amounts of evidence for

debris-floods observed in the middle range of *R* and semi-equal amounts observed either side of these values.

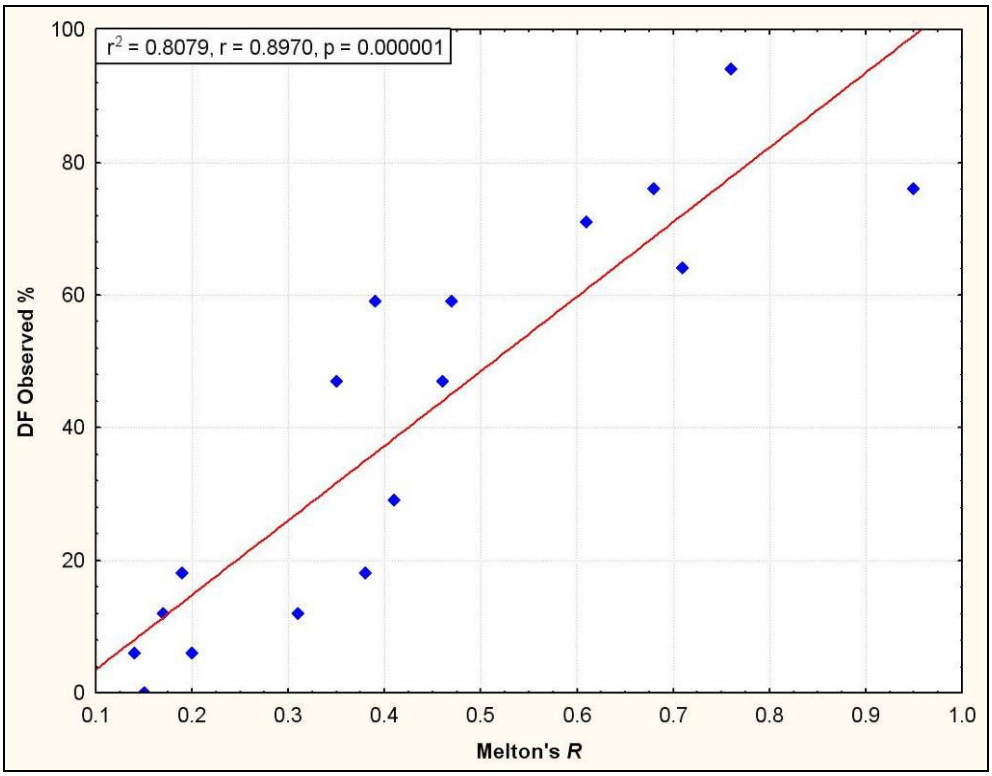

Figure 5.16: Relationship between observed evidence for debris-flows (DF) and Melton ratio (*R*) for stream watershed locations in the study area.

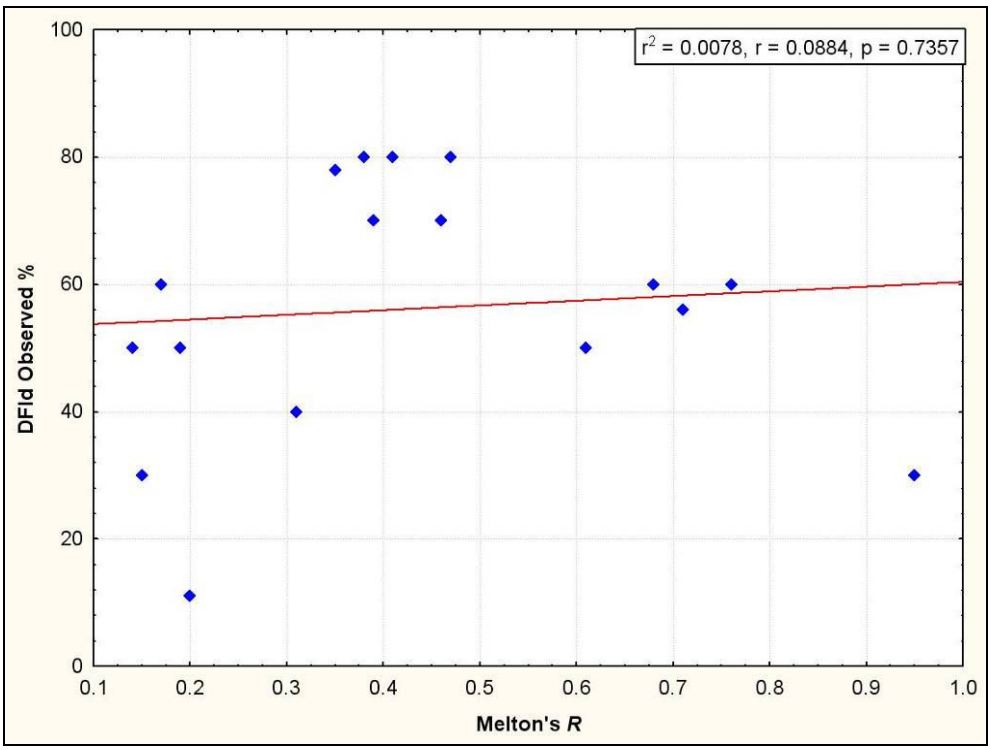

Figure 5.17: Relationship between observed evidence for debris-floods (DFld) and Melton's *R* for stream watershed locations in the study area.

5.4.1.3 R vs. fluvial evidence

A strong inverse relationship is evident between Melton's *R* and evidence for fluvial processes at stream watershed locations in the study area (Figure 5.18). Values derived for r^2 (-0.77) and r (-0.88) are close to -1 (perfect inverse relationship). In addition, the correlation is considered to be statistically significant as the derived p-value is <0.01.

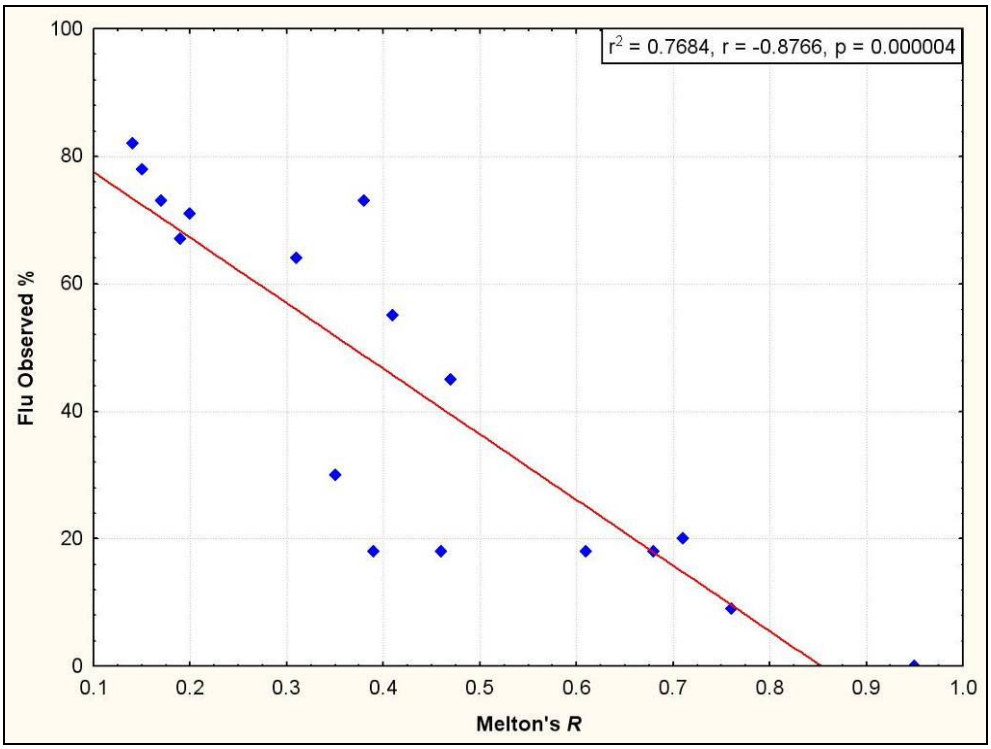

Figure 5.18: Relationship between the amounts of criteria observed for fluvial processes (Flu) and Melton's *R* for stream watershed locations in the study area.

5.4.2 Categories of R vs. observed evidence

5.4.2.1 R Categories vs. debris-flow evidence

Figure 5.19 shows the range in evidence observed for debris-flows at stream watershed locations exhibiting *R* values <0.30 (category 1), 0.30 – 0.60 (category 2) and >0.60 (category 3). The range in evidence observed differs significantly between categories. Stream watershed locations with *R* values in category 1 show minimal evidence for debris-flows (range 0 – 18 %) while the opposite holds true for those in category 3 (range 64 – 94 %). Locations with *R* values in category 2 show a much

broader range in evidence observed (18 - 59 %). No overlap is apparent between the categories.

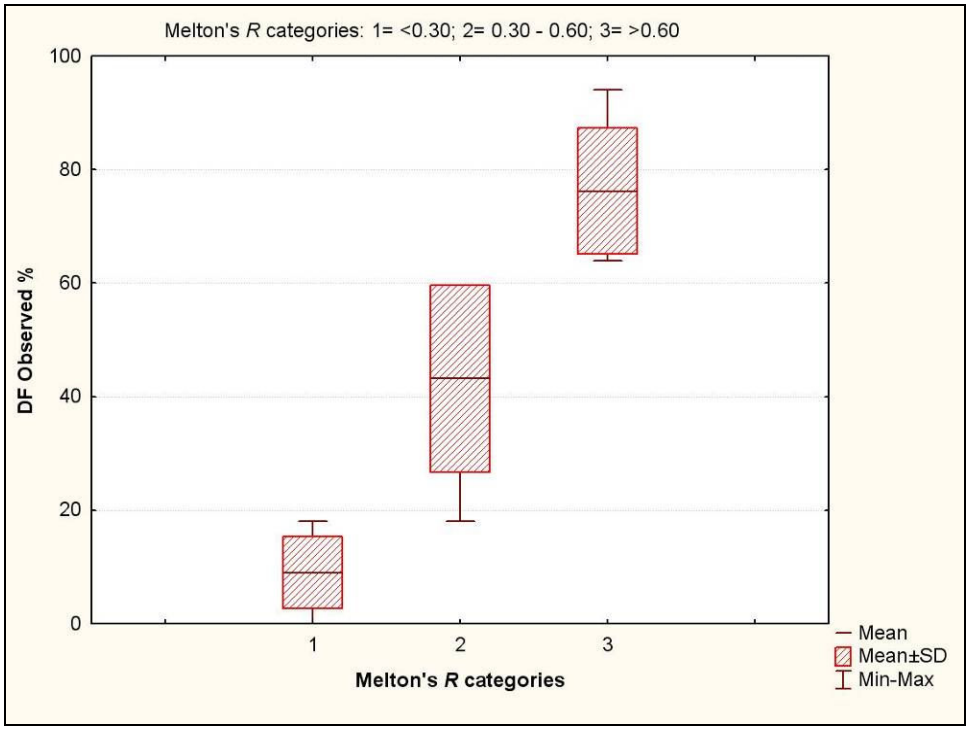

Figure 5.19: Evidence observed for debris-flows (DF) at stream locations in the study area in terms of categories of Melton's *R*.

5.4.2.2 R categories vs. debris-flood evidence

Significant overlap is evident between *R* categories 1 and 3 in the range of evidence observed for debris-floods at stream watershed locations in the study area (Figure 5.20). Stream watershed locations with *R* values in category 2 however, show no overlap with the other two categories. Highest amounts of evidence for debris-floods are observed in this category (range 70 – 80 %) whilst lowest amounts of evidence are observed at stream locations with *R* values in Category 1 (range 11 – 60 %).

5.4.2.3 R categories vs. fluvial evidence

The amount of evidence observed for fluvial processes, as with debris-flows, differs significantly between the 3 categories of Melton's *R* with only a minor overlap observed in the lower and upper quarters of categories 2 and 3, respectively (Figure 5.21). All 3 categories have distinctly different means. Streams locations with *R* values in category 1 show the highest amount of evidence for fluvial processes (range 64 – 82 %) and those in category 3 the lowest (0 – 20 %). The greatest range in

evidence observed is apparent at stream locations with *R* values in category 2 (range 18 – 73 %).

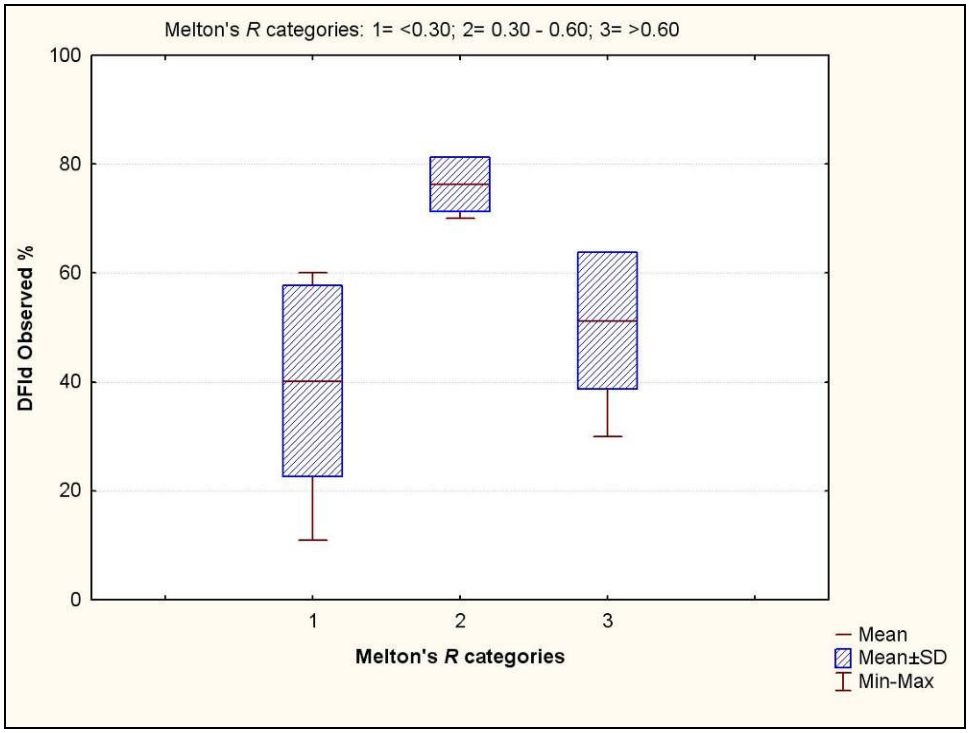

Figure 5.20: Evidence observed for debris-floods (DFld) at stream locations in the study area in terms of categories of Melton's *R*.

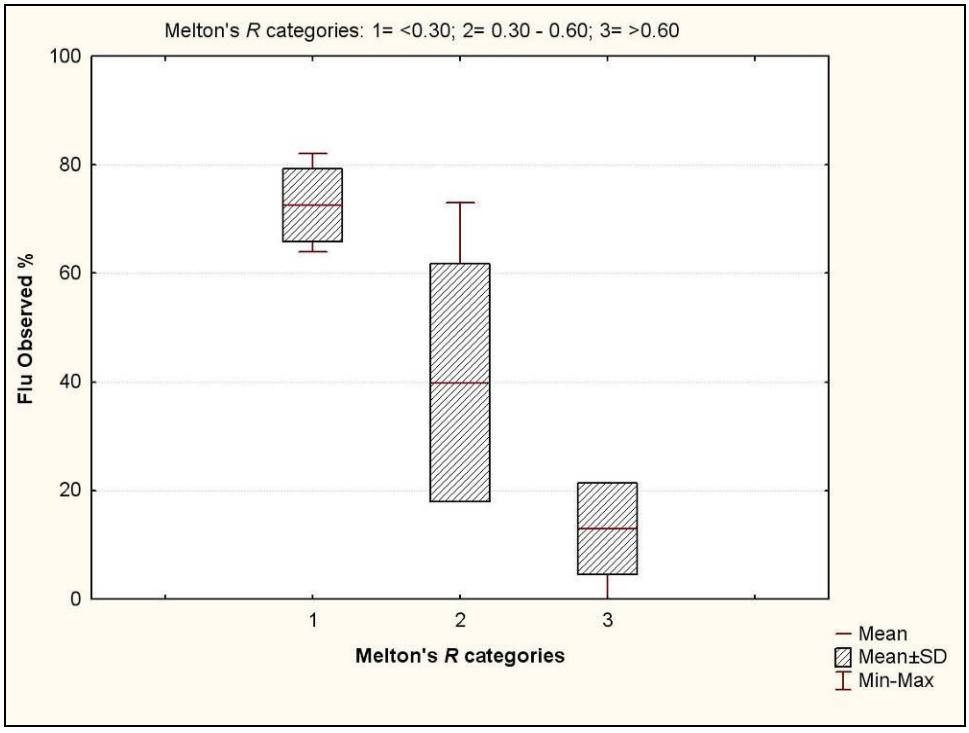

Figure 5.21: Evidence observed for fluvial processes (Flu) at stream locations in the study area in terms of categories of Melton's *R*.

5.4.3 Watershed length (WSL) vs. observed evidence

5.4.3.1 WSL vs. debris-flow evidence

Figure 5.22 demonstrates the relationship between watershed length and observed evidence for debris-flows at stream watershed locations in the study area. Although some scatter is evident in the data (r^2 = 0.61), a statistically significant (p <0.01) strong, inverse correlation (r = -0.78) is apparent between the variables.

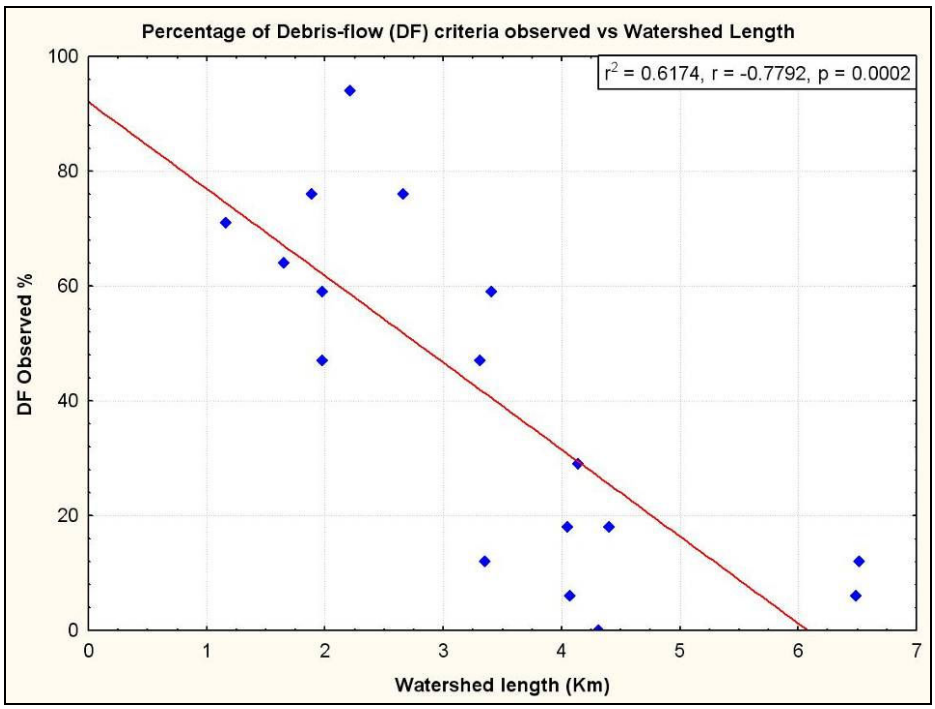

Figure 5.22: Relationship between observed evidence for debris-flows (DF) and watershed length for stream locations in the study area.

5.4.3.2 WSL vs. debris-flood evidence

No relationship is apparent between watershed length and observed evidence for debris-floods at stream locations in the study area (Figure 5.23). Extremely low values are obtained for r^2 (0.0013) and r (-0.004). A high p-value (0.89) is also derived indicating the correlation is not statistically significant.

5.4.3.3 WSL vs. fluvial evidence

A strong and statistically significant positive relationship exists between the amount of evidence observed for fluvial processes in the study area and watershed length

(Figure 5.24), with high values for r^2 (0.76) and r (0.87) and a very low p-value (0.000006) obtained in the regression.

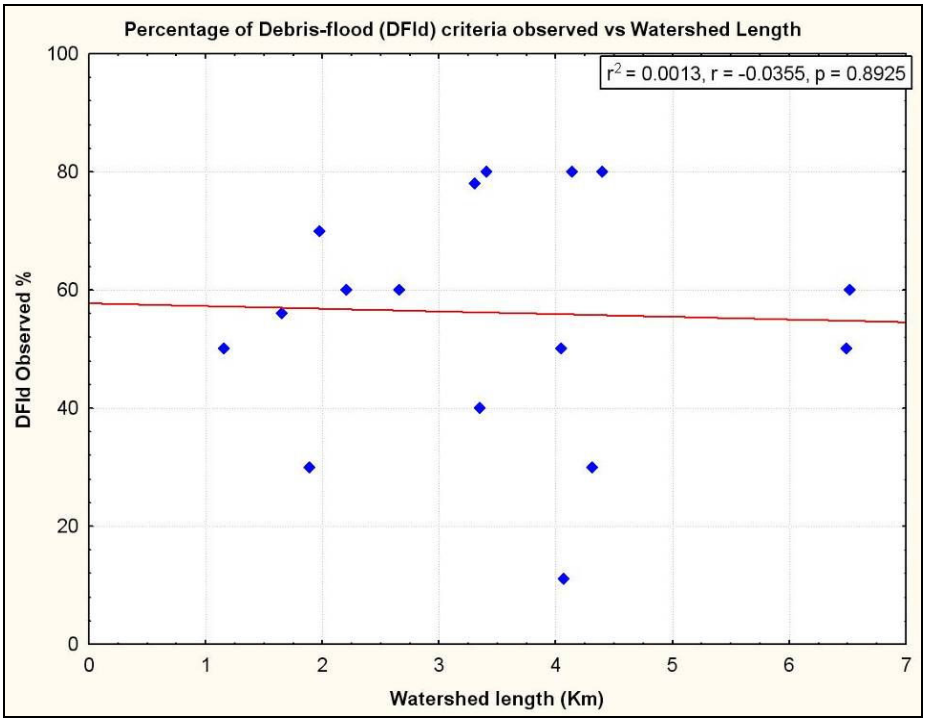

Figure 5.23: Relationship between observed evidence for debris-floods (DFld) and watershed length for stream locations in the study area.

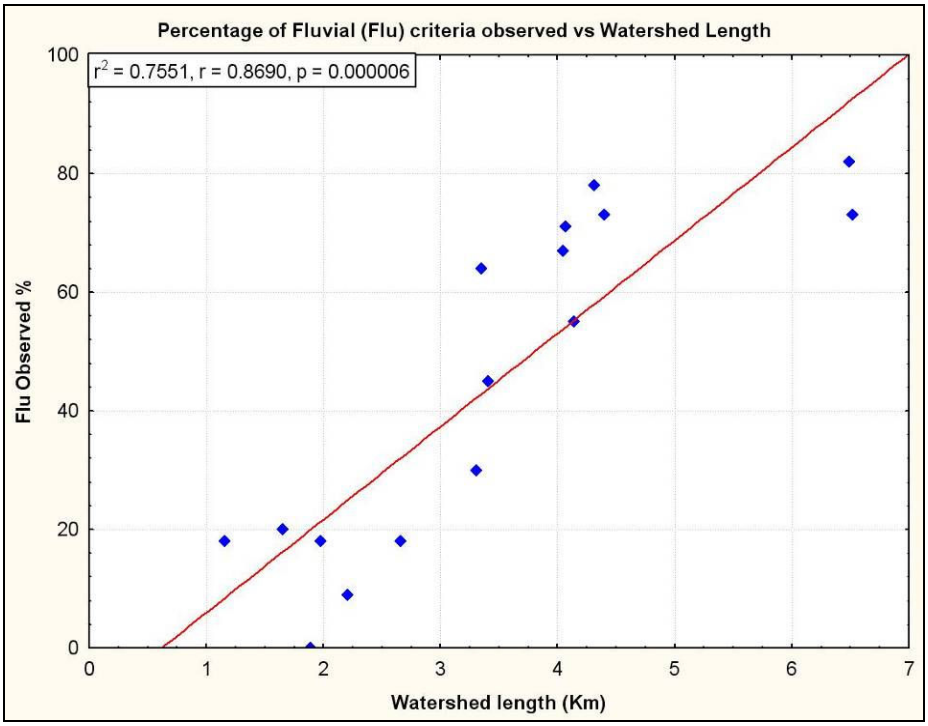

Figure 5.24: Relationship between observed evidence for fluvial processes (Flu) and watershed length for stream locations in the study area.

5.4.4 Categories of WSL vs. observed evidence

5.4.4.1 WSL categories vs. debris-flow evidence

The range in evidence observed for debris-flows at stream locations exhibiting watershed lengths >2.7 km (category 1) and <2.7 km (category 2) is illustrated in Figure 5.25. The range in evidence observed is clearly distinct between the 2 categories, with those stream locations exhibiting watershed lengths <2.7 km showing the highest amount of evidence for debris-flows (range 47 – 94 %). The means of the two categories are significantly different with only a small overlap observed between the maximum values for evidence observed in category 1 and minimum values in category 2.

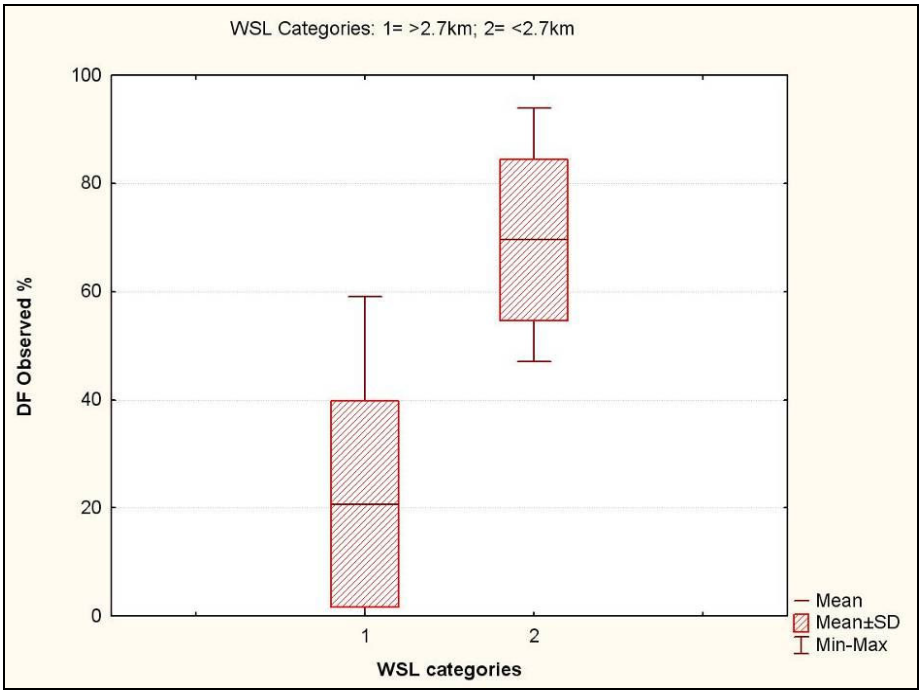

Figure 5.25: Evidence observed for debris-flows (DF) at stream locations in the study area in terms of categories of watershed length (WSL).

5.4.4.2 WSL categories vs. debris-flood evidence

Substantial overlap exists between watershed length categories in regard to the range in evidence observed for debris-floods at stream locations in the study area (Figure 5.26). No significant difference is observed between the mean values of the two categories. Stream locations with watershed lengths in category 1 exhibit both the highest and lowest amounts of evidence for debris-floods in the study area.

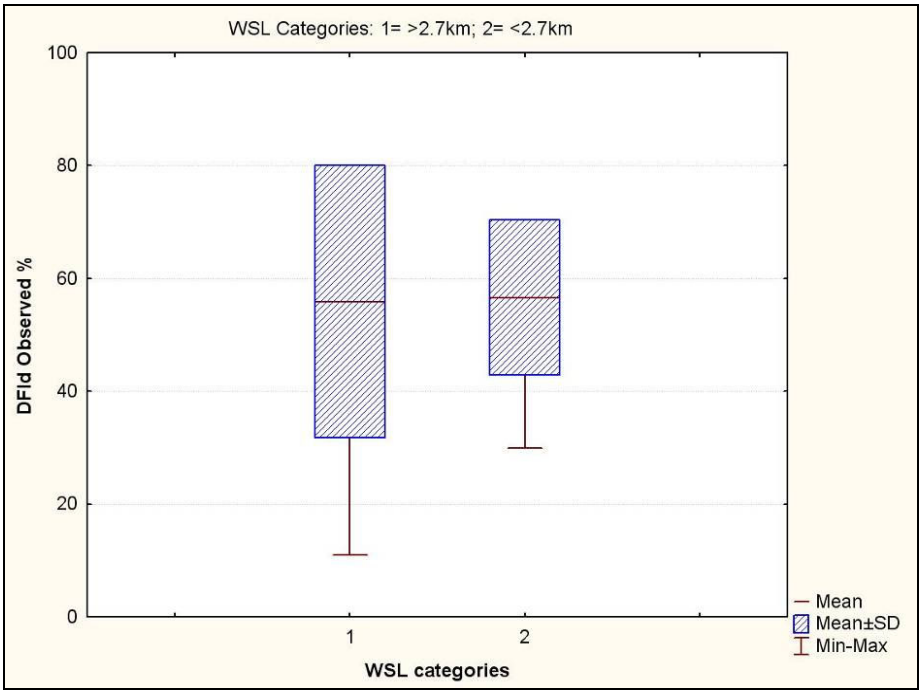

Figure 5.26: Evidence observed for debris-floods (DFld) at stream locations in the study area in terms of categories of watershed length (WSL).

5.4.4.3 WSL categories vs. fluvial evidence

Figure 5.27 shows the range in the amount of fluvial evidence observed at streams locations with watershed lengths >2.7 km (category 1) and <2.7 km (category 2). Similar to that seen for debris-flows in section 5.4.4.1, the range in evidence observed for fluvial processes at stream locations in the study area differs substantially between categories with no overlap in values seen between them Stream locations with watershed lengths in category 1 show the highest amounts of fluvial evidence (range 30 - 82 %) whilst those in category 2 show not more than 20 % evidence for fluvial processes.

5.5 Melton ratio (R) and watershed length values derived for other stream watershed locations outside the study area

In addition to the watershed data derived for stream locations in the study area, Melton ratios (*R*) and watershed lengths were also derived for 18 other stream locations in New Zealand known to have experienced debris-flows in the past. Melton ratio (*R*) and watershed lengths derived for each of these stream watersheds are shown in Table 5.2, and their general geographic locations shown in Figures 5.28 and 5.29.

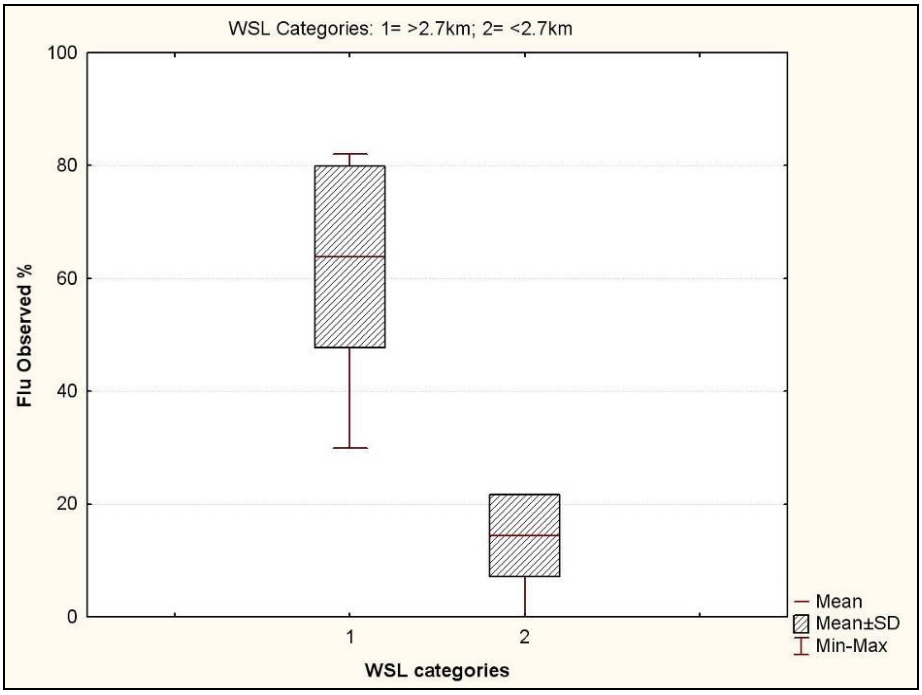

Figure 5.27: Evidence observed for fluvial processes (Flu) at stream locations in the study area in terms of categories of watershed length (WSL).

Table 5.2: Melton ratio(*R*) and watershed lengths (WSL) derived for 'other' stream locations outside the study area

Stream watershed location	Melton ratio (*R*)	WSL (km)
Bullock Ck, Mt Thomas	0.58	1.51
Stoney Ck, Tatare	0.86	2.63
Yellow Ck, Fox	1.18	1.53
Bullock Ck, Fox	0.57	4.46
Pipson Ck, Makarora	0.89	3.11
Waterfall Ck, Lake Hawea	0.94	3.15
Candy's Ck, Otira	1.31	1.15
Halpin Ck, Arthurs Pass	0.52	3.18
Greyneys Ck, Arthurs Pass	1.07	1.80
Unnamed Ck 1, Boyle River	0.92	2.05
Unnamed Ck II, Boyle River	1.08	1.97
Carew Ck 1, Lake Brunner	1.02	1.77
Turiwate Ck, Turiwhate	1.06	1.58
Grahams Ck, Turiwhate	0.88	2.33
Unnamed Ck, Turiwhate	1.17	1.48
Kowhai R, Peel Forest	0.69	2.32
Awatarariki Stm, Matata	0.17	3.68
Waitepuru Stm, Matata	0.25	2.38

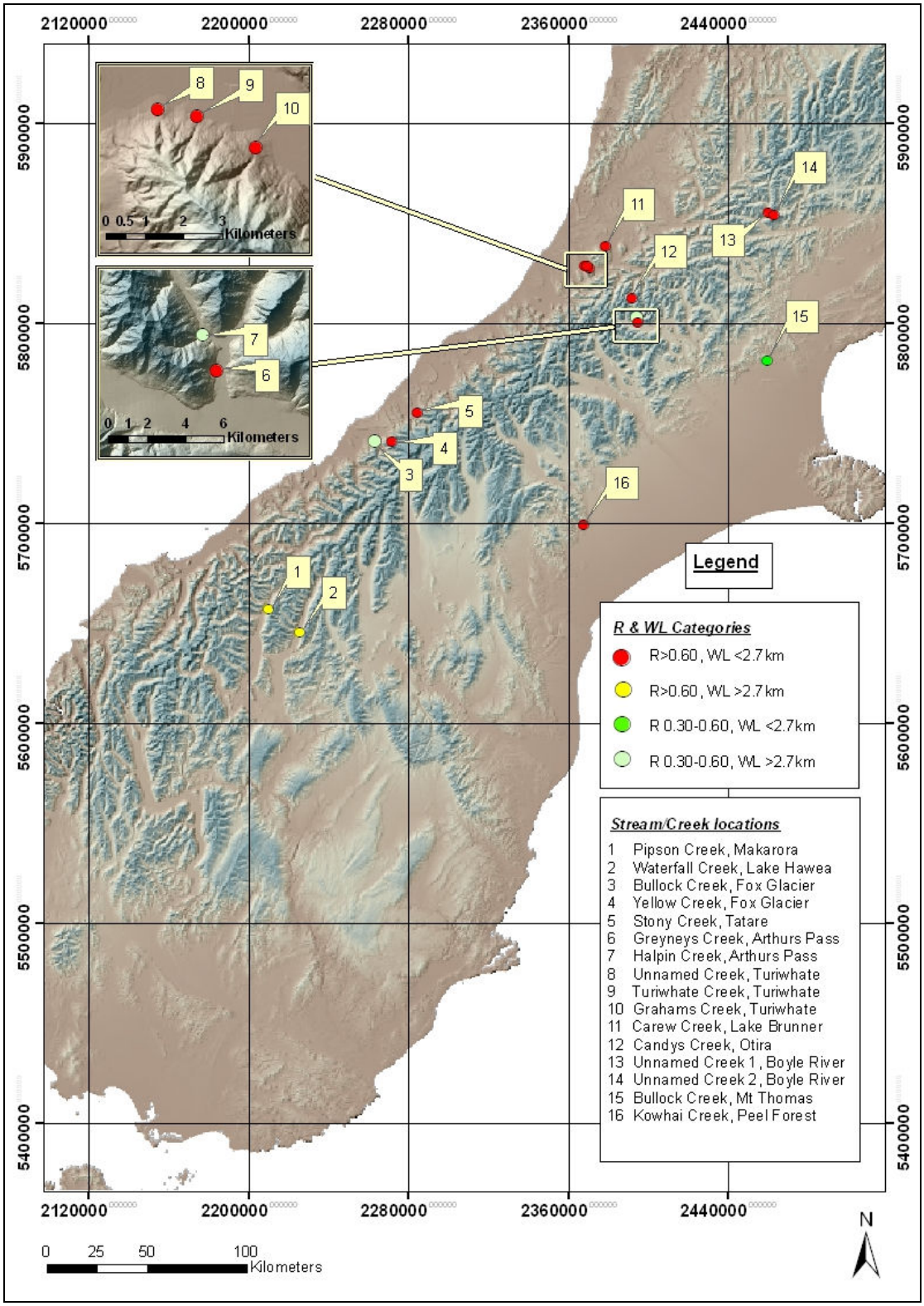

Figure 5.28: South Island locations and allocated Melton ratio (*R*)/watershed length (WL) categories (see section 5.2) for stream watersheds outside the study area known to have produced debris-flows.

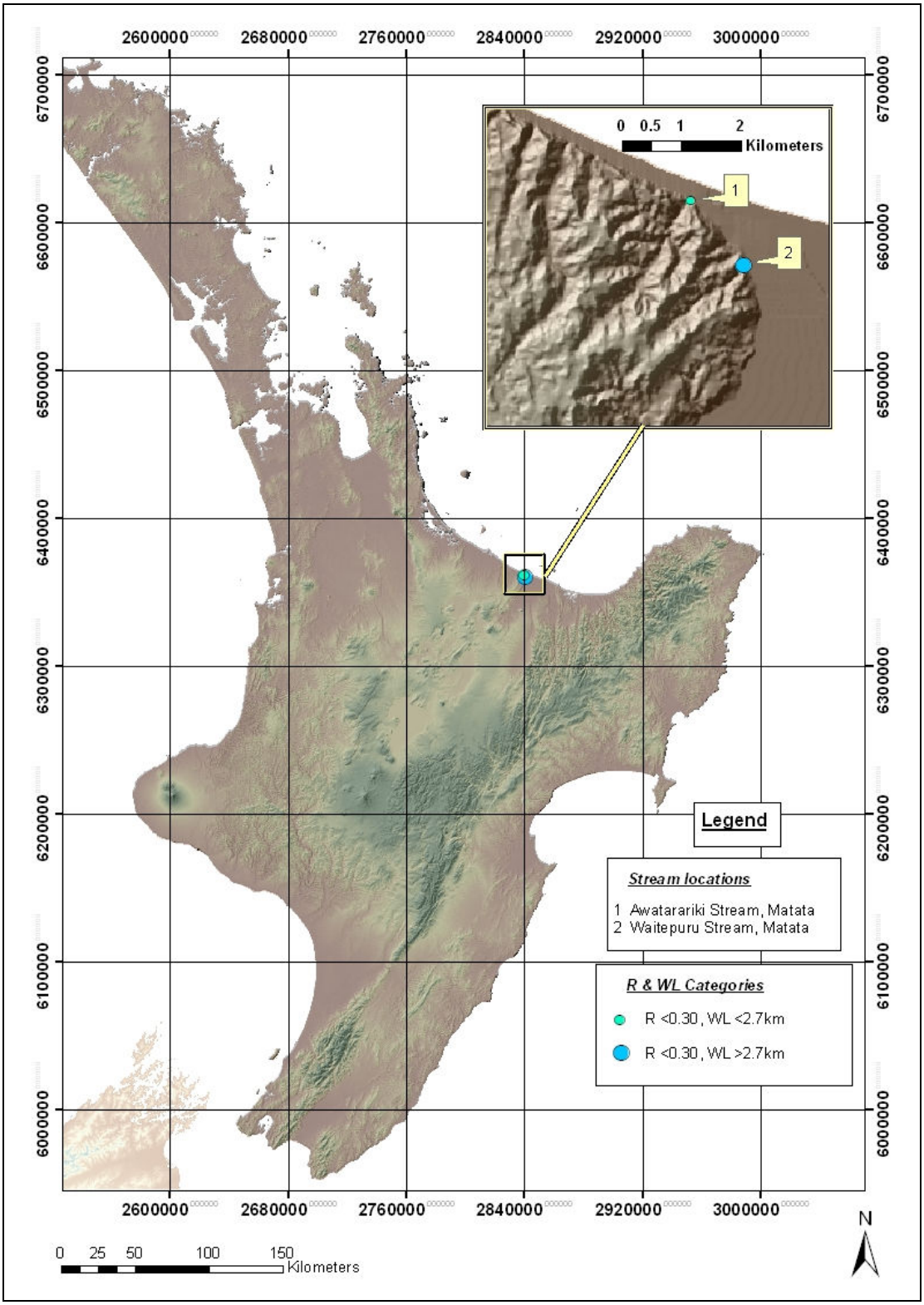

Figure 5.29: North Island locations and allocated Melton ratio (*R*)/watershed length (WL) categories (see section 5.2) for stream watersheds outside the study area known to have produced debris-flows.

Melton ratio (*R*) values for the stream watersheds range from 0.17 at Awatarariki Stream in Matata to a maximum of 1.31 at Candys Creek, Otira, and watershed lengths from 1.15 km at Candys Creek, Otira, to 5.56 km at Cascade Creek, Milford Road. A scatter plot of *R* against watershed length for these stream watershed locations is illustrated in Figure 5.30. The majority of stream watersheds (11/18; 61 %) plot in category F (stream watersheds exhibiting *R* values >0.60 and lengths <2.7 km). The next highest frequencies are observed in categories C (2/19; 11%) and E (2/19; 11 %).

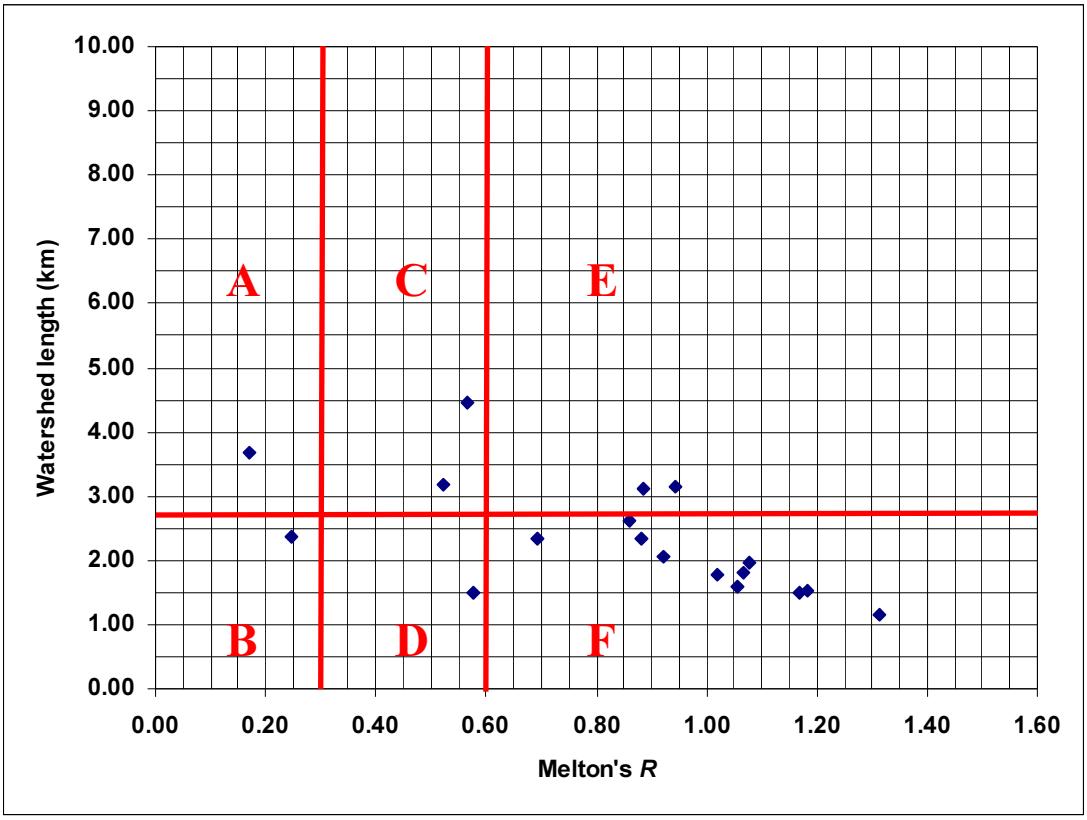

Figure 5.30: Scatterplot of Melton ratio (*R*) and watershed lengths for stream watersheds outside the study area known to have experienced debris-flows. Quadrants A – F represent categorical combinations of *R* and watershed length (described in section 5.2).

Chapter Six

Discussion

6.1 Introduction

The key results of this research can be summarised as follows:

- Strong relationships/correlations exist between the evidence observed for debris-flows, debris-floods and fluvial processes at stream watershed locations (i.e. drainage points of watersheds) in the study area, and the Melton ratio (R) values of contributing watersheds
- Equally strong relationships/correlations are apparent between the evidence observed for debris-flows and fluvial processes, and the lengths of contributing watersheds
- No correlation is evident however, between watershed length (WSL) and the evidence observed for debris-floods at stream locations in the study area
- Highest amounts of evidence for debris-flows were observed at stream watershed locations plotting in R/WSL category F (Melton's R >0.60; watershed length <2.7 km), while highest evidence for fluvial processes was found at locations plotting in category A (R <0.30; length >2.7 km), and debris-floods in categories C and D (R 0.30-0.60; lengths <2.7 km and >2.7 km)
- The majority of stream watersheds outside the study area that are known to have experienced debris-flows plot in category F, although there is some spread evident between categories

This chapter begins with a discussion and interpretation of the key results with respect to the literature in order to evaluate the hypothesis that 'debris-flow, debris-flood and flood hazards can be related to specific catchment/watershed parameters and these parameters used to indicate hazard levels at the drainage points of watersheds in the Coromandel/Kaimai study area'. Implications for debris-flow hazard in the study area are then discussed utilising results outlined in sections 5.2 and 5.3. Finally, a critical appraisal of the methods used in this research is provided.

6.2 The use of Melton ratio (*R*) for the identification of areas prone to debris-flow, debris-flood and fluvial-flood hazards in the study area

6.2.1 Interpretation of results

Results presented in Chapter 5 show strong relationships to exist between the ruggedness (*R*) of watersheds in the study area and the geomorphic evidence observed for debris-flows, debris-floods and fluvial processes at the corresponding drainage points of these watersheds (Figures 5.16, 5.17 and 5.18, Chapter 5). The deposits observed at the drainage points (i.e. fan heads) of watersheds are a direct reflection of the sediment transport mechanisms operating within the basin at that particular point in time (Kostaschuk et al., 1986; Jackson et al., 1987; Kellerhals and Church, 1990; Hungr et al., 2001; de Scally and Owens, 2004). Thus, it can be argued that the ruggedness of watersheds in the study area has an important influence on the type and dominance of hydrogeomorphic processes acting within the watershed to transport sediment to the fanhead. In order to understand how and why these relationships are apparent, it is first useful to revisit the concept of the Melton ratio (Melton, 1965).

Equation 6.1: Melton's *R* = $H_b / \sqrt{A_b}$

A_b denotes the total area of the basin, and H_b basin relief

As mentioned in Chapter 3, the Melton ratio (*R*) is an index of watershed 'ruggedness' that normalises watershed relief by area (Equation 6.1). In effect, it is a measure of watershed steepness and reflects the gradients down which sediment is transported to the fan; i.e. high *R* values are associated with steep gradients, low *R* associated with shallow gradients (Church and Mark, 1980; de Scally and Owens, 2004) The channel gradients in a watershed can influence the type and dominance of sediment processes acting to transport sediment to the fan (Van Dine, 1985; de Scally and Owens, 2004; Patton, 1988). For example, sufficient gradients are required to promote and maintain momentum in debris-flows (de Scally and Owens, 2004). In less inclined watersheds (e.g. those with $R < 0.30$ in the study area), channel gradients are generally insufficient to maintain motion of debris-flows to the fan. Consequently, fluvial processes, characterised by bed-load transport (sliding, rolling and saltation), are the main means by which sediment is transported to the drainage point of the

watershed. These processes are well reflected at the drainage points of low-gradient watersheds in the study area. Combined correlation trends for each of the hydrogeomorphic processes vs. Melton's R are illustrated in Figure 6.1. At watersheds exhibiting low ruggedness values (R <0.30), more evidence is observed for fluvial processes at the drainage point of the watershed than for debris-floods or debris-flows, thus suggesting the dominance of fluvial sediment transport mechanisms.

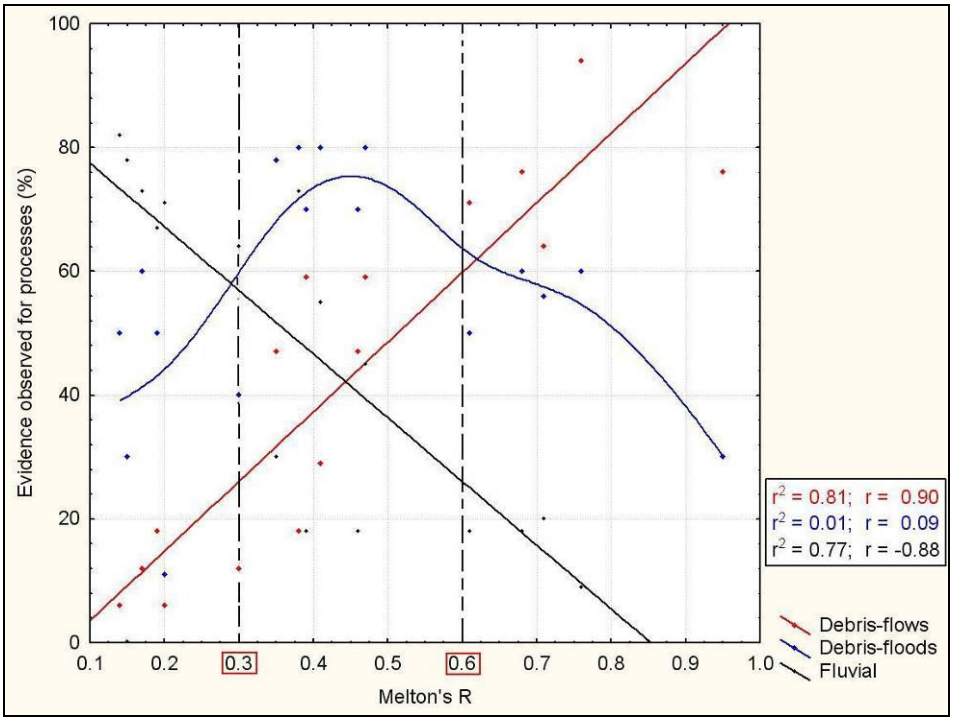

Figure 6.1: Correlation trends between observed evidence for debris-flows, debris-floods and fluvial processes at drainage points of watersheds in the study area and Melton's R of the contributing watershed. Dashed lines at R 0.30 and 0.60 represent thresholds (after Wilford et al., 2004) used to discriminate between processes.

Conversely, in steeper watersheds (e.g. those exhibiting R >0.60 in the study area) normal bed-load transport is replaced by massive bed instability with increasing slope angle (Hungr, 2005). The steeper stream gradients render sediment stored on slopes more susceptible to gravity induced mass movement, and debris-flows become a dominant mechanism by which sediment is transported to the drainage point of the watershed (Kostaschuk et al., 1986). Deposits observed at the drainage points of steep-gradient watersheds in the study area reflect these processes, with those

exhibiting high values of ruggedness (R >0.60) showing much more evidence for debris-flows relative to that for debris-floods and fluvial processes.

In watersheds that exhibit mid-range R values (0.30 – 0.60 in the study area), transitional processes between those of fluvial floods and debris-flows (collectively termed debris-floods; see section 2.5, Chapter 2) act to transport sediment (Hungr, 2005). In such watersheds channel gradients are insufficient to sustain motion of debris-flows. As a result, debris-flows will often terminate well before they reach the drainage point of the watershed (Hungr, 2005; McSaveney et al., 2005). Gradients are however generally steep enough to maintain motion of debris-floods, thus the water and loose debris draining from the debris-flow deposit will usually form a debris-flood downstream to reach the fan (Hungr, 2005). Again, these processes are well reflected at the drainage points of mid-range gradient watersheds ($0.30 < R < 0.60$) in the study area, with more evidence observed for debris-floods than that for the other two processes.

In addition to channel gradient, the sediment supply conditions can have a major influence on the type and dominance of sediment transport processes in the watershed (Jakob et al., 2005; see section 3.2.2, Chapter 3). For example, if limited sediment is available for transport in steeper-gradient watersheds (e.g. R >0.60), the development of debris-flows can be inhibited (de Scally et al., 2001). As a consequence, debris-floods can become a more important mechanism of sediment transport (Jakob et al., 2005). In such cases, more evidence for debris-floods than for debris-flows would be expected at the drainage point of the watershed (in contrast to the study area results). Moreover, much less evidence would probably be observed for both processes (this depending however on the way in which processes initiate and develop i.e. draining of debris-flows to form debris-floods vs. spontaneous in-channel initiation). The strong relationships observed between R and the evidence observed for all three hydrogeomorphic processes thus suggest that sediment supply is not a limiting factor in the study area. This is plausible, considering that the study area is largely characterised by steep, rugged terrain, is chiefly underlain by erodible volcanic rocks, and receives high annual precipitation (see section 4.2, Chapter 4) - characteristics that are largely conducive to the development of debris-flows and debris-floods (de Scally et al., 2001; de Scally and Owens, 2004; Hungr, 2005).

6.2.2 Comparison to the literature

The study area results show that in watersheds exhibiting *R* values >0.60, debris-flows are a dominant sediment transport mechanism (i.e. more evidence is observed for debris-flows than for debris-floods and fluvial processes hence it is assumed debris-flows are the major mechanism transporting sediment to the fan), while in watersheds exhibiting *R* values <0.30, fluvial processes are dominant and in watersheds with *R* values between 0.30 and 0.60, debris-floods are the main means of sediment transport.

These results generally compare well with the literature. For example, studies by Bovis and Jakob (1999), de Scally et al. (2001), de Scally and Owens (2004) and Wilford et al. (2004) all identify debris-flow-prone watersheds to exhibit much higher *R* values than those prone to fluvial processes (Table 6.1); a trend that is well observed for watersheds in the study area (Figures 6.2 & 6.3).

Table 6.1: Comparison between mean *R* and standard deviation ranges of *R* for debris-flow and fluvially-prone watersheds

Study	D-Flow mean R	D-Flow SD range	Fluvial mean R	Fluvial SD range
Bovis & Jakob (1999)	1.01	0.55 - 1.47	N/A	N/A
de Scally et al. (2001)	1.12	0.75 - 1.49	0.59	0.15 - 1.03
de Scally & Owens (2004)	1.17	0.91 - 1.43	0.62	0.38 - 0.86
Wilford et al. (2004)	0.95	0.76 - 1.14	0.23	0.13 - 0.33

With regard to individual studies, the study area results fit well with that of Wilford et al. (2004); all debris-flow watersheds are found to exhibit *R* values >0.60 (defined lower threshold for debris-flows-prone watersheds), all debris-flood watersheds have *R* between 0.30 – 0.60 (range of *R* for debris-flood-prone watersheds) and all fluvial watersheds plot below *R* = 0.30 (upper threshold defined for fluvial watersheds; Figure 6.4). In addition, the lower threshold of *R* (0.53) defined for debris-flow watersheds by Bovis and Jakob (1999) fits closely with Wilford et al. (2004) and hence the study area results.

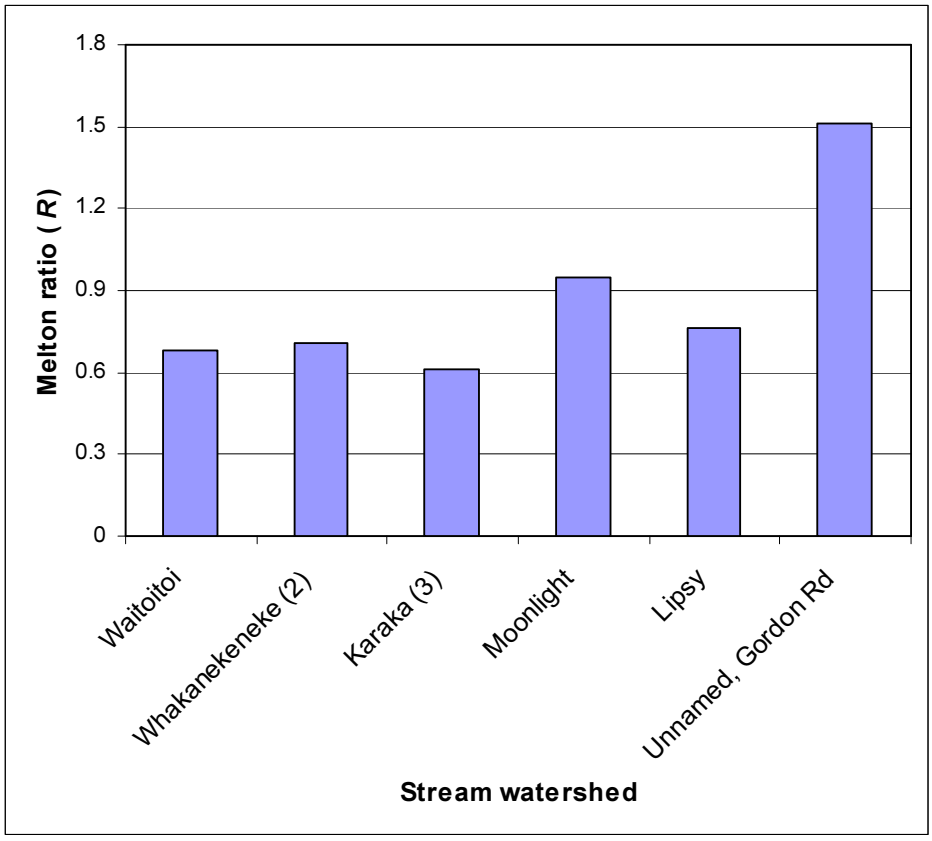

Figure 6.2: Melton ratios (*R*) of debris-flow-prone watersheds in the study area

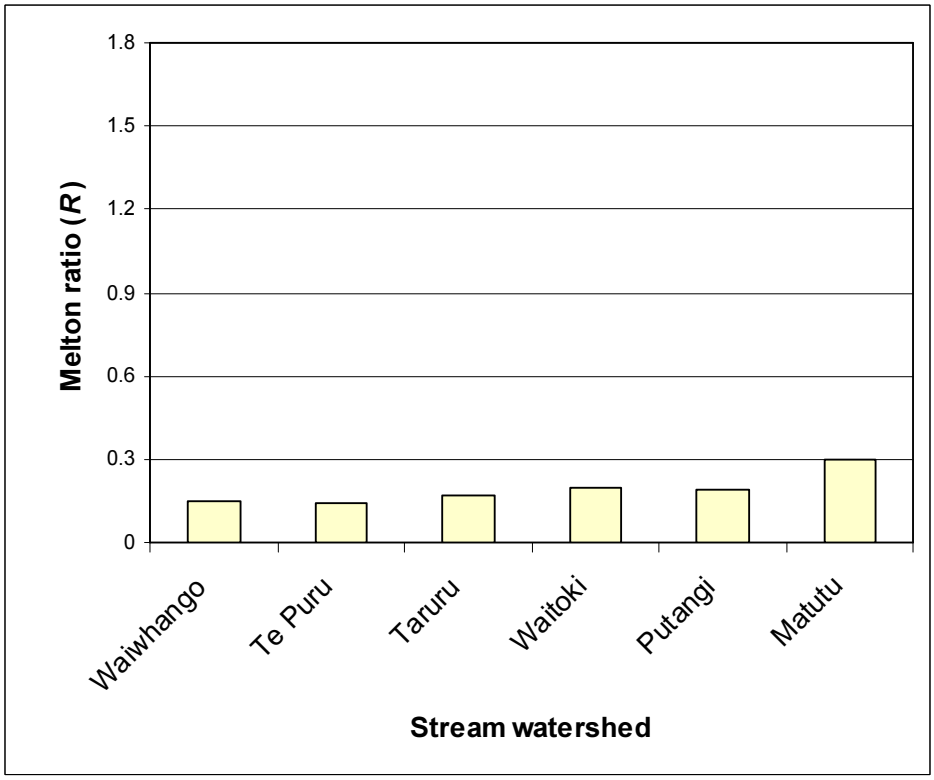

Figure 6.3: Melton ratios (*R*) of fluvially-prone watersheds in the study area

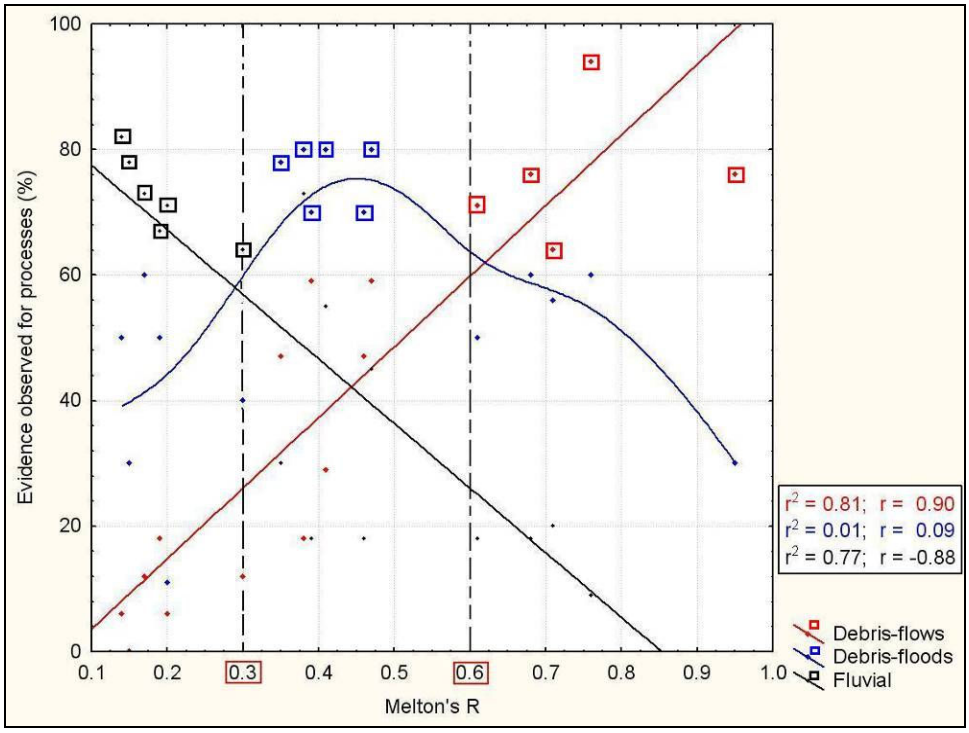

Figure 6.4: Correlation trends between observed evidence for processes at stream locations in the study area and Melton's R of contributing watersheds. Boxes enclosing points indicate those watersheds that are dominated by debris-flows (red), debris-floods (blue) and fluvial (black) processes in the study area. Dashed lines at 0.30 and 0.60 R represent thresholds used to discriminate watersheds by process, defined by Wilford et al. (2004).

A number of other studies however, identify dissimilar thresholds of *R* for debris-flow-prone watersheds. Jackson et al. (1987, *R* = 0.30), Coe et al. (2003, *R* = 0.35) and de Scally et al. (2001, *R* = 0.38) identify much lower thresholds of *R* for debris-flow watersheds, while a much higher threshold of 0.75 *R* is identified by de Scally and Owens (2004). It is possible that these lower thresholds identified by Jackson et al. (1987), Coe et al. (2003) and de Scally et al. (2001) are in part due to the fact that debris-floods are not included in their schema i.e. the thresholds of ~0.30 *R* probably reflect the lower thresholds for debris-floods rather than debris-flows, thus debris-flow thresholds may well be closer to that identified by Wilford et al. (2004) and Bovis and Jakob (1999). Similarly, the higher (*R* = 0.75) threshold recognized for debris-flow watersheds by de Scally and Owens (2004) may be due in part to the combining of fluvial and debris-floods, as debris-floods are also not considered in their study.

Most of the debris-flow watershed thresholds identified above, also act as the upper *R* thresholds for fluvial watersheds (i.e. differentiating fluvial from debris-flow-prone watersheds; e.g. Jackson et al. (1987; de Scally et al. (2001), de Scally and Owens (2004); Coe et al. (2003)). In this respect, the study area results compare quite well; study area watersheds classed as fluvially-dominated all exhibit *R* values below the 0.30 and 0.35 thresholds identified by Jackson et al. (1987) and Coe et al. (2003) respectively. Despite this however, the upper *R* threshold for fluvial watersheds defined by de Scally and Owens (2004) is again much higher than identified in the studies mentioned above and hence disagrees somewhat with the study area results. This is also the case for de Scally et al. (2001) in which the upper threshold of *R* for fluvial watersheds (1.34) is shown to overlap considerably with the lower threshold of *R* (0.38) identified for debris-flow watersheds.

These discrepancies can be attributed to the influence of sediment traps in the watersheds, associated with past glacierization (Jackson et al., 1987; de Scally and Owens, 2004). As previously mentioned in section 3.3.1, Chapter 3, low-gradient reaches associated with glacial erosion can act to trap debris-flows in generally steeper watersheds before they reach the fan. The deposits are then reworked and transported to the fan by conventional fluvial processes. As a result, watersheds dominated by fluvial processes can exhibit much higher values of *R* and thus higher upper thresholds (as observed in de Scally et al. (2001) and de Scally and Owens (2004)) in comparison to *R* values for fluvial watersheds in unglacierized areas such as the Coromandel/Kaimai region study area.

Despite the discrepancies identified above, the study area results generally compare favourably with the literature, and hence support the research hypothesis (see section 6.1). The next section will now investigate the use of watershed length for the identification of areas susceptible to debris-flow and related hydrogeomorphic hazards in the study area.

6.3 The use of watershed length for the identification of areas prone to debris-flow, debris-flood and fluvial-flood hazards

6.3.1 Interpretation of results

The results presented in Chapter 5 show strong relationships to exist between the total planimetric lengths of watersheds in the study area and the evidence observed for debris-flow and fluvial processes at the corresponding drainage points of these watersheds. Debris-flow-prone watersheds in the study area (i.e. those exhibiting more evidence for debris-flows than for debris-floods and fluvial processes at the drainage point) are observed to exhibit much shorter watershed lengths than those prone to fluvial processes (Figure 6.5).

This relationship probably exists for the reason that watersheds exhibiting longer lengths are generally much larger (Bridge, 2003), exhibit higher stream orders and generally have lower channel gradients than shorter watersheds (Knighton, 1998; Ritter et al., 2002; Summerfield, 1991; Patton, 1988; Kostaschuk et al., 1986; DesLodges and Gardner, 1984). As mentioned in section 2.3.1, Chapter 2, debris-flows are generally restricted to steep, lower order streams/watersheds (e.g. 1st or 2nd order) because they require sufficient channel gradients to maintain momentum (Benda and Cundy, 1990; Hungr, 2005). In longer (and thus larger) watersheds, channel gradients may therefore be largely insufficient to maintain momentum in debris-flows (de Scally and Owens, 2004). Furthermore, in watersheds characterised by higher order streams, the presence of more lower-gradient stream junctions may act to slow debris-flow motion to the fan as these locations are generally associated with reductions in channel gradients and increases in channel widths (Benda, 1985; Benda and Cundy, 1990). Evidence for fluvial processes is thus likely to be dominant at the drainage points of longer watersheds in the study area, while in shorter and hence smaller watersheds, steeper gradients associated with lower order streams ensure debris-flows are a more dominant mechanism of sediment transport to the drainage point of the watershed.

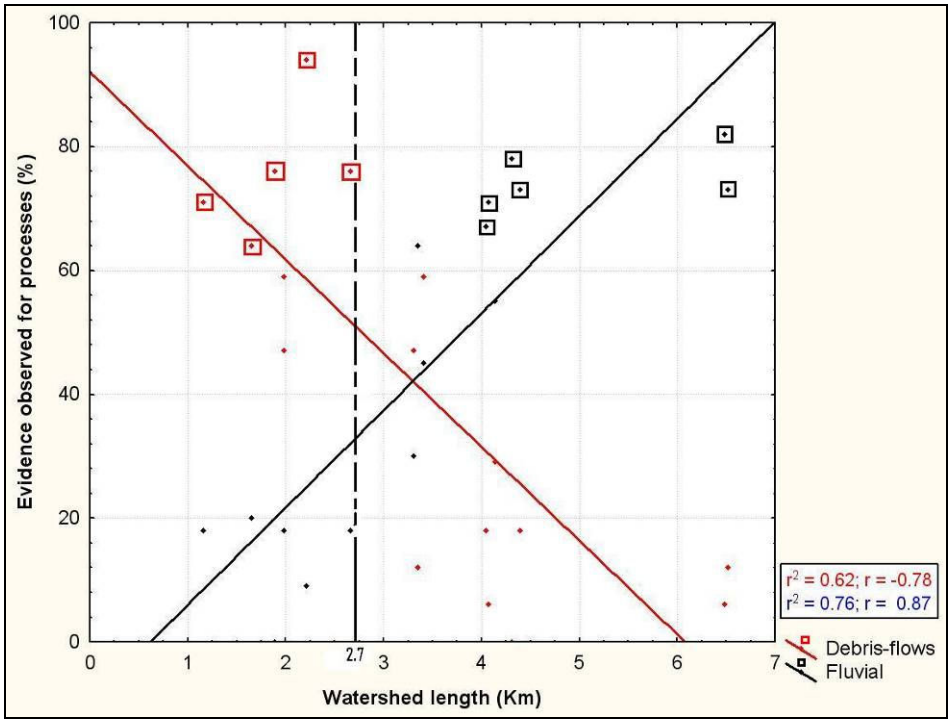

Figure 6.5: Correlation trends between evidence for debris-flow and fluvial processes and watershed length for stream watershed locations in the study area. Dashed line at watershed length 2.7 km represents the threshold (defined by Wilford et al. (2004)) used to differentiate watersheds by dominant process.

In contrast to the strong relationships observed between watershed length and the evidence observed for debris-flows and fluvial processes in the study area, no linear relationships are observed to exist between the evidence observed for debris-floods and watershed length (Figures 5.23 & 5.26, Chapter 5). This is probably due to the fact that debris-floods are transitional in nature between debris-flow and fluvial processes (see section 2.3.3, Chapter 2) and thus can occur in both longer, larger watersheds (deposits would probably exhibit a higher fluvial component) and shorter, smaller and steeper watersheds (higher debris-flow component). In this regard, the ruggedness of watersheds and sediment supply conditions are probably more important controls on the occurrence of debris-floods in the study area.

6.3.2 Comparison to the literature

Wilford et al. (2004) is one of the only studies to date to have explored the use of watershed length (amongst other parameters) for the identification and discrimination of watersheds prone to debris-flow, debris-flood and fluvial-flood processes. In their

study, watershed lengths were found to vary considerably between debris-flow, debris-flood and fluvial-prone watersheds. Watersheds prone to fluvial processes were found to exhibit mean lengths more than four times longer than those subject to debris-flows, and the ranges in watershed lengths for all three processes were found to differ significantly.

The study area results for the present research agree closely with Wilford et al.'s (2004) findings, with much longer lengths also identified for fluvial watersheds relative to those prone to debris-flows. As shown Table 6.2, similar trends are also evident in the ranges of lengths for watersheds, with those prone to debris-flows identified to have the shortest lengths, those prone to fluvial processes the longest, and those dominated by debris-floods exhibiting mid-range lengths between the two end members.

Table 6.2: Comparison of ranges in watershed lengths (km) identified for specific hydrogeomorphic processes by Wilford et al. (2004) and the present study.

Study	**Debris-flow**	**Debris-flood**	**Fluvial**
Study area results	1.16 – 2.66 km	1.98 – 4.40 km	4.05 – 6.52 km
Wilford et al. (2004)	0.28 - 4.68 km	1.68 -10.73 km	2.27 - 18.46 km

Wilford et al. (2004) also identified 83 % of debris-flood, and 94 % of fluvial watersheds to exhibit lengths >2.7 km, but only 8 % of those prone to debris-flows. Again, the study area results compare very well with these findings. All debris-flow watersheds in the study area exhibit lengths less than the 2.7 km threshold identified by Wilford et al. (2004), while all fluvial watersheds and 67 % of those prone to debris-floods exhibit lengths >2.7 km.

6.4 Results derived for stream watersheds outside the study area

The Melton's *R* and watershed length values derived for debris-flow watersheds outside the study area compare relatively well with the study area results, despite contrasting geological/lithological and meteorological settings (i.e. metamorphic and glacial geology of the Southern Alps vs. volcanic geology of the Coromandel; see

Chapter 4, section 4.6). As shown in Figure 5.30 (Chapter 5), most of these watersheds exhibit high R values and short watershed lengths, in agreement with the *R* values identified for debris-flow-prone watersheds in the study area and the literature.

A handful of the watersheds however, display much lower Melton ratios and longer watershed lengths than expected. In particular, Awatarariki (R = 0.17) and Waitepuru (R = 0.25) stream watersheds in Matata display abnormally low *R* values. The values fall well below all thresholds identified in the literature and are consistent with that defined for fluvial watersheds (R<0.30) (Jackson et al., 1987; Wilford et al. (2004). Despite this, both Awatarariki and Waitepuru watersheds are identified to have produced large debris-flows in the past, in addition to the event in 2005 (described in Chapter 2, section 2.4.3). It is thus likely that other factors such as the local topography near the drainage point of the watershed and sediment supply conditions are more important controls on the potential for debris-flows in these watersheds. For example, examination of the DEM for Awatarariki Stream watershed shows a number of small tributaries to lie adjacent to each other and in relatively close proximity to the fan. Rainstorm-generated debris-flows in these tributaries may thus have potential to coalesce at stream junctions (as was the case in the 2005 event; McSaveney et al, 2005). This may have the effect of forming one large debris-flow capable of flowing further than any flow on its own. Furthermore, the weak, fine-grained, sedimentary and volcanic deposits that underlie the Matata region (McSaveney et al. (2005) may cause resultant debris-flows to be more fluid and hence capable of flowing on shallower gradients than expected.

Bullock Creek, Fox Glacier, exhibits a much longer watershed length (4.46 km) than the 2.7 km upper threshold for debris-flow watersheds identified by Wilford et al. (2004). Despite this, it does show an *R* value close to 0.60, indicating that channel gradients within the basin are relatively sufficient to maintain momentum in debris-flows. It is possible that glacial conditions within the area may have had an influence on the ability of debris-flows to reach the fan in this watershed (e.g. as a result of glacial out-break floods; Jackson et al., 1987). In addition to Bullock Creek, a handful of other debris-flow watersheds (Halpin Creek – WL 3.18 km; Waterfall Creek – WL 3.15 km; and Pipson Creek – WL 3.10 km) exhibit longer watershed lengths than 2.7

km. They also however, exhibit high *R* values (e.g. 0.52, 0.94 and 0.88 respectively). In light of this, it is possible that a slightly higher threshold of watershed length may exist for differentiating debris-flow from non-debris-flow watersheds in the Southern Alps.

6.4 Combinations of *R* and watershed length for the identification of debris-flow hazards in the study area

The results discussed above confirm the utility of the Melton ratio and watershed length for the differentiation of watersheds by dominant hydrogeomorphic process. When used in combination, thresholds of *R* and watershed length can be used to define class limits for debris-flow, debris-flood and fluvially-prone watersheds in the study area (Wilford et al. (2004). Furthermore, these class limits can be used to indicate the likelihood of debris-flows to reach the fan of a watershed because they reflect fundamental catchment characteristics/requirements that are necessary to promote and maintain momentum in debris-flows (de Scally et al. (2004; Church and Mark, 1980). In this regard, each categorical combination of *R* and WL, as defined by the class limits for specific processes, can be assigned a particular level of debris-flow hazard (Figure 6.6).

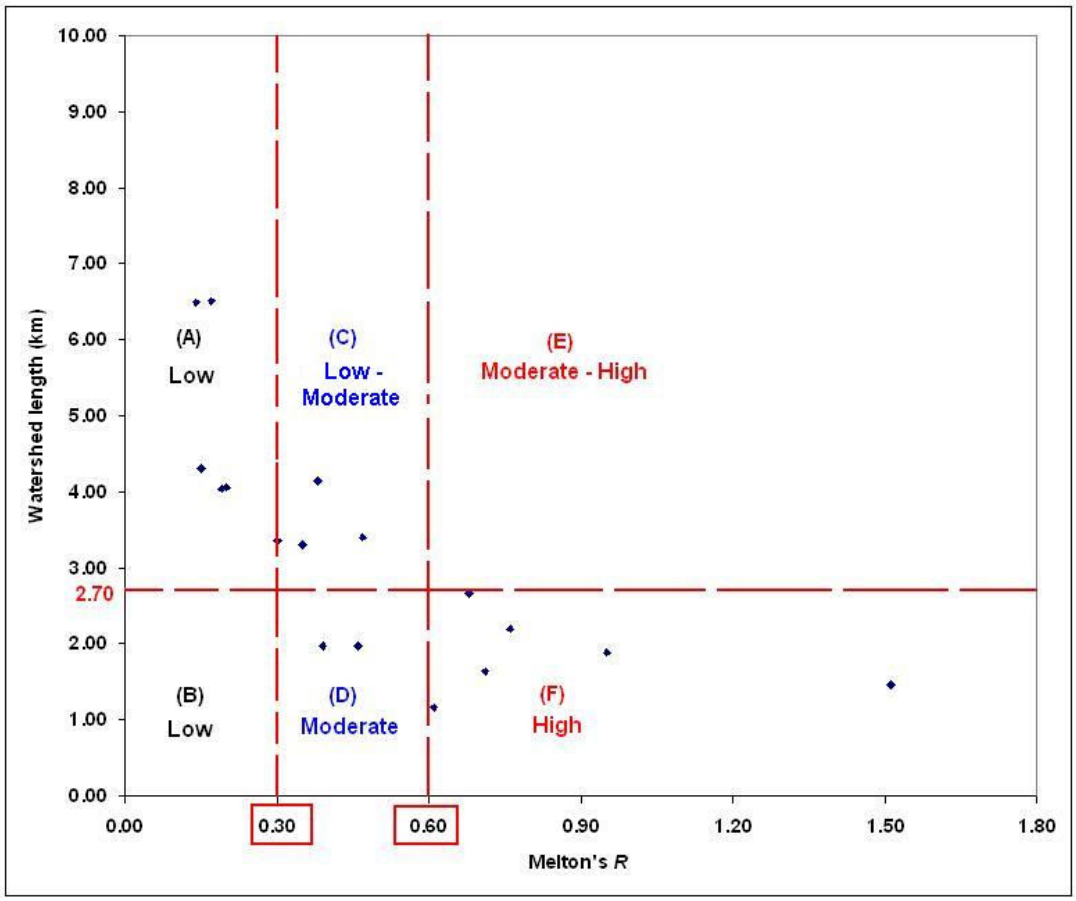

Figure 6.6: Scatterplot showing debris-flow hazard levels assigned to each categorical combination of *R* and watershed length (A-F). Data points represent *R*/WL combinations for/of watersheds surveyed in the field investigation.

In Figure 6.6, watersheds plotting in Categories A and B are assigned a low debris-flow hazard because channel gradients are largely insufficient to promote and maintain motion of debris-flows to the fan. Categories C and D are assigned a low-moderate and moderate debris-flow hazard respectively. Channel gradients are more sufficient to maintain momentum in debris-flows in these categories. Category C is assigned a lower hazard because at longer watershed lengths (>2.7 km), there is a greater likelihood debris-flows will terminate/deposit before they can reach the fan (see section 6.3.1). Categories E and F are assigned a moderate-high and high debris-flow hazard as channel gradients are optimal for maintaining momentum of debris-flows. Category E is assigned a lower hazard than category F because the longer watershed lengths (>2.7 km) means there is greater travel distance to the fan and thus a greater likelihood that debris-flows will slow and deposit or be diluted at channel junctions before they reach the drainage point of the watershed.

6.6 Implied debris-flow hazard at stream locations in the Coromandel/Kaimai region

Utilising the hazard classification outlined in Figure 6.6, a level of debris-flow hazard can be implied for all streams in the study area for which watershed data is derived. Table 6.3 shows the frequency distribution of stream watersheds in the study area in terms of categories of Melton ratio (*R*) and watershed length (WL), and assigned debris-flow hazard level. The majority of stream watersheds (71 %) exhibit a low, to low-moderate debris-flow hazard (*R*/WL categories A, B and C). These watersheds are well-spread throughout the study area and are particularly common in the eastern regions of the Coromandel Peninsula (see Figure 5.2, Chapter 5).

In contrast, those exhibiting moderate, moderate-high and high debris-flow hazard are largely restricted to the western range front of the Coromandel and Kaimai Ranges. Highest concentrations are noted in the vicinity of Te Aroha, and at the southern extent of the Kaimai range (adjacent to Matamata) (Figures 6.7 and 6.8). Two smaller clusters also exist in the vicinity of Thames and in the far north of the Coromandel Peninsula (just south of Port Jackson). In total, 88 watersheds in the study area (29 %) exhibit a moderate, moderate-high and high debris-flow hazard. General locations for each of these moderate to high debris-flow hazard watersheds are shown in Figure 6.7 (Coromandel region) and Figure 6.8 (Kaimai region), with the list of names for watersheds and their respective *R*/WL categories and debris-flow hazard levels illustrated in Table 6.4.

Table 6.3: Frequency of stream watersheds within categories of *R*/WL and associated debris-flow hazard

Category of *R*/WL and assigned debris-flow hazard level	**Frequency (no.)**	**Frequency (%)**
(A) Low	117	39
(B) Low	64	21
(C) Low-moderate	33	11
(D) Moderate	58	19
(E) Moderate - high	3	1
(F) High	27	9
Total:	**302**	**100**

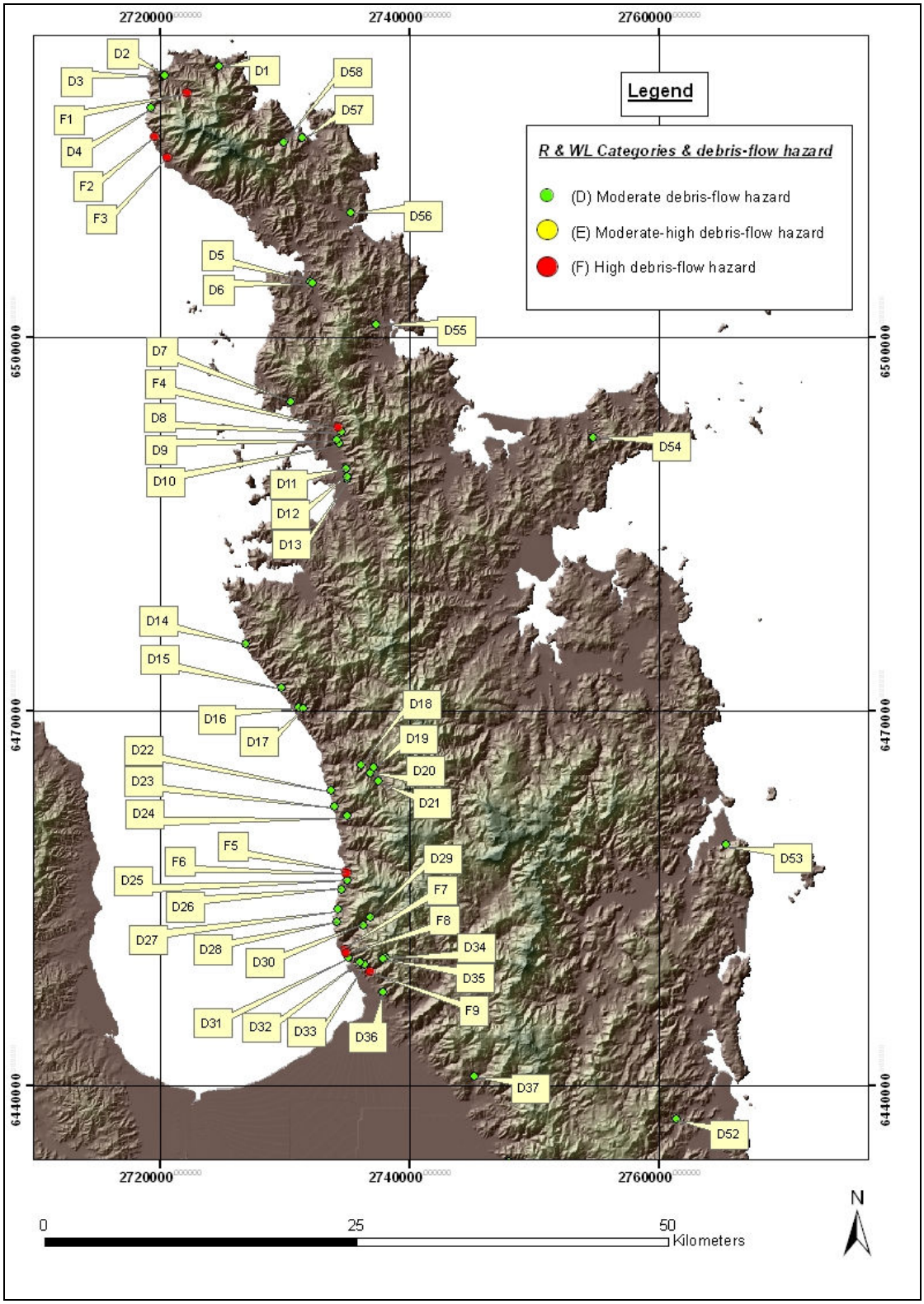

Figure 6.7: Stream watersheds in the Coromandel region exhibiting moderate, moderate-high and high debris-flow hazard. See Table 6.4 for corresponding stream watershed names associated with labels.

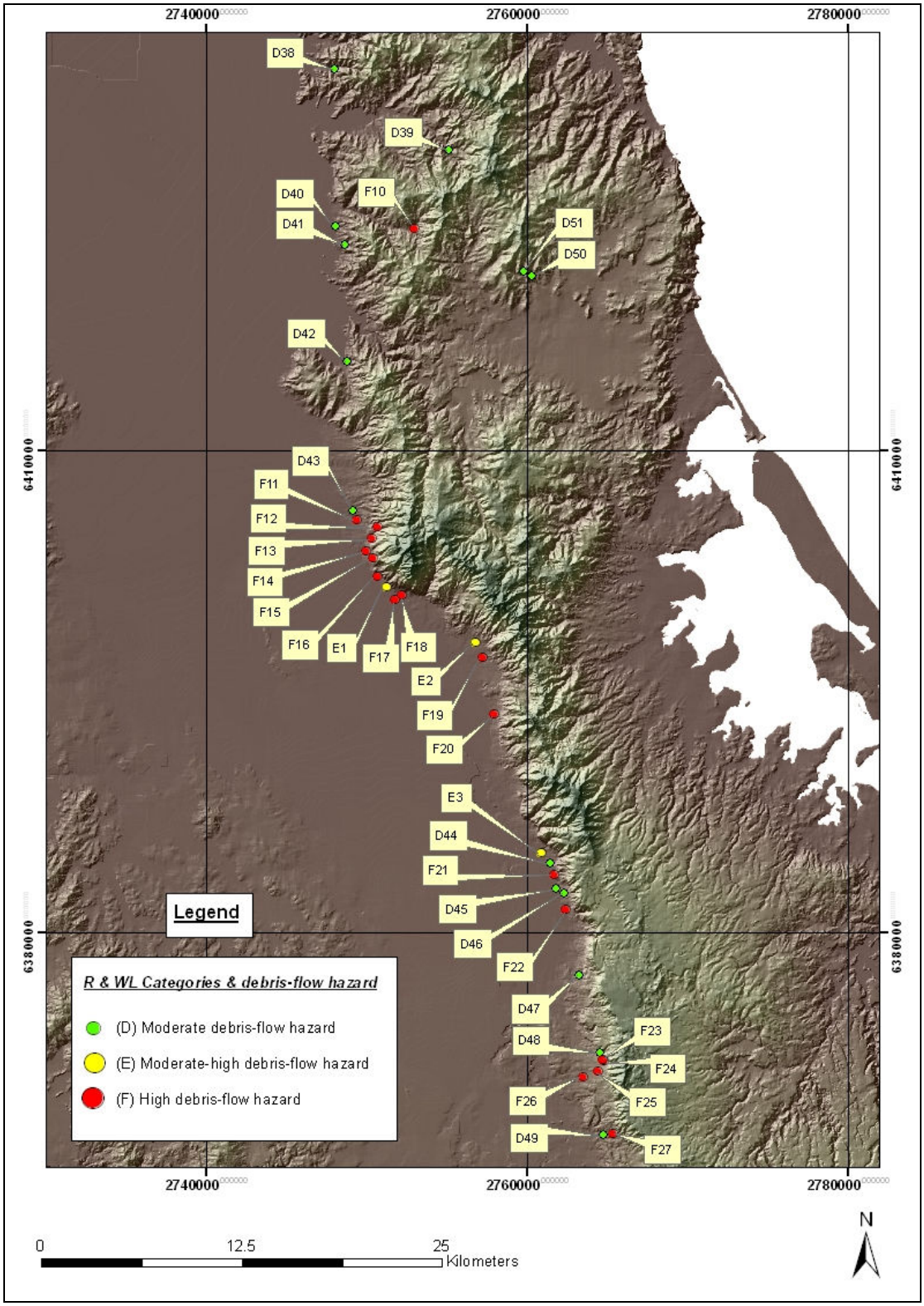

Figure 6.8: Stream watersheds in the Kaimai region exhibiting moderate, moderate-high and high debris-flow hazard levels. See Table 6.4 for corresponding stream watershed names associated with labels.

Table 6.4: Names for stream watersheds in the study area, their respective R/WL categories and associated debris-flow hazard levels

Stream watersheds - Moderate debris-flow hazard (Coromandel region)	**R/WL category & Stream watershed no.**	**Stream watersheds - Moderate debris-flow hazard (Kaimai Region)**	**R/WL category & Stream watershed no.**
Holland Creek	D1	Onetai Stream	D45
Pahi Stream (4)	D2	Whakamoehau Stream	D46
Pahi Stream (3)	D3	Unamed Stream, Morrison Rd.	D47
Pouretu Stream	D4	Kapukapu Stream	D48
Umangawha Stream (4)	D5	Rotokohu Stream (3)	D49
Umangawha Stream (3)	D6	Omahu Stream (2)	D50
Koputauaki Stream	D7	Maurihoro Stream	D51
Whakanekeneke Stream	D8	Turanga Stream	D52
Taumatawahine Stream (2)	D9	Sheehan Stream	D53
Taumatawahine Stream	D10	Mangangarara Stream	D54
Huaroa Stream	D11	Unnamed, Barton Rd. (1)	D55
Huaroa Stream (2)	D12	Omahine Stream	D56
Huaroa Stream (3)	D13	Waitete Stream (3)	D57
Paraunahi Stream	D14	Waitete Stream (2)	D58
Omako Creek	D15		
Wharekawa Stream (3)	D16	**Moderate-High debris-flow hazard**	
Wharekawa Stream (2)	D17	Haohaenga Stream	E1
Te Kaka Stream (2)	D18	Wahine stream	E2
Te Kaka Stream	D19	Martin Stream	E3
Unnamed Stream, Mt Misery	D20		
Black Swan Stream	D21	**High debris-flow hazard (Coromandel)**	
Whalebone Stream	D22	Pahi Stream	F1
Otuturu Stream	D23	Fantail stream (2)	F2
Pohue Stream	D24	Waitoitoi Stream	F3
Pokopokoru Stream	D25	Whakanekeneke Stream (2)	F4
Otohi Stream	D26	Pokopokorua Stream (3)	F5
Hongikore stream	D27	Pokopokorua Stream (2)	F6
Bone Mill Stream	D28	Sunbeam Stream	F7
Argosy Stream	D29	Opitmoko Stream	F8
Ohio Stream	D30	Karaka Stream (3)	F9
Pukehinau Stream	D31	Komata Reefs	F10
Moanataiari Stream	D32		
Waiotahi Stream	D33	**High debris-flow hazard (Kaimia)**	
Alabama stream	D34	Omahu Stream (3)	F11
Karaka Stream (2)	D35	Tui Stream	F12
Herewaka Stream	D36	Tunakohoia Stream	F13
Ruapekapeka	D37	Moonlight Stream (Tunakohoia 3)	F14
Wentworth River (3)	D38	Lipsy Stream	F15
Unnamed Stream, Pauanui	D39	Unnamed Stream, Baldspur	F16
Waitaia Stream	D40	Unnamed Stream, Gordon Rd. (1)	F17
Mangatu Stream	D41	Unnamed Stream, Gordon Rd. (2)	F18
Waikawau River (3)	D42	Wahine Stream (3)	F19
Oneuru Creek	D43	Motutupere Stream	F20
Okahutahi Stream	D44	Garrett Stream	F21
		Goodwin Stream	F22
		Unnamed Stream, Barton Rd. (2)	F23
		Unnamed Stream, Barton Rd. (3)	F24
		Mangakara Stream	F25
		Te Weraiti Stream	F26
		Omahine Stream (2)	F27

(*n*) Indicates watershed derived for an unnamed tributary draining into the main stream

6.7 Limitations of the research

Having discussed the key results with respect to the literature and implied a debris-flow hazard for stream watersheds in the study area (sections 6.2 to 6.6), it is now appropriate to discuss the main limitations associated with the GIS and field investigation methodologies, in order to provide a balanced understanding of the results obtained in the research.

6.7.1 Limitations of the GIS procedure

A number of drawbacks were associated with the use of the NZ 25 x 25 m DEM in the GIS procedure. For example, the relatively coarse resolution of the DEM meant that spatial details of small-scale features in the modelled landscape were lost (DeMers, 2002). Consequently, as the DEM was the source dataset utilised in the watershed model, it constrained the quality of all subsequently derived outputs in the model. In particular, this affected the representation of the drainage network in that streams were modelled as one cell wide (25 m – minimum grid size), in general much wider than that observed in reality. Despite this shortcoming, the resolution of the DEM was considered only a minor hindrance in the present research as the main aim was to look at the broader details of the landscape, at watershed level/regional scale as opposed to at local-scale. Furthermore, the TM wrap air photographs (1 m resolution), when draped over the DEM, allowed identification of small-scale features where necessary.

The age of the DEM may have also been a possible constraint on the accuracy of the results obtained in the present research. For example, since 2000 (date the DEM was generated) it is possible that some streams in the study area may have changed course as result of storm-related flooding and avulsion. Such changes are not reflected in the outputs of the present research. Therefore it is possible that some steep streams that are not considered in the present research (because they were interpreted to lack a debris-flow hazard i.e. had no developments in close proximity to the active stream channel) may in fact now have a debris-flow hazard.

A number of limitations also existed in relation to the placement of pour points and the identification of suitable streams for watershed generation. As mentioned in Chapter 4, section 4.3.3.2, the accurate initial placement of pour points was largely affected by the resolution of the on-screen display at the time. This issue was overcome using the snap pour tool which enabled initially placed pour points to be snapped to the desired cell of highest flow accumulation (streams). A small limitation existed in relation to the snap pour tool however, in that if the initial placement of pour points was grossly inaccurate (i.e. many grid cells off the intended placement location) the accuracy of the tool became dependent on the snap distance chosen (see Chapter 4, section 4.3.3.2). For example, if the desired cell (for final pour point placement) lies within a snap distance of 50 m of the initially placed pour point, but the user sets the snap distance at 100 m, cells other than that desired showing high flow accumulation (other nearby streams) maybe snapped instead of the desired cell. It is thus imperative that initial placement of pour points is carried out at individual cell level (i.e. display magnified to show individual cells) to promote the accuracy of the snap pour tool and subsequently derived outputs.

A degree of subjectivity was associated with the identification of suitable streams for watershed generation. For example, the desired proportions of steep slopes for prospective locations to derive watersheds (criterion (a) in section 4.3.3.1) and the presence of housing with a possible hydrogeomorphic hazard (criterion (b)) were both estimated visually on-screen. In this regard both techniques were largely subjective. It could be argued that more objective methods (e.g. deriving the watershed first and then calculating slope proportions within this feature) should have been used to estimate proportions of steep slopes for criterion (a). It should be noted however that the purpose of criterion (a) was preliminary identification of areas suitable for watershed generation, thus an objective method such as that suggested above may have taken more time that it was worth. Despite this, it is possible that some streams with border-line proportions of suitable slopes according to criterion (a) may not have been considered for watershed generation and subsequent morphometric and debris-flow hazard analysis in the present research.

The visual estimation method used to identify housing/developments with a possible debris-flow hazard (criterion (b)) was also subject to limitation. For example,

identifying those houses strictly within the 4 cell radius of the active stream channel became challenging when stream channels were oriented at an angle (i.e. other than perpendicular or parallel to the regular grid tessellation – in this case the boundary of 4 cell radius became arbitrary). A more objective method such as creating a buffer at a specified distance around stream channels in the drainage network could have proved a more accurate approach for the identification of housing with a debris-flow hazard.

Some minor limitations can also be identified in relation to data entry and processing in the GIS procedure. Despite the fact that the 'watershed model' was able to iterate and thus process large amounts of data automatically the preparation of lists to contain relevant data was time-consuming, and the correct iteration of the model sensitive to the order of data entry. This enhanced the potential for human error (i.e. due to loss of concentration), especially where large datasets were to be processed. In addition, statistical data (morphometric information on watersheds) derived using the model also had to be exported manually into the relevant analysis programmes (e.g. Microsoft Excel; Statistica), as opposed to automatically as is possible via scripting. Consequently, this was also a time-consuming task. Despite this, the manual procedure did have an advantage in that each output could be scrutinised for any possible errors before export (as opposed to automated procedures where it may prove difficult to identify earlier sources of error subsequent to processing large amounts of data).

6.7.2 Limitations of the field investigation

A number of limitations exist in relation to the field investigation methodology for the research, these primarily associated with: the sample size of sites chosen for field reconnaissance, the use of supplementary techniques to support the field observations and the influence of land modification and subsequent fluvial activity on the geomorphic record for debris-flows. As described in section 4.4.1, Chapter 4, a total of 18 sites (stream locations draining watersheds) were selected for field investigation in the Coromandel/Kaimai study area. In statistical terms, this is considered a small sample size (Statistica, 2005). Consequently, there exists a higher probability (i.e. in comparison to a larger sample size) that the results obtained in the investigation are perhaps due to 'chance' or 'fluke' rather than fact (Statistica, 2005). Despite this, the

overall results of this research are shown be highly significant ($p < 0.001$) and thus unlikely to be due to a chance outcome. Nevertheless, in a similar investigation it would be preferable to field test a larger sample size (e.g. 50-100 sites) to effectively eradicate the possibility of chance outcomes affecting the results. Due to time constraints however, such extensive field reconnaissance was not considered feasible in the present research.

The sample size issue was also a significant limitation with regard to the number of watersheds selected for investigation within categorical combinations of *R* and watershed length (WL). For example, only 2 stream watersheds were selected from category D (see Table 4.2, Chapter 4), while 6 were chosen/selected from categories A and F, and 4 in category C. Furthermore, no stream watersheds were selected in categories B and E for field investigation (refer to section 4.4.1 for explanation). Consequently there exists a high probability that the results were due to chance (particularly for watersheds in category D). Again, it would have been preferable to have selected equal numbers of watersheds within each category to reduce bias and skewness in the results.

A further shortcoming of the field investigation methodology related to the fact that no supplementary techniques such as age dating of deposits, slope stability analysis or air photograph interpretation were utilised to supplement the observations made in the field. As mentioned in section 4.5, Chapter 4, air photos were acquired but were of inadequate resolution and expense to be a useful supplement to the field investigation. Dating of deposits and slope stability analyses were not considered due to time constraints and the considerable expense associated with these methods. This meant that the field investigation for hydrogeomorphic processes was based solely on observational evidence. Further, this meant the field investigation was subject to limitations associated with subsequent fluvial activity, landuse changes and the general influence of forested fans on sediment deposit signatures typical of particular hydrogeomorphic processes. For example, post-event fluvial reworking of sediments and anthropogenic alteration of the stream fan (e.g. housing developments) can mean the characteristic sediment deposit signatures indicative of past debris-flows or debris-flood occurrence are removed from the landscape (Wilford et al., 2004; Davies, 1997). Additionally sediment deposit signatures can be altered by the presence of

trees on fans (e.g. turbulence around trunks; downed woody debris can alter clast orientation and obscure or enhance characteristic sediment deposit signatures; Wilford et al., 2004). These limitations could have affected the accuracy of the results obtained in the present research and hence the overall classification of debris-flow hazard for stream watershed locations in the study area.

Overall however, the results demonstrate that specific watershed morphometric parameters (Melton ratio (*R*) and watershed length), derived using the GIS procedure developed in this research, can be used to give a preliminary indication of debris-flow potential at the drainage points (fan-heads) of watersheds in the Coromandel/Kaimai region. In this regard, the specific GIS procedure devised in this research could thus prove a useful tool for regional councils and CDEM groups in regional debris-flow hazard assessment by facilitating the identification of existing developments at risk of debris-flow disaster.

\

Chapter Seven

Summary and Conclusions

7.1 Introduction

This thesis has developed and tested a new procedure for identifying areas prone to debris-flow hazards in the Coromandel/Kaimai region, North Island, New Zealand. This chapter will summarise and conclude the main findings of the research with respect to the aims and objectives set out in Chapter 1. In addition, some direction will be given regarding the future use of GIS technology and watershed morphometric variables to identify debris-flow hazard-prone areas, both in New Zealand and abroad.

7.2 Restatement of thesis aims and objectives

As outlined in Chapter 1, the primary objective of this research was to develop and test a new procedure for identifying debris-flow hazard-prone areas in the Coromandel/Kaimai region. The procedure was developed in relation to the following hypothesis:

"That debris-flow, debris-flood and flood hazards can be related to specific catchment/watershed parameters and these parameters used to indicate hazard levels at the drainage points of watersheds in the Coromandel/Kaimai study area"

In order to test the hypothesis and hence validate the utility of the GIS procedure, the primary aims of the research were to:

1. Generate useful definitions and distinctions between debris-flows, debris-floods, conventional floods and related hydrogeomorphic processes as these phenomena present vastly different hazards

2. Identify suitable morphometric parameters to be derived using the procedure to be developed

3. Develop a simple, automated GIS-based procedure to derive watersheds and their morphometric parameters for selected stream locations in the study area

4. Test the hypothesis and hence the procedure by:

   (a) Examining selected stream locations for geomorphic evidence indicative of debris-flow, debris-flood and flood processes.

   (b) Correlating the field evidence observed at selected stream locations for each hazard with the GIS-derived morphometric measures to enumerate relations between these variables.

   (c) Using the GIS procedure to derive watershed morphometric measures for streams in other areas of New Zealand known to have produced debris-flows.

5. Imply a debris-flow hazard for specific stream locations in the study area for which watershed data had previously been derived

7.3 Summary of the main findings

The first aim of this research was to generate definitions and distinctions between hydrogeomorphic phenomena. Debris-flows, defined as "a rapid, highly concentrated, homogenous flows of saturated non-plastic debris and sediment in steep channels", were identified to present the greatest hazard out of the hydrogeomorphic phenomena reviewed. This was due to their ability to transport huge boulders in permanent suspension as a result of physical interactions between clasts, and clasts and the fluid during flow. In contrast, conventional fluvial floods, characterized by substantially more water than sediment in the mixture and hence Newtonian fluid flow characteristics, were identified to pose the least hazard. Transitional phenomena between these two end members: hyperconcentrated flow (a distinct flow process, fine-grained in nature in which viscous and yield strength maintained suspension of fines in water enables the intermittent suspension of large quantities of coarser sediment) and debris-flood (extreme magnitude sediment-rich flood events in which prodigious quantities of sediment and debris are transported downstream in steep

catchments and in which the flow maintains the characteristics of a Newtonian fluid) were identified to pose a greater hazard than fluvial floods for their ability to transport large quantities of sediment, but still presented a lower hazard than debris-flows.

The second aim of this research was to identify suitable morphometric parameters to derive using the procedure to be developed. Through review of the literature, Melton ratio (R) and watershed length were identified to offer the greatest potential for discrimination of basins and fans with a debris-flow hazard and thus were chosen for use in the present research.

The third aim of this research was to develop a GIS-based procedure to derive watersheds and their morphometric parameters for selected stream locations in the study area. In this regard, ESRI's Arc GIS Arc View, version 9.1 and 9.2 comprised the GIS within which a 2–part systematic procedure was developed (the Watershed model). This procedure was constructed linking tools within the Spatial Analyst Model Builder interface, with the NZ 25 x 25 m DEM used as primary input to the procedure. When run, it enabled a drainage network to be derived for the study area (part 1 of the model) and watersheds and their associated morphometric parameters (Melton ratio (R) and watershed length) to be derived for selected streams (part 2 of the model).

The fourth aim of the research was to test the ability of the GIS procedure (the Watershed model) to identify areas prone to debris-flows in the Coromandel/Kaimai region. This first involved field investigation of selected stream watershed locations to identify geomorphic evidence characteristic of debris-flow, debris-flood and fluvial processes. Eighteen sites were selected for field investigation. Highest amounts of evidence for debris-flows were found at Lipsy Stream (94 %) and Unnamed Stream, Gordon Rd. (87 %) in Te Aroha. Comparatively more evidence was observed for fluvial processes than for debris-flows and debris-floods at Te Puru Stream (82 %) and Waiwhango Stream (78 %) in the Coromandel Peninsula. Additionally, dominant evidence for debris-floods was found at Wahine (80 %) and Gordon (80 %) streams in the Kaimai region.

Evidence observed in the field was then correlated with the GIS-derived watershed morphometric parameters (Melton ratio (R) and watershed length) to enumerate relations between the variables. Strong relationships were found to exist between the Melton ratios (R) of watersheds in the study area and the evidence observed for debris-flows, debris-floods and fluvial processes at the drainage points of these watersheds. These relationships are interpreted to exist because Melton's R is a measure of the channel gradients within the watershed and debris-flows require a certain minimum gradient (identified at R = 0.60 (steep gradients) in the study area) to maintain motion to the drainage point of the watershed.

Equally strong relationships were also found to exist between the lengths of watersheds in the study area and the evidence observed for debris-flows and fluvial processes at corresponding drainage points of these watersheds. These relationships are interpreted to exist for the reason that longer watersheds are generally larger, exhibit higher stream orders and thus lower channel gradients than shorter watersheds. Consequently, debris-flows are rarely able to travel far enough to reach the drainage points of longer watersheds (e.g. <2.7 km in the present study) as channel gradients are generally insufficient to maintain their momentum and there exists a higher probability for termination (e.g. in watersheds characterised by higher order streams, the presence of more lower-gradient stream junctions may act to slow debris-flow motion to the fan as these locations are generally associated with reductions in channel gradients and increases in channel widths). No significant relationship was apparent between the evidence found for debris-floods at the drainage points of watersheds in the study area and the lengths of watersheds. This is probably due to the fact that debris-floods are transitional in nature between debris-flow and fluvial processes and thus can occur in both longer, larger watersheds (deposits would probably exhibit a higher fluvial component) and shorter, smaller and steeper watersheds (higher debris-flow component).

Overall, the relationships apparent between the evidence observed for debris-flows, debris-floods and fluvial processes at stream watersheds locations in the study area, and the Melton's R and watershed lengths of contributing watersheds, compare well with the literature. The results thus support the hypothesis and confirm the utility of

the parameters, and hence the GIS procedure for identifying areas prone to debris-flows in the Coromandel/Kaimai region.

In light of the results, R and watershed length were combined (displayed using a scatter plot) and critical thresholds of the two variables were used to classify the range limits for processes (defined by categorical combinations of R and watershed length: A-F). The categorical combinations were then assigned a level of debris-flow hazard e.g. Category A (R<0.30, WL >2.7 km) was assigned the lowest hazard; category F (R>0.60, WL <2.7 km) assigned highest hazard. This was based on the interpretation that each combination could be used to indicate the particular likelihood of debris-flows to reach the drainage point of a watershed because they reflect fundamental catchment characteristics/requirements that are necessary to promote and maintain momentum in debris-flows.

The GIS procedure was then used to derive R and watershed lengths for streams in other areas of New Zealand known to have produced debris-flows. The majority of these watersheds were observed to plot in category F (assigned high debris-flow hazard) therefore further supporting the utility of the GIS procedure.

The fifth and final aim of this research was to imply a debris-flow hazard for stream locations in the study area (for which watershed data had previously been derived) and produce indicative debris-flow hazard maps for the Coromandel/Kaimai region. The majority of stream watersheds (214/302; 71 %) were identified to exhibit a low or low-moderate debris-flow hazard (*R*/WL categories A, B and C), while 88 watersheds in the study area (29 %) were observed to exhibit either a moderate, moderate-high or high debris-flow hazard. Watersheds exhibiting moderate, moderate-high and high debris-flow hazards were found to be mainly restricted to the western range front of the Coromandel and Kaimai Ranges. Highest concentrations of these watersheds were noted in the vicinity of Te Aroha; towards the southern extent of the Kaimai range (adjacent to Matamata); in the vicinity of Thames and in the far north of the Coromandel Peninsula (just south of Port Jackson).

7.4 Conclusions

This research has provided a fresh insight into the preliminary evaluation of debris-flow and related hydro-geomorphic hazards and a greater appreciation of the extent and severity of such hazards in the Coromandel/Kaimai region of north-eastern New Zealand. The results demonstrate that specific watershed morphometric parameters (Melton ratio (R) and watershed length), derived using the GIS procedure developed in this research, can be used to give a preliminary indication of debris-flow potential at the drainage points (fan-heads) of watersheds in the Coromandel/Kaimai region.

Furthermore, the GIS procedure devised in this research is acknowledged to provide a simple, relatively automated and inexpensive alternative to conventional field and map based methodologies for deriving the specific morphometric characteristics of watersheds. In this regard, the procedure could prove a useful tool for regional councils and CDEM groups in regional debris-flow hazard assessment by facilitating the identification of existing developments at risk of debris-flow disaster. In particular, the procedure could provide justification for subsequent, more intensive local investigations to fully quantify the risk to people and property at stream fan and watershed locations in such areas.

7.5 Suggestions for future research

The primary findings of this research confirm the utility of watershed morphometric parameters (Melton ratio (R) and watershed length), and hence the GIS procedure, for the identification of areas prone to debris-flows in the Coromandel/Kaimai region. The method developed in this research however, only investigates one of the factors (morphological characteristics of the watershed) that can influence the spatial occurrence of debris-flows. In this respect, there still exists much to be investigated with regard to the preliminary identification of areas prone to debris-flow hazards. Possible future avenues of research could include:

- Testing the use of basin area and fan gradient watershed morphometric parameters to identify areas prone to debris-flow hazard. In combination with R and watershed length, these additional parameters could facilitate a more

complete preliminary quantification of debris-flow hazard with regard to the topographic/morphometric characteristics of watersheds

- Quantification of sediment-supply conditions within the watersheds in a particular region of interest, perhaps utilising the methods of 'basin-typing'(i.e. classifying a basin as either transport limited or weathering limited) proposed by Bovis and Jakob (1999) and Jakob et al (2005) (see Chapter 3, section 3.2.2).

- Investigation into the broad-scale meteorological trends apparent in a region of interest. This would involve investigation of region-specific precipitation characteristics (e.g. average annual precipitation; recurrence intervals of high intensity rainfall events).

- Development of a GIS database to hold the above information. A procedure could then be devised that incorporates topographical, meteorological and sediment supply information to quantify more precisely watersheds and fans prone to debris-flow hazard in a region of interest.

References:

Adams, C.J, Graham, I.J, Seward, D, Skinner, D.N.B. (1994). "Geochronological and geochemical evolution of late Cenozoic volcanism in the Coromandel Peninsula, New Zealand". *New Zealand Journal of Geology and Geophysics*, **37**: 359-379

Alcoverro, J., Corominus, J. and Gomez, M. (1999). "The Barranco de Aras flood of 7 August 1996" (Biescas, Central Pyrenees, Spain). *Engineering Geology*, **51**: 237-255

Aleotti, P. and Chowdhury, R. (1999). "Landslide hazard assessment: Summary review and new perspectives". *Bulletin of Engineering Geology Reviews*, **58**: 21-44

Aulitzky, H. (1980). "Preliminary two-fold classification of debris-torrents". In: *Proceedings of 'Interpraevent' Conference*. Austria, Bad Ischl, **4**: 285-309, translated from German by G Eisbacher). Internationale Forschungsgesellschaft, Klagenfurt, Interpraevent.

Batalla, R.J.,DeJong, C., Erginzinger, P. and Sala, M. (1999). "Field observations on hyperconcentrated flows in mountain torrents". *Earth Surface Processes and Landforms*, **24**: 247-253

Bates, R.L. and Jackson, J.A. (eds) (1987).Glossary of Geology. Alexandria, VA, American Geological Institute

Benda, L.E. (1985). "Delineation of channels susceptible to debris-flows and debris-floods". In: Takei, A (eds)(1985). Proceedings of the International Symposium on Erosion, Debris-flow and Disaster Prevention. Japan, Tsukuba

Benda, L.E. and Cundy, T.W. (1990). "Predicting deposition of debris-flows in mountain channels". *Canadian Geotechnical Journal*, **27**: 409-417

Beverage, J.P. and Culbertson, J.K. (1964). "Hyperconcentrations of suspended sediment". *ASCE Journal of Hydraulics Division*, **90**(HY6): 117-126

Birkeland, P. (1999). Soils and Geomorphology. New York, Oxford University Press

Bisson, M., Favalli, M., Fornaciai, A., Mazzarini, F., Isola, I., Zanchetta, G. and Pareschi, M.T. (2005*). "*A rapid method to assess fire-related debris flow hazard in the Mediterranean region: An example from Sicily (southern Italy)". *International Journal of Applied Earth Observation and Geoinformation*, **7** (3): 217-231

Boggs, S. (1995). Sedimentology and Stratigraphy (2nd edition). New Jersey, Prentice-Hall.

Bovis, M.J. and Jakob, M. (1999)."The role of debris supply conditions in predicting debris-flow activity". *Earth Surface Processes and Landforms*, **24:** 1039-1054

Bridge, J.S. (2003). Rivers and floodplains: Forms processes and the sedimentary record. United Kingdom, Blackwell Publishing

Broscoe, A.J. and Thompson, S. (1969). "Observations on an alpine mudflow, Steele Creek, Yukon". *Canadian Journal of Earth Science*, **6**: 219-229

Bucky, D.J. (2007). URL: bgis.sanbi.org/GIS-primer/page_15.htm. D.O.A: 15 May 2007

Burrough, P.A. and McDonnell, R.A. (1998). Principles of Geographic Information Systems. Oxford, Oxford University Press

Bull, W. B. (1964). "Alluvial fans and near-surface subsidence in western Fresno County, California". USGS Professional Paper 437-A, Reston, VA, US Geological Survey

Burrows, C. J. and Greenland, D. E. (1979). "An analysis of evidence for climatic change in New Zealand in the last thousand years: Evidence from diverse natural phenomena and from instrumental records". *Journal of the Royal Society of New Zealand*, **9**:321-73

Byrami, M., Ogden, J., Horrocks, M., Deng, Y., Shane, P. and Palmer, J. (2002). "A palynological study of Polynesian and European effects on vegetation in the Coromandel, New Zealand, showing the variability between four records from a single swamp". *Journal of the Royal Society of New Zealand,* **32**(3): 507–531

Caine, N. (1980). "The rainfall intensity-duration control of shallow landslides and debris-flows". *Geografiska Annaler*, **62**A: 23-27

Cannon, S. H. (1993). “An empirical model for the volume change behavior of debris-flows”. In: Shen, H.W, Su, S.T, Wen, F. (eds). (1993). Proceedings, Hydraulic Engineering: Volume 2. New York, American Society of Civil Engineers

Cannon, S.H. and Ellen, S. (1985). “Rainfall conditions for abundant debris-avalanches in the San Francisco Bay region”. *California. California Geology*, **38** (12): 267-272

Cheng, W., Wang, X. and Zhou, X. (1999). “Research on some characteristics of two-phase hyperconcentrated flow”. In: Jayawardena, A.W., Lee, J.H. and Wang, Z.Y. (eds) (1999). River Sedimentation: Theory and applications. Rotterdam, A.A. Balkema.

Christie, A.B., Brathwaite, R.L., Rattenbury, M.S. and Skinner, D.N.B. (2001). ‘Mineral resource assessment of the Coromandel region, New Zealand”. Science Report 2001/11, Institute of Geological and Nuclear Sciences

Church, M. and Mark, D.M. (1980). “On size and scale in geomorphology”. *Progress in Physical Geography*, **4**:342-390

Coe, J.A., Godt, J.W., Parise, M. and Moscariello, A. (2003). Estimating debris-flow probability using fan stratigraphy, historic records and drainage basin morphology, Interstate 70 highway corridor, central Colorado, USA. In: Rickenmann and Chen (eds) (2003). Debris-flow hazards mitigation: Mechanics. Prediction and Assessment. Rotterdam, Millpress.

Committee on methodologies for predicting mudflow areas (1982). Selecting a methodology for delineating mudslide hazard areas for the national flood insurance program. Washington, National Research Council, National Academy Press.

Coussot, P. (1995). "Structural similarity and transition from Newtonian to non-Newtonian behavior for clay-water suspensions". *Physical Review Letters*, **74**: 3971-3974

Coussot, P. and Piau, J.M. (1994). "On the behavior of fine mud suspension". *Rheologica Acta*, **33**: 175-184

Cronin, S.J., LeCointre, J.A., Palmer, A.S. and Neall, V.E. (2000). "Transformation, internal stratification and depositional processes within a channelised, multi-peaked lahar flow". *New Zealand Journal of Geology and Geophysics*, **43**, 117-128

Cruden, D.M. and Varnes, D.J. (1996). "Landslide types and processes". In: Turner, A.K. and Shuster, R.L. (eds) (1996). Landslides investigation and mitigation. Special report 247: 36-75. Transportation Research Board, Washington, D.C., US National Research Council.

Davies, T.R. (1997). "Using hydro-science and hydro-technical engineering to reduce debris-flow hazards". *Proceedings of the First International Conference – Debris-flow Hazards Mitigation: Mechanics, Prediction and Assessment*: 787-810, San Francisco, American Society of Civil Engineers.

Decaule, A. and Saemundson, T. (2003). "Debris-flow characteristics in the Gleidarhjalli area, northwest Iceland". *Debris-flow hazards mitigation: Mechanics,*

Prediction, and Assessment: Proceedings of the 3rd International DFHM conference, Davos, Switzerland. Rotterdam, Millpress.

DeMers, M.N. (2002). GIS modelling in raster. USA, John Wiley and Sons.

de Scally, F.A., Slaymaker, O. and Owens, I.F. (2001). "Morphometric controls and basin response in the Cascade Mountains". *Geografisca Annaler***, 83A** (3):117-130

de Scally, F.A. and Owens, I.F. (2004). "Morphometric controls and geomorphic response on fans in the Southern Alps, New Zealand". *Earth surface processes and landforms*, **29**: 311-322

Environment Waikato (2007). URL: www.ew.govt.nz/enviroinfo/profile /environment/climate.htm, D.O.A: May 4, 2007.

ESRI (2006). Arc GIS version 9.2 desktop electronic help manual.

Fannin, R.J. and Wise, M.P. (2001). "An empirical statistical model for debris-flow travel distance". *Canadian Geotechnical Journal*, **38**: 982-994

Gagoshidze, M.S. (1969). "Mud flows and their control". *Soviet Hydrology: Selected Papers*, **4:** 410-422

Garcia-Martinez, R. and Lopez, J.L. (2005). Debris flows of December 1999 in Venezuela, In: Jakob, M. and Hungr, O. (eds), (2005). Debris-flow Hazards and Related Phenomena. Berlin, Praxis. Springer.

Glade, T. (2005). "Linking debris-flow hazard assessments with geomorphology". *Geomorphology*, **66** (1-4): 189-213

Griffiith, P.G., Webb, R.H. and Melis, T. S. (1996). "Initiation and frequency of debris-flows in the Grand Canyon, Arizona". USGS Open-file report 96-491. Reston, V.A, US Geological Survey

Guzzetti, F., Carrara, A., Cardinali, M. and Richenbach, P. (1999). "Landslide hazard evaluation: A review of current techniques and their application in a multi-scale study, central Italy". *Geomorphology*, **31**:181-216

Hair, J.F; Black, W.C; Babin, B.J; Anderson, R.E and Tatham, R.L. (2006). Multivariate data analysis (6th edition). New Jersey, Pearson Prentice Hall.

Hauraki District Council (2007).URL: www.haurakidc.govt.nz/Overview/Paeroa.htm. D.O.A: 8 March 2007.

Hochstein, M.P. and Nixon, I.M. (1979). "Geophysical study of the Hauraki Depression, North Island, New Zealand". *New Zealand Journal of Geology and Geophysics*, **22**: 1-19

Hogg, A.G. and McCraw, J.D.(1983)."Late Quaternary Tephras of the Coromandel Peninsula, New Zealand: a mixed peralkaline and calcakaline tephra sequence". *New Zealand Journal of Geology and Geophysics,* **26***:* 163-187

Homer, L. and Moore, P. (1992). Vanishing volcanoes: A guide to the landforms and rock formations of the Coromandel Peninsula. Wellington, Landscape Publications.

Hungr, O. (2005). Classification and Terminology. In: Jakob, M. and Hungr, O. (eds), (2005). Debris-flow Hazards and Related Phenomena. Berlin, Praxis. Springer.

Hooke, R. LeB. (1968). "Steady-state relationships on arid-region alluvial fans in closed basins". *American Journal of Science*, **266**: 609-629

Hungr, O. (2005). Classification and Terminology. In: Jakob, M. and Hungr, O. (eds), (2005). Debris-flow Hazards and Related Phenomena. Berlin, Praxis. Springer.

Hungr, O., Evans, S.G., Bovis, M. and Hutchinson, J.N. (2001). "Review of the classification of landslides of the flow type". *Environmental and Engineering Geoscience*, **VII**: 221-238

Hurlimann, M., Rickenmann.,D. and Graf, C. (2003). "Field of monitoring data of debris-flow events in the Swiss Alps". *Canadian Geotechnical Journal*, **40**:161-176

Hutchins, G. (2006). Highwater - Floods in New Zealand. Wellington, Grantham House Publishing

Hutchinson, J.N. (1968). Mass movement. In: Fairbridge, R.W. (eds), (1968). Encyclopedia of Geomorphology, New York, Reinhold: 688-695.

Hutchinson, J.N. (1988). "General report: Morphological and geotechnical parameters of land-slides in relation to geology and hydrogeology". In: Bonnard, C. (eds) (1988). Proceedings of the 5th International Symposium on Landslides, Christchurch, New Zealand. Rotterdam, A.A. Balkema, **(1)**:3-36

Ikeya, H. (1981). “A method for designation for area in danger of debris-flow”. *Erosion and Sediment Transport in Pacific Rim steep lands*, **132**: 576-588, IAHS Publication

Inovative GIS solutions (2007). URL: www.innovativegis.com/basis/ primer/ concepts.html. D.O.A.: 5 May 2007.

Irvine, R.J. and Smith, M.J. (1990). “Geophysical exploration for epithermal gold deposits”. *Journal of Geochemical Exploration*, **36**: 375-412

Iverson, R.M. (1997). “The physics of debris-flows”. *Reviews of Geophysics,* **35(3)**: 245-296

Iverson, R.W. (2005). Debris-flow mechanics. In: Jakob, M. and Hungr, O. (eds) (2005). Debris-flow Hazards and Related Phenomena. Berlin, Praxis. Springer.

Jackson, L.E. Jr, Kostaschuk, R.A. and MacDonald, G.M. (1987). “Identification of debris-flow hazard on alluvial fans in the Canadian Rocky Mountains”. *Reviews in Engineering Geology* **7**: 115-124

Jakob, M. (2005). Debris-flow hazard analysis. In: Jakob, M. and Hungr, O. (eds), (2005). Debris-flow Hazards and Related Phenomena. Berlin, Praxis. Springer.

Jakob, M., Bovis, M. and Oden, M. (2005). “The significance of channel recharge rates for estimating debris-flow magnitude and frequency”. *Earth Surface Processes and Landforms*, **30**: 755-766

Jakob, M. and Hungr, O. (eds) (2005). Debris-flow Hazards and Related Phenomena. Berlin, Praxis. Springer.

Jakob, M. and Podor, A. (1995). "Frequency and magnitude of debris-flows". *Canadian Geotechnical Conference, Vancouver, B.C.*, **1**:491-498

Jane, T.G. and Green, T.G.A. (1984). "Ecological aspects of climate patterns within the Kaimai Ranges, North Island, New Zealand". *New Zealand Journal of Ecology*, **7**: 183-197

Jones, A. (1985). "Trouble in the town". *Soil and Water*, **21(1):** 21

Jones, A., Howarth, M. and Whitehouse, B. (1985). Town in trouble. Hamilton, Hamilton printing works

Jarrett, R.D. and Costa, J. E. (1986). "Hydrology, Geomorphology and Dam-break modeling of the July 15, 1982, Lawn Lake Dam and Cascade Lake Dam Failures, Larimer County, Colorado". USGS Professional Paper 1369. Reston, VA, US Geological Survey.

Kellerhals, R. and Church, M. (1990). Hazard management on fans, with examples form British Columbia. In: Rachocki, A.H. and Church, M. (1990). Alluvial fans: A field approach. Chichester, John Wiley and Sons

Kimbu, R.T. (1991). Catastrophic flooding in the Kowhai catchment, South Canterbury, New Zealand. Master of Arts thesis, Department of Geography, University of Canterbury.

Knighton, D. (1998). Fluvial forms and processes: A new perspective. New York, John Wiley and Sons

Komar, P.D. (1988). "Sediment transport by floods". In: Baker, V.R., Kochel, R.C., Patton, P.C. (eds), Flood Geomorphology. New York, Wiley-Interscience.

Kostaschuk, R.A., Macdonald, G.M. and Putnam, P.E. (1986). "Depositional process and alluvial fan – drainage basin morphometric relationships near Banff, Alberta, Canada". *Earth Surface Processes and Landforms*, **11**:471-484

Landcare research (2000). URL: www.landcareresearch.co.nz/databases. D.O.A: 10 June 2006.

Lin, P-S, Lin, J-Y, Hung, J-C and Yang, M-D. (2002). "Assessing debris-flow hazard in a watershed in Taiwan". *Engineering Geology,* **66** (3-4): 295-313

Lorenzini, G. & Mazza, N. (2004). Debris-flow: Phenomenology and Rheological Modelling. Southhampton, WIT Press.

Lorente, A., Garcia-Ruiz, J.M., Begueria, S. and Arnaez, J. (2002). "Factors explaining the spatial distribution of hillslope debris-flows: a case study in the Flysch sector of the central Spanish Pyrenees". *Mountain Research and Development*, **22** (1):32-39

Major, J.J., Janda, R.J. and Daag, A.S. (1996). Watershed disturbance and lahars on the east side of Mt Pinatubo during the mid-June 1991 eruptions. In: Newhall, C.G. and Punungbayan (eds) (1996). Fire and Mud: Eruptions and lahars of Mt Pinatubo,

Philippines. Quezon City, Philippine Institute of Volcanology and Seismology and University of Washington Press, Seattle.

Maunder, W. J. (1970). World survey of Climatology, volume 13. Amsterdam, Elsevier

McSaveney, M. J., Beetham, R.D., Leonard, G.S. (2005). "The 18 May 2005 debris-flow disaster at Matata: Causes and mitigation suggestions". Client Report 2005/71, Lower Hutt, Institute of Geological and Nuclear Sciences.

McSaveney, M.J. and Beetham, R.D. (2006). The potential for debris-flows from Karaka stream at Thames, Coromandel. GNS consultancy report 2006/014, Lower Hutt, Institute of Geological and Nuclear Sciences.

McSaveney, M. J. and Davies, T.R. (2005). Engineering for debris-flows in New Zealand. In: Jakob, M. and Hungr, O. (eds) Debris-flow hazards and related phenomenon. UK, Praxis

Melton, M.A. (1965). "The geomorphic and paleoclimatic significance of alluvial deposits in southern Arizona". *Journal of Geology*, **73**: 1-38

Mizuyama, T. (1981). An intermediate phenomenon between debris-flow and bed load transport. In: *Erosion and sediment transport in Pacific Rim steep lands*. IAHS Publication No. 132. Christchurch, International Association of Hydrological Sciences.

Montz, B.E. (1993). "Hazard area disclosure in New Zealand: the impacts on residential property values in two communities". *Applied Geography*, **13**(3): 225–242.

Morgan, G.C., Rawlings, G.E. and Sobkowicz, J.C. (1992). Evaluating total risk to communities from large debris-flows. In: Geotechnique and natural hazards: a symposium sponsored by the Vancouver Geotechnical Society and the Canadian Geotechnical Society, May 6-9. Vancouver, BC, BiTech Publishers

Newsome, P.F.J. (1987). The vegetative cover of New Zealand. Wellington, National Water and Soil conservation Authority

Ni, J.R., Liu, R.Z., Onyx, W.H., Wai, A., Borthwick, G.L. and Ge, X.D. (2006). "Rapid zonation of abrupt mass movement hazard: Part 1, General Principles". *Geomorphology*, **80** (3-4): 214-225

NIWA Science, (2007). URL: http://www.niwascience.co.nz/edu/resources/climate, (8 March 2007).

O'Brien, J.S. and Julian, P.Y. (1985). "Physical properties and mechanics of hyperconcentrated sediment flows". *Proceedings Specialty Conference on Delineation of Landslides, Flash Flood and Debris-flow Hazards in Utah*, 260-279.

Pasuto, A. and Soldati, M. (2004). "An integrated approach for hazard assessment and mitigation of debris-flows in the Italian Dolomites". *Geomorphology*, **61** (1-2): 59-70

Patton, P.C. (1988). Drainage Basin Morphometry and Floods. In: Baker, V.R., Kochel, R.C. and Patton, P.C. (1988). Flood Geomorphology. New York, John Wiley and Sons

Piako Post, (1985). Death and disaster swoop down on sleeping town. February 20, 1985 Supplement to the Piako Post

Pierson, T.C. (2005). Hyperconcentrated flow – transitional process between water-flow and debris-flow. In: Jakob, M. and Hungr, O. (eds) (2005). Debris-flow Hazards and Related Phenomena. Berlin, Praxis. Springer.

Pierson, T.C. and Costa, J.E. (1987). "A rheological classification of sub-aerial sediment-water flows". *Geological Society of America Reviews in Engineering Geology*, **7**: 1-12

Qian, Y., Yang, W., Zhao, W, Cheng, X., Zhang, L. and Xu, W. (1981). "Basic characteristics of flow with hyperconcentration of sediment". *Proceedings of International Symposium on River Sedimentation*. Beijing, Chinese Society of Hydraulic Engineering

Rickenmann, D. (1991). "Hyperconcentrated flow and sediment transport at steep slopes". *Journal of Hydraulic Engineering*, **117**: 1419-1439

Ritter, D.F., Kochel, R.C. and Miller, J.R. (2002). Process Geomorphology: Fourth Edition. New york, McGraw-Hill

Rodolfo, K.S., Umbal, J.V., Alonso, R.A., Remotigue, C.T., Paladio-Melosantos, M.L., Salvador, J.H.G., Evangelista, D. and Millar, Y (1996). "Two years of lahars on the western flank of Mount Pinatubo: Initiation, flow processes, deposits, and attendant geomorphic and hydraulic changes". In: Newhall, C.G. and Punungbayan (eds) (1996). Fire and Mud: Eruptions and lahars of Mt Pinatubo, Philippines. Quezon City, Philippine Institute of Volcanology and Seismology and University of Washington Press, Seattle.

Roger, J.D. and Beckmann, N.H. (2003). West Lost Trail Creek Sturzstrom: A composite landslide, URL: http://web.umr.edu/~rogersda/composite_landslides. D.O.A: 12 March 2007.

Rowbotham, D., de Scally, F. and Louis, J. (2005). "The identification of debris torrent basins using morphometric measures derived within a GIS". *Geografiska Annaler*, **87**A (4): 527-537

Scoot, K.M. and Gravlee, G.C. (1968). "Flood surge on the Rubicon River, California: Hydrology, Hydraulics and Boulder Transport". USGS Professional Paper 422-M, Reston, VA, US Geological Survey

Scott K.M., Janda, R.J., de la Cruz, E.G., Gabinete, E., Eto, I., Isada, M., Sexon, M. and Hadley, K.C. (1996). "Channel and sedimentation responses to large volumes of 1991 volcanic deposits in the east flank of Mt Pinatubo". In: Newhall, C.G. and Punungbayan (eds) (1996). Fire and Mud: Eruptions and lahars of Mt Pinatubo, Philippines. Quezon City, Philippine Institute of Volcanology and Seismology and University of Washington Press, Seattle.

Sharpe, C.F.S. (1938). Landslides and related phenomena. New York, Columbia University Press

Skempton, A.W. and Hutchinson, J.N. (1969). "Stability of natural slopes and embankment foundations". *Proceedings of the 7th International Conference on Soil Mechanics and Foundation Engineering* (State of the art volume: 291-340)

Skinner, D.N. B. (1976). Sheet N40 and part sheets N35, N36 and N39 – northern Coromandel. Geological Map of New Zealand 1:63 360. Wellington, Department of Scientific and Industrial research.

Skinner, D.N. B. (1986). Neogene volcanism of the Hauraki Volcanic Region. In: Smith, I.E.M.(eds) (1986). "Late Cenozoic volcanism in New Zealand". *Royal Society of New Zealand Bulletin*, **23**: 21-47

Skinner, D.N. B. (1995). Geology of the Mercury Bay area, Sheet T11BD and part U11. Scale 1:50 000. *Institute of Geological and Nuclear Sciences geological map 4.*

Slaymaker, O. (1988). "The distinctive attributes of debris-torrents". *Hydrological Sciences Journal,* **33**: 567-573

Smith, K. (2001). Environmental Hazards: Assessing risk and reducing disaster. London, New York, Routledge.

Staley, D.M., Wascklewicz, T. A., Blaszczynski, J.S. (2006). "Surficial patterns of debris-flow deposition on alluvial fans in Death Valley, CA, using airborne laser SWATH mapping data". *Geomorphology*, **74** (1-4):152-163

Statistica, (2005). Statistica version 7.1 desktop electronic help manual.

Stiny, J. (1910). Die Muren. Verlag der Wagner'schen Universitats-buchhandlung, Innsbruck. (Debris-flows (English translation by Jakob, M. and Skermer, N. (1997)). Vancouver, EBA Engineering Consultants.

Stirling, S. and Slaymaker, O. (2006). "Lithologic control of debris-torrent occurrence". Geomorphology, **86** (3-4): 307-319

Summerfield, M.A. (1991). An Introduction to the Study of Landforms. New York, John Wiley and Sons.

Swanston, D.N. (1974). "Slope stability problems associated with timber harvesting in mountainous regions of the south-western United States". (Forest Services General Technical Report PNW -021). Washington, US Department of Agriculture

Takahashi, T. (1981). Debris-flow. *Annual Reviews in Fluid Mechanics,* **13:** 57-77

Takahashi, T. (1991). Debris-flow. Monograph series of IAHR, Rotterdam, A.A. Balkema

Thornton, J. (2000). The reed field guide to New Zealand Geology: An introduction to rocks, minerals and fossils. Auckland, Reed Publishing.

Tourism Coromandel (2007). URL: http://thecoromandel.com/2007, (15 May 2007).

Van Dine, D.F. (1985). "Debris-flows and debris-torrents in the southern Canadian Cordillera". *Canadian Geotechnical Journal*, **22**: 44-68

Varnes, D.J. (1954). “Landslide types and processes”. In: Eckel, E.B. (eds) (1954). *Lanslides and Engineering Practice* (Special Report 28: 20-47). Washington, Highway Research Board, National Academy of Sciences.

Varnes, D.J. (1978). “Slope movement and types of processes”. In Schuster, R.J. and Krizek, R.J. (eds) (1978). *Landslides, Analysis and Control* (Special Report 176: 11-33). Washington, Transportation Research Board, National Academy of Sciences.

Volker, H.X., Wasklewicz, T.A. and Ellis, M.A. (2006). “A topographic fingerprint to distinguish alluvial fan formative processes”. *Geomorphology*, In Press, Corrected Proof.

Waananen, A.O., Harris, D.D. and Williams, R.C. (1970). “Floods of December 1964 and January 1965 in the far western states, part 2: Stream flow and sediment data”. USGS Water-Supply Paper 1866B. Reston, VA, US Geological Survey.

Walsh, S.J., Butler, D.R. and Malanson, G.P. (1998). “An overview of scale pattern process relationships in geomorphology: A remote sensing and GIS perspective”. *Geomorphology*, **21**: 183-205

Wan, Z. and Wang, Z. (1994). Hyperconcentrated Flow. Rotterdam, A.A. Balkema.

Wardle, P. (1991). The vegetation of New Zealand. Cambridge, Cambridge University Press

Watanabe. and Ikeya, H, (1981). “Investigations and analysis of volcanic mudflows on Mt Sakurajima, Japan”. *Proceedings Erosion and Sediment Transport Measurements*, **133:** 245-256, IAHS Publication

Weiczorek, G.F., Larsen, M.C., Eaton, L.S., Morgan, B.A. and Blair, J.L. (2001). “Debris-flow and flooding hazards associated with the December 1999 storm in coastal Venezuela and strategies for mitigation”. USGS Open File Report 01 – 0144. Reston, VA, US Geological Survey,

Whitehouse, I.E. and McSaveney, M.J. (1992). “Assessment of geomorphic hazards along an alpine highway”. *New Zealand Geographer*, **48**(1): 27-32

Wieczorek, G.F. and Glade, T. (2005). Climatic factors influencing occurrence of debris-flows. In: Jakob, M. and Hungr, O. (eds), (2005). Debris-flow Hazards and Related Phenomena. Berlin, Praxis. Springer.

Wieczorek, G.F, Morgan, B.A. and Campbell, R.H. (2000). “Debris-flow hazards in the Blue Ridge of central Virginia”. *Environmental and Engineering Geoscience*, **6** (1): 3-23

Wilson, R.C. and Wieczorek,G.F. (1995). “Rainfall thresholds for the initiation of debris-flows at La Honda, California”. *Environmental and Engineering Geoscience*, **1**(1): 11-27

Wilford, D.J., Sakals, M.E., Innes, J.L., Sidle, R.C. and Bergerud, W.A. (2004). “Recognition of debris-flow, debris-flood and flood hazard through watershed morphometrics”. *Landslides*, **1**: 61-66

Wilson, R.C. and Wieczorek, G.F. (1995). "Rainfall thresholds for the initiation of debris-flows at La Honda, California". *Environmental and Engineering Geoscience*, **1**(1): 11-27

Wohl, E. and Oguchi, T. (2004). Geographic information systems and mountain hazards. In: Bishop, M.P. and Shroder, J.F.(eds) (2004). Geographic Information Science and Mountain Geomorphology, Chichester, Praxis.

Xu, J. (1999). "Erosion caused by hyperconcentrated flow on the Loess Plateau of China". *Catena*, **36**: 1-19

Xu, J. (2002b). "Implication of relationships among suspended sediment size, water discharge and suspended sediment concentration, the Yellow River Basin, China". *Catena,* **49**: 289-307

Xu, J. (2003). "Hyperconcentrated flows in the lower Yellow River as influenced by drainage basin factors". *Zeitschrift fur Geomorphologie*, **47**, 393-410

Appendices

Appendix 1: Aeromagnetic anomalies in the Coromandel/Kaimai region (Christie et al., 2001)

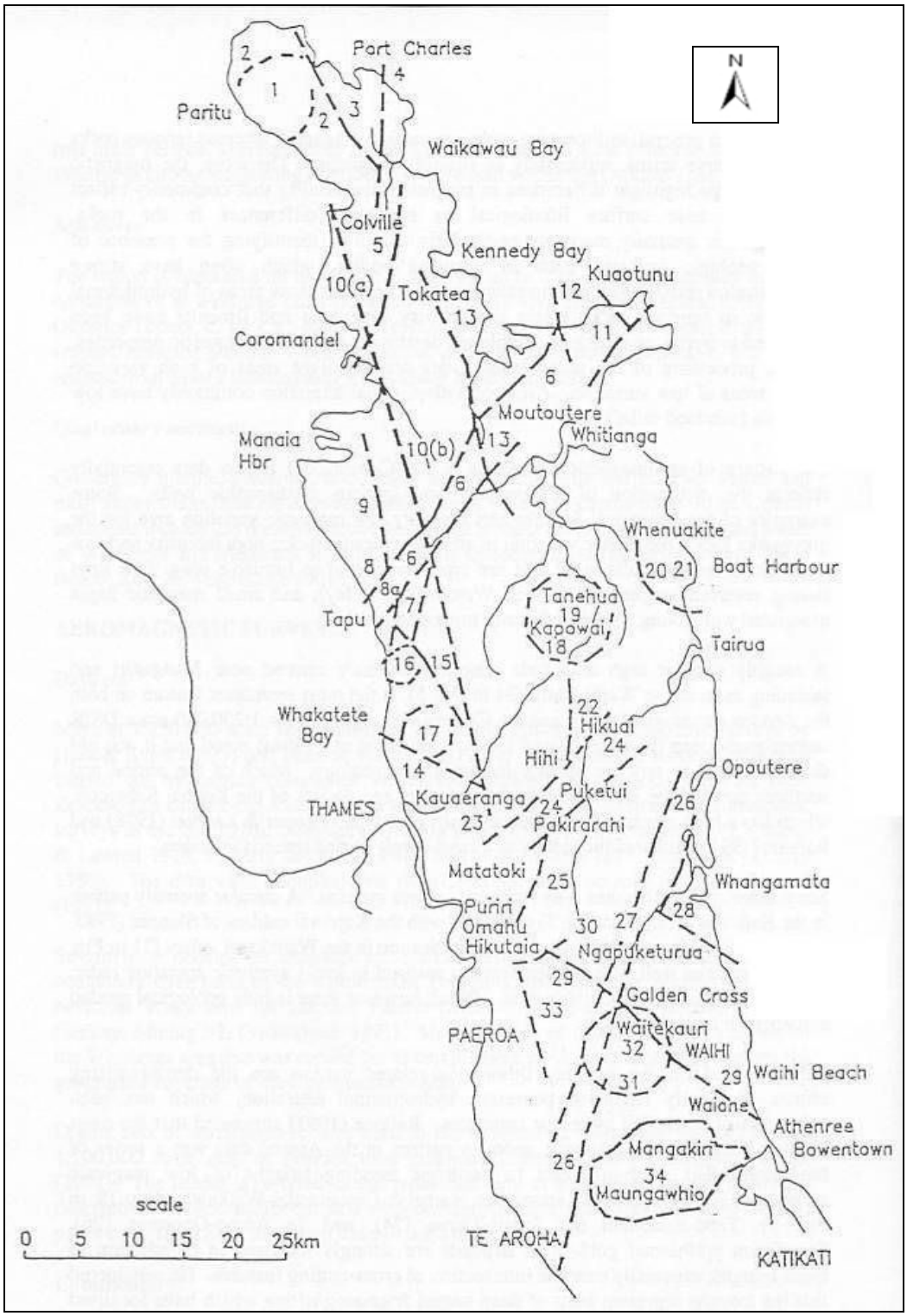

Appendix 2: Major fault zones in Coromandel/Kaimai region (Christie et al., 2001)

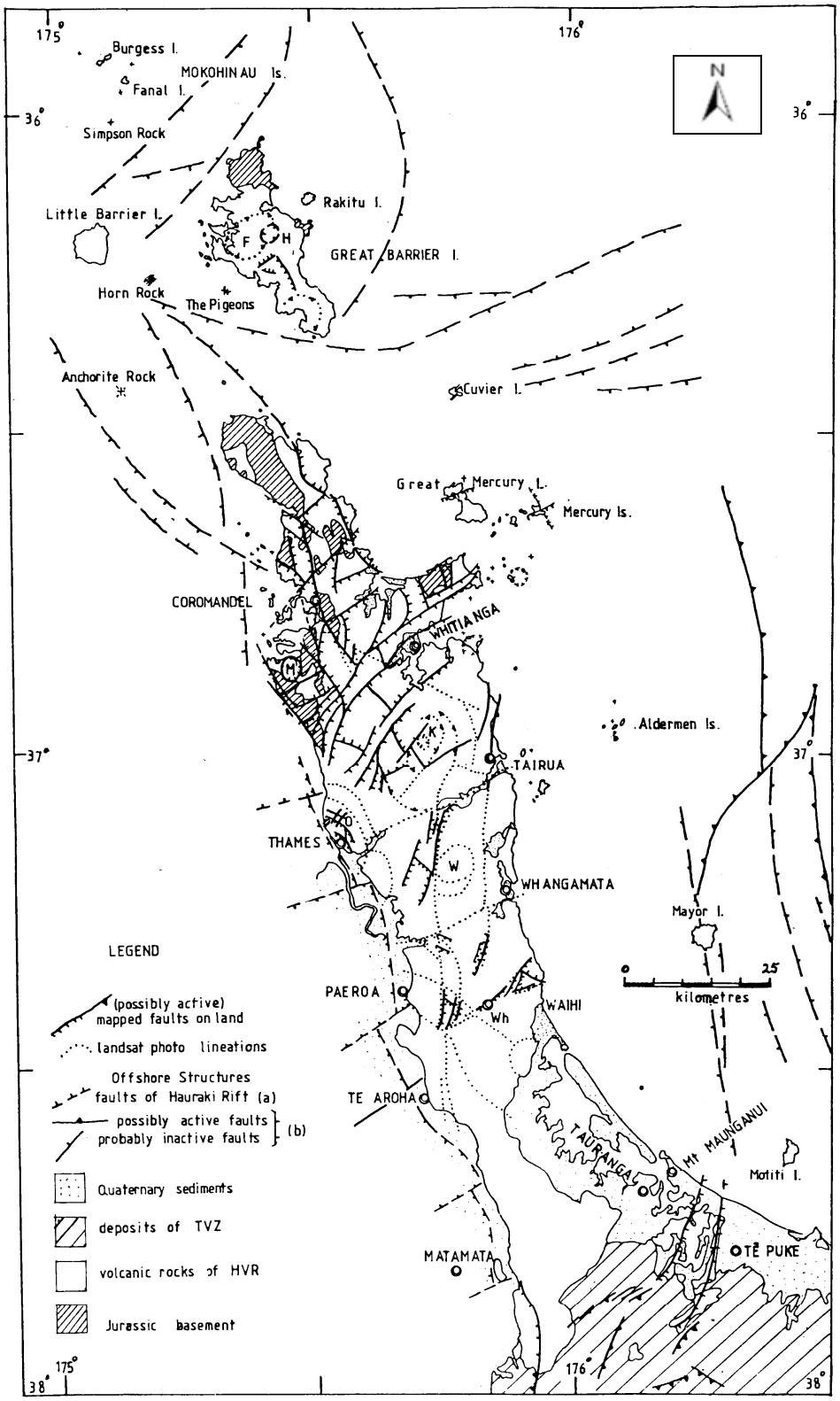

Appendix 3: Epithermal gold-silver deposits and porphyry copper deposits in the Cormandel/Kaimai region (Christie et al., 2001).

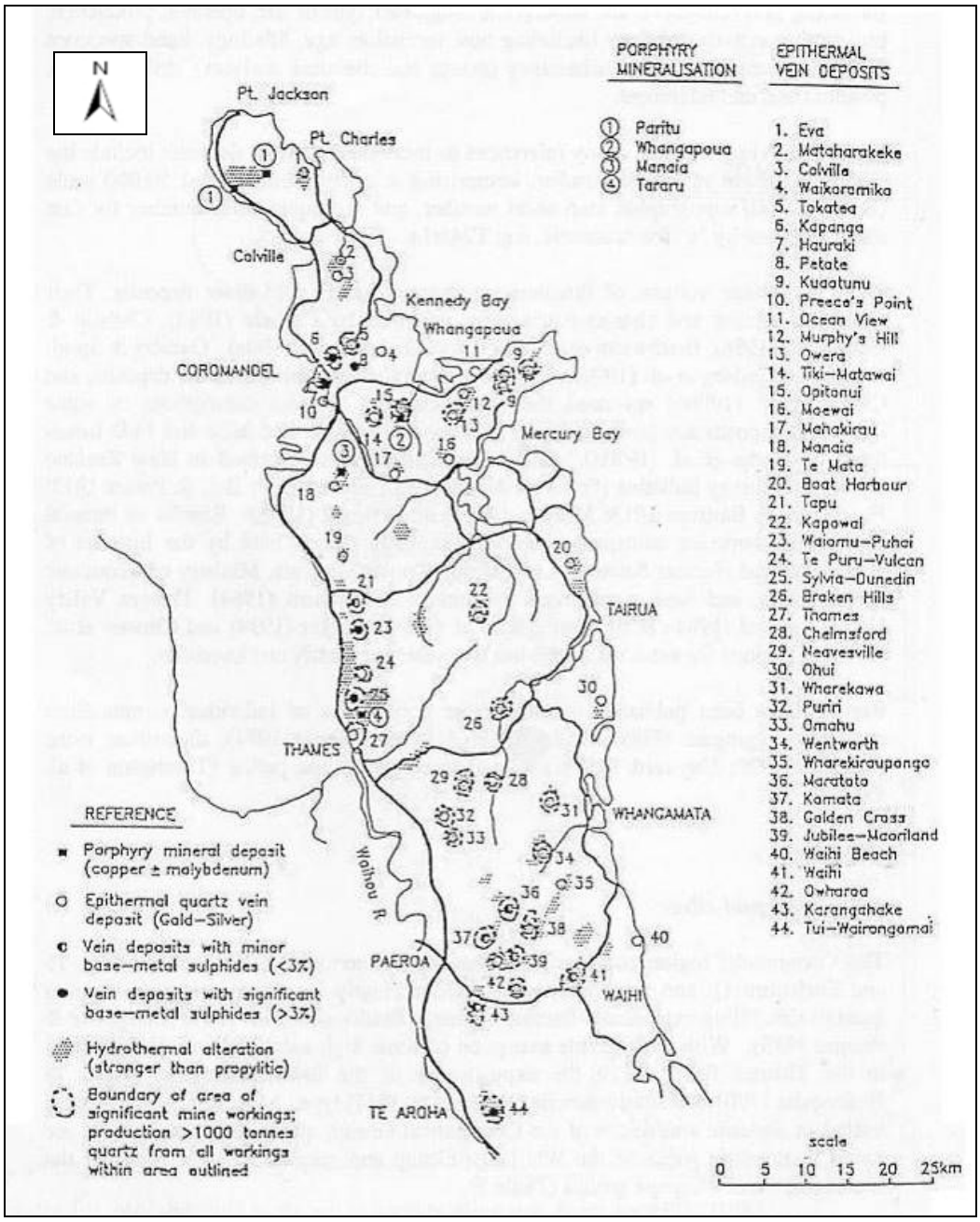

Appendix 4: Specific stream locations surveyed in the field investigation

4.1 Waitoitoi stream

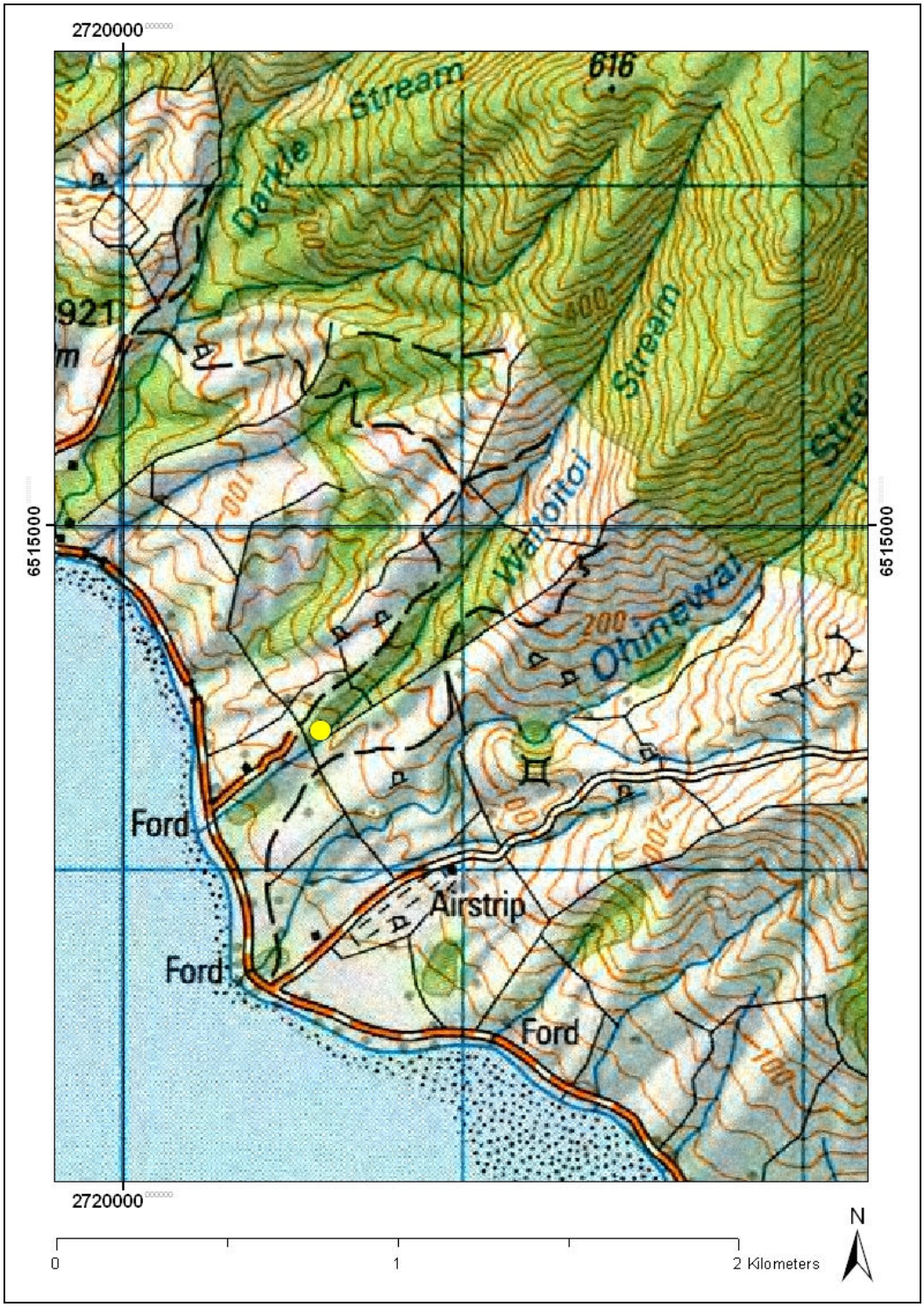

4.2 Waiwhango stream

4.3 Whakanekeneke stream (2)

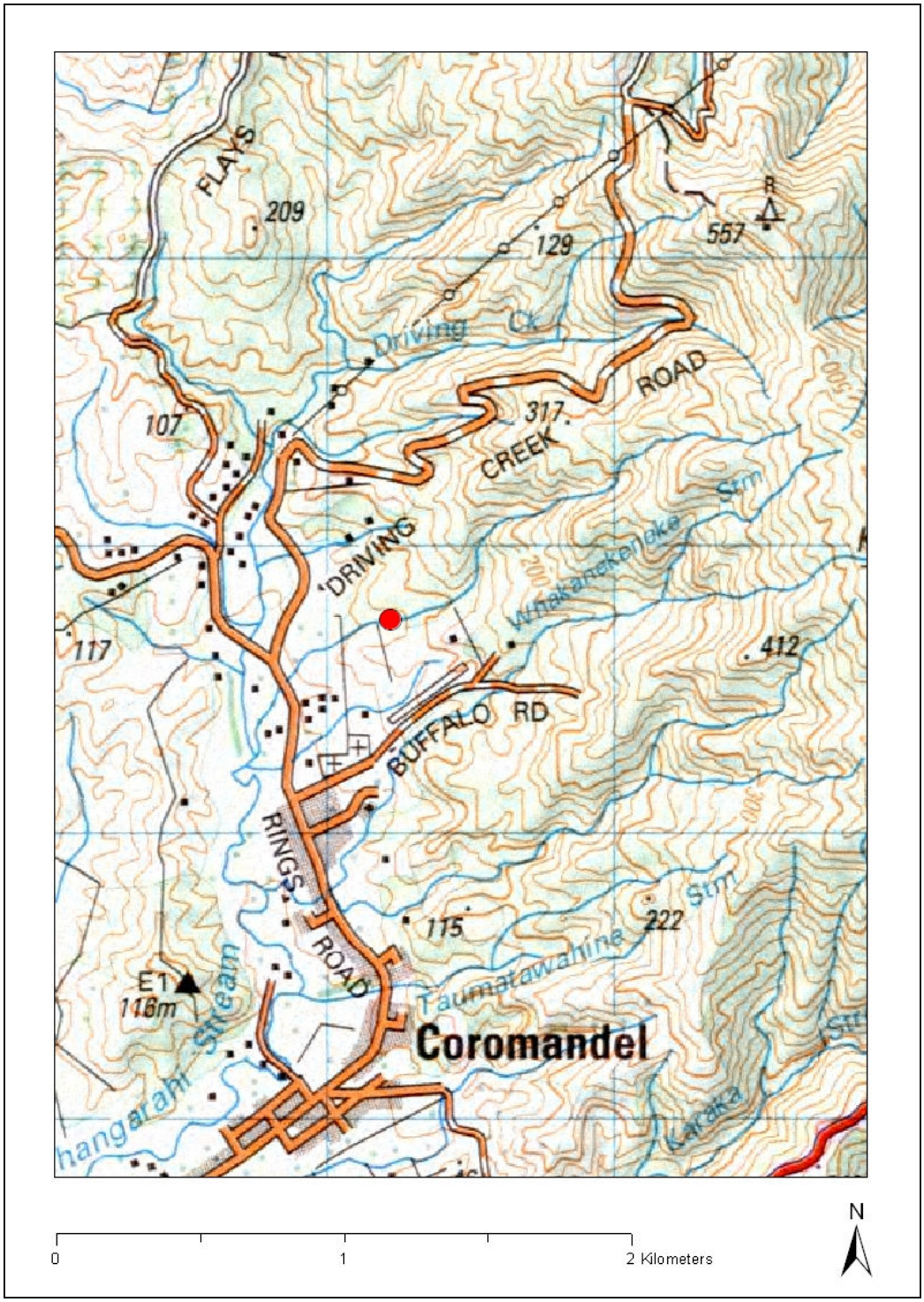

4.4 Otuturu stream

4.5 Te Puru stream

4.6 Otohi stream

4.7 Taruru stream

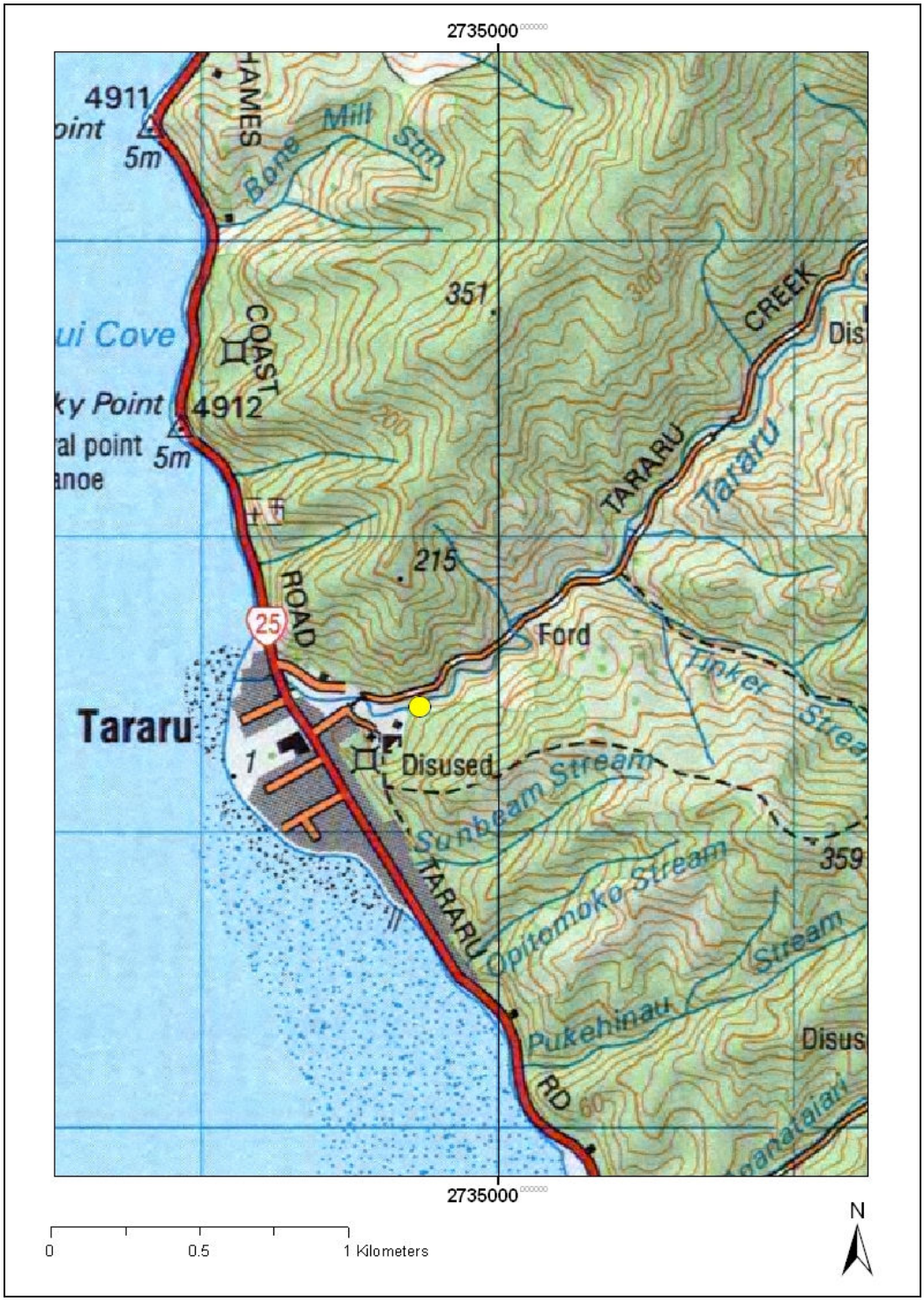

4.8 Waiotahi stream

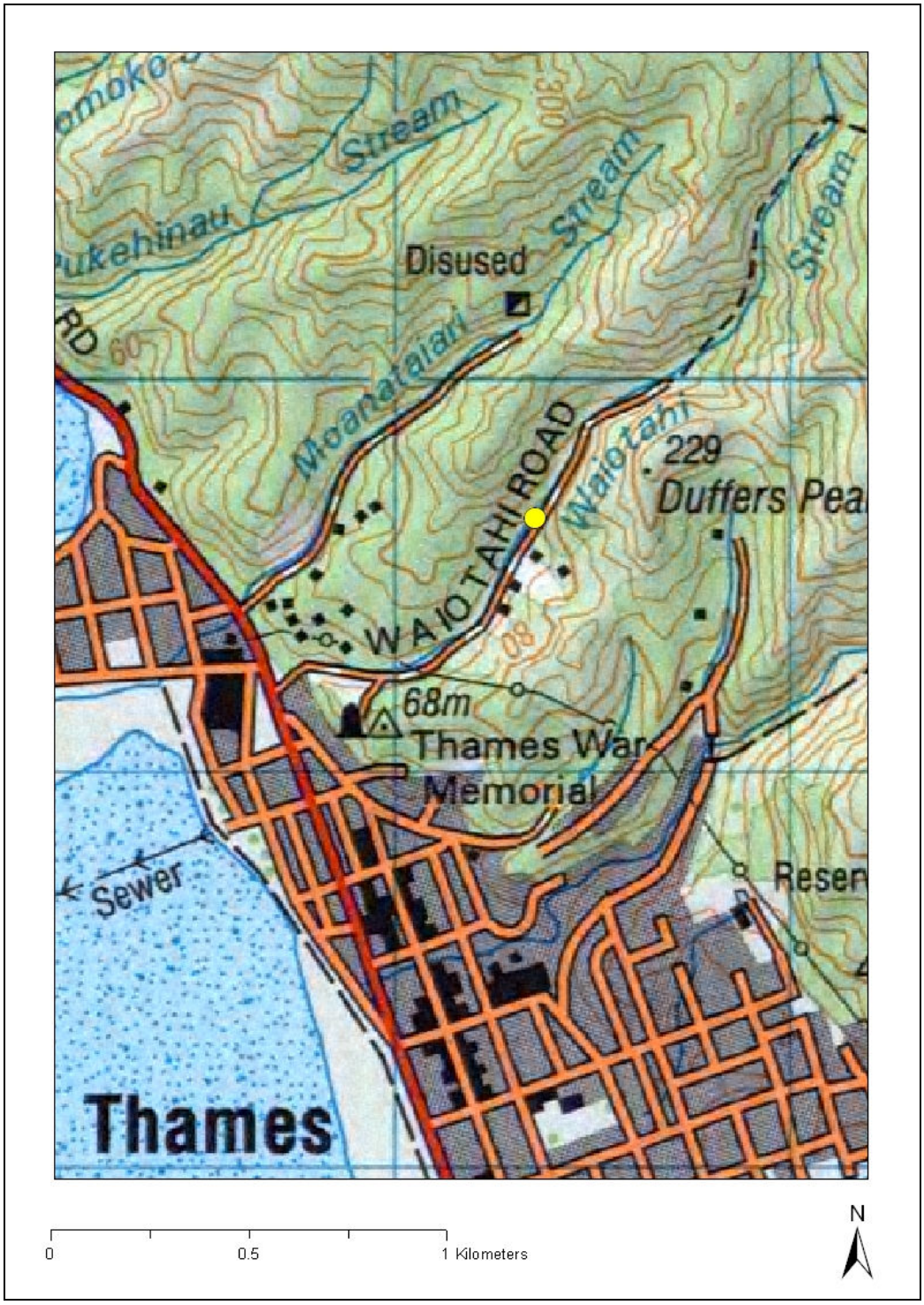

4.9 Karaka stream (3)

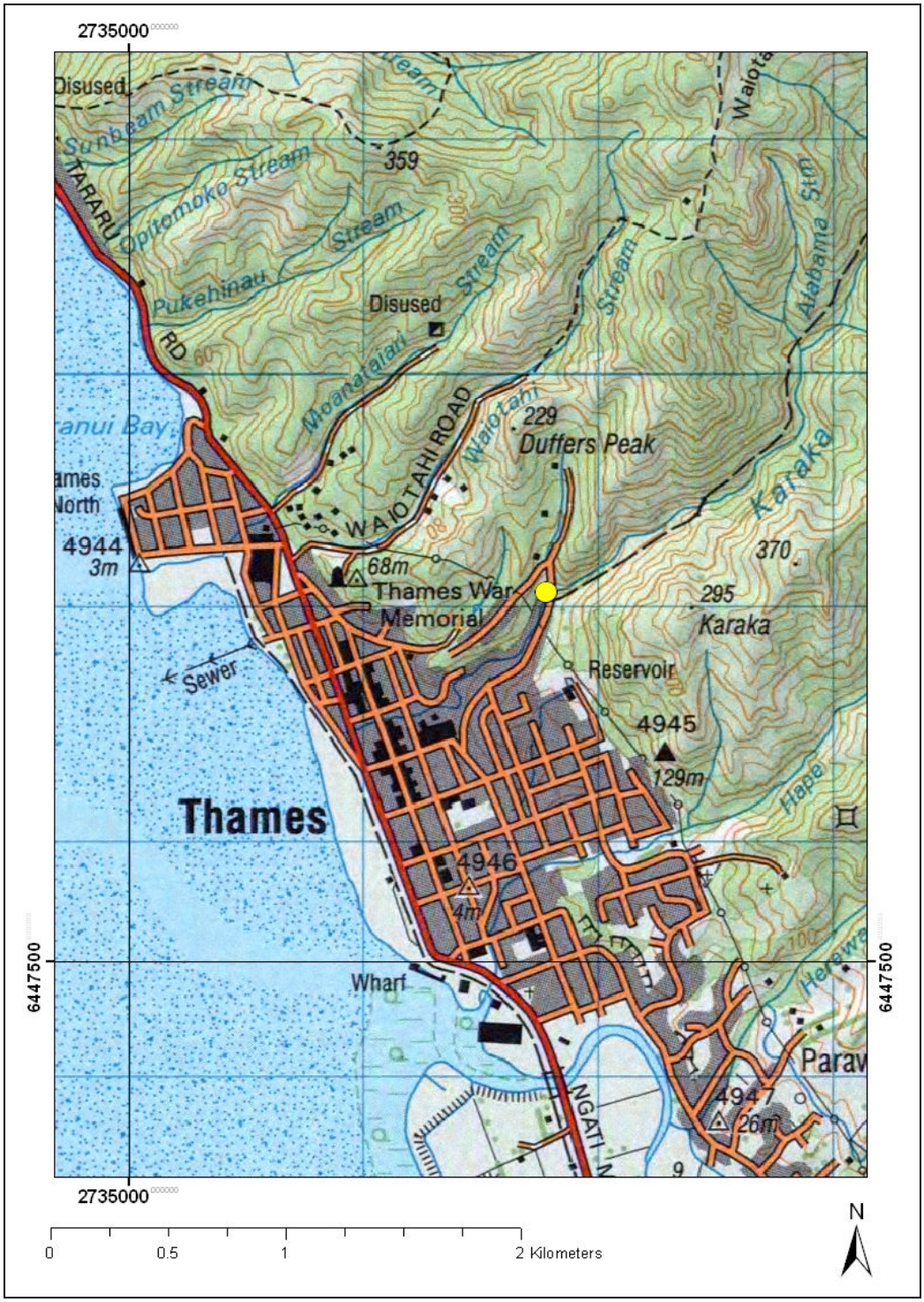

4.10 Waitoki stream

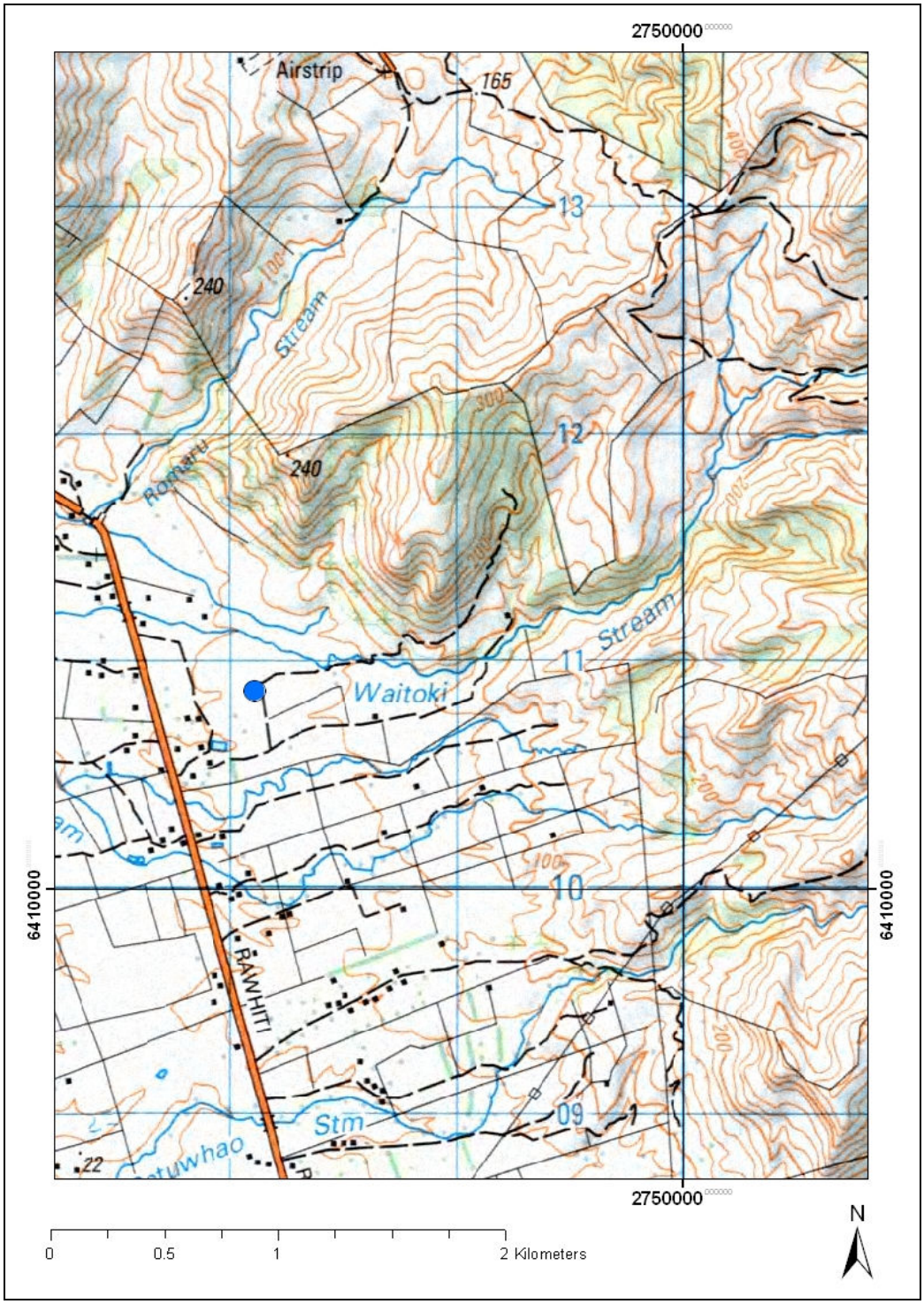

4.11 Moonlight stream

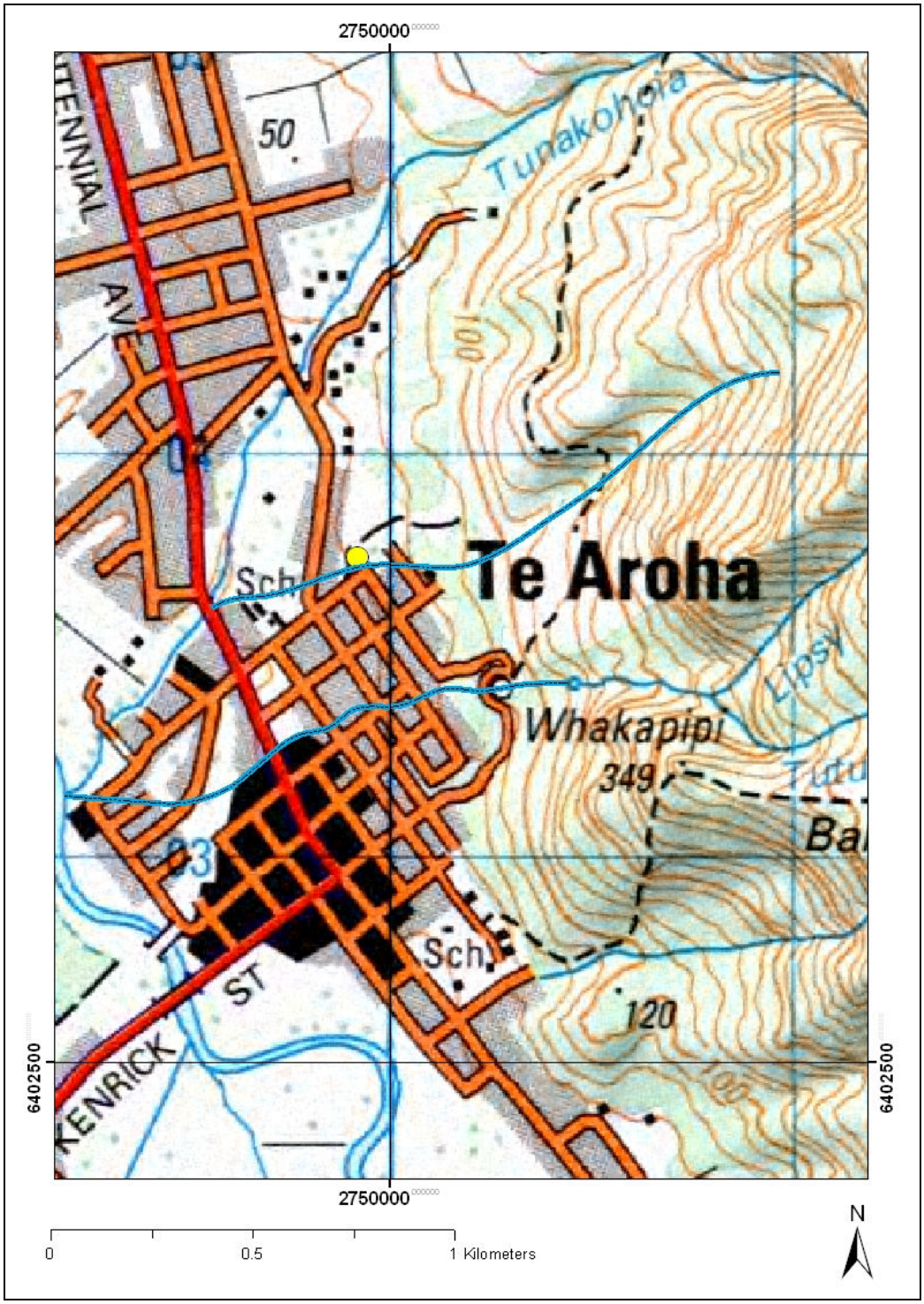

4.12 Lipsy stream

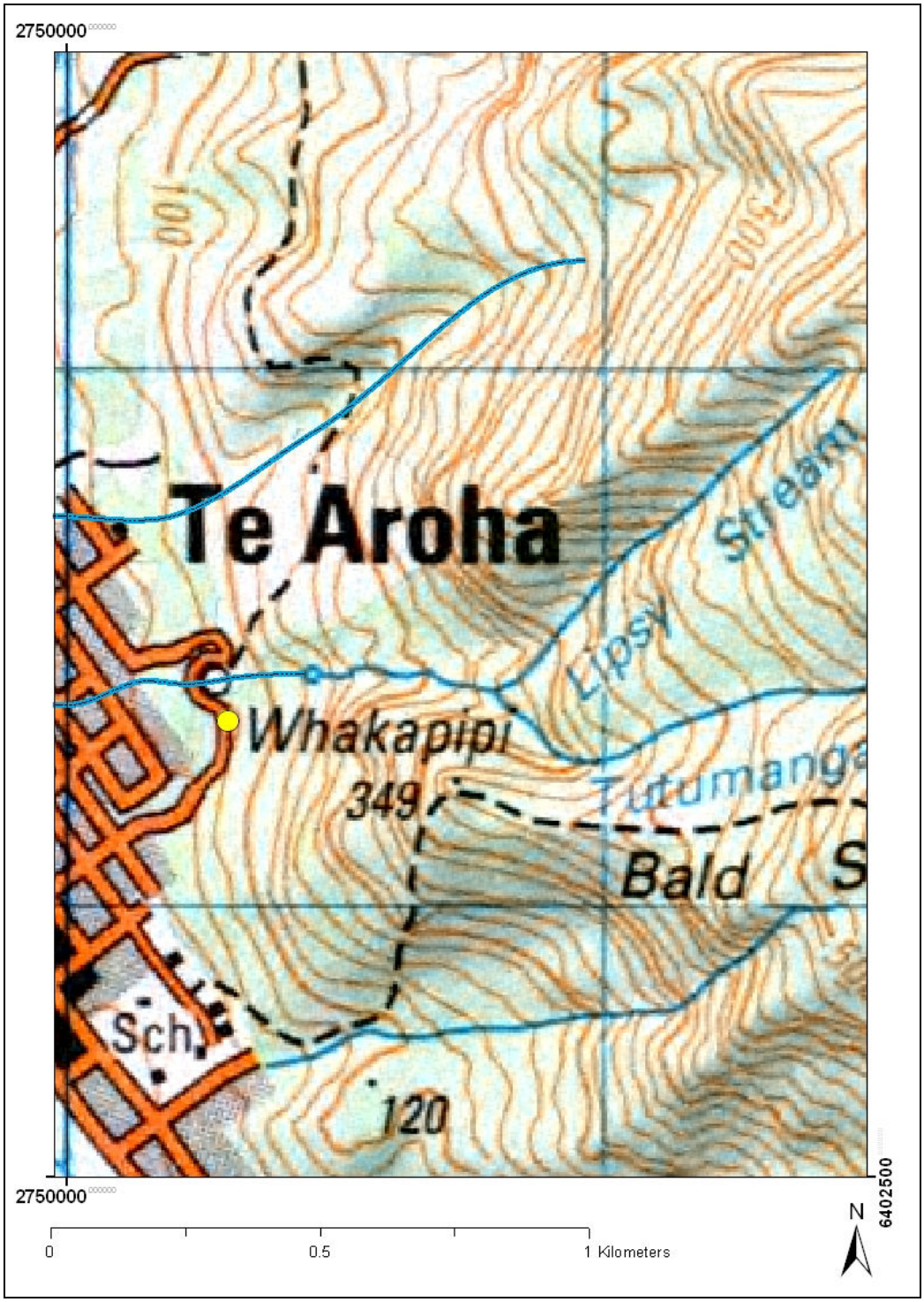

4.13 Unnamed stream, Gordon Rd.

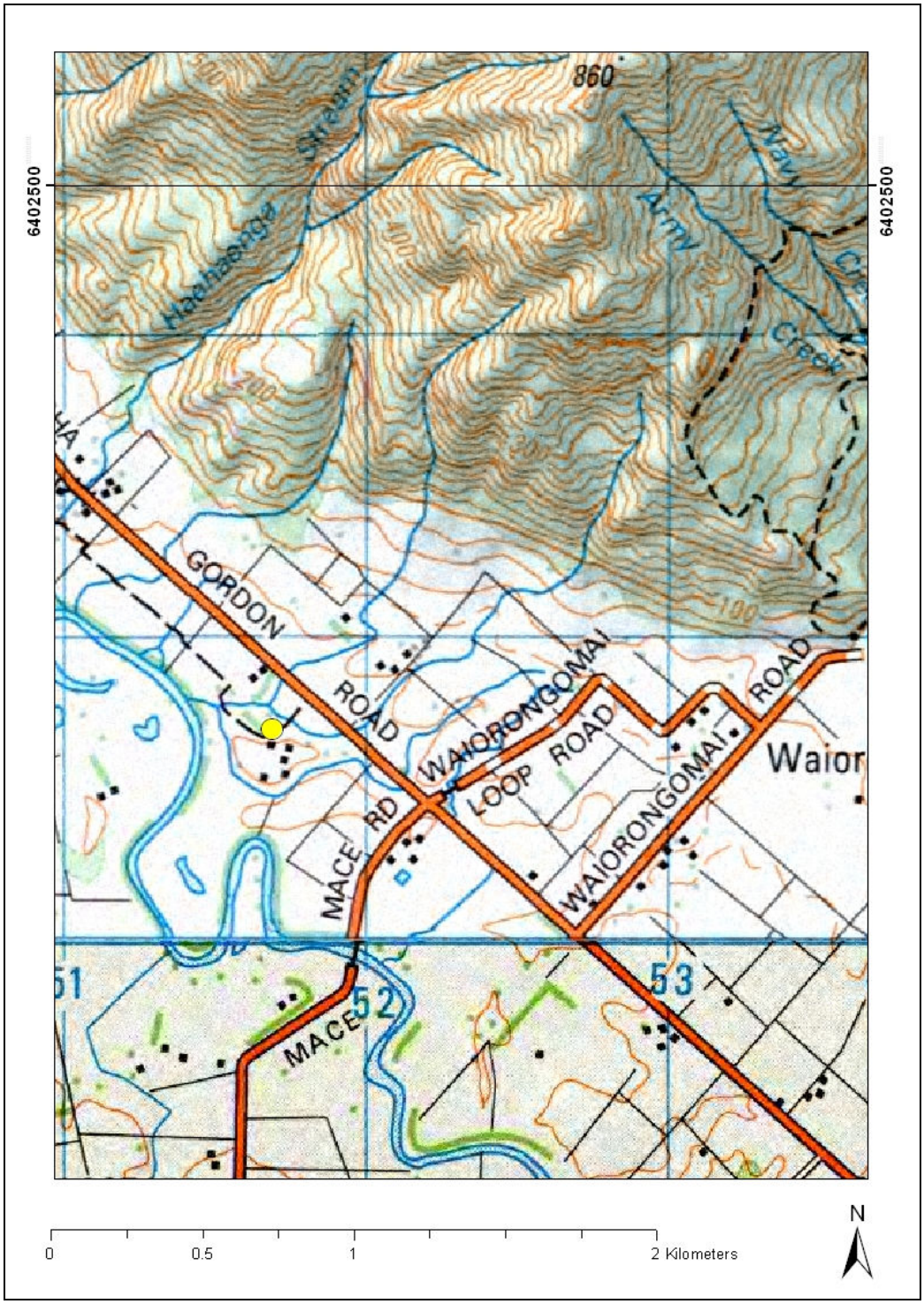

4.14 Wahine stream (2)

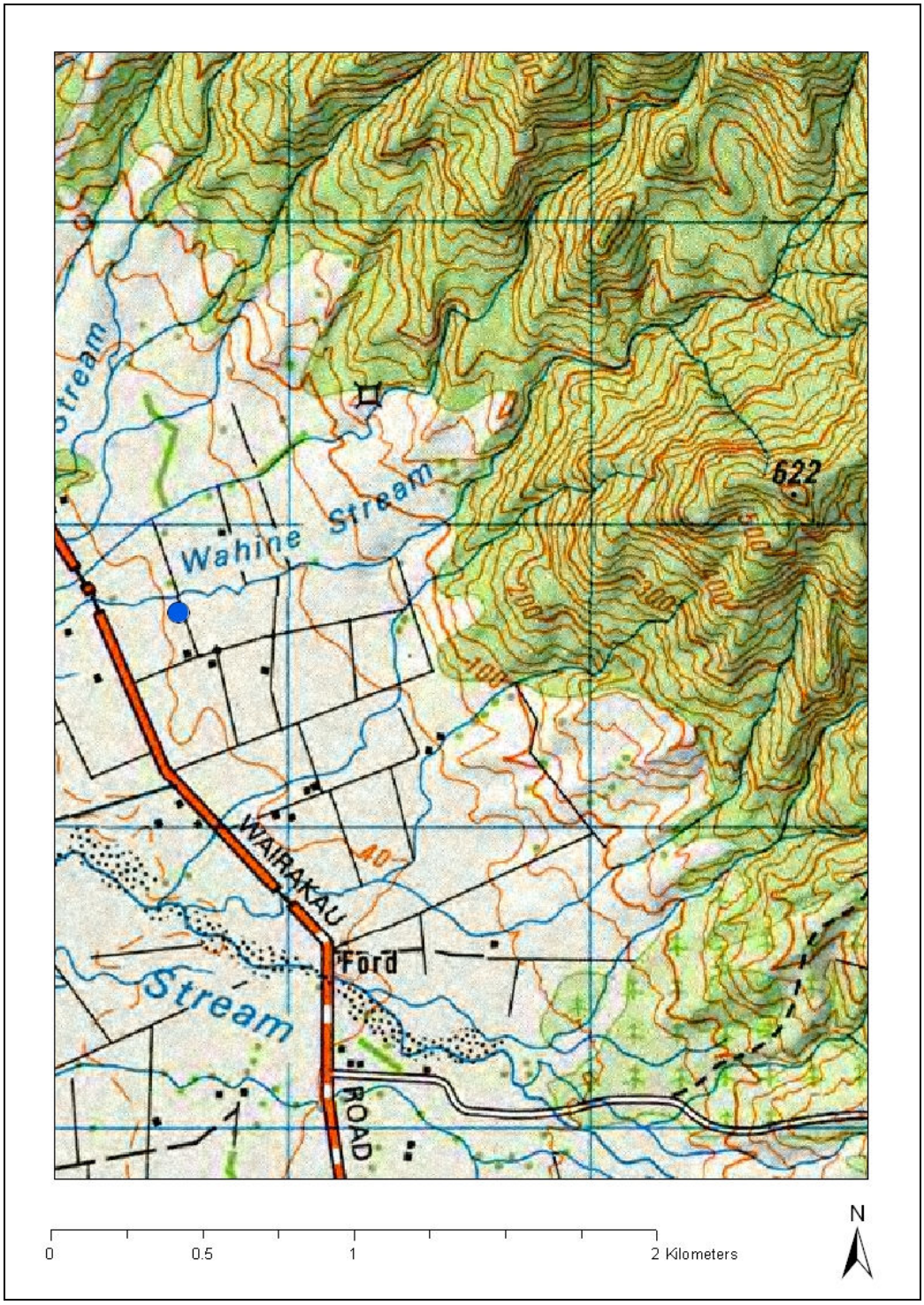

4.15 Gordon stream

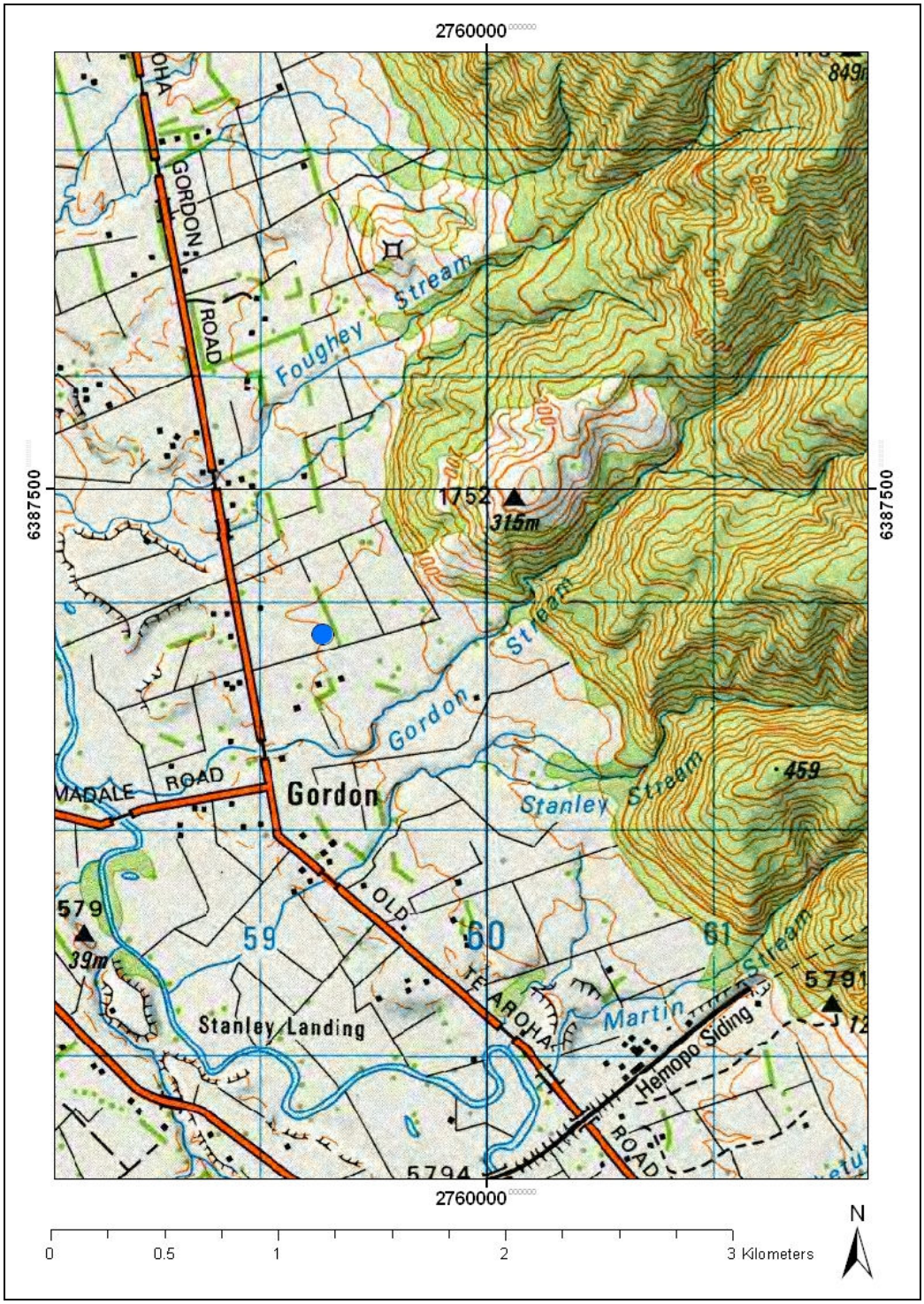

4.16 Stanley stream

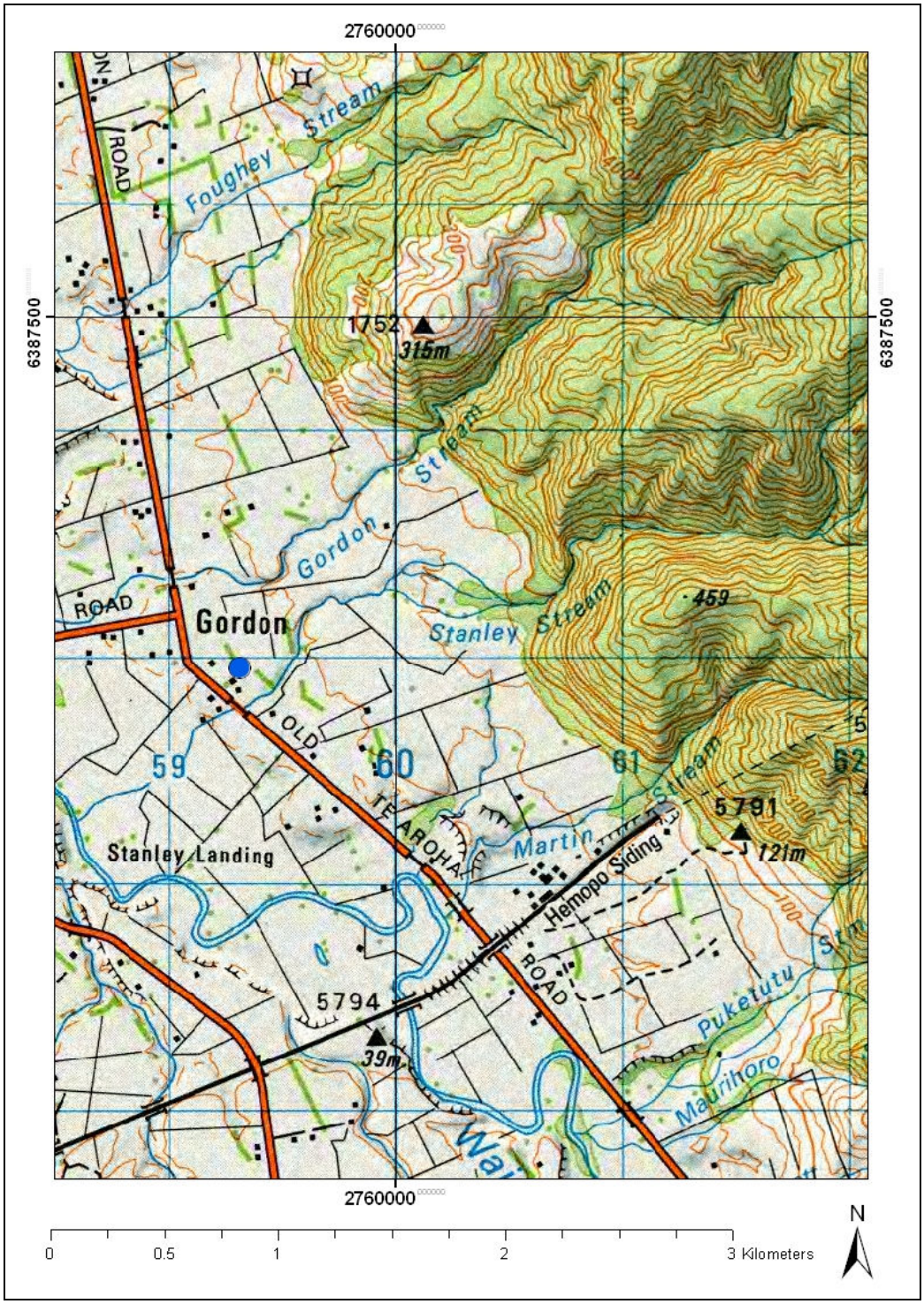

4.17 Putangi stream

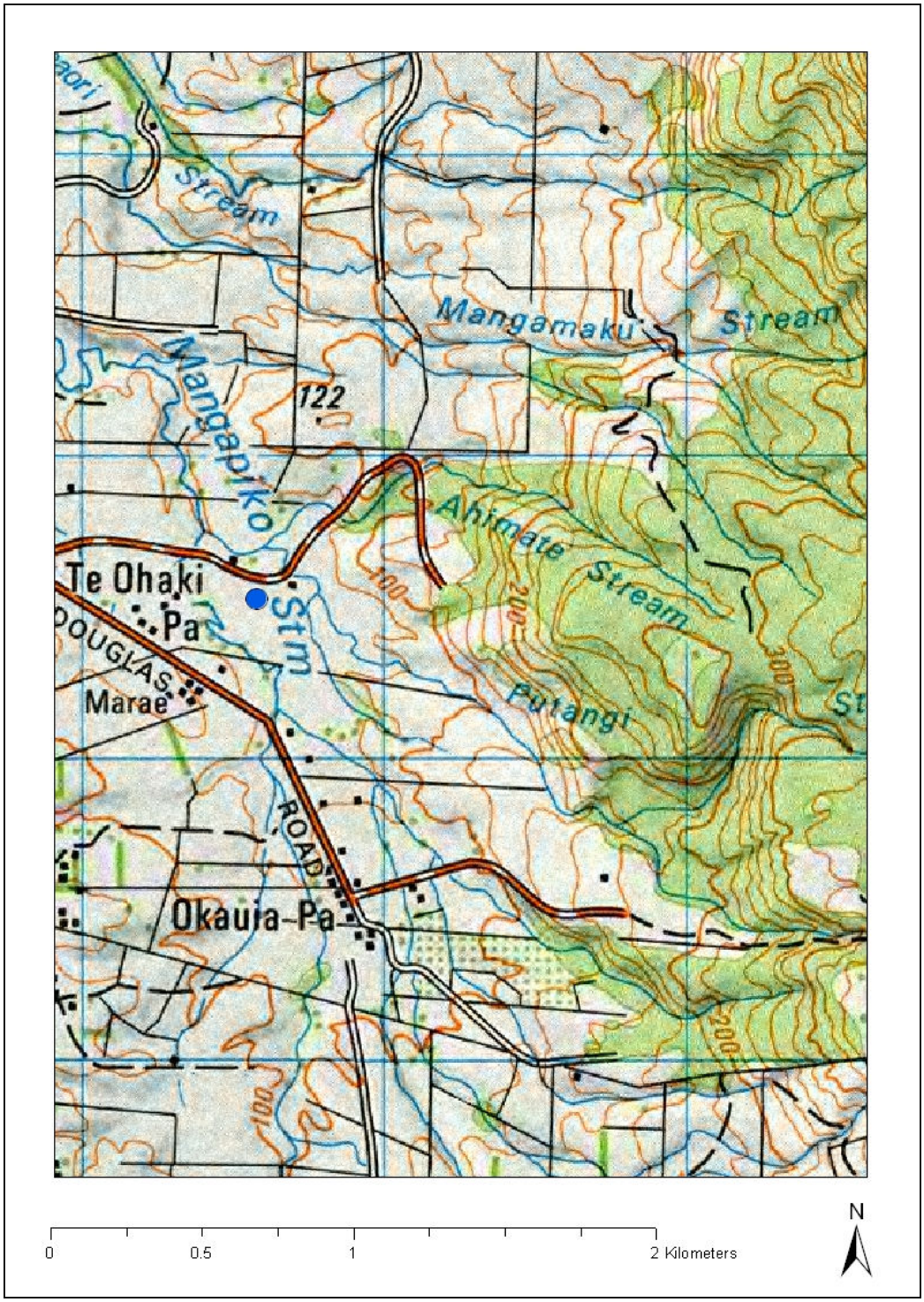

4.18 Matutu stream